Katia Imeria FERRO

The impact of oxalogenic plants on soil carbon dynamics

- formation of a millennium carbon storage as calcium carbonate -



UNIVERSITÉ DE NEUCHÂTEL

PLANT SURVIVAL
National Centre of Competence in Research

FNSNF
FONDS NATIONAL SUISSE
DE LA RECHERCHE SCIENTIFIQUE

Nr. U.00926.03.03

Institut de biologie de l'Université de Neuchâtel 2012

Université de Neuchâtel

FACULTE DES SCIENCES
Secrétariat-Décanat de la faculté
Rue Emile-Argand 11
CH-2000 Neuchâtel

IMPRIMATUR POUR LA THESE

The impact of oxalogenic plants on soil carbon dynamics – formation of a millenium storage as calcium carbonate

Katia FERRO

UNIVERSITE DE NEUCHATEL

FACULTE DES SCIENCES

La Faculté des sciences de l'Université de Neuchâtel,
sur le rapport des membres du jury

Prof. Eric Verrecchia, UniNe et Université de Lausanne, directeur de thèse
Prof. Michel Aragno, UniNe
Prof. Jean-Michel Gobat, UniNe
Dr Guillaume Cailleau, Université de Lausanne,
Dr David Sebag, Université de Rouen F

autorise l'impression de la présente thèse.

Neuchâtel, le 19 septembre 2012

Le doyen :
P. Kropf

Téléphone : +41 32 718 21 00 E-mail : secretariat.sciences@unine.ch www.unine.ch/sciences

Université de Neuchâtel
Institut de biologie

The impact of oxalogenic plants on soil carbon dynamics - formation of a millennium carbon storage as calcium carbonate -

Thèse

Présentée à la Faculté des Sciences de l'Université de Neuchâtel

Pour l'obtention du grade de *Docteur ès Science*

par

Katia Imeria Ferro

Acceptée sur proposition du jury :

Prof. Eric P. Verrecchia, Université de Neuchâtel (Directeur de thèse)
Prof. Michel Aragno, Université de Neuchâtel
Prof. Jean-Michel Gobat, Université de Neuchâtel
Dr. David Sebag, Université de Rouen (France)
Dr. Guillaume Cailleau, Université de Lausanne

Soutenue le 6 septembre 2011
Université de Neuchâtel
2012

Abstract

South of Burkina Faso, thousands of years of pedogenesis result in “Plinthic Ferralsols (Arenic)” (according to the WRB). However, it was observed that under the influence of oxalogenic trees, such as *Milicia excelsa*, *Afzelia africana*, and *Bombax costatum*, the soils evolved into “Ferralic Calcisols (Arenic)” (according to the WRB) in only a few decades. It has been proposed that the driving force of this carbonate accumulation is the bacterial oxalotrophy, which generates a carbon reservoir between the atmosphere and the soil.

The principal goals of this work are (1) to provide a carbon balance, (2) to propose a model of the carbonate accumulation, and (3) to estimate the residence time of the inorganic carbon in the soil under the trees. Samples were taken from five profiles near the considered oxalogenic trees and a reference soil beyond their respective influence. Contents of total organic carbon, oxalate, and carbonate were measured. The main tools used to quantify these three different forms of carbon were the Rock-Eval pyrolysis, enzymatic digestion (Trinity Biotech), and back titration after acid dissolution of carbonate.

Analysis of organic matter indicates that the total organic carbon evolves both quantitatively and qualitatively from leaves to mineral horizons. The stock of organic carbon is incorporated in the bio-molecules at the surface horizons (A) and in stable geo-molecules in mineral horizons (B and C).

This study shows that the amount of oxalates in leaves (considered here as a first oxalate reservoir) is of 20 x 10^{-2} mg / g of dry matter. Oxalogenic fungi may also have to be added to this source. Indeed, by culturing soil samples, the following oxalogenic strains were identified: *Aspergillus sp.*, *Fusarium sp.,* and *Mucor sp.*.

Despite these contributions (leaves and fungi) of oxalate, the concentration measured in the soil is low, never exceeding 6.5 x 10^{-3} mg oxalate / g of soil at any time *t*. This unexpected outcome may be explained by the efficiency of the bacterial oxidation of oxalate, leading to low magnesium calcite precipitation. Indeed, the latter, while not present in fresh leaves, was found in litter and soils, where its concentration can reach values as high as 15% of the soil total mass.

Abiotic factors influencing the carbonate accumulation are here discussed. This work points out that, under an oxalogenic tree (such as a *M. excelsa* tree), the accumulation of carbonate between 70 and 170 years is so significant that the soil may even become cemented. Moreover it is proposed that the residence time of carbonate in soil constitutes a carbon stock of several hundred years.

Résumé

Au sud du Burkina Faso, des milliers d'années de pédogénèse ont produit des «Plinthic Ferralsols (Arenic)» (suivant la WRB). Il a toutefois été observé que sous l'influence d'arbres oxalogènes tels que *Milicia excelsa*, *Afzelia africana* et *Bombax costatum*, les sols évoluent vers des «Ferralic Calcisols (Arenic)» (selon la WRB) en quelques décennies. Il est admis que le moteur de cette accumulation carbonatée est l'oxalotrophie bactérienne, qui crée un réservoir à carbone entre l'atmosphère et les sols.

Les buts de ce travail sont (1) de dresser un bilan de carbone, (2) de modéliser son accumulation et (3) de calculer un temps de résidence du carbone minéral dans le sol sous ces arbres. Les échantillons ont été prélevés dans cinq profils à proximité d'arbres oxalogènes et un dans un sol de référence, hors de leur influence. Les teneurs en carbone organique total, en oxalates et en carbonates ont été ensuite mesurées. Les principaux outils utilisés pour quantifier ces trois formes de carbone ont été respectivement la pyrolyse Rock-Eval, la digestion enzymatique (Trinity-Biotech) et la titration en retour après dissolution acide des carbonates.

L'analyse de la matière organique indique que le carbone organique total évolue de manière quantitative et qualitative depuis les feuilles jusqu'aux horizons minéraux. Le stock de carbone organique est intégré dans les bio-molécules dans les horizons de surface (A) et dans les géo-molécules plus stables dans les horizons minéraux (B et C).

Cette étude montre que la quantité en oxalates dans les feuilles (considérées comme un premier réservoir d'oxalate) est de 20 x 10^{-2} mg/g de matière sèche. A cette source peut être ajoutée celle des champignons excréteurs d'acide oxalique. En effet, par la mise en culture d'échantillons de sol, les espèces oxalogènes suivantes ont été identifiées: *Aspergillus sp.*, *Fusarium sp.* et *Mucor sp.*.

Malgré ces deux apports d'oxalate (feuilles et champignons), la concentration mesurée dans les sols reste faible, ne dépassant pas 6.5 x 10^{-3} mg d'oxalate/g de sol à un instant *t*. Ceci-ci peut être expliqué par l'efficacité de l'oxydation bactérienne des oxalates menant à la précipitation de calcite faiblement magnésienne. En effet cette dernière, non présente dans les feuilles fraîches, a été observée dans la litière et les sols où les concentrations peuvent atteindre 15% de la masse totale.

Les facteurs abiotiques influençant l'accumulation carbonatée sont ici discutés. Ce travail permet de mettre en évidence que sous un arbre oxalogène, tel que le *M. excelsa,* l'accumulation en carbonates sur une période de 70 à 170 ans serait telle que le sol pourrait être cimenté. De plus, le temps de résidence du carbonate dans le sol est de l'ordre de plusieurs centaines d'années. Ce dernier constitue donc un puits à carbone.

Remerciements

Avec cette thèse se termine enfin une longue période de ma vie pour le plus grand bonheur des gens qui m'entourent et moi-même. Je remercie toutes les personnes qui ont participé, de près ou de loin, à l'élaboration de ce travail et qui ont patienté jusqu'à ce jour pour voir la fin de mon doctorat.

Mes remerciements vont d'abord à mon directeur de thèse le Professeur Eric Verrecchia. Je lui suis infiniment reconnaissante, non seulement parce qu'il m'a proposé cette thèse, mais aussi pour avoir répondu toujours rapidement et gentiment à mes questions, même les dimanche soirs, même en vacances, et pour tout le temps qu'il a dédié à ce travail.

Je remercie les membres du Jury qui m'ont fait l'honneur de juger cette thèse : le Prof. Michel Aragno, le Prof. Jean-Michel Gobat, le Dr. David Sebag et le Dr. Guillaume Cailleau. Aux Professeurs Eric Verrecchia, Michel Aragno et Jean-Michel Gobat, merci de m'avoir fait découvrir avec enthousiasme les biogéosciences. J'adresse un grand merci au Dr. Daniel Job pour ses cours fascinants de mycologie et les recommandations qu'il a apportées à cette thèse.

Je tiens à remercier particulièrement la Dr. Nadia Khammar pour ses précieux conseils au début de cette thèse. Je remercie aussi Sonia pour la campagne d'échantillonnage à Salina parmi les cactus et les câpres.

Un grand merci à Christophe Dupraz pour les observations au microscope électronique ainsi que pour ses conseils forts utiles. Je remercie Nicole Jeanneret du laboratoire de microbiologie pour son aide, sa gentillesse et sa disponibilité.

Je remercie la Dr. Claire Arnold et la Dr. Elena Havlicek pour leurs recommandations lors du rapport de demi thèse.

Merci de tout cœur aux personnes rencontrées au Burkina Faso: le guide ainsi que l'éducateur Mikaïlou Namoro, le pépiniériste Sankara, l'infatigable Ya Ya et Mamadou, les habitants de Mangodara, Farakorosso et Nianmango qui ont permis la réussite de cette expédition. Il m'importe d'exprimer ma gratitude aux membres de L'Ecole Nationale des Eaux et Forêts (ENEF) de Bobo-Diulasso, ainsi qu'aux membres du Ministère du cadre de l'environnement à Banfora, et tout particulièrement à l'Ingénieur Directeur Général Léonard O. Zouré (Ingénieur Agro- sylvo-pastoraliste), l'Ingénieur Ouedrago P. Alassane (Ingénieur des eaux et des forêts, botaniste), Monsieur Sité Jean-Albert Somé (Technicien supérieur d'agriculture, spécialiste en apiculture tropicale) ainsi que le directeur et Ingénieur forestier Adama Dulcom. Tous m'ont fourni de précieux renseignements qui nous ont permis de trouver les irokos.

Je remercie Guillaume Cailleau. Son travail de thèse sur la voie oxalate-carbonate précède le mien et il a consacré beaucoup de son temps à discuter avec moi sur les stratégies à adopter et lors de la rédaction du manuscrit.

Un grand merci à Gilles, Gaëlle, Géraldine, Matthieu, Claire, Gaétan, Matteo des laboratoires de mycologie et pédologie.

Mes remerciements s'adressent aussi à Thierry Adatte, Virginie Matera et Tiffany pour leur aide, leurs conseils et leur patience lors de l'interprétation des résultats de l'ICPMS et du Rock-Eval.

A Flurin mon copain-de-bureau : merci pour avoir toujours trouvé une solution à tout et pour ton amabilité. Alla Sere, la Criss-Felicità, Sara et Joel, Fiore et Ana, Mari-Sol et Lina, Oli, Olivier, Saskia, Christina, et Grand-papa Louis grazie per la vostra amicizia.

A Anouk un merci spécial. Grazie Anouk pour nos discussions sans conclusions, notre vie commune à la Tchò,

le voyage au Burkina, les bons repas et les gros rires! Ces moments sont à jamais gravés dans mon cœur!

A Giò, mio ex-assistente di fisica, compagno di vita, a colui che ha reso il mio inglese approssimativo leggibile, ma soprattutto mio Amicone di San Vittore: Tank you very much!

A Ralph, l'homme qui partage ma vie un merci spécial chargé de tant de significations ! Allez ma période oxalate-carbonate arrive à son terme ! Finis les bâillements!

A nos filles, Gaïa Mathilde, Charlotte Iris et à Eliot Albert. Merci d'être ma joie, mes perles de soleil et ma fierté. Je remercie « Grand-maman-Nona » Marianne pour avoir gardé mes enfants pendant la rédaction de ce travail.

Un grazie carico di emozione va ai miei genitori ed ai miei fratellli, Sacha, Benni e Stefano per avermi sempre sostenuta ed incoraggiata, e per aver creduto in me.

Grazie Natura!

Ce projet de doctorat a été financé par le Fonds National Suisse.

Contents

Figure list
Table list

Chapter 1 INTRODUCTION
Presentation of the oxalate-carbonate pathway

1.1	Introduction	1
1.2	Problem statement	1
1.3	Research questions	2
1.4	Objectives	2
1.5	Hypotheses	2
1.6	Organization of the manuscript	2
1.7	Background	3
1.7.1	The global carbon cycle	3
1.7.2	The land carbon cycle	4
1.7.3	Carbonate precipitation processes	6
1.7.4	Pedogenic carbonate	10
1.7.5	The primary calcium (and magnesium) source: a limiting factor for calcite formation	10
1.7.6	The carbon dioxide-oxalate-carbonate pathway	11
1.7.7	Oxalic acid and oxalate salts	12
1.7.8	Plants and oxalates	13
1.7.9	Fungi and oxalates	15
1.7.10	Soils and oxalates	16
1.7.11	The oxalate degradation: the oxalotrophy	17
1.7.12	Carbonate related to the *M. excelsa* ecosystem	18

Chapter 2 MATERIAL AND METHODS
The tools used to quantify the oxalate-carbonate pathway

2.1	Carbonate detection and pH measurement on field	21
2.2	The analysed material	21
2.2.1	“Fresh organic material” and pure Ca-oxalate samples	21
2.2.2	Soil samples	22
2.2.3	Water samples	23
2.3	Soil intrinsic characteristics	23
2.3.1	pH measurement	23
2.3.2	Residual humidity	23
2.3.3	X-ray diffraction	23
2.3.4	Scanning electron microscopy (SEM)	24
2.3.5	Soil grain size distribution	24
2.3.6	ICP-MS	24

2.3.7 Base cation saturation ratio (S/(S+AE) *100) 25
2.3.8 Thin sections 25
2.4 Carbon quantification 25
2.4.1 The Rock-Eval6 principle 25
2.4.2 Deconvolution of S2 curves 26
2.4.3 Carbonate titration 27
2.4.4 Oxalate quantification 2
2.4.5 CHN 27
2.5 Fungi manipulation 27
2.5.1 Fungal isolation 27
2.5.2 The Malt-Agar medium + gypsum 28
2.5.3 Ergosterol quantification 28

Chapter 3 PRESENTATION OF THE STUDIED SYSTEMS
An African and an Italian example

3.1 Geographical settings: Mangodara and Niangoloko 29
3.1.1 The *Milicia excelsa* tree 29
3.1.2 The *Afzelia africana* tree 33
3.1.3 The *Bombax costatum* tree 34
3.1.4 Description on the *Milicia excelsa* trees location and soils 35
3.1.5 The *Afzelia africana* system 41
3.2 The Salina ecosystem 41
3.2.1 Geographical setting: Pollara 41
3.2.2 The *Opuntia sp.* cactus 43
3.2.3 The Pollara studied soils 44

Chapter 4 THE ORGANIC CARBON QUALIFICATION
A Rock-Eval pyrolysis approach

4 Introduction 45
4.1 Soil organic matter 45
4.1.1 Carbohydrates 47
4.1.2 Nitrogenous compounds 47
4.1.3 Lipids 48
4.1.4 Lignin 49
4.1.5 Humified organic substances 49
4.2 Objectives of the chapter 52
4.3 Samples 52
4.4 Results and discussion: usual Rock-Eval parameters 52
4.4.1 Fresh organic material 52
4.4.2 The reference soil: F3 54
4.4.3 Soil related to oxalogenic trees 59

4.4.4 Salina soils 61
4.5 Results: the acquisition and processing of pyrolysis and oxidation curves 62
4.5.1 Pure mineral material: Ca-oxalate 63
4.5.2 Plant material: wood and leaves 64
4.5.3 Fungal material: *Boletus sp.*, *Fusarium sp.*, and melanin 65
4.5.4 Insect material: ants, termites, and termite nest 65
4.5.5 Soil material 66
4.6 Discussion: pyrolysis and oxidation curve analyses 66
4.7 Conclusions 73

Chapter 5 OXALATE QUANTIFICATION
Analysis of two oxalate sources: plants oxalate and fungal oxalate

5.1 Introduction 75
5.2 Results and discussion 76
5.2.1 Results: oxalate and plants 76
5.2.2 Discussion: oxalate and plants 79
5.2.3 Partial conclusions: oxalate and plants 81
5.2.4 Results: oxalate and fungi 81
5.2.5 Discussion: oxalate and fungi 82
5.2.6 Partial conclusions: oxalate and fungi 84
5.2.7 Results: oxalate and soil 86
5.2.8 Discussion: oxalate and soil 89
5.2.9 Partial conclusions: oxalate and soil 90
5.3 General conclusions 91

Chapter 6 CARBONATE QUANTIFICATION
The soil, a reservoir of inorganic carbon

6.1 Introduction 93
6.2 Results 94
6.3 Qualification of the carbonate state in soil profiles related to *M. excelsa* and *A. africana* trees 97
6.4 Quantification of carbonate in the rhizosphere of *M. excelsa* trees and the *A. africana* stump from Burkina Faso 103
6.5 Carbonate leaching rate and carbon residence time in tropical soils under a *M. excelsa* tree 104
6.6 Comparison of carbonate content in the soils of *M. excelsa* trees from Burkina Faso, Ivory Coast, and Cameroon 104
6.7 A particular case: the Salina ecosystem 109
6.8 Summary 110

Chapter 7 CONCLUSIONS
The carbon balance

7.1	Carbon in its organic form	111
7.2	Carbon in oxalate form	111
7.3	Carbon in carbonate form	112
7.4	Distribution of carbon forms in Burkina Faso and Ivory Coast ecosystems	112
7.5	The Burkina Faso reservoir capacity	114
7.6	A carbon flux estimation	118

Chapter 8 OUTLOOKS 119

REFERENCES 121

ANNEXES 137

Figure list

CHAPTER 1

Fig. 1.1- Simplified global carbon cycle (modified after Asst. Prof. C. Dupraz). Fluxes are in GtC/years (Gigatons of carbon/years). Numbers between brackets refer to stored carbon pools. **4**

Fig. 1.2- Land carbon cycle that takes into account soil carbon in carbonate form. Unities are in Pg of carbon. Modified after Prentice et al. (2001) and Cailleau (2005), "Inert" carbon: charcoal and decaying resistant organic matter; τ: pool turnover. **5**

Fig. 1.3- Equilibrium fields of carbonate species in function of pH and three different temperatures (dashed line: 0°C, dotted line: 10°C, and solid line: 25°C). Modified after Verrecchia (2004). **8**

Fig. 1.4- The CO_2-oxalate-carbonate pathway. Oxalic acid is produced by plants (A.1), fungi and bacteria (A.2). Metals (M), such as Ca or Mg, bind with oxalic acids in order to form oxalate salts. The release of plant oxalate is the consequence of litter biodegradation (B. 1 and 2). The root exudates actively release oxalic acid in the rhizospheric environment (B.3). The bacteria oxalate consumption (oxalotrophy; C.1), combustion (C.2), plant enzymatic absorption (C.3), and fungal enzymatic degradation (C.3) transform oxalate. During these steps, a part of the carbon returns to the atmosphere in the CO_2 form. Carbonate results from bacteria and fire attack. To form a long-term carbon storage a metal is necessary to fix the ionic carbon in the carbonate form. This metal may have different origins (D). **12**

Fig. 1.5- Upper part: oxalic acid, oxalate (modified from Gadd 1999), and calcium oxalate monohydrate molecules; Central part: crystal morphologies of calcium oxalate. A) Prisms of whewellite belonging to the monoclinic system: I, oblique; II, III, prismatic; IV, tablet. B) Whewellite crystals: I styloid; II, II, raphide. C) Weddellite belonging to the tetragonal system: I, II, III, bipyramid; IV, tablets; V, long prism with a pyramid at each end. D) Elongation of initial tetragonal crystals (in C) leading to needles with different termination: I, bevelled edge; II, tetragonal pyramid; III, complex (modified from Verrecchia et al. 1993). Below: On the left calcium oxalate druse under natural light observed in Salina *Opuntia sp.* and right druses aggregates present between fibers of an *Opuntia sp.* cactus (from Cailleau 2005). **14**

Fig. 1.6- Diagram of two main pathways for calcium oxalate production by fungi. Biosynthesis of calcium oxalate is often accompanied by other low-molecular-weight organic acids, such as citrate or acetate (Verrecchia et al. 2006). **16**

CHAPTER 3

Fig. 3.1- A pedological map of the Comoé province, Burkina Faso, showing the sites of the studied systems (Pottier 1969). **30-31**

Fig. 3.2- Burkina Faso maps of climatic regions, vegetation, relief and hydrography (Lerebours-Pigeonnière and Menager 2001), and geology (Béziat et al. 2008) with location of the studied systems. The red star

indicates the position of the *M. excelsa* tree, near the Mangodara site. The blue star stands for the *A. africana* tree, near the Njangoloko site. **32**

Fig. 3.3- A *Milicia excelsa* tree and leaves situated in the Mangodara village (South of Burkina Faso), near "Le Commissariat". **33**

Fig. 3.4- The *Afzelia africana* tree (A), leaves (B), and mineralized stump (C, D, and E) found near Njangoloko. Stars indicate carbonate accumulations on stump surface. **34**

Fig. 3.5- General features of the *Bombax costatum* tree (http://database.prota.org). A: the tree shape (http://www.mi-aime-a-ou.com); B: the flower (http://www.fleurdestropiques.net); C: the fruit containing white floss called kapok (http://database.prota.org); and D: the typical conical, stout, sharp-pointed spines on stems and branches (http://gardenmalaysia.blogspot.com). **35**

Fig. 3.6- The *M. excelsa* ecosystem. A: general view of the relict forest with the emplacement of the *M. excelsa* trees. B: sketch of the *M. excelsa* trees and the studied soils emplacement. C: HCl test reactions from core sampling prospection. **36**

Fig. 3.7- Above: Pictures of a soil profile section under a living *M. excelsa* tree, showing a root with a white carbonate accumulation zone (1) and below: granitoid outcrops present in the proximity of the *M. excelsa* trees location. **37**

Fig 3.8- P1, P2 and P3 soil profiles.
§**38**

Fig. 3.9- Profiles of the di ferent studied soils. OM: organic matter. See also Fig 6.8 and Annex 11. **39-40**

Fig. 3.10- A) Aeolian Island on South Italy; B) Pollara location in Salina Island; C) ombrothermic diagram from Messina (Sicily). D) emplacement of the two soil profiles located at the border of the Mediterranean Sea at the Pollara crater; E) geological sketch map of Salina Island modified from the original sketch of Barca and Ventura (1991). F) pyroclastic material from the Pollara crater, composing the soil parent material. **42**

Fig. 3.11- A) the chosen *Opuntia sp.* tree; B and C) two different degradation states of Salinas *Opuntia sp.* cladodes displaying carbonate reaction to HCl (10%) test. **43**

CHAPTER 4

Fig. 4.1- Main functional groups in organic molecules. **46**

Fig. 4.2- Example of carbohydrate molecules. A) glucose, B) fructose, C) sucrose, and D) basic unit and supramolecular structure of cellulose with β-(1-4)glycosidic bond. **47**

Fig. 4.3- Some nitrogenous compounds molecule structure: A) RNA, DNA, and associated nucleotides, B)

urea, C) uric acid, D) amino acid E) chitin showing the two N-Acetylglucosamine units F) murein, and G) primary structure of a protein. **48**

Fig 4.4- Example of a lipid molecule. **49**

Fig. 4.5- Chemical structures of three monolignols: A) H-monomer (p-coumaryl alcohol), B) G-monomer (coniferyl alcohol) and C) S-monomer (sinapyl alcohol). D) Structure of the major bonds in lignin (from Kögel-Knabner 2002). **50**

Fig. 4.6- Molecular structure (A and B**)** and general structure (C and D) of fulvic acid (A and C) and humic acid (B and D; from Buffle et al. 1977; Stevenson et al. 1982; Gobat et al. 2010). **51**

Fig. 4.7- HI vs. OI diagram for "fresh organic material" completed with soil layer results showing high HI values for fresh material. See Fig. 4.10 for soils data. **54**

Fig. 4.8- S2 FID (left blue line), S3 CO (left red line), S3 CO2 (left green line), S4 CO (right red line), and S4 CO2 (right blue line) spectra for Ca-oxalate and "fresh organic material". X-axis: oven temperature (°C); Y-axis: relative intensity of released compounds. See also Annex 7 and Annex 8. **55-58**

Fig. 4.9- Detail from a root from the *M. excelsa* stump colonized by fungal mycelia. **59**

Fig. 4.10- Oxygen and hydrogen indices of Burkina Faso samples plotted on a modified van Krevelen diagram. **60**

Fig. 4.11- HI vs. TOC diagram for Burkina Faso soils (A, B, C, D; F1, and P1 to P4) and Salina soils (E; PC1 and PC2). **61**

Fig. 4.12- Oxygen and hydrogen indices of Salina samples plotted on a modified van Krevelen diagram. **62**

Fig. 4.13- Temperature range (°C) for F Gaussian descriptors found in this study compared to those found by Sebag et al. (2006). OM: organic matter; BF: Burkina Faso. **63**

Fig. 4.14- Contribution of the Gaussian F peaks for the analyzed "fresh organic material" and associated average T°C. **64**

Fig. 4.15- Results from mathematical deconvolution of 64 soil samples (A to C layers) from Burkina Faso. Relationships between bio-molecules (F0 + F1 + F2) - immature geo-molecules (F3a + F3b) - stable/ stabilised geo-molecules (F4). **68**

Fig. 4.16- S4CO2 spectra for "fresh organic material" compared to Figure 5 from Lafargue et al. (1998) showing the dolomite and calcite oxidation peaks. 1) and 2) are the two characteristic peak reactions resulting from the dolomite oxidative decomposition. **69**

Fig. 4.17- X-ray diffraction spectra of *Milicia excelsa* and *Afzelia africana* leaves, wood, and branches

showing the presence of Ca-oxalate salts and a carbonate phase. Peak between 20 and 24°2θCuKα1 is cause by the presence of amorphous silica. **71**

Fig. 4.18- Total Rock-Eval6 diagrams (S2, S3, and S4) for profile P4 (at 4.5 m from a living *M. excelsa* tree). X-axis: oven temperature (°C); Y-axis: relative intensity of released compounds. **72**

CHAPTER 5

Fig. 5.1- Degradation states (from 0 to 4) of cladodes in the studied *Opuntia sp.* (Salina, Italy). **76**

Fig. 5.2- Scanning electron microscope (SEM) micrographs of *M. excelsa* wood and leaves; arrows show Ca-oxalate crystals; h: fungal hyphae. A: Ca-oxalate crystals on *M. excelsa* wood surface. B: details from picture A. C: *M. excelsa* wood colonized by fungi. Ca-oxalates are of vegetal and fungal origin. D: Ca-oxalate crystal associated to fungal hyphae (cf. Fig. 5.4-N). E: *M. excelsa* wood colonized by a thick fungal hyphae or actinobacteria. Ca-oxalate crystals are associated to hyphae and are observed near organic matter (OM). F: Detail from picture E (cf. Fig. 5.3). G: Ca-oxalate prisms clustered (druses) in fascicles arranged in the shape of a spiral observed on *M. excelsa* rotten leaves. H: detail from G. **80**

Fig. 5.3- Ca-oxalate crystals visible under natural light microscope and associated to fungi grow in laboratory conditions. A) Details from Ca-oxalate bipyramids ("envelope" shape) associated with *Aspergillus sp.* grown in Malt-Agar medium. B) Twinned Ca-oxalate crystal on Malt-Agar substrate from *Aspergillus sp.* (cf. Fig. 5.2- F and Fig. 5.4-N). C) Ca-oxalate crystals associated with *A. niger* hyphae grown in Malt-Agar medium (cf. Fig. 5.2- D). D and E) Complex structure of overlapping Ca-oxalate crystals observed with *A. niger* in Malt-Agar medium added with gypsum. **84**

Fig. 5.4- From A to L: scanning electron microscope (SEM) micrographs of Ca-oxalate crystals found associated with fungi grown in Malt-Agar and gypsum (50 g/l) medium; arrow indicate Ca-oxalate crystals; OM: organic matter; h: fungal hyphae; s: fungal spore. A, B, C, and D: *Aspergillus type ochraceus*; E, F, G, H, I, and L: *A. niger*. A and B: Ca-oxalate dipyramids (cf. N and Fig. 5.3- A, B, and C); C and D: Ca-oxalate tablets (cf. N and Fig. 5.3- I); E, F, I, and L: complex structures of Ca-oxalate tablets (twinned crystals); G: Ca-oxalate crystals develop around a fungal hyphae; H: detail from G. M: EDS chemical element spectrum of a Ca-oxalate crystal. N: Fig. 38 from Khan (1995). **85-86**

Fig. 5.5- Oxalate profiles measured in soils. F3, P3, P4 and L2 are Burkina Faso soils, PC1 and PC2 are Salina (Italy) soils. **87**

Fig. 5.6- Ca-oxalate crystals (Ox) observed in soil thin sections (crossed-polarized light); Qtz: quartz; Cc: carbonate; Pl: plagioclase; v: void; w: wood. A, B, C and D) soil related to *M. excelsa* tree. A and B) P4 5 cm, first soil horizon. C) P4 12 cm, second soil horizon. Ca-oxalate crystals are visible in wood tissues. D) P4 50 cm, fifth soil horizon. Ca-oxalate crystals are visible in root tissues. E) soil related to *A. africana* tree; L2 4 cm, first horizon. **88**

Fig. 5.7- Box plots of oxalate content in studied soils (Burkina Faso and Italy) compared to similar systems studied in Cameroon and Spain (Cailleau 2005). *n*: number of samples. **89**

CHAPTER 6

Fig. 6.1- Box plots of pH_{H2O} found in the studied soils. *n* is the number of soil pH measurements. **94**

Fig. 6.2- Carbonate content and pH values in function of depth in the different studied soil profiles. **95**

Fig. 6.3- Percentage of magnesian calcite in the profile under the *A. africana* tree (black circle) with the respective XR diffraction spectra (L2 0-8), at 4 cm deep showing a pure calcite component (A). White square indicate the magnesium percentage found for the profile under the living *M. excelsa* tree (P4) and black square the values calculated for the soil under the *M. excelsa* stump. B and C are XR spectra from P4 profile at 0 cm and 20 cm deep respectively. CC: Calcium carbonate; LMC: Low magnesian calcite; HMC: high magnesium calcite. **96**

Fig. 6.4- SEM view of a pore in *A. africana* wood. The border cells are partially mineralised (star symbol). EDS signal indicates a magnesian carbonate content ("Mg", "Ca", "C", and "O" peaks). "Au" peak is due to gold coating, whereas the "Si" and "Al" (silicon and aluminium) peaks are probably clay mineral contamination. **97**

Fig. 6.5- *M. excelsa* calcified wood by sparite. A, B, and G: crossed-polarised light. C-F: fluorescence light. A) Wood under the *M. excelsa* stump at 3 cm of depth (arrows). B) Wood under the living *M. excelsa* tree at 5 cm of depth (arrow). Mineralized roots found in the soil at 11 cm under *A. africana* (C and D) and at 3 cm under *M. excelsa* (E, F, and G) stumps. Roots show at least three mineralization types: 1) sparite mineralisation of central root cells (nr. 1), 2) sparite mineralisation in external cells (nr. 2), or 3) coating on root surface (arrows in C). Qtz: quartz. **98**

Fig. 6.6- A) Carbonate features found in soils surrounding *A. africana* (A) and *M. excelsa* trees (from B to F). A) sparite crystals present at 11 cm under *A. africana* (arrow); OM: organic matter; Qtz: quartz crystal. B) sparite crystals found at 3 cm under *M. excelsa* stump. C) sparite assemblage at 3 cm under the *M. excelsa* stump. A flowe -shaped structure with a dark centre is visible in the dashed lined circle. D) Micritic ped (arrow) at 7 cm under the *M. excelsa* stump. E) Ped composed of carbonate and organic matter including a quartz crystal present at 5 cm under the living *M. excelsa* tree (PL). F) Ped composed of carbonate, organic matter, and quartz found at 12 cm under the living *M. excelsa* tree. A: natural light; B: fluorescence light; C-F: crossed-polarized light. **99**

Fig. 6.7- Carbonate features (crossed-polarised light) found in soils surrounding *M. excelsa* trees. A) Carbonate and oxalate accumulation around a wood remain found at 5 cm under the living *M. excelsa* tree. B) Ped composed of quartz, carbonate, oxalate, and organic matter present at 5 cm under the living *M. excelsa* tree. C and D) Carbonate and oxalate crystals including silicate and organic matter at 5 cm under the living *M. excelsa* tree. E and F) carbonate coatings (arrows) at 40 cm and 50 cm under the living *M. excelsa* tree. **100**

Fig. 6.8- Grain size ternary diagram of Burkina Faso soils compared to soils surrounding *M. excelsa* from Cameroon and Ivory Coast (Cailleau, 2005). **101**

Fig. 6.9- Thin section detail (natural light), showing burned wood tissues present in the soil surrounding *A. africana* stump probably resulting from the bush-fire practice. **102**

Fig. 6.10- West African average annual rainfall isohyetes in mm/yr (Breman and de Ridder 1991). Stars indicate sites of studied *M. excelsa* trees. Burkina Faso: this study; Cameroon and Ivory Coast: Cailleau (2005) and Braissant (2005). **106**

Fig. 6.11- A and B) Thin section details (crossed-polarized light) of soil under a living *M. excelsa* tree showing quartz (A) and plagioclase (B) with corrosion gulfs (arrows). Plagioclase remains attest the calcium origin from silicate minerals. C and D) Silicified wood remains in soil under *A. africana* stump (C) and *M. excelsa* stump (D). **107**

Fig. 6.12- Calcium and magnesium balance from literature (*) and this study. **108**

Fig. 6.13- X-ray spectrum of Salina dust showing a magnesium component of 5%. **109**

CHAPTER 7

Fig. 7.1- Distribution of total organic carbon (TOC) Burkina Faso (A) and residual carbon (RC) Ivory Coast (B; Cailleau 2005), carbon in oxalate form and carbon in carbonate form in the soil related to a *M. excelsa* tree. Values are standardized. The Burkina Faso *M. excelsa* tree is a living tree, having an estimated age of about 70 years, whereas the Ivory Coast *M. excelsa* tree is the stump of a 170 year-old tree. **113**

Fig. 7.2- Amounts of carbon forms present in the 3 soil layers under a living *M. excelsa* tree from Burkina Faso. **114**

Fig. 7.3- Carbon stock and residence times in the studied *M. excelsa* tree ecosystem. **116**

Fig. 7.4- Seasonal evolution of the litter in a dense *Celtis* semi-evergreen forest at Ivory Coast. A: leaves fall (cumulative distribution function). B: Evolution of the litter weight on soil. C: Monthly values calculated for the absolute rate of decomposition (adapted from Devineau 1982). **117**

Fig. 7.5- Carbon fluxes in the studied *M. excelsa* tree ecosystem. Only calculated fluxes are shown (see Annex 15). TOC : Total organic carbon ; Ox : measured oxalic acid ; Carb: carbonate; TOT C: total carbon. This last is calculated as follow: carbon represent 26.68 % in oxalate and 12 % in carbonate. **118**

Table list

CHAPTER 1

Table 1.1- Estimated major reservoirs of carbon on Earth. **3**

CHAPTER 4

Table 4.1- Average proportion of the broad categories of organic substances in plant and soils (from Gobat et al. 2010). **46**

Table 4.2- Rock-Eval 6 parameters for "fresh organic material". See Annex 4 for soils. **53**

CHAPTER 5

Table 5.1- Oxalate content of some plant species found in literature completed with results from this study. Results are expressed in milligrams of total oxalate per 100 grams of oven-dried material. The plant species are listed in order of increasing oxalate content. n.s.: not specified; T.s.: this study.
References: 1. Hönow and Hesse, 2002; 2. Ogawa et al., 1994; 3. Ciba-Geigy, 1977; 4. Elmadfa et al., 1992/1993; 5. Chandler, 1937; 6. Haytowicz and Matthews, 1984; 7. Souci et al., 1986; 8. Noonan and Savage, 1999; 9. Schelstraete and Kennedy 1980; 10. Nakata and McConn, 2007; 11. Nakata and McConn, 2000; 12. Guil et al., 1996; 13. Guil-Guerrero et al., 1998; 14. Kasidas and Rose, 1980; 15. Suvachittantont et al., 1973; 16. Awadalia et al., 1985 ; 17. Kmiecik et al .2004; 18. Vickery, 1955; 19. Zarembski and Hodgkinson, 1962; 20. Massey et al., 1993; 21. Perez et al., 2001; 22. Savage et al., 2000; 23. Sotomayor et al., 2001; 24. Valyasevi, 1974 ; 25. Kamchan et al., 2006; 26. Siener et al., 2006. **77-78**

Table 5.2- Oxalogenic and non-oxalogenic strains isolated from Burkina Faso soils. P4, P3, P2, and P1 are soils related to *M. excelsa* oxalogenic tree. L2 is a soil situated under an *A. africana* stump, and F3 is the Burkina Faso reference soil. **82**

Table 5.3- Oxalate presence on some fungal strains cultivated on Malt-Agar (MA) added with gypsum. **83**

CHAPTER 6

Table 6.1- Main factors present in *M. excelsa, A. africana*, and *Opuntia sp.* ecosystems. A.m.s.l.: above mean sea level. References: 1. Cailleau (2005); 2. Braissant (2005); 3. This study. **105**

CHAPTER 7

Table 7.1- Estimates of soil organic carbon pools found in literature (Prentice 2001) compared to those calculated under a living *M. excelsa* tree from Burkina Faso. **115**

Chapter 1 INTRODUCTION

Presentation of the oxalate-carbonate pathway

1.1 Introduction

Vegetation, especially in forests, is known for accumulating various amounts of carbon, depending on species and geographic location. The possibility of using vegetation and soil as long term carbon reservoirs has been identified as a potential measure to mitigate the greenhouse gas effect of global warming (Lal 2004). The accumulation of carbon by the vegetation is defined generally as a mean of "Carbon Stock". This stock is present in all living materials, from leaves, to stems, barks, roots, and microbial biomass, but is also present in dead material such as litter and humic material (IPCC 2001; Prentice et al. 2001; Janzen 2004; Bell and Lawrence 2009).

There are currently various methods and models to estimate the carbon stock over vegetation types (Lindner and Karjalainen 2007) and soils (Lal 2004). In this study, we follow the carbon from leaves to soil in the so-called oxalate-carbonate pathway. In order to get a better understanding of the oxalate-carbonate pathway, we have taken into consideration three different systems. Two systems were chosen in Burkina Faso: *Milicia excelsa* trees in Mangodara and an *Afzelia africana* stump in Njangoloko. Another system was taken in Salina Aeolian Island (Italy), which is the *Opuntia ficus indica* cactus system in Pollara. This particular choice was based on sites presenting an oxalogenic plant and the absence of carbonate in the rock basement.

1.2 Problem statement

This study describes an effort to estimate pedogenic carbon stock in a tropical ecosystem composed of an oxalogenic tree and related soil. The whole carbon is separated in organic carbon, carbon present in oxalate, and carbon present in carbonate. This thesis deals with the carbon cycle or more precisely with a way called the oxalate-carbonate pathway (Braissant et al. 2002; Braissant et al. 2003; Braissant et al. 2004; Cailleau et al. 2004; Braissant 2005; Cailleau 2005; Cailleau et al. 2005; Verrecchia et al. 2006) as a powerful mechanism to catch atmospheric CO_2 and form a long-term carbon sink (Cailleau et al. 2004). But until now no residence time estimation has been given.

The literature proposes a carbon stock in soils that is constituted principally by organic carbon (Lal 2004). This carbon content is measured in the first soil meter without dynamic compartment separation. In terrestrial ecosystems the admitted new formed carbonates are the carbonate produced in arid environment (Rasmussen 2006) by the silicate alteration process (Kraimer et al. 2005). The oxalate-carbonate pathway remains at this moment an under estimated atmospheric carbon pump.

1.3 Research questions

This thesis was considered and implemented in a way to answer the following questions:

- Is the *Milicia excelsa* tropical tree, and related soil, the only system able to accumulate pedogenic carbonate?
- Which it is the best soil compartimentation in relation to the carbon dynamics generated by oxalotrophy?
- Are fungi an important source of oxalate?
- Which is the residence time of carbon, resulting from the oxalate-carbonate pathway, in a tropical soil?
- What is the carbon balance in this ecosystem?

1.4 Objectives

The aim of this thesis is to provide both new insights and pertinent results about the natural creation of a pedo-carbonate storage as the result of the oxalate-carbonate pathway. The studied model is composed of an oxalogenic tree and its related soil in tropical environment. The carbon forms are quantified and the factors influencing the carbonate accumulations are discussed. The final objective is to give a carbon dynamic model where stock and fluxes are quantifi
In a previous work, G. Cailleau and O. Braissant (under the supervision of Prof. E.P. Verrecchia, from the University of Neuchâtel, Switzerland) already highlighted the importance of a tropical system, composed of an oxalogenic tree, in the formation of a pedospheric carbon storage. Indeed, these authors found that this oxalogenic tree-soil system runs like a pump, driving carbon from the atmosphere to the hydrosphere through the pedosphere and, therefore, inscribes it in the global carbon cycle.

1.5 Hypotheses

The following hypotheses were formulated prior to this study:

- The oxalate-carbonate pathway is more widespread than expected.
- The pedogenic carbonate found in tropical soil constitutes a long-term carbon sink.

1.6 Organization of the manuscript

The studied oxalate-carbonate pathway is presented in three main chapters, each of them discussing the carbon chemical nature present in a tropical system, and composed by an oxalogenic plant and its related soil. After the general introduction in Chapter 1, in Chapter 2 are described the tools allowing the carbon quantification found in the studied ecosystems described in Chapter 3. Chapter 4 deals with the organic carbon present in leaves and soil. The chosen method for this study is the Rock-Eval pyrolysis, that allows the quantification of, but also the differentiation

between, different carbon thermal resistance forms and consequently between different carbon pools. Moreover with Rock-Eval pyrolysis the calcium oxalate presence in the sample is rapidly detected. Chapter 5 is dedicated to the quantification of oxalates, present both in leaves and soil, obtained using the conventional enzymatic protocol. The carbonate content in soil and wood is measured using a titration method. The obtained results are explained in Chapter 6. All these results, supported by those of G. Cailleau and O. Braissant, allow us to calculate the residence time of carbon in its carbonate form in the soil under *M. excelsa* trees. Finally, a carbon balance is presented and discussed in Chapter 7.

1.7 Background

Here are summarized the principal acquaintances on which this work is based.

1.7.1 The global carbon cycle

Between the major terrestrial cycles thus of carbon is one of the most important because it constitutes with the oxygen and the hydrogen the basic unit for the life $\langle CH_2O \rangle$. Carbon can have nine oxidation states (4, 3, 2, 1, 0, -1, -2, -3, -4). It can be found in all oxidation states between +4, in CO_2, and -4 in CH_4. Passing from an oxidation state to another leads to carbon fluxes and cycles with sources and reservoirs depending on the time lag of C molecules. Principal Earth carbon sinks are present in Table 1.1 (Trumbore 1997; Eswaran et al. 2000; Amundson 2001; IPCC 2001; Prentice et al. 2001; Janzen 2004; Lal 2004; Rasmussen 2006; Dart et al. 2007; Brovkin et al. 2008). The biogeochemical terrestrial carbon cycle, which plays an undeniable role in global climate change, is defined by both the size of carbon reservoirs (such as the atmosphere, biomass,

Reservoirs	Amount in billions of metric tons (Pg of C)
Marine sediments and sedimentary rocks	66'000'000 to 100'000'000
Ocean	38'000 to 39'000
Fossil fuel reserves and combustible	27'000
Soil organic matter to 1m depth	1500 to 2000
Soil inorganic carbon	930 to 1738
Soil carbonate	940
Atmosphere	750 to 785 as CO_2
Terrestrial plants	470 to 660
Biota	400 to 600
Ocean biomass	3

Table 1.1- Estimated major reservoirs of carbon on Earth.

soil and bedrock) and the exchange between them of various mineral and organic carbon forms (Copard et al. 2007). In the global carbon cycle, the major pools are: the ocean, carbonate rocks, terrestrial ecosystems, and the atmosphere (Table 1.1 and Fig. 1.1). In the atmosphere CO_2 plays with the water vapour (H_2O), ozone (O_3), methane (CH_4) and nitrous oxide (N_2O) a major role in the total energy budget. These gases, by their structural configuration, absorb and re-emit part of the infra-red radiation emitted by terrestrial surface. This causes the greenhouse effect that allows the maintaining of the troposphere temperature approximately at 15°C. The C fluxes among the various pools, and their feedbacks, have kept the global C cycle quite stable for millennia at least, until recent decades when human activity began exerting increasing stresses on the C cycle (Janzen, 2004). It is noticed that the preindustrial atmospheric carbon concentration was of 280 ppm whereas the present day concentration surpasses 370 ppm. The main anthropogenic influences are the land use change and the fossil carbon fuel combustion (Janzen, 2004)

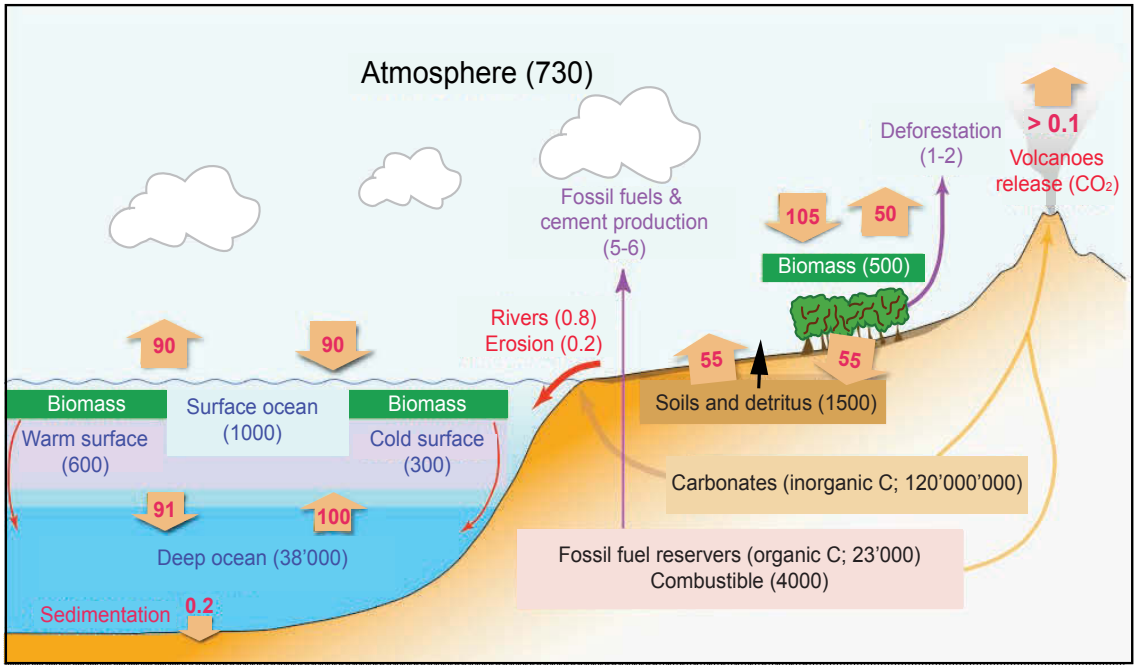


Fig. 1.1- Simplified global carbon cycle (modified after Asst. Prof. C. Dupraz). Fluxes are in GtC/years (Gigatons of carbon/years). Numbers between brackets refer to stored carbon pools.

1.7.2 The land carbon cycle

Through photosynthesis, carbon enters living phytomass, whereas respiration returns carbon into the atmosphere (Fig. 1.2). Inland organic carbon is present in living phytomass, necromass, and soil organic matter (Golubyatnikov and Svirezhev 2008). Carbon in living vegetation is estimated at 466 PgC (Lal 2004) to 610 PgC (Schimel 1995). Accumulation of carbon in soils varies with

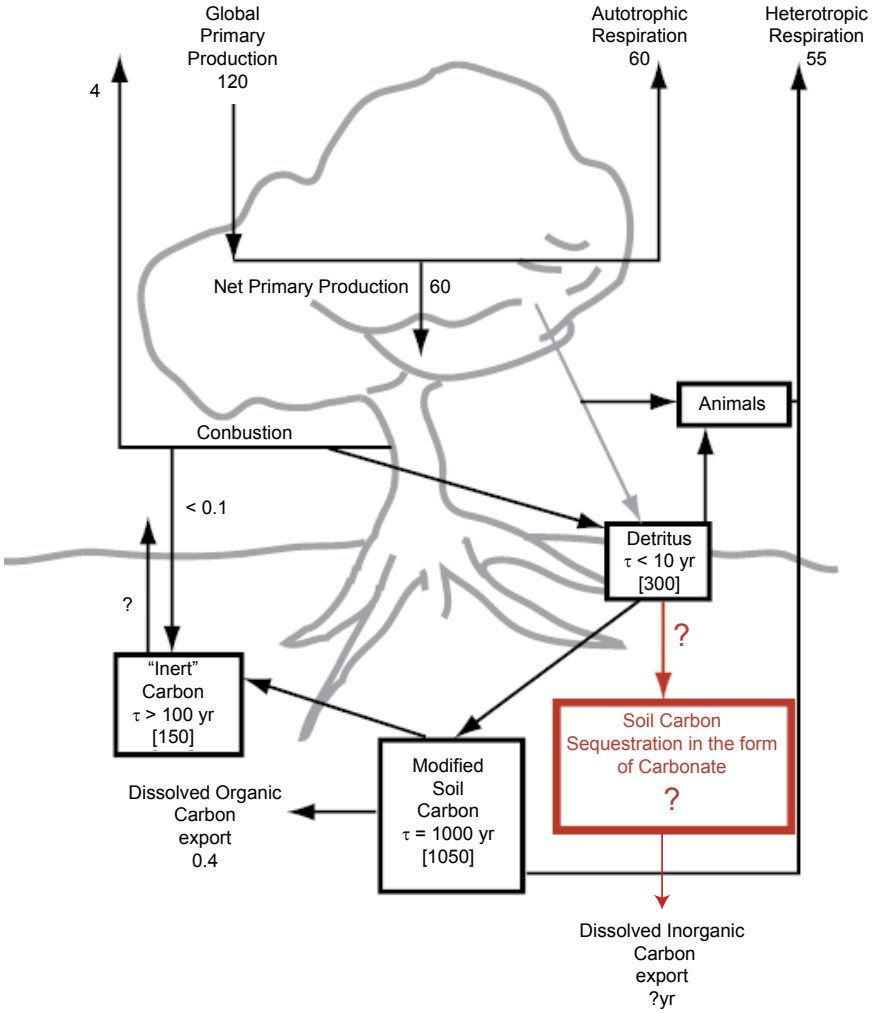


Fig. 1.2- Land carbon cycle that takes into account soil carbon in carbonate form. Unities are in Pg of carbon. Modified after Prentice et al. (2001) and Cailleau (2005), "Inert" carbon: charcoal and decaying resistant organic matter; τ: pool turnover.

soil depth and latitude (climate). At a depth of 1 m, it contains about 1500 - 2000 PgC in various organic forms, from recent plant litter to charcoal and very old humified compounds (Amundson 2001; Prentice et al. 2001). Soil layers deeper than 1 m contain several hundreds of PgC in the form of peat in Northern ecosystems and organic carbon in moist tropical forest soils (Trumbore 1997). Additionally, about 950 PgC are stored in inorganic (carbonate) form, predominantly in dry lands (Eswaran et al. 2000; Lal 2004).

To measure or infer carbon sinks, different indirect methods are used (Houghton 2002): 1) global budgets based on atmospheric data and models, 2) global budgets based on models of oceanic carbon uptake, 3) regional carbon budgets constructed from forest inventories, 4) stand-level direct measurement of CO_2 flux (from towers), 5) physiologically-based process models of ecosystems, and 6) carbon models based on changes in land use.

A missing carbon sink results from global carbon budget estimations (Schimel 1995; Prentice et al. 2001; Houghton 2002; Janzen 2004; Lal 2004) and is suspected to be present in terrestrial

ecosystems ("residual terrestrial sink"). It is evaluated at ± 3 PgC/y (Schimel 1995; Houghton 2002). In terms of fluxes, the residual terrestrial sink has been evaluated as 1.9 ± 1.3 PgC/y during the 80's and 2.3 ± 1.3 PgC/y during the 90's (Retallack 1990; Prentice et al. 2001). The time lag between photosynthetic uptake of CO_2 by plants and the subsequent return of C to the atmosphere through respiration define the transient sources or sinks in terrestrial carbon pools (Trumbore 1997). Studies show that the present terrestrial biosphere became a net carbon sink in the 90's, due to recent changes in land use and management, fertilizing effects of nitrogen, and increased levels of atmospheric CO_2 (Schimel 1995). This present sink will last until about 2050 and will turn into a source thereafter probably due to conversion of natural ecosystems into agro ecosystems (Seneviratne 2003).

Carbon of soil organic matter (SOM) has a turnover time going from a second (e.g. it is rapidly consumed when released as sugars or root exudates) to several hundred years (as stable or recalcitrant substances; Trumbore 1997; Prentice et al. 2001; Seneviratne 2003; Lal 2004). In contrast, soil inorganic carbon has potentially a residence time of 1'000'000 years (Retallack 1990; Prentice et al. 2001). Thus, the major challenge is to find ways to produce slow-turnover pools. A solution could be the promotion of carbonate formation in soils.

1.7.3 Carbonate precipitation processes

Carbonate precipitation can occur following either abiotic or biotic processes such as:

a) abiotic physico-chemical precipitation from supersaturated solutions, by evaporation, temperature increase and/or pressure decrease;
b) external or internal skeleton production by eukaryotes;
c) autotrophic processes influencing C $_2$ pressure;
d) bacterial heterotrophic processes influencing media alkalinity
e) fungal metabolism.

a) Abiotic physico-chemical precipitation

The calcium carbonate system is a heterogenic system composed of three phases (gas, solid, and liquid). The gaseous phase is constituted by carbon dioxide (CO_2) whereas the solid phase is represented by calcium carbonate ($CaCO_3$). In the solution, the chemical dissolved species are:

- protons (H^+) and hydroxyl (OH^-) ions coming from water dissociation;
- carbonic acid (H_2CO_3), bicarbonate (HCO_3^-), and carbonate (CO_3^{2-}) ions derived from hydration and dissociation of carbon dioxide into water;
- the calcium ion (Ca^{2+}).

In the liquid phase, these different chemical species are linked by the following instantaneous and reversible reactions (Sposito 1994):

$$H_2O \leftrightarrow H^+ + OH^- \quad (1)$$

$$H_2CO_3 \leftrightarrow H^+ + HCO_3^- \quad (2)$$

$$HCO_3^- \leftrightarrow H^+ + CO_3^{2-} \quad (3)$$

$$Ca^{2+} + HCO_3^- \leftrightarrow CaHCO_3^+ \quad (4)$$

$$Ca^{2+} + CO_3^{2-} \leftrightarrow CaCO_3 \quad (5)$$

Liquid and gaseous phases are linked by the dissolution/vaporization of carbon dioxide, followed by their hydration:

$$CO_2 + H_2O \leftrightarrow H_2CO_3 \quad (6)$$

And the solid phase by the calcium carbonate dissolution/precipitation:

$$CaCO_3 \leftrightarrow Ca^{2+} + CO_3^{2-} \quad (7)$$

The two last reactions have a time kinetic constant comprised between an hour and a day, and in the case of non equilibrium, they will drive the system (Callot 1999). Carbonate precipitation is a function of carbonate alkalinity and the availability of free calcium, which are combined in the saturation index defined as

SI = log IAP = Ksp

where IAP denotes the ion activity product (i.e. $[Ca^{2+}]\times[CO_3^{2-}]$), and Ksp the solubility product of the corresponding mineral. The Ksp for aragonite and calcite is respectively of $10^{-6.19}$ and $10^{-6.37}$, at 25 °C, 1 bar of atmospheric pressure and 35 PSU salinity (Dupraz et al. 2009). The carbonate equilibrium can be written as:

$$H_2CO_3 \leftrightarrow HCO_3^- \leftrightarrow CO_3^{2-} \quad (8)$$

which has pKa of 5.9 and 8.9, respectively, at 25 °C, at 1 bar atmospheric pressure and 35 PSU salinity, depending on the pH (Fig. 1.3). H_2CO_3 is formed from CO_2 dissolution in the water, which depends of the Henry's Law constant (K_H) for this gas, which is temperature dependant. At 25°C, $K_H = 3.38 \cdot 10^{-2}$ mol/L/atm (Andersen 2002).

b) External or internal skeleton production by eukaryotes

In eukaryotes, organo-minerals are the product of biologically-controlled mineralization, where cellular activity drives the nucleation, growth, morphology, and final location of a mineral, forming an external or internal skeleton (Lowenstam and Weiner 1989).

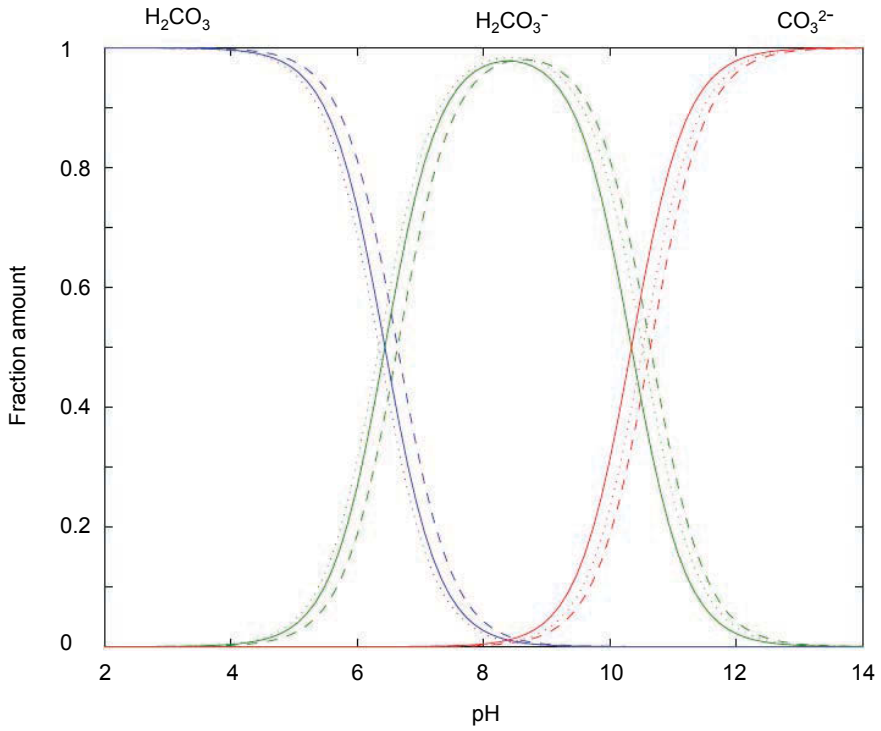


Fig. 1.3- Equilibrium fields of carbonate species in function of pH and three different temperatures (dashed line: 0°C, dotted line: 10°C, and solid line: 25°C). Modified after errecchia (2004).

c) Autotrophic processes influencing C_2 pressure

In Plant kingdom, carbonatation can result from photosynthetic activity. The reaction, characteristic for plants and algae, that linked the proton excretion/uptake with the oxygenic photosynthesis reaction is the following (Verrecchia 2002):

$$Ca^{2+} + 2\,HCO_3^- \rightarrow CaCO_3 + \langle CH_2O \rangle + O_2 \quad (9)$$

Where $\langle CH_2O \rangle$ symbolises the biomass. In prokaryotic autotrophic metabolism, three metabolic pathways are involved (Castanier et al. 1999):

1) autotrophic methanogenesis

$$3\,HCO_3^- + 4\,H_2 + Ca^{2+} \rightarrow CaCO_3 + CH_4 + 3\,H_2O \quad (10)$$

2) anoxygenic photosynthesis, under strict anaerobiosis environmental conditions, carried out by purple and green sulphur or non-sulphur bacteria:

$$3\,HCO_3^- + Ca^{2+} + HS^- \rightarrow 2\,\langle CH_2O \rangle + SO_4^{2-} + CaCO_3 \quad (11)$$

3) Oxygenic photosynthesis (Castanier et al. 2000), under aerobic condition, performed by cyanobacteria:

$$2\ HCO_3^- + Ca^{2+} \rightarrow CaCO_3 + \langle CH_2O \rangle + O_2 \quad (12)$$

d) Prokaryotic heterotrophic process influencing media alkalinit

In this heterotrophic pathway, two metabolic cycles are involved, the nitrogen and the sulphur cycle (Castanier et al. 1999). The following processes allow carbonate precipitation:

1) ammonification of amino acids in aerobiosis, performed by aerobic and anaerobic bacteria

$$2\ NH_4OH + Ca(HCO_3)_2 \rightarrow CaCO_3 + (NH_4)_2CO_3 + 2\ H_2O \quad (13)$$

and

$$(NH_4)_2CO_3 + CaSO_4 \rightarrow CaCO_3 + (NH_4)_2SO_4 \quad (14)$$

2) dissimilatory reduction of nitrates in anaerobiosis or microaerophily:

$$Ca(NO_3)_2 + 3\ H_2 + C_{org} \rightarrow CaCO_3 + 3\ H_2O + N_2 \quad (15)$$

3) degradation of urea in the presence of calcium:

$$H_2N\text{-}CO\text{-}NH_2 + 2\ H_2O + Ca^{2+} \rightarrow CaCO_3 + 2\ NH_4^+ \quad (16)$$

4) dissimilatory reduction of sulfates (sulfato-reduction) in anaerobiosis:

$$CaSO_4 + 2\ \langle CH_2O \rangle \rightarrow CaCO_3 + H_2S + CO_2 + H_2O \quad (17)$$

$$CaSO_4 + 2\ \langle CH_2O \rangle + Fe \rightarrow CaCO_3 + FeS + CO_2 + H_2O \quad (18)$$

$$SO_4^{2-} + 2\ \langle CH_2O \rangle + OH^- + Ca^{2+} \rightarrow CaCO_3 + CO_2 + 2\ H_2O + HS^- \quad (19)$$

5) methanogenesis, in anaerobic conditions, performed by Archaea

$$2\ HCO_3^- + 4\ H_2 + Ca^{2+} \rightarrow CaCO_3 + CH_4 + 3\ H_2O \quad (20)$$

6) oxalotrophy, performed by oxalotrophic aerobic and anaerobic bacteria (Verrecchia et al. 2006)

$$1000\ CaC_2O_4 \cdot nH_2O + 372\ O_2 + 32\ NH_4^+ \rightarrow 32\ C_4H_8O_2N^+_{biomass} + 936\ CaCO_3 + 64\ Ca(OH)_{2aq} + \ldots$$
$$\ldots + (1000 \cdot (n - 2) + 1872)\ H_2O + 936\ CO_2 \quad (21)$$

e) Fungal metabolism

Carbonate is also observed to precipitate near fungal hyphae as Needle Fiber Calcite (Callot et al. 1985) resulting from the development of fungal hyphae at a soil depth where the $CaCO_3$ concentration in soil solution is high. Moreover, it was observed that CO_2 produced during growth and characteristic proteins released from *Verticillium sp.* and *Thermomonospora sp.*, may be react with aqueous Ca^{2+} to produce biogenic $CaCO_3$ crystals (Rautaray et al. 2004).

1.7.4 Pedogenic carbonate

Carbonate in soil can be of different origins: (1) inherited from an *in situ* or an exogenous (detritical) carbonate rock, (2) generated from the dissolution and recrystallization of an existing carbonate material (in Kraimer et al. 2005), (3) derived from the dissolution of silicate Ca-bearing minerals (in Kraimer et al. 2005), (4) resulting from biological induced mineralisation (active mineralisation allowing the formation of microbialites), (5) influenced mineralisation (passive mineralisation allowing the formation of other types of microbialites), or (6) controlled mineralisation (e.g. external or internal skeleton; Dupraz et al. 2009). Soil carbonate is the major form of soil inorganic carbon (SIC). SIC forms an estimated reservoir ranging from 930 PgC to 1738 PgC (Rasmussen 2006), surpassing the atmospheric (Lal 2004). The ability of pedogenic carbonate to sequester atmospheric C depends on the source of calcium (Ca) present during carbonate pedogenesis (Kraimer et al. 2005). A net carbon sink is a system where the carbonate accumulation involves only atmospheric CO_2 and Ca from Ca-carbonate-free sources (Cailleau et al. 2004). C sink for a reservoir mean that the amount of C in the reservoir increases. Time lag of C molecules in a reservoir is important to establish if a reservoir behaves as a sink or a source of carbon. Regarding the rapid increase of CO_2 into the atmosphere and the potential problems due to the greenhouse effect caused by this gas, the challenge is now to slow down the CO_2 increase in the air. There are two different ways: reduction of emissions and looking for stocks. The *M. excelsa* system is a natural pump for atmospheric CO_2 allowing the formation of the oxalate-carbonate pathway with the result of a long term carbon stock in soil in the form of carbonate (Cailleau et al. 2004; Cailleau 2005; Cailleau et al. 2005; Verrecchia et al. 2006).

1.7.5 The primary calcium (and magnesium) source: a limiting factor for calcite formation

Silicate weathering provides the necessary Ca and/or Mg to fix the atmospheric CO_2 and form a long-term carbon sink. The weathering rate of a mineral in a given environment can be considered as a function of intensity (temperature, moisture, pH and Eh) and capacity (specific surface area and nature of the mineral) factors (McKeague and Cline 1963). Silicate weathering counterbalances the volcanoes and the metamorphic CO_2 emissions and thus regulates the level of atmospheric CO_2 during geological times (Urey 1952), following these equations:

$$CaSiO_3 + CO_2 \rightarrow CaCO_3 + SiO_2 \quad (22)$$

$$MgSiO_3 + CO_2 \rightarrow MgCO_3 + SiO_2 \quad (23)$$

Physical, chemical, and biochemical processes can modify silicate structure. Fragmentation and fracturing (physical agents) driven by climate (wind and frost) and biology (fungal hyphae, tree roots, burrowing organisms, and biomineralizing organisms) increase the crystal surface exposition facilitating chemical attack. Chemical attack is caused by water through hydration, hydrolysis, and dissolution processes. Silicate hydrolysis, the main dominant process observed in tropical environments, follows the equation below:

$$CaAl_2Si_2O_8\ (anorthite) + 3\ H_2O + 2\ CO_2 \rightarrow Al_2Si_2O_5(OH)_4\ (kaolinite) + Ca^{2+} + 2\ HCO_3^- \quad (24)$$

Depending on the CO_2 amount (pCO_2) dissolved in the water, the process that prevails is the acidolysis or the hydrolysis. Subsequently, the formed carbonic acid can: 1) enter in the water-table, 2) follows the $HCO_3^- \leftrightarrow H^+ + CO_3^{2-}$ equilibrium (see above), and/or 3) be transformed by the carbonic anhydrase and follows this reaction:

$$H_2O + CO_2 \leftrightarrow H_2CO_3 \leftrightarrow HCO_3^- + H^+ \quad (25)$$

in order to maintain the acid-alkaline balance. In the presence of water, organisms influence silicate weathering by their metabolism, with the production of acids, ligands, CO_2, biofilms, etc., or by active ion uptake, equilibrium displacing, changes in redox conditions, etc. Some of the chemical reactions and processes that control the CO_2 concentration of natural surface waters include weathering of minerals, photosynthesis and respiration, anaerobic bacteria consumption of organic matter (e.g., sulphate reduction, respiration), and carbon dioxide dissolution and ex-solution (Andersen 2002). Alkaline conditions (pH > 9) lead to silicate dissolution enhancement, whereas a very acidic environment (pH < 3) can alter silicate structure (Millot et al. 1977). Alkaline environments are the result of alkaline media induced by bacterial oxalotrophy (Braissant 2005; Verrecchia et al. 2006), or alkaline water-solution containing dissolved carbonate after they passed through the carbonate phase (Millot et al. 1977).

1.7.6 The carbon dioxide-oxalate-carbonate pathway

The CO_2-oxalate-carbonate pathway implies the processes that transform carbon-bearing molecules, present in the air in the form of CO_2, to oxalate salts (XC_2O_4; X = Ca or Mg) and finally to soil carbonate ($CaCO_3$; Fig. 1.4). Two oxalate producers are well documented: plants and fungi. In addition, bacterial oxalate (Hodgkinson 1977) could be used as a third source. Plant oxalate is released in the soil environment both by root exudation and by plant material decay. Fungi are involved in the oxalate-carbonate pathway with at least two different processes: the so-called indirect way is the enzymatic and acid organic matter degradation, whereas the direct way is the oxalate production (Verrecchia et al. 2006). Moreover, as cited in Hodgkinson (1977),

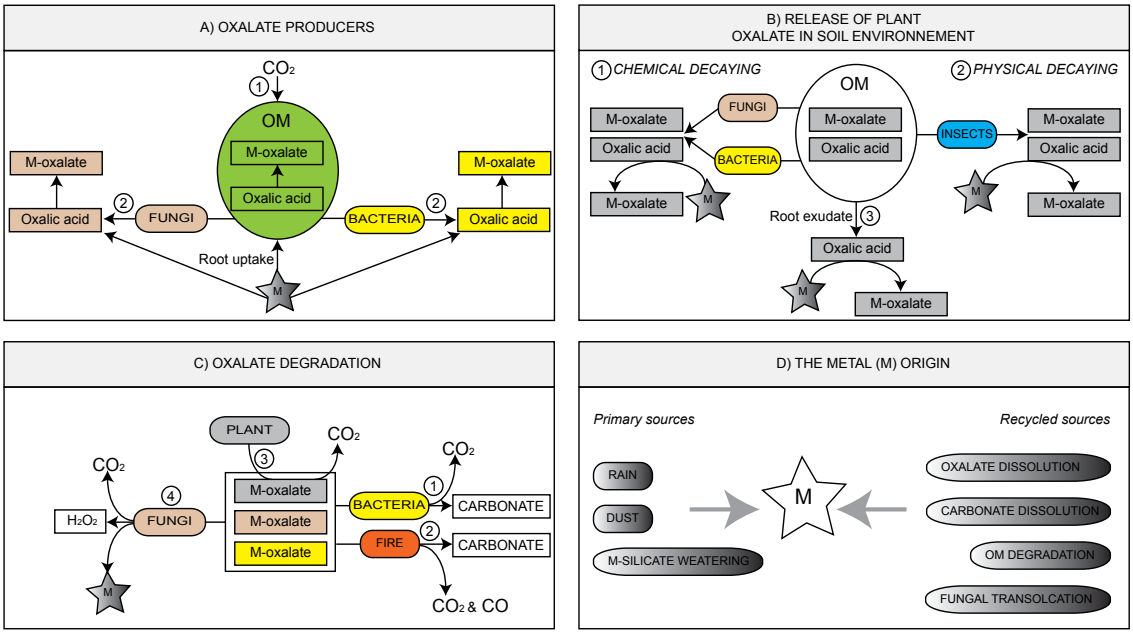


Fig. 1.4- The CO_2-oxalate-carbonate pathway. Oxalic acid is produced by plants (A.1), fungi and bacteria (A.2). Metals (M), such as Ca or Mg, bind with oxalic acids in order to form oxalate salts. The release of plant oxalate is the consequence of litter biodegradation (B. 1 and 2). The root exudates actively release oxalic acid in the rhizospheric environment (B.3). The bacteria oxalate consumption (oxalotrophy; C.1), combustion (C.2), plant enzymatic absorption (C.3), and fungal enzymatic degradation (C.3) transform oxalate. During these steps, a part of the carbon returns to the atmosphere in the CO_2 form. Carbonate results from bacteria and fi e attack. To form a long-term carbon storage a metal is necessary to fix the ionic carbon in the carbonate form. This metal may have different origins (D).

the fungal enzymatic degradation of oxalate (such as oxalate oxidase, Pr. Aragno pers. comm.), under particular pH conditions, could be considered as an additional way. Because Ca-oxalate is energetically stable, only the activation energy given by bacterial consumption transforms oxalate into carbonic acid. This transformation increases the pH values of the soil solution. If the pH reaches carbonate stability conditions (*i.e.* pH = 8.4; Fig. 1.3) and divalent cations (Ca^{2+} or Mg^{2+}) available in the soil solution, complexation with carbonic acid results in carbonate precipitation.

1.7.7 Oxalic acid and oxalate salts

Oxalic acid is probably one of the most widespread organic acids. In fact, excessive oxalate absorption via vegetable ingestion occurs in some type of intestinal disease causing hyperoxaluria and renal stone (Hodgkinson 1977). Oxalic acid (ethanedioic acid) is the simplest of the dicarboxylic acids and the most highly oxidized organic compound, with the formula: $C_2H_2O_4$ (Gadd 1999). It is found extensively in nature, rocks, soils, microorganisms, fungi, plants, and animals. It occurs as a free acid, or as water-soluble salts with Na^+, K^+, and NH_4^+ ions, or as insoluble salts with Ca^{2+}, Fe^{2+}, and Mg^{2+} (Hodgkinson 1977; Savage et al. 2000; Nakata 2003). Among these insoluble salts, the most soluble is magnesium oxalate (Mg-oxalate) and the least soluble is calcium oxalate (Ca-oxalate; Ksp = 1.78 x 10^{-9} at 18°C; Ksp = 2.57 x 10^{-9} at 25°C; Gadd, 1999). The principal

forms of Ca-oxalate occurring in nature are monohydrate Ca-oxalate (whewellite, $CaC_2O_4 \cdot H_2O$) and dihydrate Ca-oxalate (weddellite, $CaC_2O_4 \cdot 2\ H_2O$). The monohydrate Ca-oxalate (the more stable) is monoclinic, whereas the dihydrate is tetragonal. Both crystallize in a variety of forms (Fig. 1.5) prisms, druses, styloids, raphides, and crystal sand (Hodgkinson 1977; Franceschi and Horner 1980; Verrecchia et al. 1993). Ca-oxalate dihydrate could be authigenic in bottom muds and in peat sediments, in calcareous lake-bottom sediments, and may be formed by reaction of calcite with oxalic acid produced by lichens or from solutions derived from bat guano (Palache et al. 1951). Oxalic acid and oxalate salts are widely distributed in the Plant kingdom and are a common metabolic product of fungi, algae, and lichens (Gadd 1999). Moreover oxalate has been detected in cultures of *Mycobacterium*, *Acetobacter* and *Gluconobacter*, and in cell-free extracts of *Lactobacillus* (Hodgkinson 1977). Only simple oxalates can occur in biological systems because the excess of oxalate ions required for complex stability would be toxic (Gadd 1999).

1.7.8 Plants and oxalates

Oxalate in plants can be found as oxalic acid, a soluble and/or an insoluble oxalate salt (Hodgkinson 1977). In plants, oxalic acid can be present in cytoplasmic vacuoles and in sap. In addition to accumulate oxalate, plant roots are able to excrete oxalate in response to environmental stress, and use its chelating properties to facilitate nutrient mobilization and rhizosphere detoxification (Nguyen 2003; Tu et al. 2007). Ca-oxalate is the most common insoluble salt. Nevertheless, relatively large amounts of Mg-oxalate (glushinskite) are found associated with Ca-oxalate in plants such as beetroot, spinach, and buckwheat (Hodgkinson 1977). Ca-oxalate can be found in all major groups of photosynthetic organisms including algae, lower vascular plants, gymnosperms, angiosperms, and have been found in members of more than 215 plant families as monohydrate and/or dihydrate (Arnott and Pautard 1970; Hodgkinson 1977; Franceschi and Horner 1980; Nakata 2003; Franceschi and Nakata 2005). Sometimes, the oxalate content is so important that it can represent up to 85% of the dry weight of the plant such as in *Cactus senilis* (Cheavin 1938).
Ca-oxalate occurs in specialized cells (idioblasts) in vegetative, reproductive, storage, and developing organs, as well as in photosynthetic and non photosynthetic tissues (Arnott and Pautard 1970; Hodgkinson 1977; Franceschi and Horner 1980; Nakata 2003; Franceschi and Nakata 2005). Plant crystals display a variety of morphologies (Fig. 1.5): 1) prisms, 2) druses, 3) styloids, 4) raphides, and 5) crystal sand (Franceschi and Horner 1980). The morphology of crystals produced may be a single type throughout the plant, multiple types, each one being specific for certain organ or multiple types that may exist within the same organ but in different tissue regions. The crystal morphology and distribution are constant within species. This constancy is used as a taxonomy character and indicates tight genetic regulation of crystal deposition (Franceschi and Horner 1980).
Two oxalate formation pathways have been examined extensively in higher plants (Franceschi and Loewus 1995): 1) conversion of the photorespiratory products, glycolate and glyoxylate, to oxalate and 2) ascorbic acid catabolism, which yields oxalate and threonic or tartaric acid. Additional possibilities include cleavage of isocitrate or oxaloacetate (Chang and Beevers 1968),

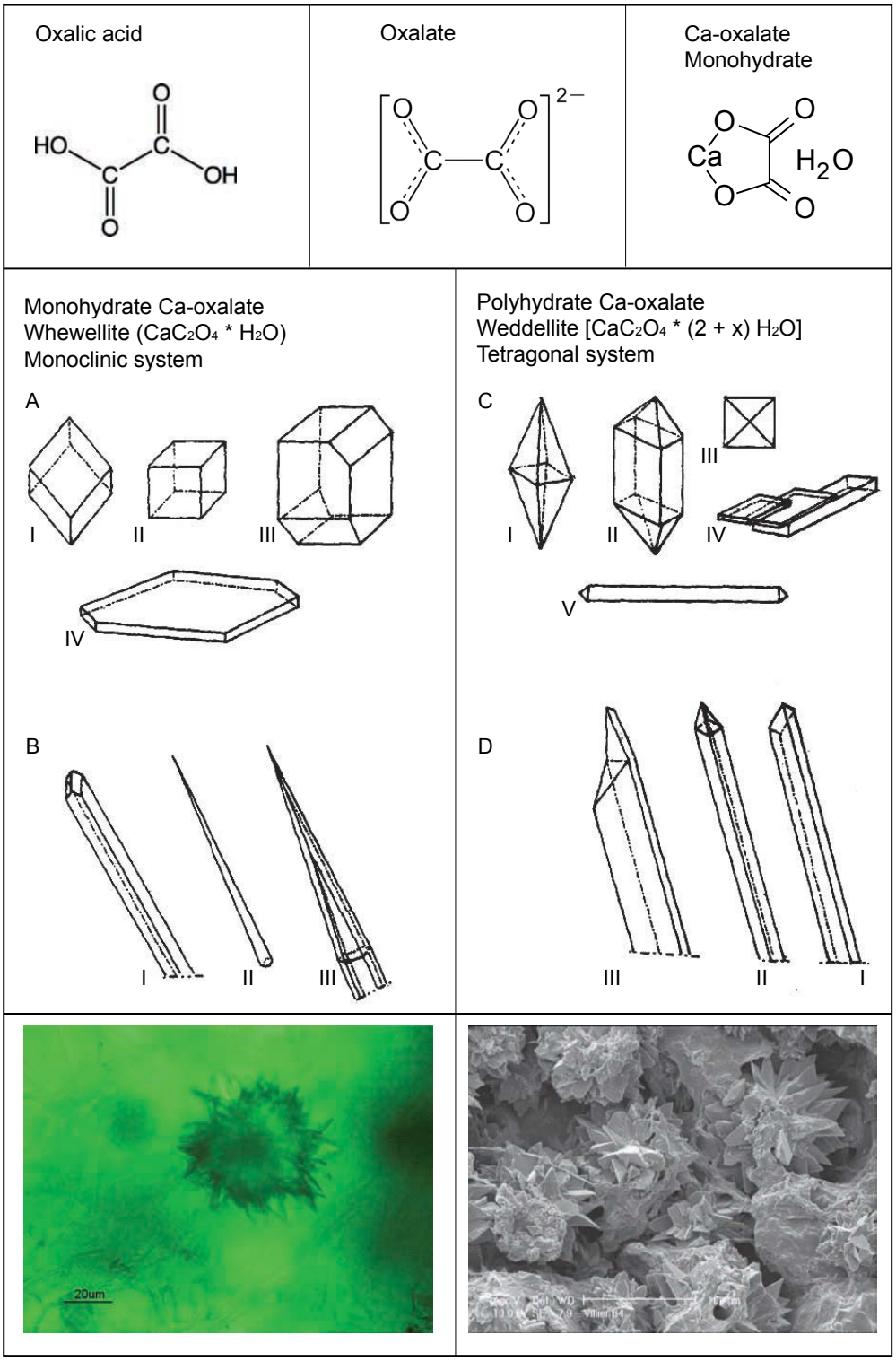


Fig. 1.5- Upper part: oxalic acid, oxalate (modified from Gadd 1999), and calcium oxalate monohydrate molecules; Central part: crystal morphologies of calcium oxalate. A) Prisms of whewellite belonging to the monoclinic system: I, oblique; II, III, prismatic; IV, tablet. B) Whewellite crystals: I styloid; II, II, raphide. C) Weddellite belonging to the tetragonal system: I, II, III, bipyramid; IV, tablets; V, long prism with a pyramid at each end. D) Elongation of initial tetragonal crystals (in C) leading to needles with different termination: I, bevelled edge; II, tetragonal pyramid; III, complex (modified from Verrecchia et al. 1993). Below: On the left calcium oxalate druse under natural light observed in Salina Opuntia sp. *and right druses aggregates present between fibers of an* Opuntia sp. *cactus (from Cailleau 2005).*

or other pathways that produce glycolate (Franceschi and Horner 1980).
The most important functions of oxalate present in plants include: 1) calcium regulation, 2) ion balance (Nakata 2003), 3) plant protection against grazing animals (Franceschi and Horner 1980; Franceschi 2001; Nakata 2003), 4) metal (Al, Pb, Sr, Cd, and Cu) or oxalic acid detoxification (Franceschi and Horner 1980; Nakata 2003), 5) storage form for either Ca or oxalate (Franceschi and Horner 1980), 6) tissue support (plant rigidity; Franceschi and Horner 1980; Nakata 2003), 7) light gathering and reflect on (Franceschi 2001; Nakata 2003), and 8) combustion retardation (Prior and Cutler 1992). Crystals may be reabsorbed and thus provide an internal reservoir for calcium (Webb 1999). Oxidases and decarboxylases are the two enzymatic degradation ways found in plants (Franceschi and Horner 1980). Calcium is essential for the development and growth of plants. It is of vital importance for cell wall formation and membrane stabilization, and within the protoplasm, it acts as a metabolic regulator for many processes. It is involved in the maintenance of low intracellular activity of Ca ions that can be achieved by restricting the entrance of ions or by actively pumping ions out of the cytoplasm into vacuoles and possibly into the apoplast (Arnott 1976).
Non-absorbed oxalate present in plant tissues is then transferred to the litter. Decay of organic matter by microorganisms, especially fungi, liberates oxalate crystals inside the soil or the litter, increasing the proportion outside the living tissues (Verrecchia et al. 2006). Until in soil environment oxalates are readily oxidized by oxalotrophic bacteria (Braissant et al. 2002).

1.7.9 Fungi and oxalates

Oxalic acid is produced in large amounts by species belonging to all classes of Fungi (Dutton and Evans 1996). Ca-oxalate crystals are commonly associated with free-living, pathogenic, and plant symbiotic fungi. This has a profound effect on biogeochemical processes in soils, acting as a reservoir for Ca, but also influencing phosphate and sulphate availability (Gharieb et al. 1998; Gadd 1999). Oxalic acid is a metabolic compound able to attack organic and mineral materials. This organic metabolite degrades not only simple organic compounds, such as cellulose, but also more complex molecules such as lignin (Gadd 1999). Moreover, oxalic acid excretion can lead to solubilisation of minerals and metal compounds, and act in fungi as a mechanism to tolerate toxic metal-containing environments (Gadd 1999). Oxalic acid excretion by fungi has different roles: 1) function in pathogenesis, 2) competition, 3) control of environmental nutrients and toxins, and 4) chemical barrier against grazing arthropods (Dutton and Evans 1996). Additionally, the secretion of oxalic acid by litter-dwelling and ectomycorrhizal fungi increased the rate of soil weathering and enhanced the availability of nutrients for uptake by associated vegetation (Dutton and Evans 1996). Recently it was demonstrated that fungi were able to dissolve and oxidize calcium oxalate (Guggiari et al. 2010) probably with extracellular enzymes (e.g. oxalate oxidase and oxalate decarboxilase) implicated in lignin degradation (ligninolytic strategy). Moreover the oxalate oxidase follows this reaction:

$$(COO)_2^{2-} + O_2 + 2\,H_2O \rightarrow CO_2 + 2\,OH^- + H_2O_2 \quad (26)$$

resulting in a pH increasing, due to hydroxide ion releasing, comparable to the bacterial oxalate catabolism (Pr. Aragno pers. comm.).

The factors affecting oxalate production by fungi are primarily the availability of carbon and nitrogen, their ratio, and the environmental pH (Dutton and Evans 1996). Carbon sources necessary to oxalic acid synthesis by fungi are glucose or citrate, with acetate and citrate as co-products (Fig. 1.6). When glucose is used, oxalate is produced through oxidation of glucose to pyruvate (Verrecchia et al. 2006). Then, carboxylation of pyruvate yields oxaloacetate and the hydrolysis of oxaloacetate allows the formation of oxalate and acetate (Verrecchia et al. 2006). When citrate is the source, oxalate is produced through the isocitrate and glyoxylate cycle involving glyoxylate hydrogenase (Dutton et al. 1993). Excreted oxalic acid reacts with Ca, present in the environment, forming Ca-oxalate crystals, either whewellite and weddellite (Gadd 1999; Verrecchia et al. 2006).

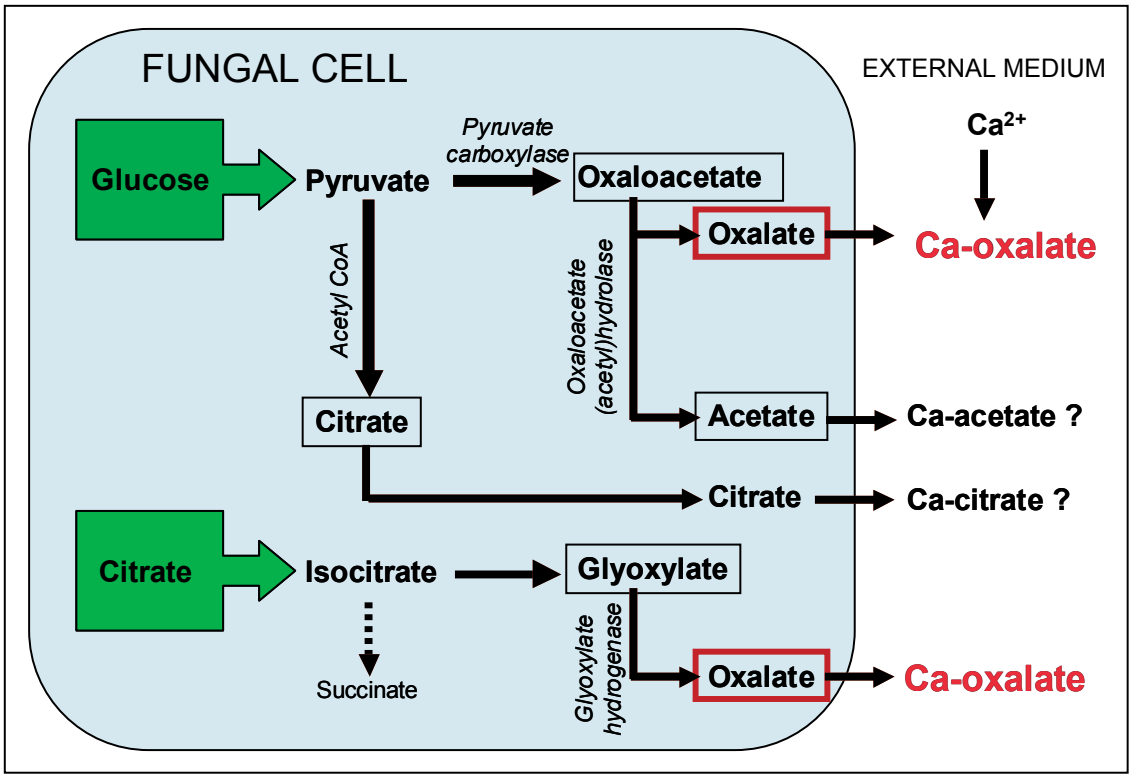


Fig. 1.6- Diagram of two main pathways for calcium oxalate production by fungi. Biosynthesis of calcium oxalate is often accompanied by other low-molecular-weight organic acids, such as citrate or acetate (Verrecchia et al. 2006).

1.7.10 Soils and oxalates

Among low molecular-weight organic acids, the oxalic acid is commonly present in soil, often even being the most abundant one (Fox and Comerford 1990). Oxalate concentrations in soils

can range from 10^{-6} to 10^{-3} M (Allison et al. 1995; Khan 1995). Despite these acids account for a small fraction of the total dissolved organic carbon, they play an important role in soil genesis, plant physiology, and microorganism metabolism. For example they affect: 1) mineral alteration (Graustein et al. 1977), 2) the availability of nutrients to vegetation (Graustein et al. 1977), 3) the transport of metals through the soil profile (Pohlmann and McColl 1988), 4) the complexation of elements with phytotoxic effect, such as Al (Hue et al. 1986), and 5) the exchange of regulatory signals between plants and soils (Albuzio and Ferrari 1989). Despite plants and microorganisms release these acids continuously in the soil and although they precipitate mainly as Ca-oxalate due to the low solubility of this salt (Ksp ≈ $10^{-8.5}$), Ca-oxalate is rare in the geological record (Graustein et al. 1977). Under normal pressure and temperature conditions any metal oxalate can be considered as a compound in a metastable equilibrium. The only sub-spontaneous diagenetic evolution of Ca-oxalate is a possible transformation of weddellite into whewellite by dehydration. Additionally, for a complete oxidation of Ca-oxalate monohydrate or dihydrate, an activation energy provided by living organisms is required (Verrecchia et al. 2006). Once formed, only a few bacteria and actinomycetes (*Streptomyces* and *Nocardia*) can use Ca-oxalate as single source of carbon and energy (Cromack et al. 1977; Messini and Favilli 1990; Sahin 2003). The result of this consumption is a carbonate precipitation (Braissant et al. 2002; Braissant et al. 2003; Braissant et al. 2004; Cailleau et al. 2004; Braissant 2005; Cailleau 2005; Cailleau et al. 2005; Verrecchia et al. 2006).

1.7.11 The oxalate degradation: the oxalotrophy

While it is known that oxalates are also produced by bacteria (Hodgkinson 1977; Bonaventura et al. 1999; Wakao et al. 2002), data present in the literature about oxalogenic soil bacteria are still insufficient. On the other hand, records about bacteria degrading oxalate are abundant. Despite its low solubility (Kps = $4x10^{-9}$ mol/L for Ca-oxalate) and its high chemical stability, the accumulation of metal oxalates has rarely been observed in the geological record. This suggests a microbiologically mediated process as the main oxalate sink in natural environments (Hodgkinson 1977; Braissant et al. 2002; Braissant et al. 2004). Oxalate is used as the sole carbon and energy source by a limited number of aerobic and anaerobic bacteria (Chandra and Shethna 1975; Hodgkinson 1977; Tamer and Aragno 1980; Braissant et al. 2002; Sahin 2003). These bacteria do not constitute a phylogenetic group, but rather a functional group, that consists of diverse taxa of microorganisms. The degradation of oxalic acid molecules (catabolism) will provide the energy necessary to assimilate the carbon present in other oxalic acid molecules (anabolism; Braissant 2005). Oxalate is assimilated through either the serine pathway or the glycolate pathway (Quayle et al. 1961; Quayle 1963; Blackmore and Quayle 1970; Tamer and Aragno 1980; Sahin 2003). Due to its high oxidation degree and its low molecular weight, its growth yield is fairly low, only about 2.5 g/mol (Braissant et al. 2002).

Oxalotrophic bacterial activity increases pH with at least two processes: 1) transformation of a strong organic acid, oxalic acid (pK1 = 1:25, pK2 = 4:27), to a less acidic weak acid (pK1 = 6:35, pK2 = 10:33), carbonic acid (Verrecchia et al. 2006) and 2) the production of a proton pump, due

to oxalate metabolism, that depletes the local environment in H^+ ions (bacterial uptake). At the same time, bacterial metabolism releases CO_2, HCO_3^-, and CO_3^{2-} allowing a pH increase that, in the presence of Ca (or Mg), promotes the carbonate precipitation. At ambient conditions (T° = 25°C; P = 1 atm), a pH value higher than 8.4 is necessary to reach the carbonate stability field (Verrecchia et al. 2006).
Ca-carbonate production, by bacteria from organic acids with a low molecular weight seems to be a common and quiet fast process (Braissant et al. 2002). However, only approximately 6.4% of the carbon of oxalate is transformed in biomass, whereas the remainder 93.6% is mineralized (Verrecchia et al. 2006).

$$1000\ CaC_2O_4 \cdot nH_2O + 372\ O_2 + 32\ NH_4^+ \rightarrow 32\ C_4H_8O_2N^+_{biomass} + 936\ CaCO_3 + 64\ Ca(OH)_{2aq} + \ldots$$

$$\ldots + (1000 \cdot (n - 2) + 1872)\ H_2O + 936\ CO_2 \quad (27)$$

Carbonates, produced in controlled culture media, are spherical micritic aggregates and micritic rods made of calcite and low magnesium-calcite (Braissant 2005). While the precise metabolic role of the oxalate in bacteria remains unclear, it is generally assumed that it is used in the pH regulation and by some bacteria for aluminium detoxification, as it can easily become toxic for several strains (Hamel et al. 1999; Tanner and Bornemann 2000; Braissant et al. 2002).

1.7.12 Carbonate related to the *M. excelsa* ecosystem

Mineralization of *M. excelsa* tree (or *Chlorophora excelsa*) is studied since a long time (Harris 1933) for biological interest as well as for commercial defects of the timber (Carozzi 1967). It has been studied in Uganda (Campbell and Fisher 1932) and Ivory Coast (Carozzi 1967). Carbonate location in the tree and the kind of concretions were first studied in the aerial part of the plant (Harris 1933). First observations led to the conclusions that stones are formed by sap exudation. Calcium is present in the sap in the form of soluble calcium bicarbonate and, at the contact with the atmosphere, carbonates precipitates (stalactite principle; Harris 1933). The sap is the vector of the calcitic mineralisation, and this was confirmed isotopically using ^{13}C (Cailleau 2005).
Later research on *M. excelsa* trees from Ivory Coast showed that carbonate is also present in soils surrounding these trees. Carbonate accumulation is so important that, in the root vicinity, carbonate blocks of a size reaching 1.5 m can be observed. These carbonate blocks are constituted of pure calcite (crypto to microcrystalline) with remains of the calco-akaline granite and organic material. Near the roots and the lower part of the trunk, these carbonate concretions can be banded by zone of fibrous calcite. The origin of their formation is the same as proposed previously i.e. abundant sap exudation infilling soil pores and cementing the rhizosphere (Carozzi 1967)
Presence of carbonate in acidic soils raises the question of the origin of the carbonate and its implication in the carbon cycle. The hypothesis that soil carbonate is generated by the oxalate-carbonate pathway has also been tested (Braissant et al. 2003; Braissant et al. 2004; Cailleau et al. 2004; Braissant 2005; Cailleau 2005; Verrecchia et al. 2006), and confirmed. Oxalate salts

are synthesized by the *M. excelsa* tree and stored as a Ca salt. Release of oxalate in the soil during organic matter degradation, principally performed by saprophytic fungi, in the presence of oxalotrophic bacteria initiates the oxalate-carbonate pathway. Soil solution alkalinisation induced by bacterial oxalotrophy constitutes the starting point. If the pH increases up to 8.4 and, if calcium is present, carbonate precipitates in the soil pores. In contrast, if the pH is lower than 8.4, carbonate ions (CO_3^{2-}) present in the soil solution are pumped by roots in the same way as calcium or other nutrients, and enter in the xylem tissues or are leached out of the soil system.

Tree mineralization takes place under different conditions. As the tree is wounded until the xylem zone (Harris 1933), which contains sap with 1.4% carbonate, the contact with the atmosphere allows the carbonate precipitation like for stalactite genesis. More recent theory is that wound is exposed to bacterial contamination and the oxalate-carbonate pathway take place on the trunk (Braissant 2005). Recent observations in Bolivia (Alto Beni, Amazona, M. Mota, pers. com.) and India (Pr. Aragno pers. comm.) seem to stretch towards the presence of an oxalotrophic flora also on the bark of oxalogenic trees.

Another phenomenon could be the supersaturation induced by water stress in the dry season occurring in vessels (Cailleau 2005). Due to this process, carbonate is found in wood tissues as well as in roots tissues (Cailleau et al. 2005). Carbonate associated with the *M. excelsa* tree can also be the product of oxalate combustion (Canti 2003) due to the burning usually applied in Africa for agricultural purposes.

Generated by the oxalate-carbonate pathway, various carbonate features have been found in the soil associated with a secular *M. excelsa* tree of Ivory Coast (Cailleau et al. 2005). Biologically induced mineralisation in the *M. excelsa* system is observed as calcified wood microstructures such as parenchyma cells and cellulose fibres, different types of rhombohedra, needle fibre calcite, large blocks, micritic aggregates, and hemi-spherulites (Cailleau et al. 2005).

Chapter 2 MATERIAL AND METHODS

The tools used to quantify the oxalate-carbonate pathway

The guiding thread from this thesis is to follow the carbon from the plant to the soil. We will demonstrate the impact from the oxalate-carbonate pathway on the intrinsic soil properties and quantified the neo-formed carbonate in a normally acid soil

2.1 Carbonate detection and pH measurement on fiel

Preliminary carbonate distribution measurement under *M. excelsa* trees of different age has been conducted using a soil core sampler and HCl 10% test. A relative scale from 0/4 (no reaction) to 4/4 (maximal reaction) has been applied (Gobat et al. 2005). Hellinge-pH-meter was used to state if the soil was alkaline or acidic.

2.2 The analysed material

Three kind of material are sampled and stocked for laboratory test. To African and Italian samples some other fresh materials are added to confirm hypothesis and calibrate results

2.2.1 "Fresh organic material" and pure Ca-oxalate samples

Calcium oxalate: Ca-oxalate (CaC_2O_4) is a pure laboratory product.

Afzelia africana wood from Burkina Faso: the sample is the central part of a stump cut in 1987, which was dried and ground before analysis.

A. africana dried leaves: the leaves have been sampled directly from a Burkina Faso tree. These leaves are dried and ground before analysis.

Milicia excelsa dried leaves: the leaves have been sampled from a Burkina Faso tree and collected on the soil (litter). These leaves were dried and ground before analysis.

M. excelsa fresh leaves: the leaves are from a 70 years old Burkina Faso tree. These leaves were frozen directly after sampling. Before analysis, they were oven dried and ground.

M. excelsa rotten leaves: these air dried leaves come from a Burkina Faso tree and left in a plastic bottle for rotting during several months. Before analysis samples were oven dried and ground.

Grass (Gramineae family*)*: these leaves have been sampled near Neuchâtel University

(Switzerland), and were oven dried and ground immediately after sampling.

Rumex alpinus dried leaves: these leaves have been sampled from a Swiss plant (Val Piora, Ticino). This plant grew on a soil that developed on a moraine deposit with nearby dolomite. This material was collected for their high presence on oxalic acid.

Oak sp. dried leaves: these dried leaves from a Swiss tree (Ayent, Valais), were collected during fall directly on a tree. Carbonate is present in the surrounding soil. This material has been collected in order to compare their Rock-Eval pyrograms to the *A. africana* leaves where we suspected the presence of wax.

Boletus sp.: this sample is a dried alimentary boletus from a Swiss supermarket.

Fusarium sp.: it has been sampled from a pure *Fusarium sp.* culture, grown on a Malt-Agar substrate.

Melanin: melanin is a black pigment scraped from a polypore fungus.

Insects: they are mainly dry termites and ants sampled under the cut *M. excelsa* tree from Burkina Faso.

2.2.2 Soil samples

Burkina Faso soils:

- F3: *M. excelsa* reference soil: this soil was sampled in the savannah at about 40 m from the cut *M. excelsa* tree. Samples were taken in the middle of each soil horizon (F3Hs is the first horizon, F3A1 is the second one, F3A2 is the third horizon, and so on).
- P4: soil profile at 4.5 m from the trunk of a living *M. excelsa* tree, with a foliar crown of 9 m in diameter. Soil samples were taken each 5 cm with a round rod spoon (*cuillère multi-usages Rotilabo®, Ø tige 8 mm*). P4 0 is the soil sample taken at the surface, P4 5 at 5 cm, and so on. H1, H2, ... are the respective soil layers.
- P3: soil under a *M. excelsa* stump cut in 1987. This soil profile is located 12 m away from P4. Soils samples were taken each 5 cm.
- P2 and P1: soils profiles located at respectively 2.0 m and 3.4 m from P3. Soils samples were taken each 5 cm.
- L2: soil profile under an *Afzelia africana* tree probably cut during the same period as the *M. excelsa* stump. Soil samples were taken in the middle of the three first horizons. L2 0-8 is the first horizon that goes from 0 to 8 cm, L2 8-15 is the second horizon and L2 15-27 is the third horizon.

Salina soils:

- PC1: Salina soil under an *Opuntia sp.* cactus. Soil samples were taken each 5 cm. Moreover, samples have been taken at 1 cm (PC1 0.01) and 2 cm (PC1 0.02) from the soil surface. PC1 0.10 is the soil sample taken at 10 cm deep, PC1 0.15 is the soil sample taken at 15 cm deep, etc.
- PC2: Salina reference soil is located at about 20 m from PC1. Soils samples were taken each 5 cm.

2.2.3 Water samples

Calcium and magnesium are limiting factors. In fact, leaching of calcium diminish the potentiality of the system to fix carbon in their carbonate form. An image of the carbon leaching is done by the analysis of water.

Water sample in Burkina Faso were collected in November 2005, after the rainy season. The following samples have been analysed by ICP-MS:

- sample E1: water from a well 25 m deep located 1 km east from the *M. excelsa* site;
- sample E2: water from a well located in the Farakorosso village, about 1 km far from the *M. excelsa* forest. The water is pumped at 102 m deep in the granitic layer;
- sample E3: water from a well 100 m deep located near Sirakorosso village;
- sample E4: water collected near Diomanidougou, in a marshland.

Rainwater from Salina was collected in April 2006.

2.3 Soil intrinsic characteristics

Soil intrinsic characteristic allows discerning the properties of the soils able to stock mineral carbon and the impact of this mineralisation on carbonate accumulation.

2.3.1 pH measurement

The soft soil mass (without carbonate) is approximately of 5 g and of 8 g for those with carbonate. The pH_{H2O} of the soil is potentiometrically measured (691 pH Meter, Metrohm®) in the supernatant suspension of a 1:2.5 (volume) soil: distilled water equilibrated during 1h.

2.3.2 Residual humidity

Approximately 15 g of sample was placed at 105° C for 48 h in order to calculate their dry weight correction for the various analyses (content of dry matters).

2.3.3 X-ray diffraction

Mineralogical analyses of crushed and pressed soil samples were carried out with a “SCINTAG

XDS 2000" diffractometer (X-ray diffraction) at Neuchâtel University. Data are calibrated on quartz peak with the FitPeak program. The calibration on quartz peak allows to calculate the magnesium mole percent in calcite (Kübler 1992).

2.3.4 Scanning electron microscopy (SEM)

Scanning electron microscopy (SEM) has been performed using a Philips XL30FEG (Field Gun Emission), coupled with a sensor for secondary electrons, backscattered electrons, and an EDS microprobe (X-Ray Energy Dispersive Spectrometry). Before its analysis, organic matter requires several baths containing increasing volume of alcohol, and a last bath with hexamethyldisilizane (HMDS) in order to dry completely the sample. Progressive mixes of methanol/water volumes of 10%, 25%, 50%, and 95%, 30 minutes each, constitute the alcohol baths. The sample (0.5 cm^3) is stuck on a SEM stud with a carbon adhesive and covered by a nanometric layer of gold that ensures conductivity and better stability.

2.3.5 Soil grain size distribution

Bulk soil samples are sieved at 2 mm. Grain size distribution is performed on the fraction < 2 mm following the protocol given by Chalumeau (2003). The sample weight varies between 50 g and 90 g. Carbonates, which could cement the soil particles, are dissolved in HCl (10%). The addition of H_2O_2 removes the organic matter. Five mesh sieves (1 mm, 500 µm, 250 µm, 125 µm, and 65 µm) are used to separate the different particle-size range and to separate the fraction < 63 µm (Chalumeau 2003). Clay and silt proportions in this last fraction are measured using an Oriel analyzer (laser system).

2.3.6 ICP-MS

Chemical analyses of all samples were conducted using the method 3051 developed by the U.S. Environmental Protection Agency EPA (Soon and Abboud 1993). 250 mg of dried and ground sample were digested in a concentrated HNO_3 solution in a microwave for temperature control. The obtained solutions were filtered and then analyzed by Inductively Coupled Plasma Mass Spectrometry (ICP-MS Perkin-Elmer Elan 6100).

Comment: this method does not allow the complete dissolution of soil samples. A residue of 15 ± 10% of original material still remains as non-dissolved matter. Although the concentrations measured by this method would exclude most trace metals trapped within silicate crystal lattices, it gives a reliable analysis of the amount of metals potentially available for natural leaching by biological processes. Calcium and magnesium contents are quite low in silicate minerals compared to those found in carbonates; hence we may assume that the concentrations measured by this method are the total concentrations of Ca and Mg in the analysed samples.

2.3.7 Base cation saturation ratio (S/(S+AE) *100)

Base Cation Saturation Ratio (V) was measured to assess the potentiality of the studied ecosystems to accumulate basic cations and improve soil fertility. To calculate V two analyses are necessary. The first give the exchangeable cations (S) and the second the exchange acidity (AE)
To calculate the exchangeable cation quantity, 10 g of sieved soil (< 2 mm; 2g if carbonate is present) are mixed with 50 ml of HCl 0.1 M during 45 minutes and filtered. NaOH is adding until the methyl red, previously added, changes his colour. To calculate the acidity exchange, 50 ml of $Ca(CH_3COO)_2$ 1N are added to 10 g of sieved (< 2 mm) soil (2 g if carbonate is present). Samples are put under agitation during 1 h, filtered and phenolphthalein is added. Titration until phenolphthalein colour change is made with NaOH 0.1 M.

2.3.8 Thin sections

Samples were taken at each horizon of the following profiles: under the living tree (P4), the old stump (P3), under the cactus (PC 1), and on Salina soil reference (PC2). Samples were transported in solid boxes, dried on air and then freeze in liquid nitrogen bath. They are then soaked and hardened by Epofix resin before making thin sections (30 µm thick)

2.4 Carbon quantificatio

The following tools have been chosen for the rapidity and the accuracy on carbonate quantification on soils and fresh material.

2.4.1 The Rock-Eval6 principle

Crushed samples are analyzed in a “Turbo model Rock-Eval6 pyrolyzer” (Vinci Technologies; University of Neuchâtel). Depending on the estimated OM content, between 30 g (for pure OM) and 70 mg (for soil) of dried and crushed material are necessary for Rock-Eval6 analysis. The standards used are: 1) ifp160000 (Toarcian schist from the Paris Basin), and 2) vp143H (Cenomanian - Turonian black shale from Vergons, Vocontian basin, France). Samples undergo two successive analytical heating phases: pyrolysis and oxidation. Pyrolysis is a thermal breakdown (cracking) of organic constituents under an inert atmosphere (N_2), whereas oxidation (combustion) takes place under air atmosphere. Oven temperature starts with an isothermal stage of 2 min at 200°C. Then, the temperature rises by 30°C · min-1 steps up to 650°C, where the temperature is held for 3 min. The second phase (oxidation) starts with an isothermal stage at 400°C, then increases by 30°C · min-1 steps up to 850°C, where the temperature is held for 5 min. It is very important to know the apparatus analytical heating phases in order to compare results, since it was demonstrated that the temperature cycle and stage steps could influence the data record (Liebezeit and Wiesner 1990).

During the pyrolysis phase the hydrocarbon quantity (mg HC/g) is recorded by a flame ionisation detector (FID). The S1 and S2 curves are calculated before 200°C and after 200°C respectively,

whereas online infrared detectors measure CO and CO_2 (S3 curves; Lafargue et al. 1998; Oorts et al. 2003). S1 is usually considered a minor curve in soils and can thus be generally neglected (Disnar et al. 2003). S3CO curve represents the quantity of CO released from the organic matter pyrolysis until 550°C, whereas S3CO2 curve represents the quantity of CO_2 released from the pyrolysis of organic matter between 200°C and 400°C. This limit is fixed to avoid CO_2 released during cracking of fragile carbonates (e.g. siderite; Lafargue et al. 1998). The remaining organic C that is not linked with hydrogen or oxygen and thus did not escape during the pyrolysis phase, binds with the air oxygen during the oxidation cycle and is recorded by the S4 curves. S4CO and S4CO2 curves represent the quantity of released CO and CO_2, respectively during the oxidation cycle.

Some other indexes can be calculated from all these curves (Lafargue et al. 1998):

- PC (wt%; Pyrolyzed Carbon): is the C released during the pyrolysis derived from organic matter (OM) cracking up to 500°C;
- RC (wt%; Residual Carbon): is the C released from the OM during the oxidation phase up to 650°C;
- TOC (wt%) = PC + RC: is the total organic carbon present in the sample;
- Tmax is an OM maturity indicator in aged sediment (Espitalié et al. 1985). It represents the oven temperature recorded at the maximum of the S2 peak, thus corresponding to the maximum of hydrocarbonaceous release. As Tmax has no significance in terms of thermal maturity, therefore for recent OM the TpS2 term will be used;
- TpS2: pyrolysis temperature representing the maximum release of hydrocarbons (Marchand et al. 2008) that corresponds to the highest peak on the multilobet S2 pyrograms;
- Tpeak is the oven temperature at defined peaks or shoulders in the S2 pyrograms
- MINC (wt%): is the amount of inorganic carbon (from carbonate) calculated by the addition of CO_2 released during pyrolysis above 400°C (on the S3CO2 curves), and CO_2 from carbonate decomposition during the oxidation phase between 650°C and 850°C (on the S4CO2 curve).
- HI (mg HC · g^{-1} TOC; Hydrogen Index): is the amount of hydrocarbonaceous products released during pyrolysis reported on TOC. It is calculated as follows: S2·100/TOC.
- OI (mg CO_2 g^{-1} TOC; Oxygen Index): measures the oxygen content of the OM. It is the amount of CO_2 released during pyrolysis reported on TOC. It is calculated as follows: S3·100/TOC. We used the OICO2 oxygen index (mg CO_2 g^{-1} TOC) that can be correlated to and is numerically close to the now used OIRE6 oxygen index (mg O_2 g^{-1} TOC; Disnar et al. 2003).

2.4.2 Deconvolution of S2 curves

Deconvolution of S2 curves with the software PeakFit v4.12 allows studying the OM type, and indirectly, the allocation of organic C to some thermally stable organic class. In order to use a non-subjective protocol that allows finding the same results during the S2 pyrogram deconvolution with the Peak-Fit program, we applied the method described in Annex 1 (discussed with Dr. D.

Sebag, University of Rouen, France).

2.4.3 Carbonate titration

Carbonate quantification is based on back titration: 1 g of sieved (< 2 mm) and crushed sample is dissolved in 125 ml of deionised water and 25 ml of H_2SO_4 (0.5 N). After one hour in a *bain-marie* at 90°C, back titration using sulphuric acid is carried out with NaOH (0.5 N). At the phenolphthalein colour change, the added NaOH volume is noted. Two blanks allow to calculate the carbonate content (Pauwels et al. 1992).

2.4.4 Oxalate quantificatio

A protocol, based on the quantification of oxalic acid present in soil and leaf samples (complement to the Trinity Biotech, USA method n°591) was elaborated in collaboration with Dipl. Mateo Mota, and Dr. Nadia Khammar. This protocol is given in Annex 2.

2.4.5 CHN

The percentage of total carbon (C), hydrogen (H), and nitrogen (N) are obtained by gas chromatography in an elementary analyzer standard Carlo-Erba-Elemental-Analyser-1108. The standard used is cyclohexanone-2,4-dinitrophenyl-hydrazone ($C_{12}H_{14}N_4O_4$). 20 mg of soil are sufficient for the analysis

2.5 Fungi manipulation

The aims of these manipulations are to find oxalogenic species in studied soils and to estimate the fungal biomass. A medium added with gypsum is made to compare the oxalate crystals from laboratory culture to some of natural fungal crystals.

2.5.1 Fungal isolation

Three soil particles (of about 0.2 mm^3) were placed in a Petri dish on a medium constituted of Malt-Agar and an antibiotic (to inhibit the bacterial growth) in the following proportions: malt (12 g/L), agar (15 g/L), and chloramphenicol (50 mg/L), or streptomycin (0.1 g/L). The inoculated boxes are incubated under ambient conditions. If the developing fungal colonies do not present invading bacteria or air fungi (mucorales), then they are isolated on a simple Malt-Agar medium. Contrarily, if the colony is contaminated, the antibiotic is changed. 20% of the isolated colonies were eliminated because they were colonised by mucorales.

2.5.2 The Malt-Agar medium + gypsum

To force fungi to produce Ca-oxalate, a pure colony is inoculated on a Malt-Agar medium with gypsum ($CaSO_4$). Into 1 L of water containing Malt-Agar, gypsum is added in the following quantities: 0.5 g, 5 g, and 50 g (Tait et al. 1999). The chosen colony is deposited on filters (sterilized with UV rays) in order to avoid catchment of the substrate for observation purpose. The strains are put at room temperature until the colony develops.

2.5.3 Ergosterol quantificatio

Ergosterol, which is a component of fungal cell membranes, was used as an indicator of fungal biomass present in soils. Soil samples have been treated for liquid chromatography analysis (Gessner and Schmitt 1996). No ergosterol was found in Burkina Faso soil, probably while it is quickly degraded or for the little quantity present in these soils.

Chapter 3 PRESENTATION OF THE STUDIED SYSTEMS

An African and an Italian example

In Burkina Faso, three systems stocking carbonate in the soils have been explored: *Milicia excelsa* and *Bombax costatum* trees near Mangodara (Nyanmiango) and *Afzelia africana* tree located 100 km at the northwest of the country, near Niangoloko. The *Bombax costatum* tree was found on the Farakorosso-Nyanmiango road. Although we have not studied in-depth the *B. costatum* ecosystem, we noted the presence of carbonate inside the soil under the tree foliar crown and we give a succinct description of this tree. The studied *Opuntia sp.* ecosystem is located in Pollara (Aeolian Island, Italy).

3.1 Geographical settings: Mangodara and Niangoloko

Mangodara and Niangoloko are located in the Comoé province, in the South of Burkina Faso (Fig. 3.1 and Fig.3.2). The Comoé province is characterized by an inter-tropical continental climate, with a Sudanian tendency and two very distinct seasons. The wet season, dominated by monsoons, goes on for six months (from May to October) and the maxima cumulated rainfall can exceed 1300 mm/year (Fig. 3.2). In the dry season, the Harmattan, a hot dry wind from the Sahara, blows regularly. Temperatures vary between 16°C and 40°C (Lerebours-Pigeonnière and Ménager 2001), with an annual mean of 25°C. Soils are developed on gravels constituted by granitoïd clasts (Naba et al. 2004), lying on a vast and flat peneplain. The mean altitude is between 250 and 300 m.a.s.l. and the dominant vegetation is a wooded savannah of the Sudano-Guinean domain.

3.1.1 The *Milicia excelsa* tree

The *Milicia excelsa* (Welw.) C.C. Berg (Fig. 3.3), formerly known as the *Chlorophora excelsa* (Welw.) Benth. & Hook., belongs to the family of the Moraceae (Ofori et al. 1996). This tree is commonly known by its trading name “Iroko”, which includes the *M. excelsa* and the *M. regia* species. As a side note, the same family includes also the Common fig (*Ficus carica*). Moreover, the *M. excelsa* is classified as deciduous (Devineau 1976) and dioïc tree (Jansen 1974). Both *Milicia* species have long been considered as pioneers trees (Nichols et al. 1998; Bosu et al. 2006) and they prefer well-drained soils and intense light exposition (Ofori and Cobbinah 2007). The *M. excelsa*, although essentially a rain forest tree, extends also farther north, into the dried savannah, along stream galleries (Carozzi 1967). While the *M. regia* is more predominant in the wet forest zones, the *M. excelsa* prefers dry zones (Ofori and Cobbinah 2007). *Milicia* trees are found starting from the sea level till altitudes of more than 4500 m in Tanzania.
M. excelsa can easy reach 47 m in height and more than 2.5 m in diameter (Ofori and Cobbinah 2007). It is a large forest tree, with an umbrella-shaped crown (Jansen 1974). The bark is thick

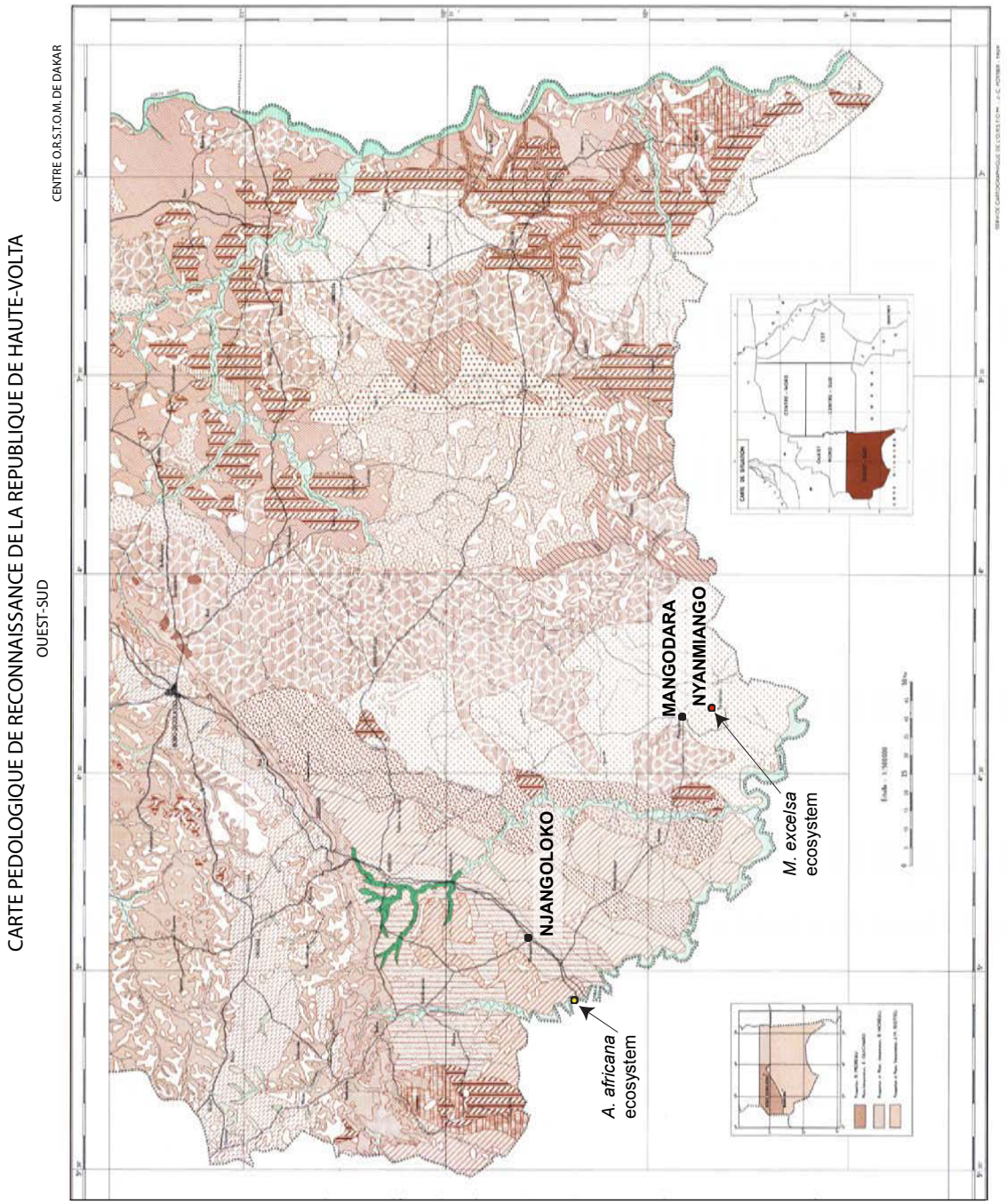


Fig. 3.1- A pedological map of the Comoé province, Burkina Faso, showing the sites of the studied systems (Pottier 1969).

LEGEND

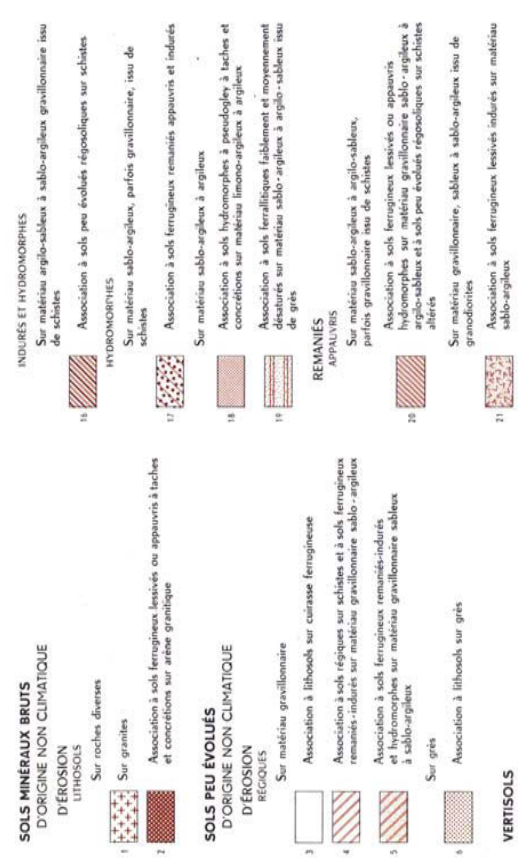


Fig. 3.1- Continued

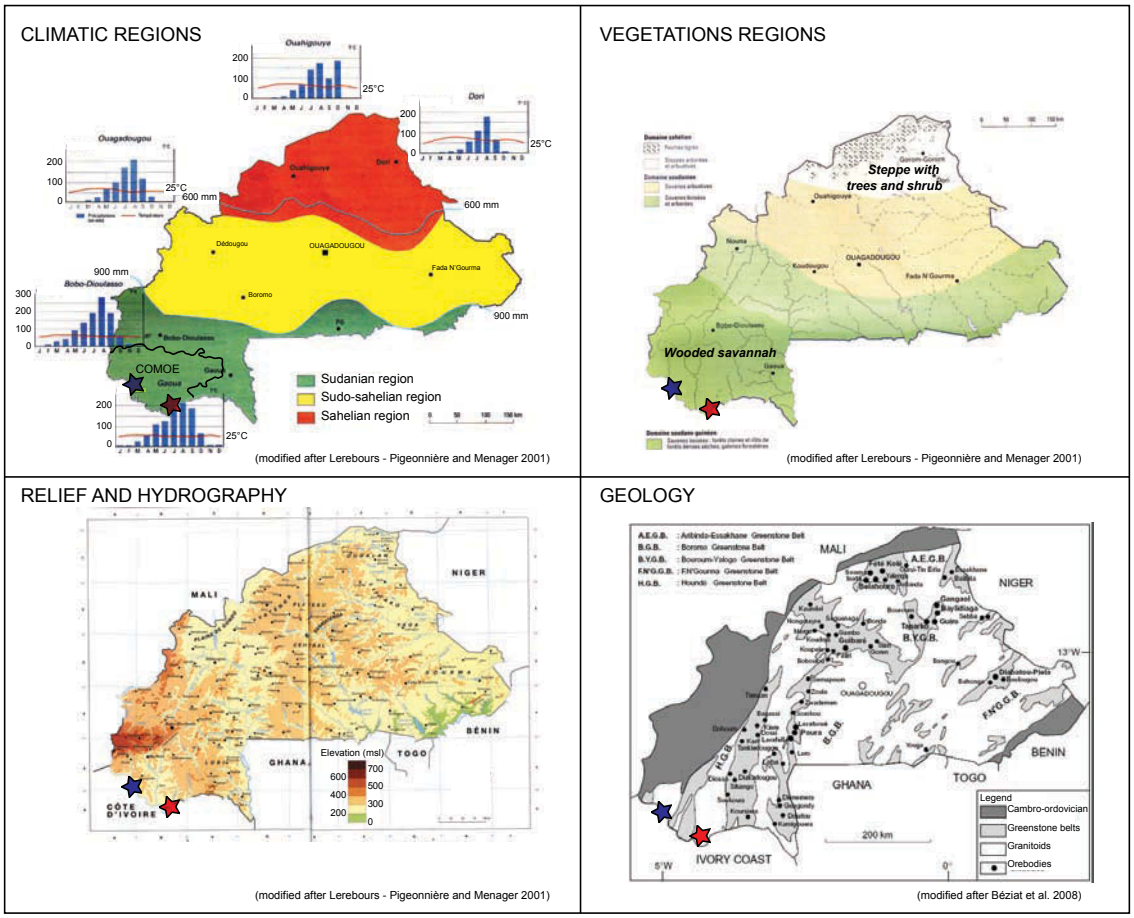


Fig. 3.2- Burkina Faso maps of climatic regions, vegetation, relief and hydrography (Lerebours-Pigeonnière and Menager 2001), and geology (Béziat et al. 2008) with location of the studied systems. The red star indicates the position of the M. excelsa *tree, near the Mangodara site. The blue star stands for the* A. africana *tree, near the Njangoloko site.*

and sclerosed, with a dark brown to blackish scaly surface, displaying yellowish lenticels, while its roots are red. The Moraceae are well known for their predisposition to siliceous and calcareous secretions (Carozzi 1967).

In local medicine, *M. excelsa* is known for its medical properties (Jansen 1974), as many parts of the tree are used to heal human diseases (Ouinsavi et al. 2005). Moreover, the *M. excelsa* tree is used to preserve cultural values and it incarnates many divinities (Ouinsavi et al. 2005). With a density of 655 kg/m^3, it is a moderately hard timber and it is very durable (Carozzi 1967; Jansen 1974), the *M. excelsa* tree is among the most economically important hardwood species in the tropical Africa (Bosu et al. 2006). As such, it is also used and exported for constructions of all kinds (Jansen 1974). However, because of its over-exploitation, combined with its poor regeneration, the *M. excelsa* tree is currently under threat of extinction (Bosu et al. 2006). All attempts to grow the *Milicia* species in plantations have generally failed due to the attack of gall-forming insects (Cobbinah and Wagner 1995; Ofori et al. 1996; Bosu et al. 2006; Ofori and Cobbinah 2007). Finally, it may be worth to add, that for its morphology, in Sao Tomé and Príncipe (western equatorial coast of Central Africa), *Milicia* trees are used as light-cover trees, for plantations such as cacao and coffee (Carvalho et al. 2004).



Fig. 3.3- A Milicia excelsa *tree and leaves situated in the Mangodara village (South of Burkina Faso), near "Le Commissariat".*

3.1.2 The *Afzelia africana* tree

The *Afzelia africana* (J.E. Smith and Pers.) tree belongs to the Fabaceae family (Caesalpinioideae subfamily). Its English common name is "Afzelia", whereas in Burkina Faso it is called with the local name of "Lingué". This tree is normally 24 till 36 m high (Fig. 3.4), with a diameter usually ranging from of 0.9 to 1.5 m (Hawthorne 1995). It can be found in West and Central Africa, where it occurs in the dense evergreen forests. It is also a common tree in the savannah and the coastal forests of East Africa (Ren et al. 2005). *A. africana* grows preferentially in gravel and dry soils (Aubréville 1970; Hawthorne 1995), at an altitude varying from 0 to 800 m.a.s.l.. Moreover, ectomycorrhizal fungi were observed associated with the *A. africana* tree (Sanon et al. 1997; Villenave and Duponnois 2002; Diedhiou et al. 2004). Among the ectomycorrhizal African trees, the *A. africana* is considered as one of the most important timber species for the reforestation of West Africa (Diedhiou et al. 2004).

From the economical point of view, those trees are very interesting (Kadiri and Olowokudejo 2008), since the Afzelia tree is a good source of timber for construction works, for soap production, and for dying processes (Ajah and Madubuike 1997; Kadiri and Olowokudejo 2008). As the *Milicia* trees, Afzelia has medicinal properties, while its foliage is a good cattle fodder (Bationo et al. 2000; Onana and Devineau 2002; Ouédraogo-Koné et al. 2006; Kadiri and Olowokudejo 2008).



Fig. 3.4- The Afzelia africana *tree (A), leaves (B), and mineralized stump (C, D, and E) found near Njangoloko. Stars indicate carbonate accumulations on stump surface.*

3.1.3 The *Bombax costatum* tree

The *Bombax costatum* (Pellegr. et Vuillet) belongs to the Bombacaceae family. Its English common names are "Red-flowered silk tree", or "Cotton tree", while its French name is "Kapokier". The *B. costatum* is a deciduous tree growing up to 25 m in height (Fig. 3.5). It flowers usually after its leaves fall, from November to February. Its bark is thick, grey brown and corky, with typical conical, stouting, and sharp-pointed spines on the stem and branches. Its tuberous roots can act both as water and sugar storage facilities during the long drought periods. The *B. costatum* grows particularly well on stony soils and it supports dry lateritic ones. The primitive habitats of the *B. costatum* are the persistent and green wet forests but also the dry and galleries forests of South and Central Africa. The *B. costatum* is a fire-resisting tree of the savannah and of the dry woodlands from Senegal to Central Africa, from Guinea, across Ghana and Nigeria, to the Southern Chad. Moreover, this tree is also cultivated in Indonesia and in Cambodge, so as in Madagascar.

The *B. costatum* provides valuable benefits to villagers in terms of fruits, fodder, and wood (Tappan and McGahuey 2007). Bark, roots, and stem bark are used in traditional medicine (Inngjerdingen

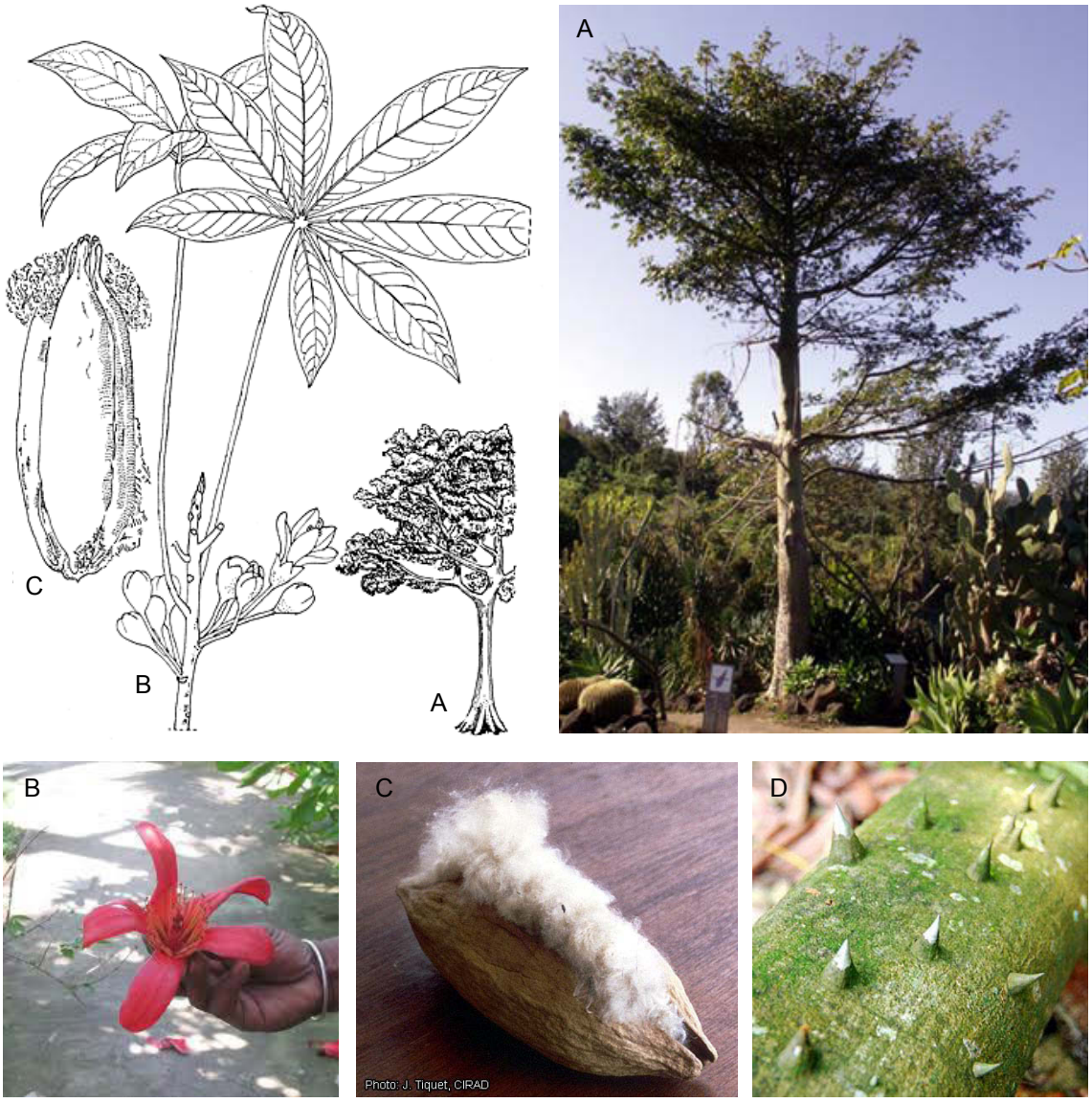


Fig. 3.5- General features of the Bombax costatum *tree (http://database.prota.org). A: the tree shape (http://www.mi-aime-a-ou.com); B: the flower (http://www.fleu destropiques.net); C: the fruit containing white floss called kapok (http://database.prota.org); and D: the typical conical, stout, sharp-pointed spines on stems and branches (http://gardenmalaysia.blogspot.com).*

et al. 2004; Magassouba et al. 2007). Fruits are consumed by humans, while leaves are given to animals as forage. Kapok fibres, obtained from the fruits, are mainly used as a filling, especially for pillows. The wood is very soft and weights only about 350-450 kg/m³, so that if untreated, it is soon attacked and destroyed by fungi and insects.

3.1.4 Description on the *Milicia excelsa* trees location and soils

M. excelsa trees are scarce in Burkina Faso. The first *M. excelsa* tree we have found was near Bobo Diulasso in a protected park, therefore impossible to study. It is in a semi-sacred relict forest near Nyanmiango (north of Farakorosso), 1 km South of Mangodara (9°54'N, 4°21'W) that some

M. excelsa trees are present and preserved since there are considered sacred trees. This forest is split by a dirt road, and in the North part, the *M. excelsa* trees are sacred and untouchables (Fig. 3.6 A). Six trees with a trunk circumference of 34.2 cm, 41.6 cm, 151 cm, 148 cm, 57 cm, and 97 cm respectively have been listed. On the South part there are three trees with a diameter of 30 and 21 cm and 92 cm. A mineralized stump of 92 cm of diameter and partially burned is also present. As Nyanmiango people told us, this last tree was cut in 1987, year in which Thomas Sankara was assassinated.

A preliminary core study allowed us to preserve the young tree roots as well as to get a general idea of the extension of the mineralisation in the soil and the trunk and to choose the position of the future soil profiles to be described and studied. Soils not influenced by the *M. excelsa* tree litter are acidic (4 < pH < 5). The following observations result from the core profiles. Reactions

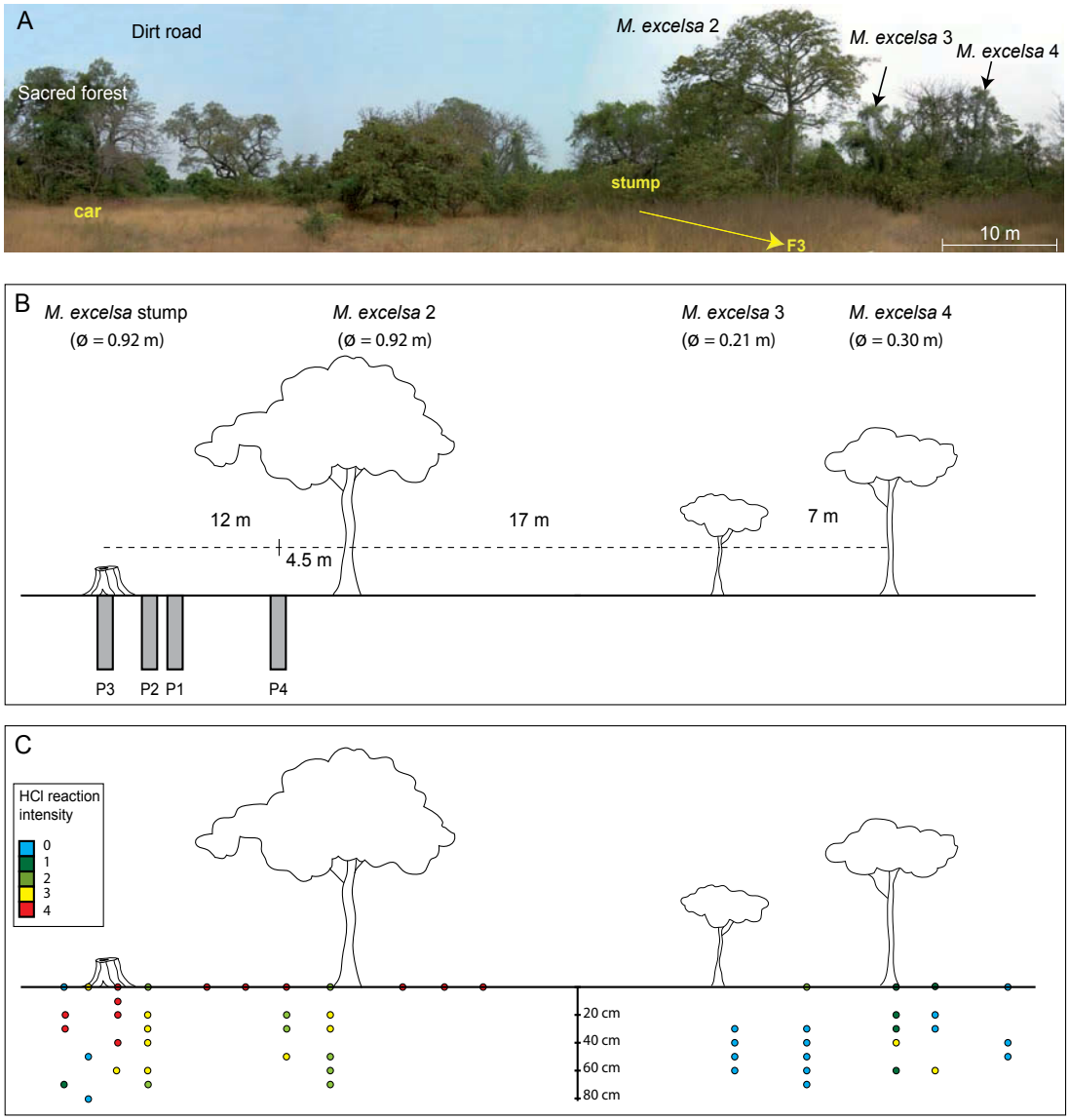


Fig. 3.6- The M. excelsa *ecosystem. A: general view of the relict forest with the emplacement of the* M. excelsa *trees. B: sketch of the* M. excelsa *trees and the studied soils emplacement. C: HCl test reactions from core sampling prospection.*

to HCl (10%) have been observed (Fig. 3.6 C):

- only under the foliar crown projection to the soil and always in the soil first centimetres
- under the youngest tree (0.21 cm in diameter) only at the soil surface;
- under the tree with a 0.30 m diameter, at the soil surface, and in relationship with its roots;
- under the oldest living *M. excelsa* tree (0.92 m in diameter) until 70 cm in depth. The strongest reactions are observed in the soil first centimetres. Carbonates are abundant around its roots (Fig. 3.7);



Fig. 3.7- Above: Pictures of a soil profile section under a living M. excelsa *tree, showing a root with a white carbonate accumulation zone (1) and below granitoid outcrops present in the proximity of the* M. excelsa *trees location.*

- under the *M. excelsa* stump, the acid reactions are the highest. The intensity is irregular with depth. Termites and ants are abundant around the stump. Moreover the stump is partially burnt.

Reactions to acid occur where the soil is basic, but a few exceptions attested a carbonate reaction in acidic parts.

The following soil profiles have been studied (Fig. 3.6 B, Fig. 3.8, and Fig. 3.9)

- P4: under the foliar crown of the oldest living *M. excelsa* tree, at 4 m distance from their trunk;
- P3: under the *M. excelsa* stump;
- P2: at 2 m distance from P3;
- P1: at 3.4 m distance from P3, at the limit of the foliar crown projection;
- F3: a reference soil located 38 m far away, southwards from P3, outside the forest.

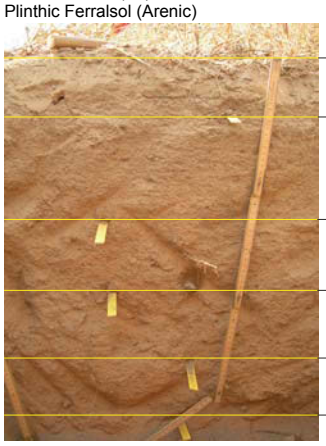
The description of the soil profiles was made November the 28th and the 29th, 2005. The last raining day was November the 5th. These soils are located in a peneplain (Fig. 3.2) where granitoids are visible at the surface (Fig. 3.7). At a depth of about 60 cm, rounded granitoids blocks are weathered, clearly indicating an alluvial plain. The Nyanmiango village is only about 300 m far from the system. The soils are strongly trampled and used for both animal pasture and agricultural purposes. Moreover, brush fire is a largely employed practice over all the Burkina Faso territory. The determinate vegetation present in this place is given in Annex 3.

A general characteristic of Burkina Faso soils considered in our study is a net limit between the different horizons (Fig. 3.9). The skeleton volume is used to distinguish the soil horizons. This skeleton occupies more and more volume with increasing depth and it is composed of crystalline (exclusively quartz) and iron nodules. At a depth of about 60-70 cm, iron nodules are molten and the soil is hand-unworkable. The soil texture is sandy and insects and insect-nests, especially from termites, are abundant. The main differences between the reference soil, located in the savannah, and the soils related to the *M. excelsa* and the *A. africana* trees are, from one side, the presence of more organic matter, both living (fungi, insects, and roots) and dead (litter), and on the other side, the presence of carbonate signals such as a pH value of 3 units higher than the profile outside



Fig 3.8- P1, P2 and P3 soil profiles

Reference soil (F3):
Plinthic Ferralsol (Arenic)



Dry Munsell color	Soil skeleton	Mechanical properties	pH	OM	TOC	Horizons	cm
							0
10YR 5/3	5%, sand	unconsolidated	5	wood, leaves, roots (2/5), mycelium, ants	0.4%	A	
							8
10YR 5/3	5%, gravel	compact	5	roots (2/5), mycelium, termites	0.2%	Bc1	
							25
10YR 5/3	10%, gravel	compact	4 - 5	roots (1/5), mycelium, spiders	0.2%	Bc2	
							37
10YR 5/3	10%, gravel and pebbles	compact	5	roots (1/5), mycelium	0.2%	Bcd	
							53
10YR 5/4	25%, gravel	compact	5	roots (1/5), mycelium, termites, ants	0.1%	C1	
							66
10YR 5/4	95%, gravel and pebbles	compact	4 - 5	roots (1/5), charcoal	0.1%	C2	

Soil related to a living *M. excelsa* tree (P4):
Ferralic Calcisol (Arenic)



Dry Munsell color	Soil skeleton	Mechanical properties	pH	OM	TOC	Horizons	cm
							0.0
10YR 4/1	5%, gravel	unconsolidated	7- 8	wood, leaves, roots (2/5), bark, seeds, mycelium, termites	3%	(OL)Ak	
10YR 5/2							4.5
10YR 4/2	5%, gravel	compact	8	roots (2/5), mycelium, termites	1.3%	Ak	
10YR 5/3							17.5
10YR 4/2	20%, gravel	compact	8	roots (3/5), mycelium, termites, ants	0.6%	Bck1	
10YR 5/3							28.5
10YR 4/2	20%, gravel	compact	8	roots (1/5), mycelium, termites	0.2%	Bck2	
10YR 5/3							
10YR 5/3							43.5
10YR 4/3	95%, gravel	very compact	8	roots (1/5), mycelium, termites, ants	0.2%	C1	
7.5YR 5/3							54.5
7.5YR 5/3	95%, gravel	hyper compact	8	-		C2	
7.5YR 5/4							
7.5YR 5/4							

Soil related to a *M. excelsa* stump (P3):
Ferralic Calcisol (Arenic)



Dry Munsell color	Soil skeleton	Mechanical properties	pH	OM	TOC	Horizons	cm
							0.0
10YR 4/1	5%, gravel	unconsolidated	8 - 9	wood, leaves, roots (3/5), bark, seeds, mycelium, termites, ants	4.8%	(OL)Ak	
10YR 5/4							6.0
10YR 5/3	2%, gravel	compact	8 - 9	roots (3/5), mycelium, termites, ants	0.6%	Ak	
10YR 5/4							
10YR 5/3							24.5
10YR 5/4	10%, gravel	compact	8 - 9	roots (3/5), mycelium, termites, ants	0.4%	Bck1	
10YR 5/3							
10YR 5/3							40.5
7.5YR 5/3	30%, gravel	very compact	8	roots (1/5), mycelium, wood, termites	0.4%	Bck2	
7.5YR 5/3							
7.5YR 5/3							
7.5YR 4/3							
7.5YR 4/3							
7.5YR 4/3	50%, gravel	hyper compact	7 - 8	roots (1/5), mycelium, wood, termites, ants	0.2%	C	62.5

Fig. 3.9- Profiles of the diffe ent studied soils. OM: organic matter. See also Fig 6.8 and Annex 11.

Soil related to an *A. africana* stump (L2):
Ferralic Calcisol (Arenic)



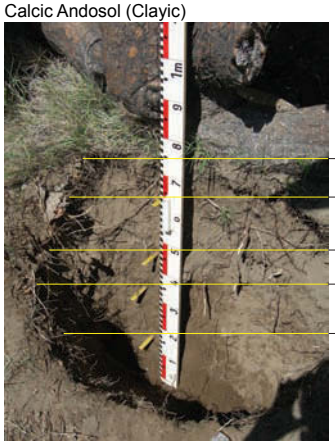
Dry Munsell color	*Soil skeleton*	*Mechanical properties*	*pH*	*OM*	*TOC*	*Horizons*	*cm*
							0
10YR 3/2	5%, gravel	unconsolidated	7-8	wood, leaves, roots (3/5), charcoal, termites, ants	3.6%	(OL)Ak	8
10YR 4/2	5%, gravel	compact	8	wood, leaves, roots (2/5), charcoal, termites, ants	5.3%	Ak	15
7.5YR 4/4	5%, gravel and pebbles	compact	6-7	wood, leaves, roots (1/5), charcoal, termites, ants	0.9%	Bck1	27

Salina Reference soil (PC2):
Calcic Andosol (Clayic)



Moist Munsell color	*Soil skeleton*	*Mechanical properties*	*pH*	*OM*	*TOC*	*Horizons*	*cm*
							0
10YR 4.5/3	30%, gravel and pebbles	unconsolidated	5	roots (5/5), mycelium	1.6%	A	5
10YR 4.5/3	45%, gravel and pebbles	poorly compact	5	roots (2/5)	0.4%	Bw11	20
10YR 3/4	45%, gravel and pebbles	poorly compact	5	roots (2/5)	0.4%	Bw12	39
10YR 3/3.5	45%, gravel and pebbles	moderately compact	5	-	0.4%	Bw2	64
10YR 3/5	45%, gravel and pebbles	compact	5	-	0.5%	BC	

Soil related to a *Cactus sp.* (PC1):
Calcic Andosol (Clayic)



Moist Munsell color	*Soil skeleton*	*Mechanical properties*	*pH*	*OM*	*TOC*	*Horizons*	*cm*
							0
10YR 4.5/3	5-10%, gravel	unconsolidated	6-7	roots (3/5), insects, pellets, brindilleas	1.7%	A	10
10YR 4/2.5	5-10%, gravel	poorly compact	7	roots (2/5), enchitreïdes, mycelium, brindilleas, humified OM	0.7%	Bw11	32
10YR 3/3	5-10%, gravel	moderately compact	6	roots (2/5), mycelium	0.1%	Bw12	51
10YR 3/4	5-10%, gravel	moderately compact	6	roots (2/5), mycelium	0.1%	Bw2	63
10YR 3.5/3	5-10%, gravel	compact	5	roots (1/5)	0.3%	BC	

Fig. 3.9- Continued

the tree influence. The *A. africana* profile, located under a stump, has similar characteristics as those under the *M. excelsa* stump: a strong presence of mycelium, termites and wood in different decomposition states.

According to the existing soil classifications, the Burkina Faso reference soil belongs to

- "Plinthic Ferralsols (Arenic)" (WRB classification)
- "Oxysols" (USDA soil taxonomy);
- "Sols à sesquioxydes et à matière organique rapidement minéralisée. Sols ferrugineux tropicaux lessivés" (Pottier 1969);

The presence of carbonates in the soils under the *M. excelsa* trees requires the following name: "Ferralic Calcisol (Arenic)" (WRB classification)

3.1.5 The *Afzelia africana* system

The difficulty to find *M. excelsa* trees in Burkina Faso prompted us to look for other mineralizing trees. So, we decided to talk with the employees from the Coulibaly sawmill in Bobo Diulasso. A man told us about the *Afzelia africana* tree on the SW of Njangoloko (10°16'N, 4°54'W; Fig. 3.1 and Fig. 3.2), who gave serious problems during its cutting since their high mineralised wood. The type of mineralisation was not clear: carbonate or silica? Is the mineralisation involving only the wood or does it take place also in the soils? In a forest on the border with the Ivory Coast there was a living *A. africana* tree of about 20 m high and an old stump cut several years ago. Carbonate was present in the soil under the foliar crown projection and surrounding the stump. Moreover the wood of the stump was highly mineralized by carbonate (Fig. 3.4). Associated soil pH is slightly acidic or alkaline ($6 < pH < 8$), whereas, out from the tree influence, pH is clearly acidic ($4 < pH < 5$). Like the soils influenced by the *M. excelsa* it is a Ferralic Calcisol Arenic (WRB classification; Fig. 3.9)

3.2 The Salina ecosystem

After the African success in finding carbonate associated with trees, the question raised about the presence of secondary carbonate in Mediterranean conditions. Salina *Opuntia sp.* ecosystem was investigated because of its well known high oxalate content and the fact that carbonate species are present in and around cactus plants such as *Carnegia gigantea* (Garvie 2003). A similar ecosystem (in the Tabernas desert, Spain) was studied by Cailleau in its thesis work (Cailleau 2005). Is the *Opuntia sp.* cactus able to generate the oxalate-carbonate pathway and act as long term carbonate storage in Aeolian Island soils? The factors controlling the formation of the carbon sink are similar to those considered in Burkina Faso or in Tabernas?

3.2.1 Geographical setting: Pollara

The studied *Opuntia sp.* system is located in the South of the Pollara caldera, NW part of the Salina Island (Aeolian Islands, Italy; Fig. 3.10), with a climate of Mediterranean type. The

average annual precipitation is about 600 mm/year, and the temperatures fluctuate between 11°C and 30°C (Fig. 3.10). Soils are developed on pyroclastic deposits (Barca and Ventura 1991; De Rosa et al. 2002; Sulpizio et al. 2008) made of andesitic, dacitic, and rhyolitic materials (Fig. 3.10). Mediterranean maquis is the dominant vegetation (Bosi 1996-1997). In the locality of Pollara, the plant associations are the *Dianthus rupicola* and *Matthiola incana* ssp. r*upestris* and the *Helichrysum litoreum* (Bosi 1996-1997).

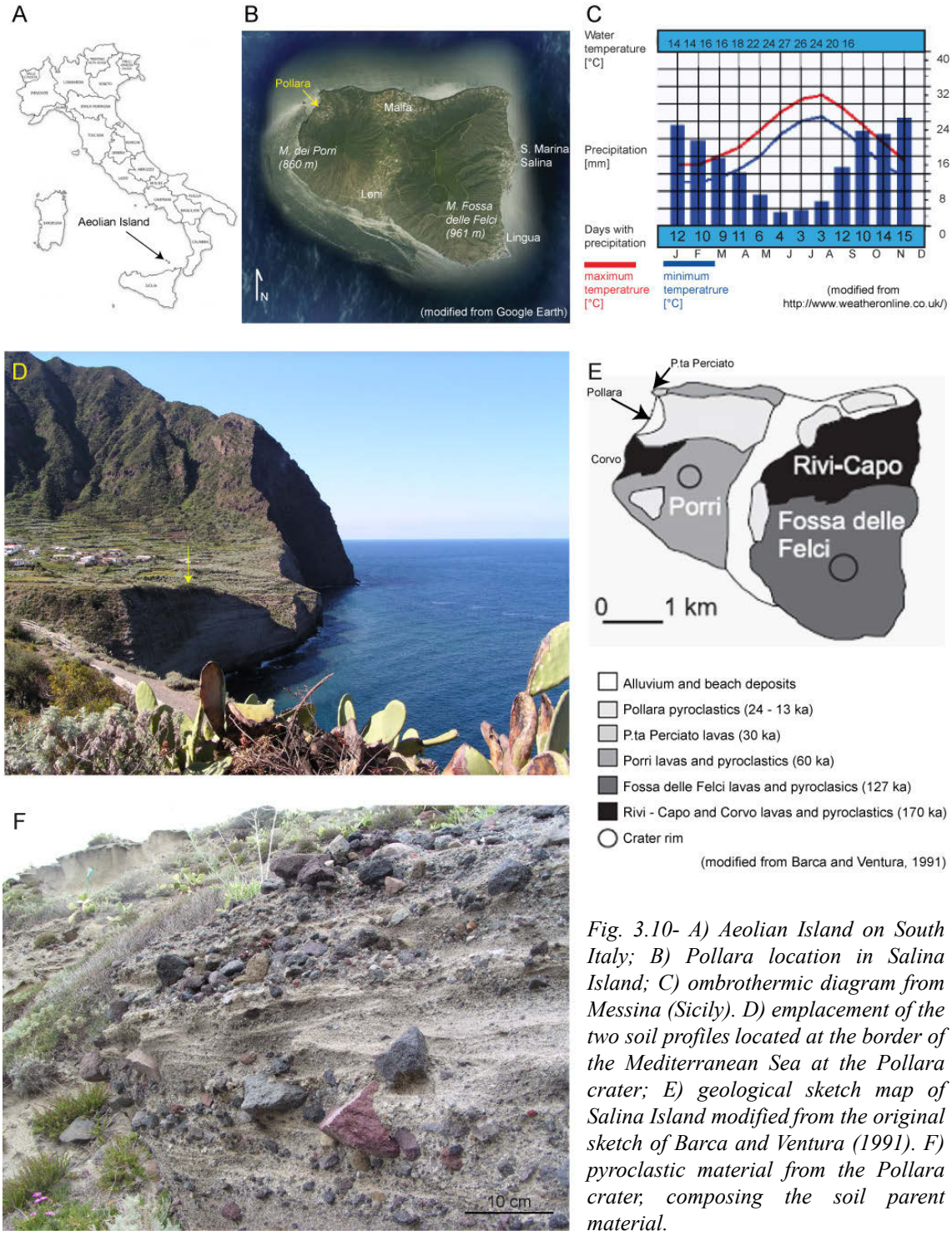


Fig. 3.10- A) Aeolian Island on South Italy; B) Pollara location in Salina Island; C) ombrothermic diagram from Messina (Sicily). D) emplacement of the two soil profiles located at the border of the Mediterranean Sea at the Pollara crater; E) geological sketch map of Salina Island modified from the original sketch of Barca and Ventura (1991). F) pyroclastic material from the Pollara crater, composing the soil parent material.

3.2.2 The *Opuntia sp.* cactus

The cactus pear (*Opuntia ficus-indic* ; *Opuntia spp.*, Cactaceae; Fig. 3.11) is a fleshy bush (or small tree), native to the desert zones of the North western Mexico and the South western United States (Knight 1980). The plant was brought to Europe by the first Spanish colonists from Mexico and has been cultivated along the Mediterranean coast since the late 17th century (Retamal et al. 1987). The *Opuntia sp.* may reach a height of 5 m and prefers calcareous soils and semi-arid climate, with temperatures ranging from 18°C to 26°C. The Opuntia is a cactus, whose branches or stems ("cladodes" or "nopalitos") have both the appearance and the function of a leaf. The plant is propagated mainly by vegetative means (cladodes or shoots), and it is characterized by superficial and fleshy roots, expanding horizontally (Tous and Ferguson 1996). The bulk absorbing-root mass is found in the surficial layers with a maximum depth of 30 cm and with a range of horizontal development that can easily reach 8 m (Mulas and Mulas 2004). The walls of the skin cells are impregnated of a thick layer of wax. The substances, composing this cuticle, are not decayed by micro-organisms, since they are not able to penetrate inside the skin (Mulas and Mulas 2004). The Opuntia genus belong to the plants called CAM (Crassulacean Acid Metabolism) obligated (Mulas and Mulas 2004).



Fig. 3.11- A) the chosen Opuntia sp. *tree; B and C) two different degradation states of Salinas* Opuntia sp. *cladodes displaying carbonate reaction to HCl (10%) test.*

3.2.3 The Pollara studied soils

The soil analysis was made April the 15th, 2006. Two soil profiles, at 45 m.s.l., are studied (Fig. 3.9, Fig. 3.10 and Fig. 3.11):

- PC1: under a living *Opuntia sp*. cactus composed by several stems. The biggest stem is made up by twelve cladodes (Fig. 3.11). Samples were taken at the following depths: 0 cm, 0.2 cm, 0.5 cm, 1 cm and then each 5 cm until a depth of 70 cm.
- PC2: the reference soil, 10 meters away from PC1. It was sampled at: 0 cm, 5 cm, 10 cm, and then every 10 cm till a final depth of 70 cm

Under the cactus, the litter is constituted by cactus cladodes and can easily reach more than 10 cm in thickness. The limits between the horizons are sharp. The soil texture is sandy and clayey (bimodal). The pH values are of 6-7 and carbonate is present in both soil profiles. Carbonate is found in dust, in cladodes showing an advanced degradation state (Fig. 3.11) and on fresh cladodes surface laying on soil. The soil skeleton is constituted of rounded mineral gravel, pebble, and volcanic blocks, and its volume increases with increasing depth. The roots that structure the soil, while channels and cavities increase the porosity support the lumps and the filter porosity of the first horizons. Fleas, springtails, mites, enchytreides, and shells fragments (gastropods) are observed. The mycelium is abundant at the soil surface and it is present till a depth of 60 cm. Gramineae essentially constitutes the vegetation, on the reference soil PC2.

According to existing soil classifications, the Salina reference soil belongs to

- “Calcic Andosols (Clayic)” (WRB classification)
- “Andosols” (Classification française)

Chapter 4 THE ORGANIC CARBON QUALIFICATION

A Rock-Eval pyrolysis approach

4.1 Introduction

In this part, the Rock-Eval method is used to appreciate the evolution of soil organic matter in soils of Burkina Faso and Salina Island (Italy). In addition to soils, some organic non-decayed samples (fungal and plant material) are exposed to a pyrolysis and oxidation cycle with the aim to characterize their Rock-Eval signature. Moreover, a laboratory calcium oxalate is analyzed as well, due to the fact that oxalate salts are present in the studied system.

Due to its heterogeneous nature, soil organic matter (SOM) is difficult to study (Golubyatnikov and Svirezhev 2008). Various physical and chemical methods exist to separate or determine SOM, but only a few of them are used routinely because of their conventional needs for preliminary sample preparation (e.g. decarbonation, extraction, or purification; Gobat et al. 2010; Sebag et al. 2006). Rock-Eval technique (see also Chapter 2) destroys molecule bonds present in the organic matter and quantify released effluents (hydrocarbons, CO and CO_2). For immature organic matter, during the pyrolysis phase, released hydrocarbons are reported in a multimodal spectrum (S2) where the shape is related to the quality of organic matter nature. CO and CO_2 quantities released during pyrolysis are reported on a S3 diagram, whereas the CO and CO_2 released during oxidizing conditions are described on a S4 diagram.

SOM consists of a variety of components, from intact original plant and animal tissues to a substantial mixture of decayed and recombined materials known as humus (Bot and Benites 2005; Gobat et al. 2010). The organic matter input forming the SOM comes from above ground (aerial litter) and below ground (roots senescence, rhizodeposition) and can be divided into two major groups: plant residues (primary resources) and microbial residues and exudates (secondary resources). Animal material, especially invertebrates, can to be added but their contribution remains fairly small. Essentially, two different types of plant tissues reach the soil for decomposition: parenchymatic and woody tissues. Plant tissues can be divided into various classes of compounds including storage material and structural components. Storage material is easily degradable thus constituting important carbon and energy sources for microorganism (Kögel-Knabner 2002). A brief description of some organic material present in soil is given below.

4.1.1 Soil organic matter

Dry plant material is composed to the extent of 99 % of eleven major element: C, H, O, N, P, S, Ca, Mg, K, Cl, and Na (Callot et al. 1982). Every carbon atom in an organic molecule has four bonds, which allows the molecule to have a complex structure with carbon as a “backbone”. At each end of the molecule is a functional group (Fig. 4.1). The functional groups determine the

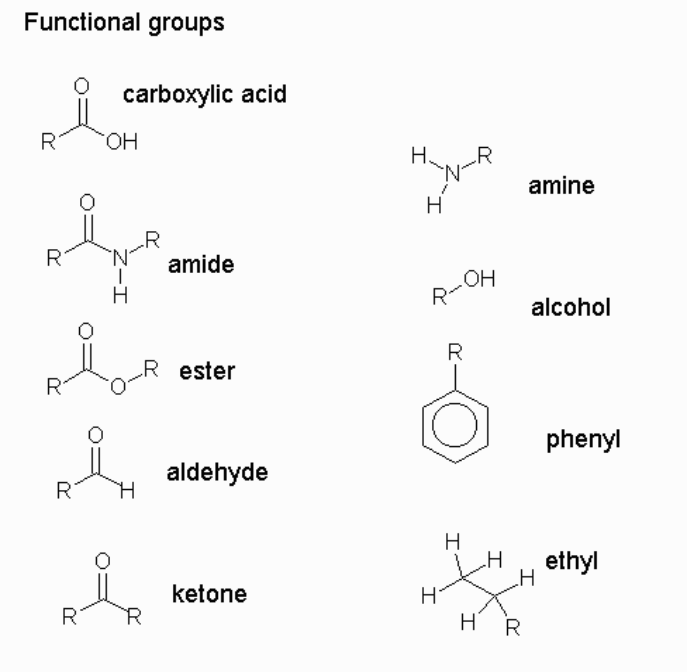


Fig. 4.1- Main functional groups in organic molecules.

reactivity and the types of chemical reactions that molecules can involve. The major classes of biomolecules found in soils are (Kögel-Knabner 2002; Gobat et al. 2010): carbohydrates, lipids, lignins, and nitrogenous compounds (amino acids, proteins, nucleic acids, nucleotides).

Their respective proportion in soils is very variable (Table 4.1) according to the horizon considered, the physicochemical environment, the type of vegetation, and the applied analytical method (Gobat et al. 2010). Non-humic organic molecules are released directly from cells of fresh residues, such as proteins, amino acids, sugars, and starches. This active fraction is strongly influenced by weather conditions, moisture status of the soil, growth stage of the vegetation, addition of organic residues, and cultural practices, such as tillage. It is the main food supply for various soil organisms.

Category of organic substance	Proportion in plant (% of category)	Proportioin in soil (% of category)
Cellulose	20 - 50	2 - 10
Hemicellulose and proteins	10 - 30	0 - 2
Lignin	10 - 30	35 - 50
Proteins	1 - 15	28 - 35
Lipids, waxes, other	1 - 8	1 - 8

Table 4.1- Average proportion of the broad categories of organic substances in plant and soils (from Gobat et al. 2010).

4.1.2 Carbohydrates

The empirical formula of carbohydrate is: $C_m(H_2O)_n$. The carbohydrates (or saccharides) are divided into the following chemical groupings (Fig. 4.2): monosaccharides (ex. glucose, fructose, galactose), disaccharides (ex. sucrose, lactose, and maltose), and polysaccharides (ex. starch, cellulose and hemicellulose). The main carbohydrates forms occurring in soils are: 1) free sugars in the soil solution, 2) cellulose (Fig. 4.2 D) and hemicelluloses, 3) complex polysaccharides, and polymeric molecules of various sizes and shapes that are attached strongly to clay colloids and humic substances (Stevenson, 1994).

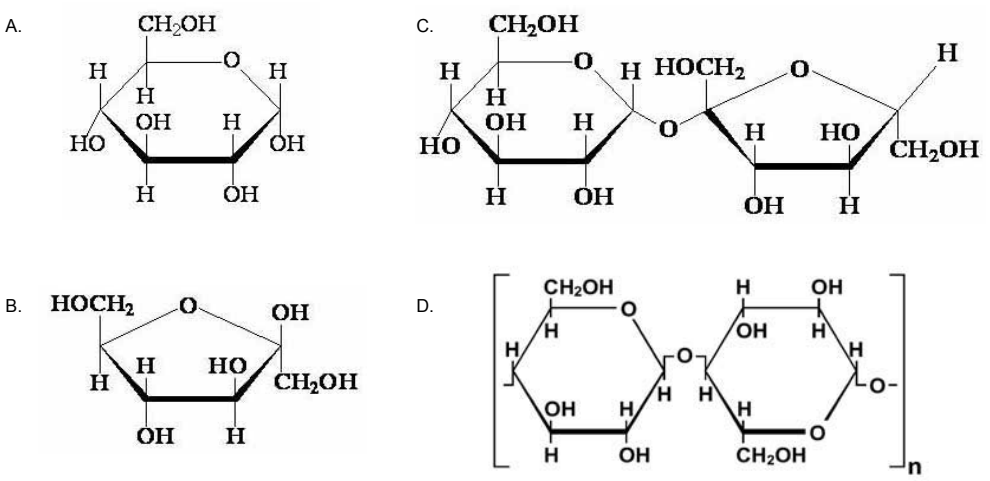


Fig. 4.2- Example of carbohydrate molecules. A) glucose, B) fructose, C) sucrose, and D) basic unit and supramolecular structure of cellulose with β-(1-4)glycosidic bond.

4.1.3 Nitrogenous compounds

Nitrogenous compounds (Fig. 4.3), which can constitute more than a third of the SOM and can contain 95 % of the total nitrogen, form a wide variety of molecules: nucleic acids (DNA, RNA, and their bases), chitin, murein, urea and uric acid, amines and proteins, and their constituents, the free amino acids (Gobat et al. 2010).

Nucleic acids are linear polymers (chains) of nucleotides. Each nucleotide consists of three components: a purine or pyrimidine nucleobase, a pentose sugar, and a phosphate group. Chitin $(C_8H_{13}O_5N)_n$ is a long-chain polymer of a N-acetylglucosamine, a derivative of glucose. It is the main component of fungal cell walls, exoskeletons of arthropods, such as crustaceans and insects, radulas of mollusks, and beaks of cephalopods, including squids and octopuses. Murein (or peptidoglycan) is a polymer consisting of sugars and amino acids that form a mesh-like layer outside the plasma membrane of bacteria (but not Archaea), forming the cell wall. Urea is an organic compound with the chemical formula $CO(NH_2)_2$. The molecule has two $-NH_2$ groups joined by a carbonyl (C=O) functional group. The formula of uric acid is: $C_5H_4N_4O_3$. It is a product

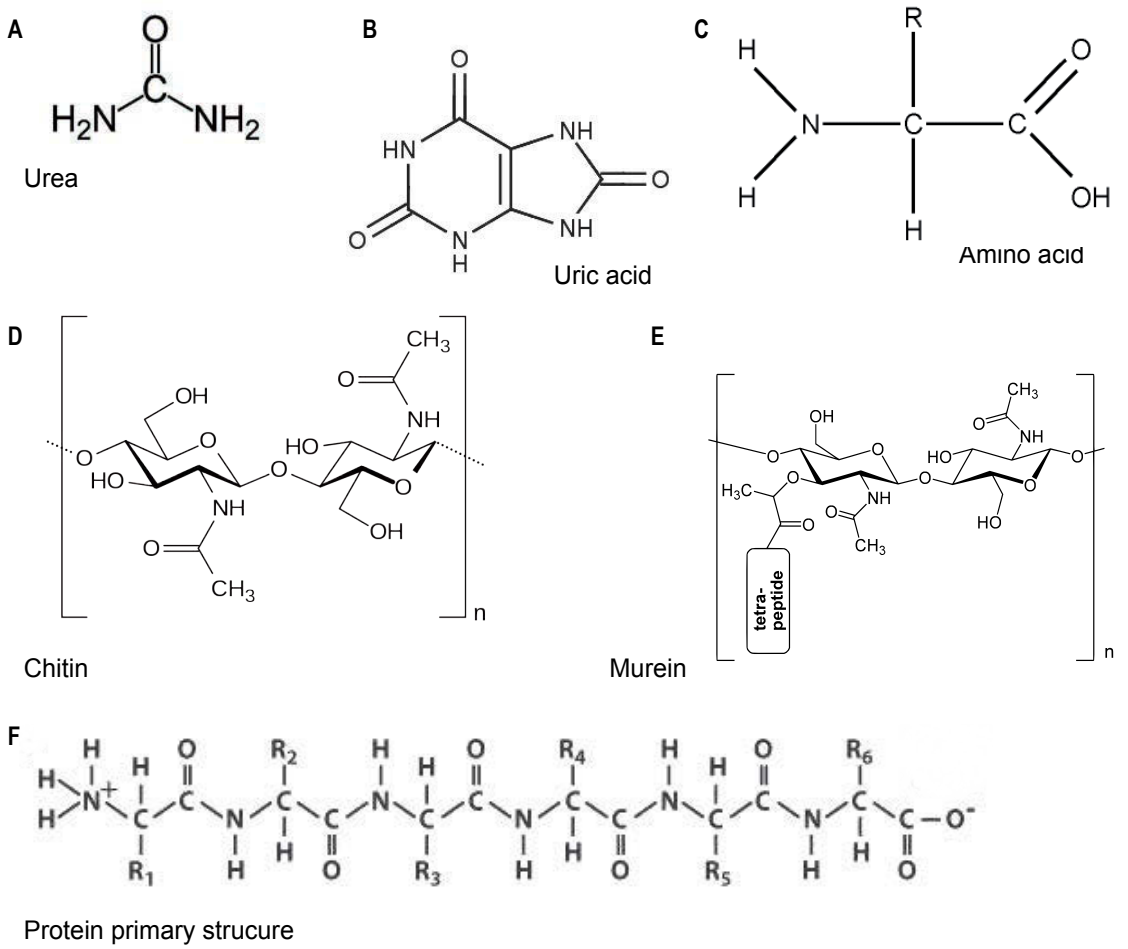


Fig. 4.3- Some nitrogenous compounds molecule structure: A) RNA, DNA, and associated nucleotides, B) urea, C) uric acid, D) amino acid E) chitin showing the two N-Acetylglucosamine units F) murein, and G) primary structure of a protein.

of the metabolic breakdown of purine nucleotides. Proteins consist of one or more polypeptides. A polypeptide is a single linear polymer chain of amino acids bonded together by peptide bonds between the carboxyl and amino groups of adjacent amino acid residues. Amines are organic compounds and functional groups that contain a basic nitrogen atom with a lone pair. Finally, amino acids are molecules containing an amine group, a carboxylic acid group, and a side-chain that is specific to each amino acid

4.1.4 Lipids

Lipids (Fig. 4.4) constitute a mixed group of organic compounds. The difference between them and carbohydrates is that they have a lower proportion of oxygen in their constitutive molecule. Lipids are a distinct and diverse set of small molecules consisting of eight general compound classes including 1) fatty acids, 2) glycerolipids, 3) glycerophospholipids, 4) sphingolipids, 5) sterol lipids, 6) prenol lipids, 7) saccharolipids, and 8) polyketides. Soil lipids and associated

compounds, fatty acids, waxes, and resins can be as high as 1 % to 20 % of total OM. Some fatty acids (about fifteen in soils) are able to bond humic and fulvic acids. Waxes and resin come directly from plant tissues (the former from cuticles), whereas porphyries derived mostly from chlorophyll and are generally found in small amounts (Gobat et al. 2010). Waxes are organic compounds that characteristically consist of long alkyl chains. Natural waxes are typically esters of fatty acids and long chain alcohols.

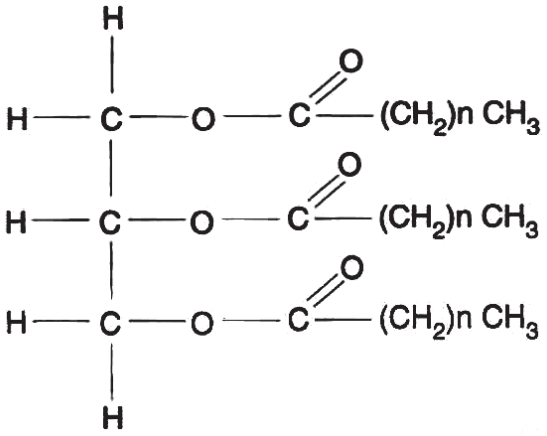


Fig 4.4- Example of a lipid molecule.

4.1.5 Lignin

Lignins are heterogeneous polymers derived from phenylpropanoid monomers (Fig. 4.5), mainly the hydroxycinnamyl alcohols, coniferyl alcohol (G-monomer) and sinapyl alcohol (S-monomer), and small amounts of p-coumaryl alcohol (H-monomer). These monolignols differ in their degree of aromatic methoxylation (-OCH_3 group). The resulting units in the lignin polymer are the guaiacyl (G), syringyl (S), and p-hydroxyphenyl (H) units. They are linked by a variety of chemical bonds that have different chemical properties. Lignin composition varies among cell types and can even be different in individual cell wall layers. Developmental and environmental parameters also influence the composition and thus the structure of the lignin polymer (van Parijs et al. 2010). After polysaccharides, lignin is the most abundant biopolymer in nature and a large contributor to terrestrial biomass residues because only a few organisms are able to degrade it (mainly Fungi).

4.1.6 Humified organic substance

When organic matter falls on mineral substrate, it undergoes three possible types of transformations: mineralization, humification or assimilation by microorganisms. Organic substances resulting from humification are broadly grouped according to their molecular mass (Buffle et al. 1977; Stevenson 1982; Gobat et al. 2010). They are described as crenic, hymatomelanic, fulvic, and humic acids (grey and brown) and humins (Fig. 4.6).

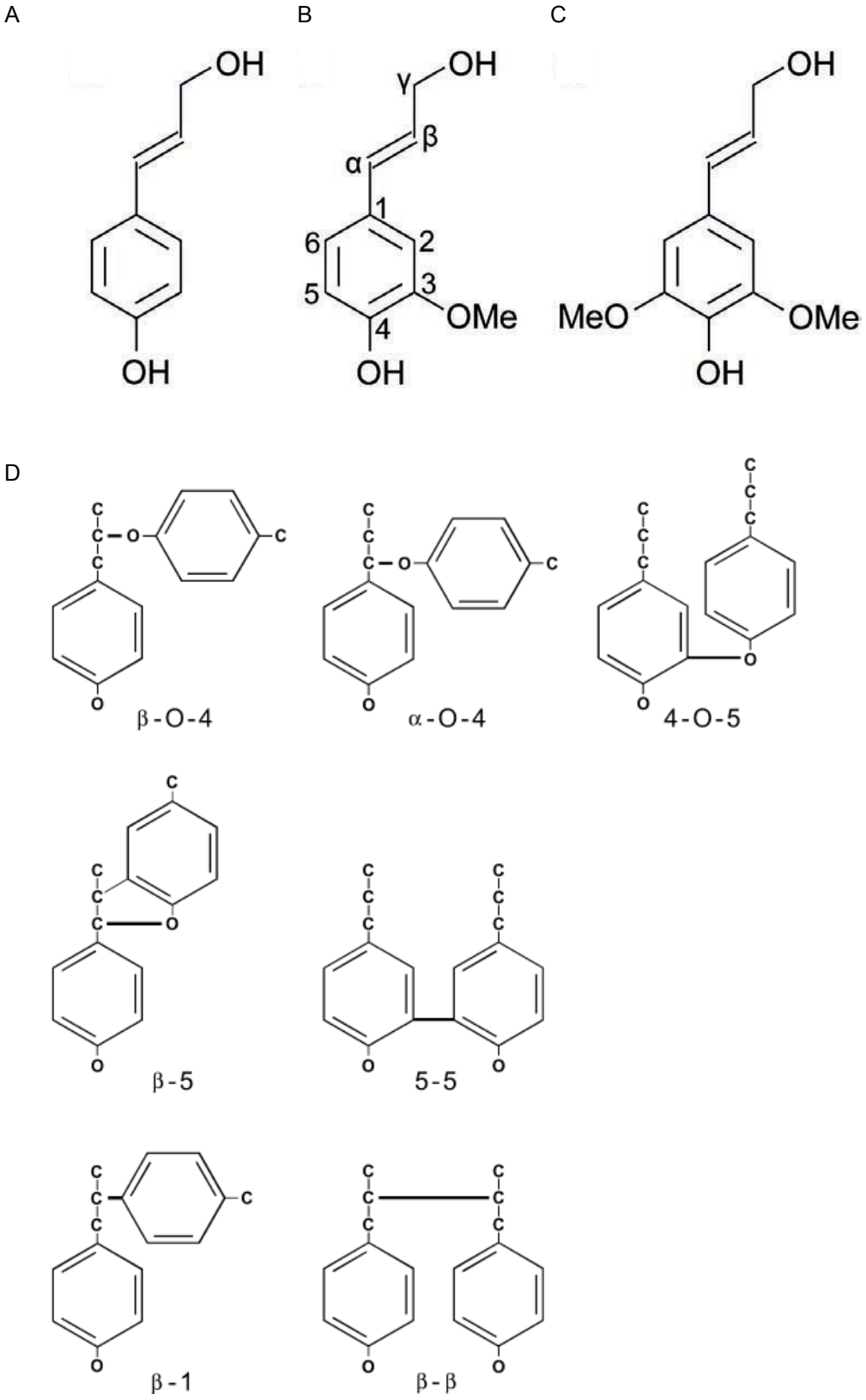


Fig. 4.5- Chemical structures of three monolignols: A) H-monomer (p-coumaryl alcohol), B) G-monomer (coniferyl alcohol) and C) S-monomer (sinapyl alcohol). D) Structure of the major bonds in lignin (from Kögel-Knabner 2002).

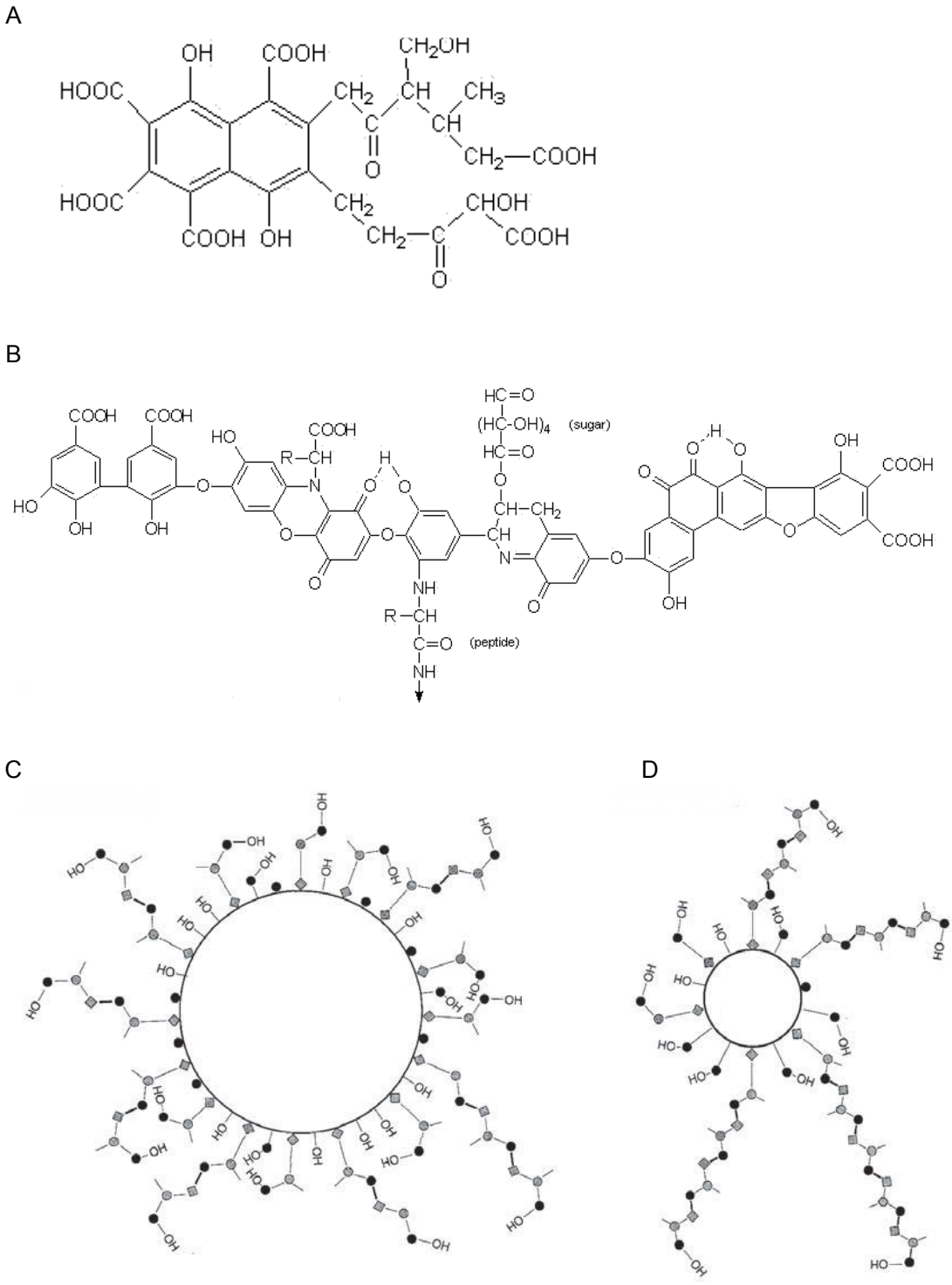


Fig. 4.6- Molecular structure (A and B) and general structure (C and D) of fulvic acid (A and C) and humic acid (B and D; from Buffle et al. 1977; Stevenson et al. 1982; Gobat et al. 2010)

4.2 Objectives of the chapter

In the Rock-Eval apparatus, bulk dry samples are heated in an inert atmosphere. During pyrolysis, the main emission products (hydrocarbons, CO_2, CO) are quantified by flame-ionization (FI) and infrared (IR) detection. These measurements are used to calculate several basic parameters, such as total organic carbon content, thermal maturity, and Hydrogen and Oxygen Indices, which are correlated to H/C and O/C values, respectively (Espitalié et al. 1977). Recent studies have shown that these various parameters, completed with morphological study of pyrolysis curves, constitute a powerful tool to study soil OM (Disnar et al. 2003; Lal 2004; Sebag et al. 2006; Disnar et al. 2008). Thus Rock-Eval technique allows bulk immature organic matter to be characterized and accurately describes soil C stocks and C dynamics in soil profiles

Fresh and decayed organic matter (soil organic matter) is characterized by a large variability in its structure and consequently in the nature and strength of chemical bonds (see paragraph 1.1). This organic matter will crack when pyrolysis conditions are applied, giving rise to a large diversity of pyrograms. The objective of this chapter is to evaluate if it would be possible to identify some particular tissue signature. In other words, this study aims at testing if any characteristic shape found in some pyrograms of non-decayed materials can be correlated to a particular stage of organic matter (fresh organic matter, decayed organic matter, or soil organic matter).

Based on Chapter 1, we saw that part of carbon (the one bound to organic components) can be followed through the oxalate-carbonate pathway in the studied system. The total organic carbon (TOC) amount will be used to draw a carbon balance of the system presented in Chapter 7. The C/N value, measured with a Carlo-Erba-Elemental-Analyser, will give information on the mineralization stage of the soil layer.

4.3 Samples

Analysed samples are plant material (wood and leaves at different degradation stages), fungal melanin, fungal and herbaceous material (grass and Rumex), soils from Burkina Faso and Salina. As the oxalate-carbonate pathway influences these soils, pure Ca-oxalate crystals are analysed as well.

4.4 Results and discussion: usual Rock-Eval parameters

4.4.1 Fresh organic material

Rock-Eval6 results of analysed “fresh OM” are given in Table 4.2. Analysed fungal material, wood, and leaves have a pyrolysable carbon (PC), varying between 11% (melanin) and 23% (*A. africana* leaves) and a residual carbon (RC), varying between 15% (fresh *M. excelsa* leaves) and

Samples	PC [%]	RC [%]	TOC [%]	MINC [%]	HI [mg HC/g TOC]	OI [mg CO2/g TOC]	HI/OI	Weight [mg]	File
Boletus sp.	18	21	39	0	504	183	2.75	50.7	1850A21.r00
Fusarium sp.	12	25	37	1	340	170	2.00	30.2	1850A20.r00
Melanine	11	32	43	1	253	143	1.77	39.6	1850A24.r00
A. africana wood	14	18	31	2	478	138	3.47	45.7	1850A23.r00
A. africana dried leaves	23	16	40	1	669	130	5.14	22.5	1586B26.r00
M. excelsa dried leaves	14	20	34	3	425	192	2.21	61.6	1586D33.r00
M. excelsa rotted leaves	14	15	29	1	441	189	2.33	49.7	1700d24.r00
M. excelsa fresh leaves	19	15	34	2	578	270	2.15	62.0	1586D31.r00
Grass fresh leaves	16	19	36	1	467	252	1.86	52.2	1586D32.r00
Rumex alpinus dried leaves	15	28	43	1	309	314	0.98	56.6	1586D29.r00
Oak dried leaves	17	20	37	2	473	244	1.94	48.6	1586D30.r00
Insects (termites and ants)	23	20	43	1	590	168	3.50	44.2	1586D35.r00
Termite nest	0	0	0	0	0	1104	0.00	63.4	1586D34.r00
Ca-oxalate	0	0	0	8	0	325	0.00	56.6	1850A22.r00

Table 4.2- Rock-Eval 6 parameters for "fresh organic material". See Annex 4 for soils.

32% (melanin). As a consequence, total organic carbon (TOC) varies between 31% (*A. africana* wood) and 43% (*R. alpinus*, melanin, and insect material), whereas mineral carbon (MINC) spans from 0% (*Boletus sp.*) to 3% (dried *M. excelsa* leaves). Rock-Eval6 analyses of leaves and wood of different species from a mangrove display TOC contents varying from 34% to 42% (Marchand et al. 2008), i.e. in the same range as the values obtained in this study. *A. africana* leaves contain 40% of carbon (C). This result is in agreement with data obtained with a CN analyzer-mass spectrometer (ANCA-GSL Preparation Module+20-20 Stable Isotope Analyzer, Europa Scientific; Oorts et al. 2003). Oorts et al. (2003) measured the C loss from fresh to litter leaves and the C present in the first 10 cm of a soil; these three samples contain 467 ± 5 g/kg, 286 ± 39 g/kg, and 8 ± 1 g/kg of C, respectively. This result shows that, in litter leaves, the C content is about half of the fresh leaves and 98% of the total C is lost during decaying. In contrast, the difference between fresh and dried leaves from *M. excelsa* tree is close to zero. This result is probably depending on sample properties, conservation methods, or sampling period. The mineral carbon signal could also have a different origin (see below).

A high Hydrogen Index (HI) is normally typical for fresh and fragmented litter (Disnar et al. 2003). It is comprised between 253 (melanin) and 669 mg HC/g TOC (*A. africana* leaves; Fig. 4.7). These results do not show a significant difference in the HI index between wood and leaves, as pointed out as well by Marchand et al. (2008).

The Oxygen Index (OI) varies between 138 (*A. africana* wood) and 314 mg CO_2/g TOC (*R. alpinus*). Scattered data points in the HI-OI diagram are emphasizing the varying composition of analysed material (Disnar et al. 2003). Surprisingly, *Oak sp.* and grass have the same HI and OI index values, whereas no difference is recorded for M. *excelsa* dried and rotten leaves. The HI/OI index varies from 0.98 (*R. alpinus*) to 5.14 (*A. africana* dried leaves) and is typical of

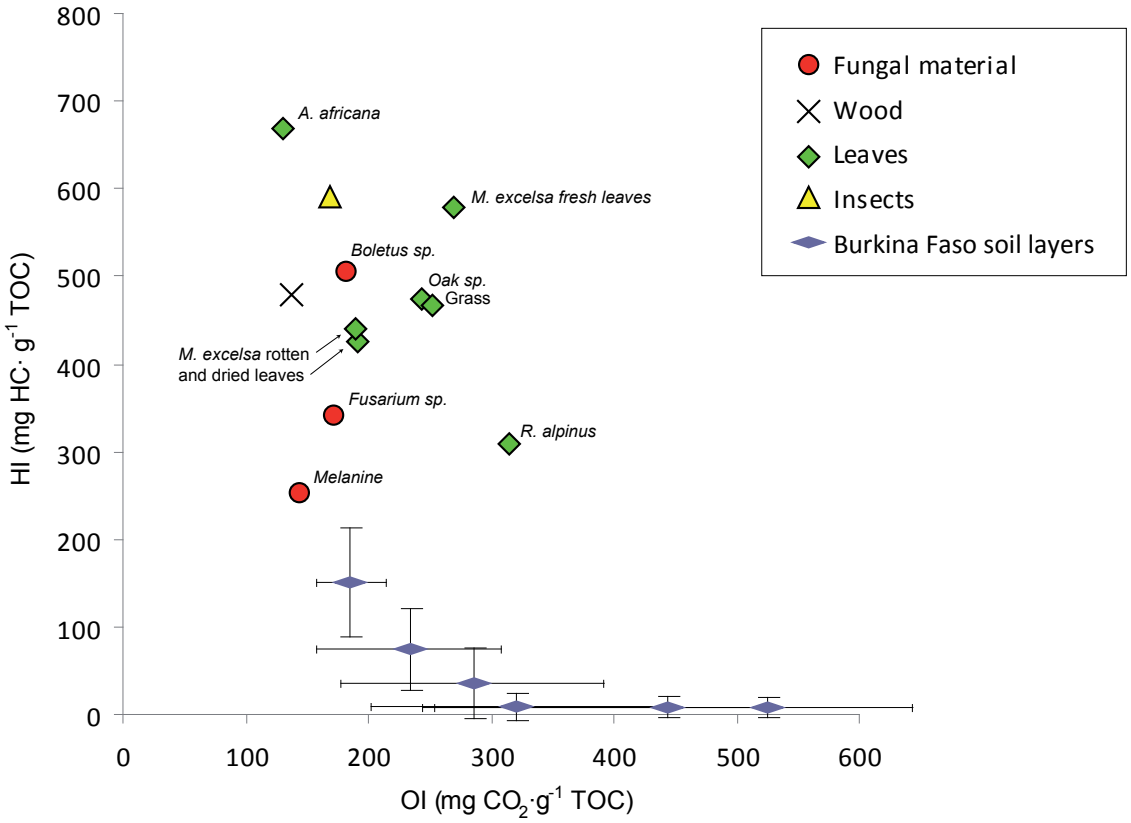


Fig. 4.7- HI vs. OI diagram for "fresh organic material" completed with soil layer results showing high HI values for fresh material. See Fig. 4.10 for soils data.

non-degraded organic material (Disnar et al. 2003). The maximum release of hydrocarbonaceous compounds (TpS2; Fig. 4.8) takes place between 251°C (grass) and 353°C (ants and termites) and is typical of immature OM (i.e. Tmax < 435°C; Espitalié et al. 1985). The termite nest shows very particular results. The TOC is 0.22%, whereas MINC yields 0.11%. The HI index shows 0 mg HC· g^{-1} TOC, whereas the OI is surprisingly high, showing 1104 mg CO_2· g^{-1} TOC. The organic carbon only contains a few hydrocarbonaceous products.

4.4.2 The reference soil: F3

Results are presented in Annex 4. The *M. excelsa* reference soil (F3 profile) is characterized by a TOC < 0.43%, with a dominant RC signal (85% of the TOC), and a MINC < 0.08%. TC (total carbon) reaches 0.51% in the first horizon (F3 Hs) and has a constant value of 0.23 ± 0.05% in the underlying layers. The C reservoir of this soil is very low if compared to those found in Cameroon or Congo Savannah (Disnar et al. 2003). This is probably due to 1) the sandy properties of this soil (70% of sand) promoting leaching, 2) and/or the content of clay minerals with insufficient absorbing properties (kaolinite clay type), 3) and/or the sampling period (November, after the rain period), 4) and/or the organic matter quality (predominance of grass). HI (hydrogen index) values are close to 0 mg HC g^{-1} TOC with three exceptions in Ak1 horizon (36 mg HC g^{-1} TOC), H2

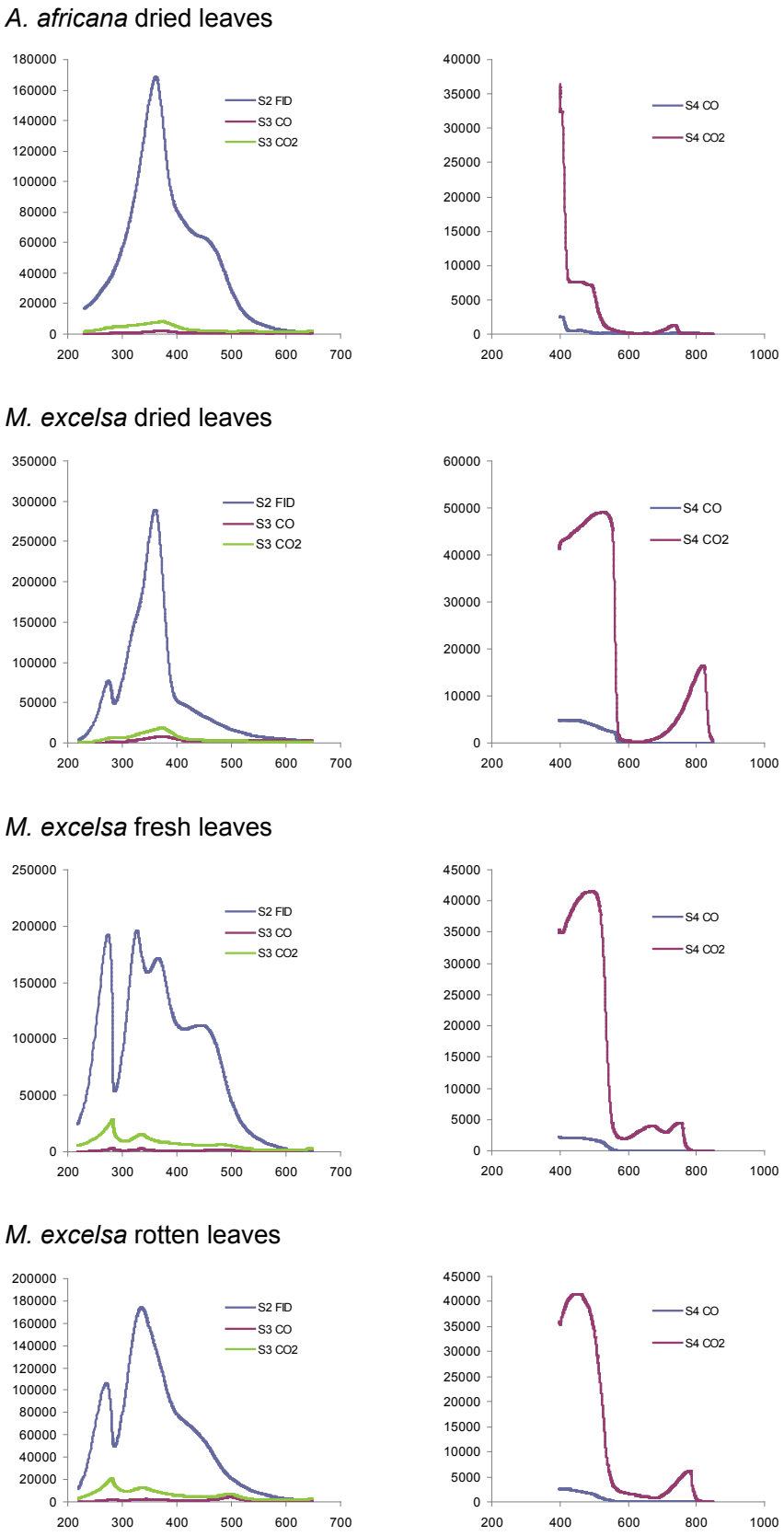
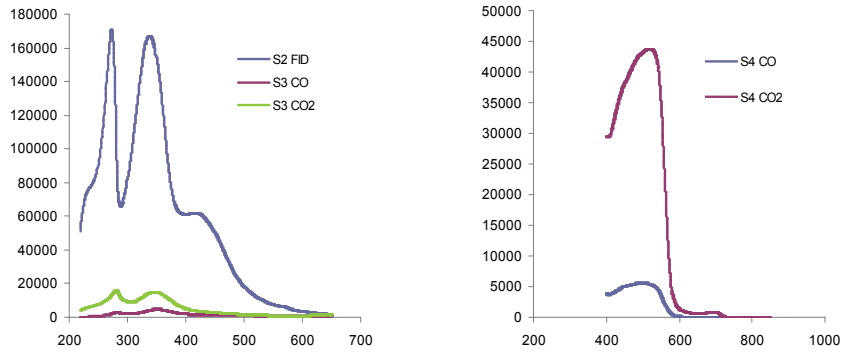
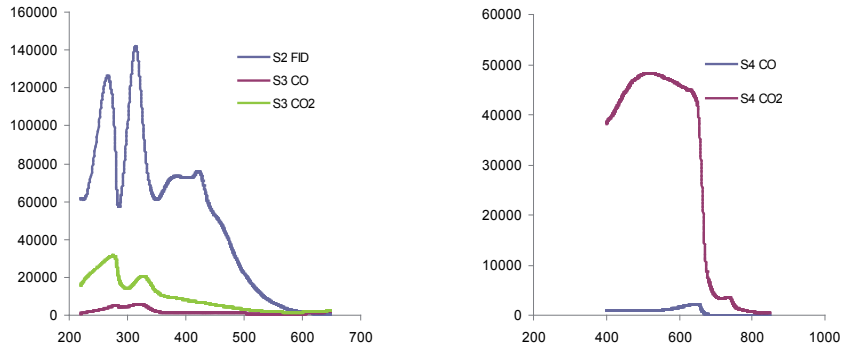


Fig. 4.8- S2 FID (left blue line), S3 CO (left red line), S3 CO2 (left green line), S4 CO (right red line), and S4 CO2 (right blue line) spectra for Ca-oxalate and "fresh organic material". X-axis: oven temperature (°C); Y-axis: relative intensity of released compounds. See also Annex 7 and Annex 8.

Grass



R. alpinus



Oak sp.

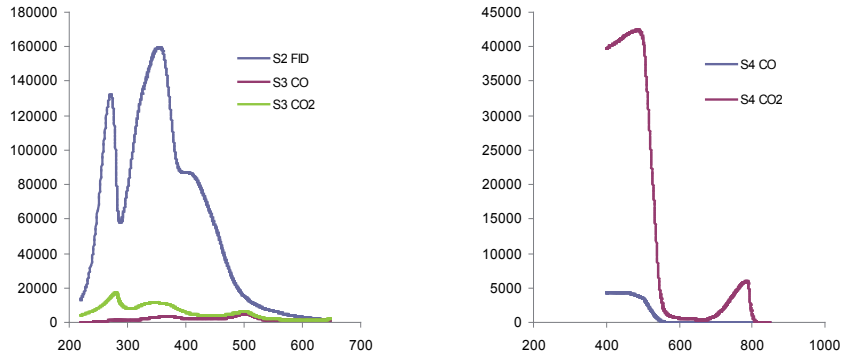
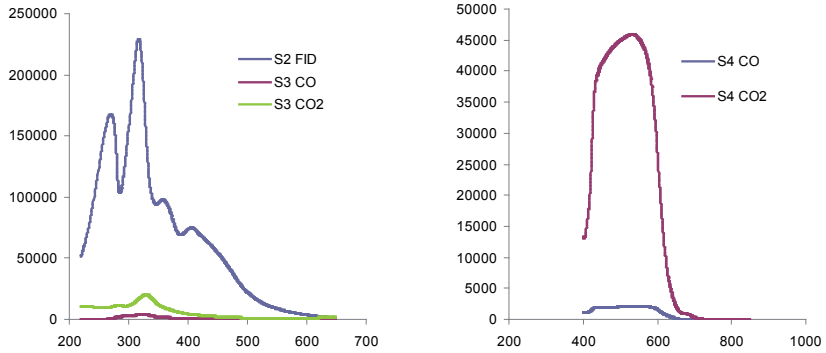
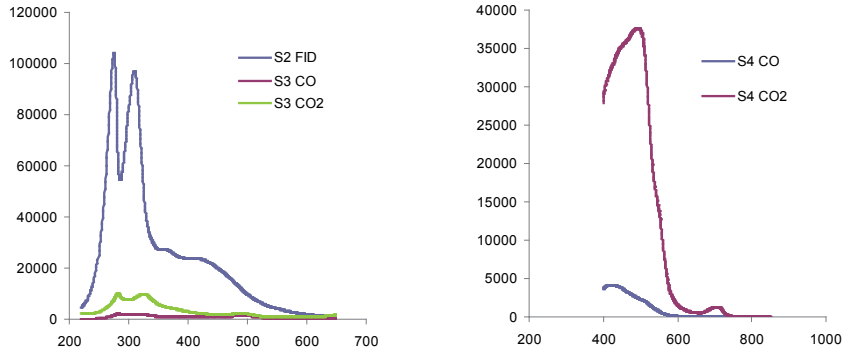


Fig. 4.8- Continued

Boletus sp.



Fusarium sp.



Melanin

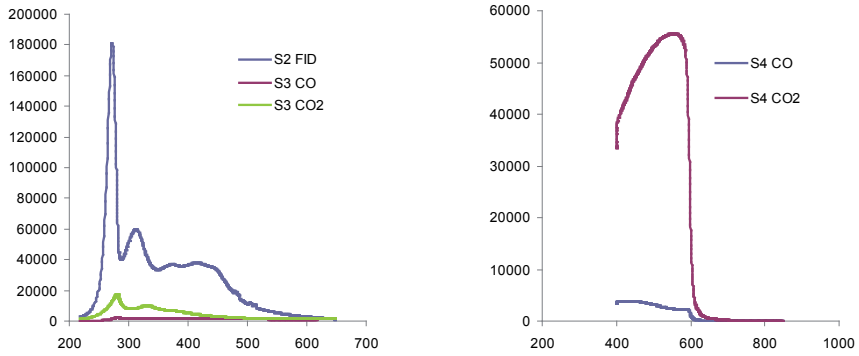
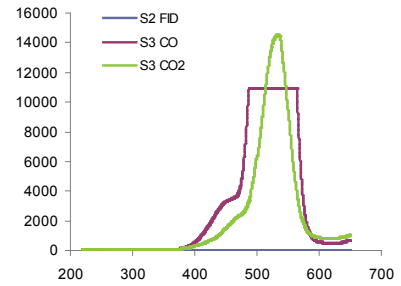
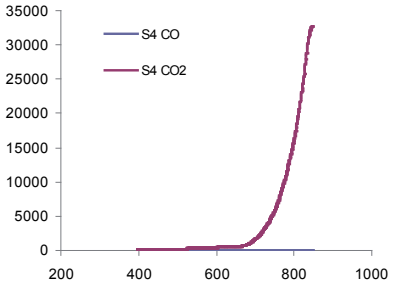


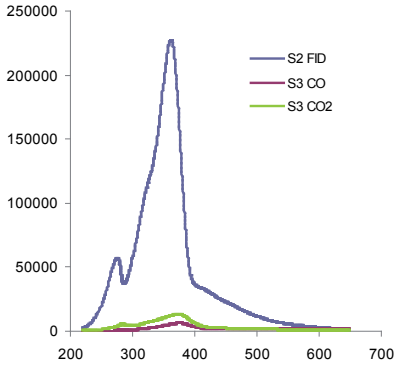
Fig. 4.8- Continued

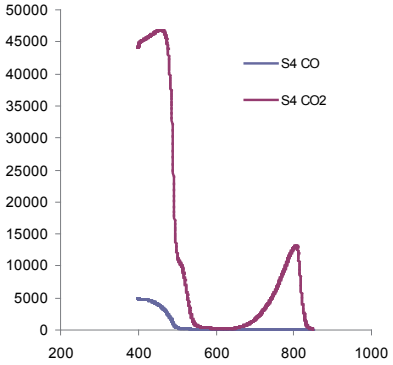
Ca-oxalate salt



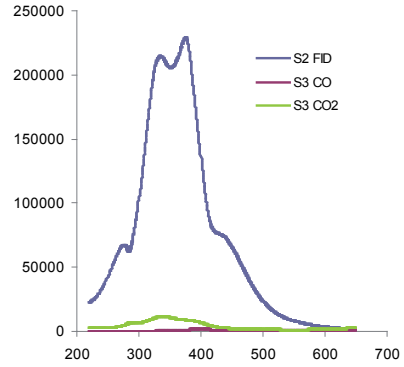


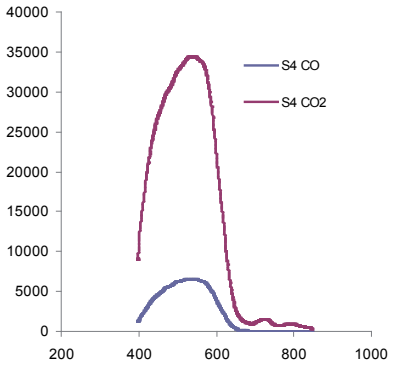
A. africana wood



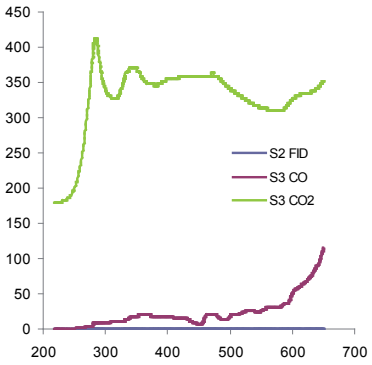


Insects





Termite nest



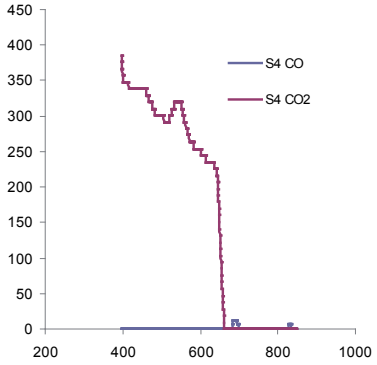


Fig. 4.8- Continued

horizon (17 mg HC g^{-1} TOC), and Bck2 horizon (18 mg HC g^{-1} TOC) replicates. A third analysis would be necessary to calculate a standard deviation, but the low HI values confirm the total and rapid dehydrogenation of the litter (grass type) from 400 to 0 mg HC g^{-1} TOC in the first soil layer (this study and Disnar et al. 2003). Moreover, with N (nitrogen) values closed to 0% (Annex 5), the essentially mineral character of this soil is confirmed. OI (oxygen index) values increase with depth from 224 to 892 mg CO_2 g^{-1} TOC, indicating that, with increasing depth, the C stock is present in oxygenated rather than hydrocarbonaceous material. The C/N ratio, usually regarded as a mineralization rate, has not been used. In fact, the variation amplitude of this ratio is low and its relationship with the speed of mineralization is not very precise. The relevance of information given by this technique would thus be very limited.

4.4.3 Soil related to oxalogenic trees

In soils related to *M. excelsa* trees (P1, P2, P3, and P4 profiles) 7.21% to 0.03% TOC is present. The general trend is a decrease with depth. About 70% of TOC is present in the first 10 cm: 2.34 ± 1.94% vs. 0.39 ± 0.26% in the following centimetres. Values of 2% for MINC are imputable to carbonate concretions and the presence of Ca-oxalate crystals (see Chapter 6 and Chapter 7). So, total carbon (TC) could represent a range of 9.23% to 2.86% at the soil surface (0 cm). Average value of TC in the soil first horizons is 4.54 ± 2.26%. The second horizon (Ak2) contains 1.24 ± 1.01% TC and the following horizon contains 0.45 ± 0.25% TC. The C stock is thus located principally in the first millimetres of the soil and is also appreciable in the first soil layers. The HI values for the first soil layer (Ak1) range from 554 to 134 mg HC g^{-1} TOC. In the Ak2 horizons, HI is comprised between 139 and 25 mg HC g^{-1} TOC, in Bck1, HI values are < 290 mg HC g^{-1} TOC, whereas in Bck2, C1, and C2, it is < 66 mg HC g^{-1} TOC. OI values are distributed between 143 and 1053 mg CO_2 g^{-1} TOC.

HI/OI values greater than 1.4 found in P1 and P2 profiles at the surface indicate the presence of relatively little transformed biopolymers as well as slow biological activity caused by xeric conditions. The high presence of wood fragments and fungal hyphae in P3 profile (Fig. 4.9) is indicated by high HI and OI values and a HI/OI ratio < 0.9.



Fig. 4.9- Detail from a root from the M. excelsa *stump colonized by fungal mycelia.*

The HI vs. OI diagram (Fig. 4.10) highlights the decrease of HI values from Ak1 to Ak2 and Bck1 in soils, influenced by M. *excelsa* tree material (leaves and wood). This trend shows the high transformation of plant input, due to high biological activity, and evidences the three main layers

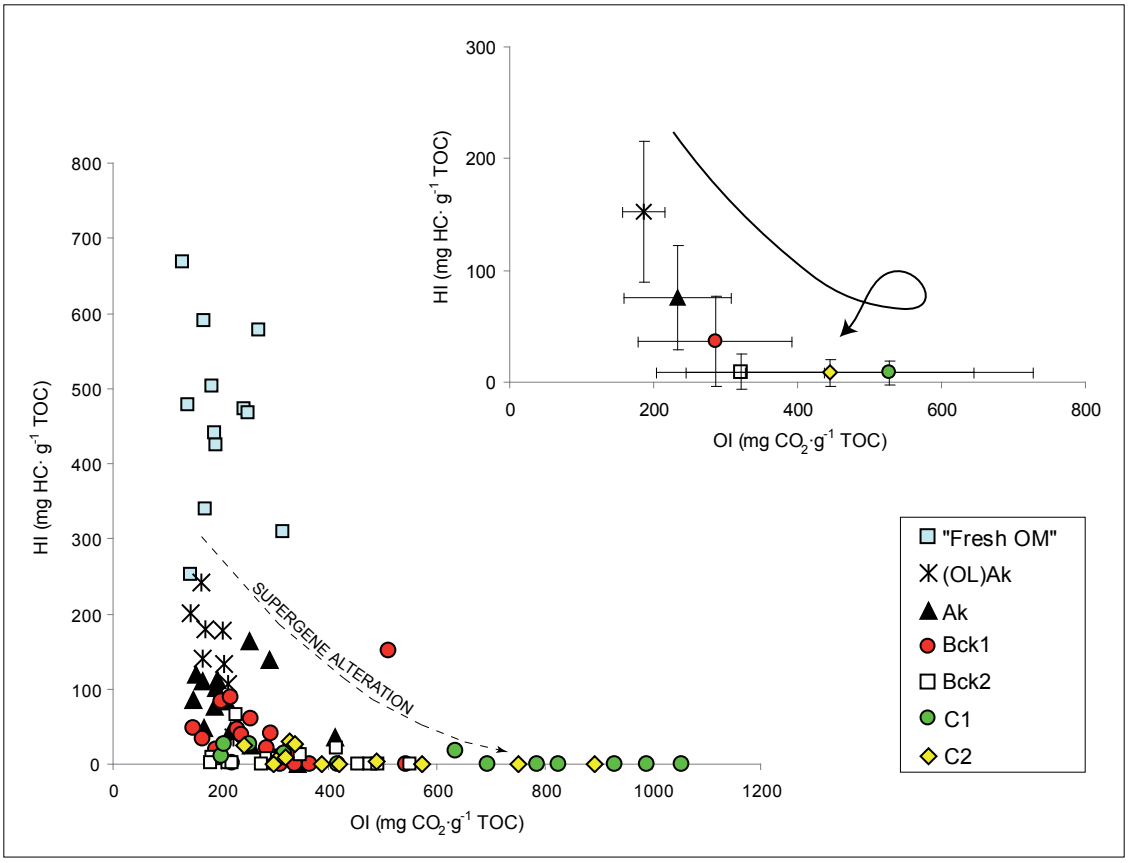


Fig. 4.10- Oxygen and hydrogen indices of Burkina Faso samples plotted on a modified van Krevelen diagram.

implicated in the quasi total loss of the C stock in its organic form. A functional transition, taking place in the second and third soil layers (Ak2 and Bck1), is also pointed out. Profile trend is a decrease of the HI parameter in Ak1, Ak2, and Bck1 horizons with an increase of OI values in the Bck2, C1, and C2 horizons: there is a dehydrogenation and a subsequent oxygenation with depth. Loss of hydrogen (dehydrogenation) could be imputable to an increasing humification (Disnar et al. 2003). Increase of O/C ratio could be related to a gain in oxygen but also an impoverishment in hydrogen atoms, as well as a loss of C. Organic chains are shorter and shorter and are dominated by oxygen ions. A decrease of oxygen rich molecules takes place between the C1 and C2 layers showing the degradation of the last organic chains.

The difference of SOM quality in examined soils is well evidenced in the HI vs. TOC diagram (Fig. 4.11). Each analyzed profile plots in a linear trend from relative high HI and TOC values in surficial layers close to null value in deeper layers

In the soil under the *A. africana* stump (L2 profile), TOC is < 5.31% (middle part of the second horizon, 11 cm in depth; Annex 4). RC represents about 80% of the TOC. MINC decreases from 0.88% to 0.25% in the first three horizons and is imputable principally to carbonate occurrence

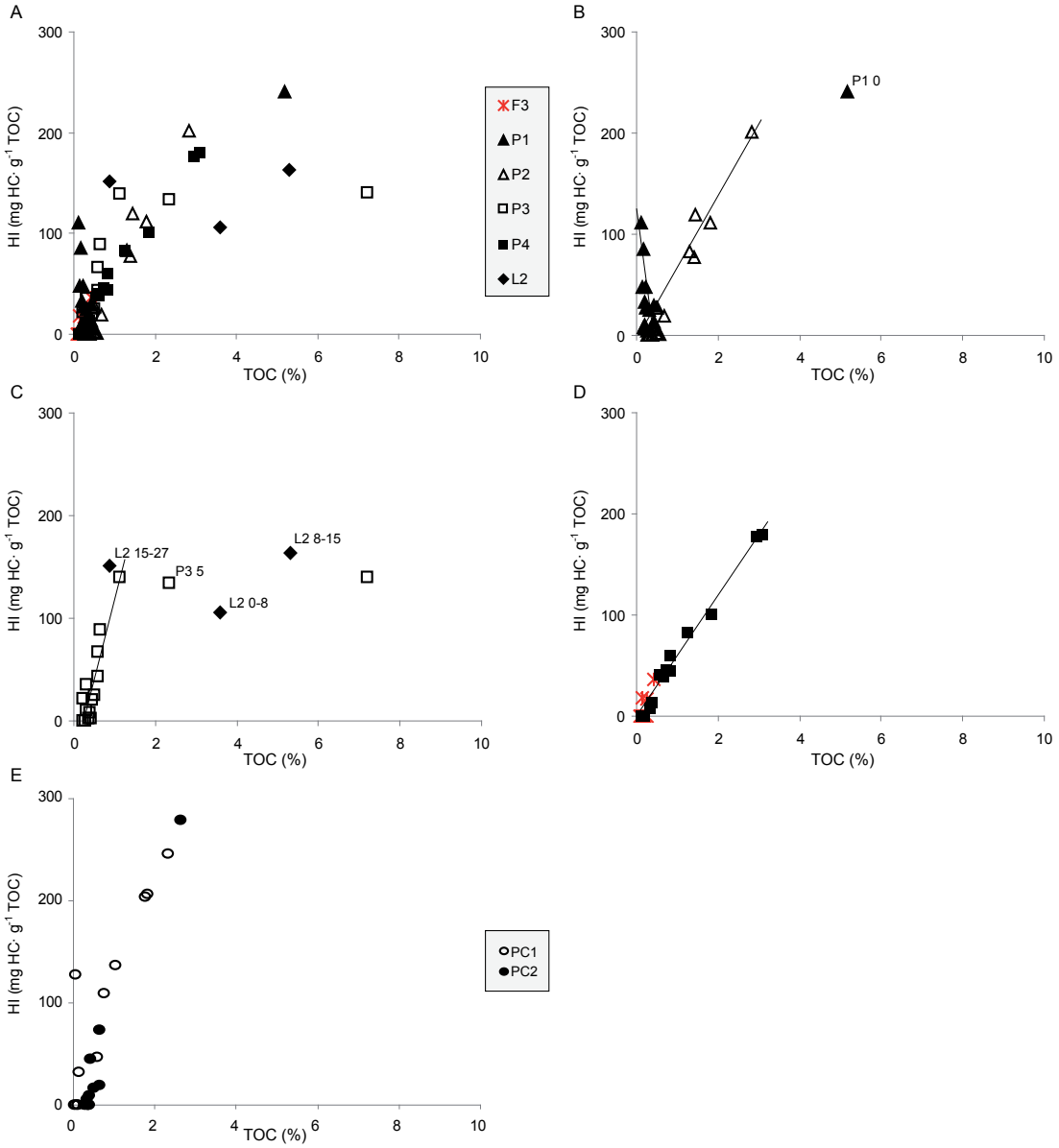


Fig. 4.11- HI vs. TOC diagram for Burkina Faso soils (A, B, C, D; F1, and P1 to P4) and Salina soils (E; PC1 and PC2).

(Chapter 6). HI is comprised between 0.88 and 0.25 mg HC g^{-1} TOC, whereas OI increases from 213 mg CO_2 g^{-1} TOC in the Ak1 to 511 mg CO_2 g^{-1} TOC in the Bck1.

4.4.4 Salina soils

Results are presented in Annexes 4 and 6. TOC in the soil under the *Opuntia sp.* (PC1 profile) varies between 2.33% and 0.59% in the first 30 cm. The deeper layers have < 0.39% TOC. The reference soil (PC2 profile) has 2.63% of TOC at the surface, decreasing to 0.45 ± 0.14%. RC is always dominant and represents more than 70% of the TOC. MINC is always < 0.16% and is imputable principally to the presence of carbonates (27.5 ± 4.5 g of carbonate/kg of soil; see

Chapter 6). In the A horizon under the cactus, HI values are between 246 and 209 mg HC g^{-1} TOC, and in Bw11 it is between 128 and 0 mg HC g^{-1} TOC, with only one exception at 55 cm (588 mg HC g^{-1} TOC). In the underlying layers, HI is close to 0 mg HC g^{-1} TOC. OI values vary between 209 and 3367 mg CO_2 g^{-1} TOC. In PC2, the HI at the soil surface accounts for 279 mg HC g^{-1} TOC. In the underlying layers, values are < 73 mg HC g^{-1} TOC. OI has a constant value of 308 ± 48 mg CO_2 g^{-1} TOC. The HI trend from Salina soils is similar to those found in Burkina Faso soils, but OI values vary between 200 and 500 mg CO_2 g^{-1} TOC with exceptions of Bw12 and Bw2 horizons, where values often exceed 700 mg CO_2 g^{-1} TOC and can reach up to 3500 mg CO_2 g^{-1} TOC (Fig. 4.12).

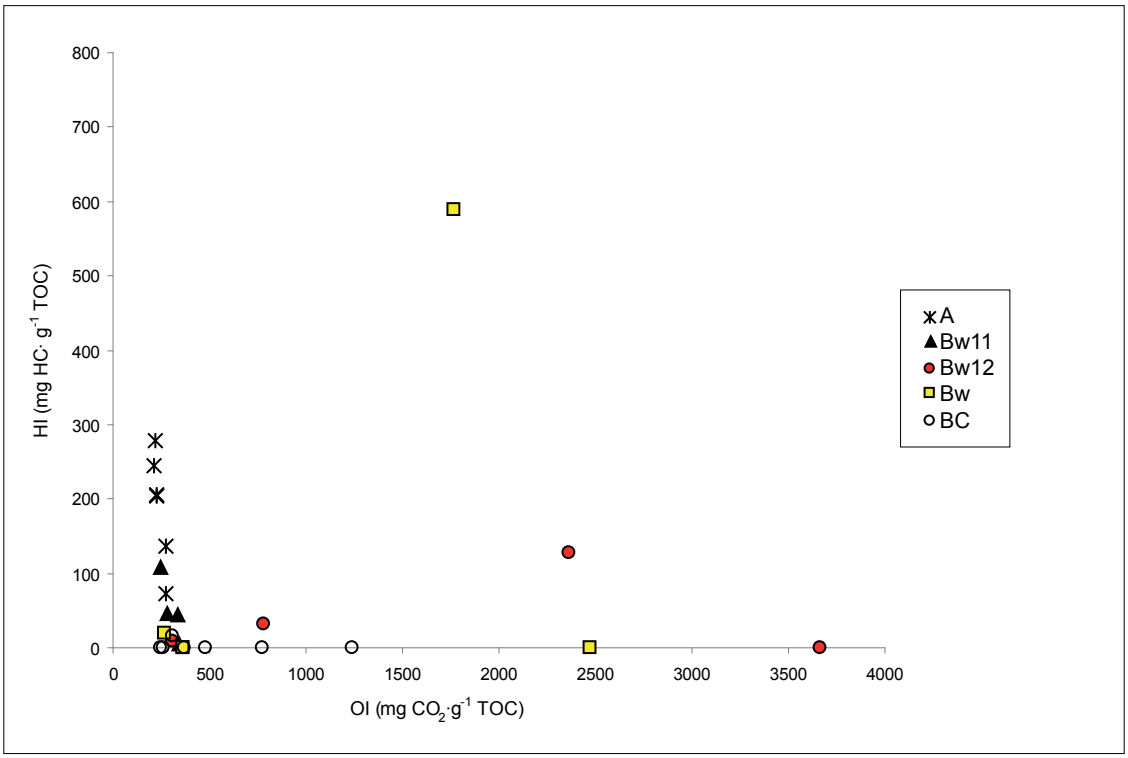


Fig. 4.12- Oxygen and hydrogen indices of Salina samples plotted on a modified van K evelen diagram.

4.5 Results: the acquisition and processing of pyrolysis and oxidation curves

The temperature record begins at 200°C. In all analysed samples, S2 peaks are non-Gaussian and display a multi-modal spectrum, typical for immature samples (Disnar et al. 2003). This multi-modal shape of S peaks indicates that the organic matter crack is not uniform but with similar chemical bonds breaking at the same temperature liberating HC (hydrocarbon). A way to study and to describe such complex S2 shapes and the associated temperature range of hydrocarbon releasing is based on deconvolution of the S2 curve in a sum of elementary descriptors (F). The employed method is called the "residual method" (Sebag et al. 2006) and processed using PeakFit v4.12 software. The goodness-of-fit is measured by correlation between the initial S2 pyrolysis signal and the sum of the resulting elementary components. This correlation is characterized by a

Pearson correlation coefficient (r; Sebag et al. 2006)

The deconvolution of the S2 pyrograms is based on four main unimodal Gaussian sub-signals F1 to F4, i.e. labile biological constituents (F1), resistant biological constituents (F2), immature non-biotic constituents (F3) and a mature refractory fraction (F4). As stipulated, these sub-peaks are reliable to major classes of organic components differing in origin and resistance to pyrolysis (Sebag et al. 2006). In the analysed samples, a component F0 has also been detected at low temperatures (± 270°C), whereas the F3 component is split into F3a and F3b (Fig. 4.13; Annex 7 and Annex 8).

Application of the residual method on S2 pyrograms from Burkina Faso (64 samples) and Salina soils (23 samples), results in a reconstruction of the initial signal at 97% with four elementary Gaussian distributions, or 99% with five elementary Gaussian distributions. Finally, six Gaussian distributions have been applied because some of them are present in some samples but not in

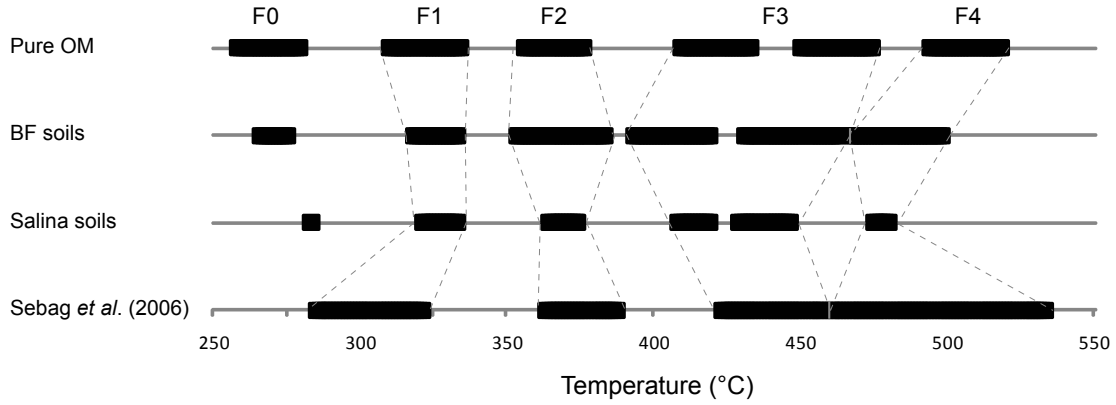


Fig. 4.13- Temperature range (°C) for F Gaussian descriptors found in this study compared to those found by Sebag et al. (2006). OM: organic matter; BF: Burkina Faso.

others. To complete the study of carbon stocks, S3 and S4 diagrams have been analysed as well.

4.5.1 Pure mineral material: Ca-oxalate

Calcium oxalate (CaC_2O_4) shows a flat pyrolysis S2 curve (Fig. 4.8) because it is not constituted of any hydrocarbons. On the other hand, the S3CO graph is bimodal with two Tpeak (the highest peak) at 460°C and 525°C. During oxalate cracking, one part of the forming CO is degassing at two different temperatures and calcium carbonate forms as well. This reaction is expressed in the following equation (Patnaik and Muralidhar 1996):

$$CaC_2O_4 \leftrightarrow CaCO_3 + CO \quad (1)$$

Similarly, the S3CO2 graph shows three peaks at 420°, 500°C, and a main peak at 530°C, with a surface proportion of 3%, 13%, and 84%, respectively. In the absence of oxygen, we suppose

(discussion with Dr. C. Glunk) that these signals are due to the cracking of a partly instable carbonate, formed by reaction (1) that can be explained by the following equation:

$$CaCO_3 \leftrightarrow CaO + CO_2 \quad (2)$$

The oxidation graph S4CO is flat. No CO is released during oxidation. The S4CO2 graph seems to be a Gaussian curve that starts around 650°C with a peak temperature close to 840°C. At this temperature, the Ca-carbonate formed during pyrolysis (reaction 1) decomposes following equation (2).

4.5.2 Plant material: wood and leaves

TpS2 (maximal hydrocarbon release) of *A. africana* wood (Fig. 4.8) appears at 360°C (F2) with a contribution area of about 50% (Fig. 4.14; Annex 7). Peaks at 270°C and 320°C represent 10% and 20%, respectively. The F3a, F3b and F4 peaks represent less than 5%. S3CO2 peaks show their maxima at 275°C and 365°C, whereas only the latter is present in the S3CO diagram. In the oxidation graph, there are two principal peaks S4CO2; a first one between 400°C and 600°C and a second one beginning at about 650°C.

S2 pyrograms from leaf material (Fig. 4.8) show similarities among the various samples. Three principal peaks are detected at 270°C, 320°C, and 370°C (Annex 7 and Annex 8; Fig. 4.14). The area underneath these three peaks can represent 20% to 30% of the total spectrum area. In *A. africana* and *M. excelsa* dried leaves, the highest contribution area is defined by the peak around 365°C. A shoulder around 460°C is also present in all leaf samples, accounting for a contribution

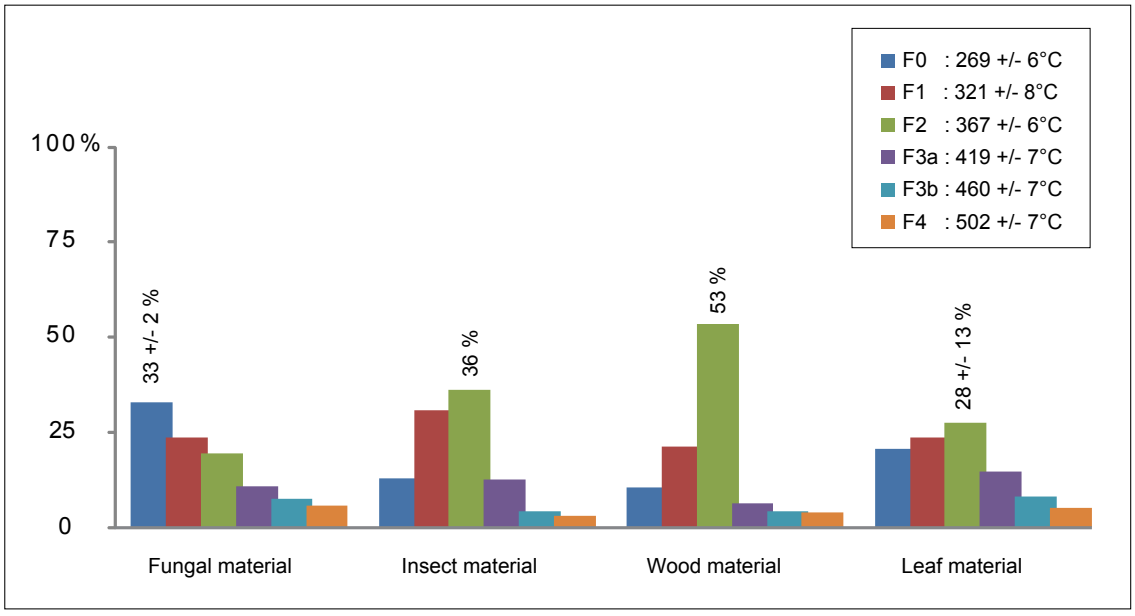


Fig. 4.14- Contribution of the Gaussian F peaks for the analyzed "fresh organic material" and associated average T°C.

area between 5% and 15%. Fresh *M. excelsa* leaves have a more complex S2 pyrogram than dried or rotten leaves. In comparison to dried leaves, dried and rotten leaves free the main hydrocarbonaceous components at temperatures of ± 270°C and ± 330°C (Fig. 4.8). *Rumex alpinus* and grass have two quasi-equivalent Tpeak around 265°C and 320°C, likely showing the mostly herbaceous quality of these two samples, when compared to *A. africana*, *M. excelsa*, and *Oak sp.* leaves, which only have one TpS2 around 360°C. This result could also represent the difference between degradation stages of leaves, if compared to the fresh *M. excelsa* pyrogram, which also contains two Tpeak at 260°C and 320°C. F3b and F4 peaks, at 460 ± 5°C and 500 ± 5°C, respectively, represent a mature refractory fraction (Sebag et al. 2006; Disnar et al. 2008) and have a small contribution to the leaf pyrograms (less than 10%; Fig. 4.14).

The S3CO2 peak of *M. excelsa* and *A. africana* leaves (Fig. 4.8) is present around 380°C, whereas other leaves show a peak maximum around 270°C. The S3CO contribution is very small. So, the main CO_2 release during pyrolysis takes place just 5°C above the release of hydrocarbon components. All the analysed leaves show a S4CO2 and S4CO peak between 400°C and 600°C (Fig. 4.8) and at least one peak around 670°C, 720°C, or 790°C. For fresh *M. excelsa* leaves, there are two peaks at 650°C and 730°C.

4.5.3 Fungal material: *Boletus sp.*, *Fusarium sp.*, and melanin

For *Boletus sp.*, *Fusarium sp.*, and melanin, the three higher peaks in the S2 pyrogram are at 270°C, 315°C, and 365°C (Fig. 4.8), representing about 80% of the hydrocarbon release (Fig. 4.14). The first peak at 270°C has a high intensity also in rotten *M. excelsa* leaves, probably due to the presence of fungi (Fig. 4.8). The following peaks at 420°C, 460°C, and 500°C represent between 5% and 15% of the signal area.

Rock-Eval6 analysis of melanin material shows a major peak (30% of contribution) at 270°C (Fig. 4.8). The following peak at 310°C and 370°C represent 20% of the FID signal. The S3CO signal is very weak; however there are two visible peaks in the S3CO2 graph, at 270°C and 315°C.

4.5.4 Insect material: ants, termites, and termite nest

The insect material S2 pyrolysis graph shows two principal peaks at 330°C and 375°C (Fig. 4.8) with a contribution area of 30% and 35%, respectively (Fig. 4.14). In the S4 oxidation graph, the organic matter peak is present between 400°C and 600°C. Two mineral S4CO2 peaks at 710°C and 780°C have been detected. The termite nest S2 pyrogram is flat. The signal of CO during the pyrolysis cycle is very weak. In the CO_2 pyrolysis graph, two peaks are present at 280°C and 330°C as well as a shoulder between 400°C and 500°C. In the CO_2 oxidation graph, there is a signal between 400°C and 600°C.

4.5.5 Soil material

Tpeak at the soil surface (0 cm) is depending on the type of organic matter that is incorporated into the mineral matrix. It appears between 360°C and 375°C for soils influenced by grass (F3) and leaves (P1 and P2), at 440°C for soils enriched in wood fragments (lignin and cellulose signal), soil attacked by termites (chitin signal) and burnt soil (P3 and L2), and at 410°C in the soil under the living tree (P4) that receives daily fresh litter (Annex 6). In deeper layers, Tpeak is between 410°C and 450°C. These temperatures are typical for immature humic substances. These results attest the rapid degradation of biological constituents in the first centimetres of soil

The displacement of Tpeak is evidenced in the mathematical deconvolution of the S2 pyrograms (Annex 6). In soils, the S2 pyrogram exhibits multiple local maxima. Consequently, deconvolution of S2 curves allows 1) classes of constituents belonging to the same energy range (cracking at the same temperature) to be separated, 2) follow up, and 3) quantification of their morphological evolution in a soil profile, 4) definition of C stock allocation, 5) maturity, and 6) stability characterization.

For Burkina Faso soils, the general depth trend for F Gaussian distributions is (Annex 6) the following: disappearance with depth of F0 and F1, increase or constancy of F2 and F3a and F3b, and decrease, disappearance or constant values of F4. Moreover, S2 curves become more and more simple (i.e. smoothing of shoulders) with soil depth, and hydrocarbon intensity becomes < 700, soon after 10 cm deep. The first peak or shoulder at 270°C (F0 descriptor) is only present at the soil surface (< 20 cm in depth) in 11 analysed soil samples and with a contribution of about 5%.

4.6 Discussion: pyrolysis and oxidation curve analyses

In general in “fresh organic material” pyrograms, the three most intense peaks appear around 270°C, 320°C, and 370°C (Annex 7 and Annex 8; Fig. 4.8), and represent more than 70% of the released hydrocarbons. In contrast, for soils, the maximum production of hydrocarbonaceous compounds (Tpeak), is not well discriminated as in fresh organic material. There are often several peaks with similar intensities in the temperature range between 350°C and 500°C (Annex 6). It is admitted that pyrolysis of biological compounds is virtually achieved at 400°C, while temperatures of 420°C and/or 440°C to 470°C are typical for humic substance decomposition (Disnar et al. 2003) and thus, normally found in soils. Moreover, in soil samples, the peaks at low temperatures disappear rapidly with increasing soil depth, in the same way as TOC. The rationale for this evolution is the progressive disappearance of the labile biological components, which are predominant in the litter, and an increase in the proportions of rather refractory geopolymers (Disnar et al. 2008).

In 11 analysed soil samples, the first peak or shoulder at 270°C (F0 descriptor) is only present at

the soil surface (< 20 cm in depth) with a contribution of about 5%. This peak does not appear in the profile under the living tree (P4) or in Salina soil (PC1 and PC2) but is present in the reference soil (F3) and in the soil near a tree stump (P1, P2, P3, and L2). Similar temperatures are also found in OF-OH, A11, and A12 horizon from a Distric ferralsol sampled in the savannah from Cameroun (Annex 9; Disnar et al. 2003). These low values of hydrocarbon release are also found in all fresh organic material, especially fungi and herbaceous material and are dominant in sugar pyrolysis graphs (see Fig. 1.b in Sebag et al. 2006). This labile fraction will be quickly degraded in soils that could in part explain its absence in the P4 profile. Salina soils are not rich in litter material whereas the African stumps are in an advanced decayed state and largely attacked by fungi and termites.

The second peak or shoulder around 330°C (F1 descriptor) is present in all soil profiles, in general between 0 and 20 cm deep. Its contribution is about 15%. This temperature range was found in Distric ferralsol (Disnar et al. 2003) and in lipid free samples, humin, and marsh soil (Hetényi et al. 2005), and was attributed to thermally labile biological compounds (Disnar et al. 2003).

The third descriptor (F2) is at 370°C and is absent only at depth > 50 cm, generally representing 8% to 100% of the S2 pyrogram area. A similar peak temperature is described in Disnar et al. (2003) as well as in Sebag et al. (2006) in pure material and soil organic matter. We also found that this is the principal release of hydrocarbon for wood, *A. africana* and *M. excelsa* dried leaves samples. During pyrolysis of pure cellulose and lignin, the maximal releasing of hydrocarbonaceous compounds take place at this temperature (Fig. 1b in Sebag et al. 2006). Cellulose is the most abundant biopolymer in soils as it comprises the major structural component of cell walls of plants and, under aerobic conditions, it decomposes slowly (Kögel-Knabner 2002). Lignin is a complex macromolecule that fills out the cell walls providing structural rigidity. Lignin is very resistant to microbial decomposition and only a limited group of fungi are able to decompose it. During biodegradation, lignin undergoes a gradual oxidative transformation process that introduces carboxyl groups in the molecule, so that the transformed molecule is thus found in the humic acid fraction (Kögel-Knabner 2002). The same process could take place in the Rock-Eval oven and explain in part the peaks present at higher temperatures than 370°C. This peak is also present in fungal material and insects. The presence of this signal in samples like fungi and insect indicates that any molecule present in these substances has the same cracking temperature than those from structural components, such as cellulose and lignin. Structural substance found typically in fungi and insects is chitin.

The other peaks are found at temperatures > 400°C, indicating more recalcitrant molecules binding hydrocarbon. F3a and F3b are present in all the analysed soil samples and represent 30 ± 20% of the S2 pyrogram area. These two peaks can also be found in pure biological components, where they represent about 10% of the S2 signal. The last shoulder is located at 480 ± 10°C. This signal could be found until a depth of 45 cm. Tpeak values greater than 470°C are usually characteristic of thermally mature organic constituents. This last fraction includes numerous constituents of

varying origin and/or nature such as stable or stabilized organic constituents, fire residues, and pollutants (Sebag et al. 2006).

In order to describe the soil hydrocarbon stock, we grouped F0, F1, and F2 that represent bio-molecules, F3a and F3b that represent labile geo-molecules, and F4 that represents stable or stabilised geo-molecules (Fig. 4.15). Bio-molecules decrease with depth but are always present, which means that 1) the production takes place in all the soil horizons, as roots and fungal mycelia are always observed, and/or 2) there is trapping and sequestration of OM in soil aggregates, such as iron concretions and, in surficial layers, carbonate concretions (see Chapter 6). The F3 contributions, with Tpeak between 410°C and 450°C, are characteristic of humic substances (Sebag et al. 2006). These components are dominant (relative contribution of 53 ± 24%) from the second to the last analysed soil horizons but represent also the highest standard deviation, signifying that, in these soils, the highest hydrocarbon stock is present as an immature, but inconstant geo-molecule form. Stable and/or stabilised hydrocarbon molecules are represented by the F4 contribution detected until a depth of 45 cm. This last fraction could represent a slower turnover of the C stock.

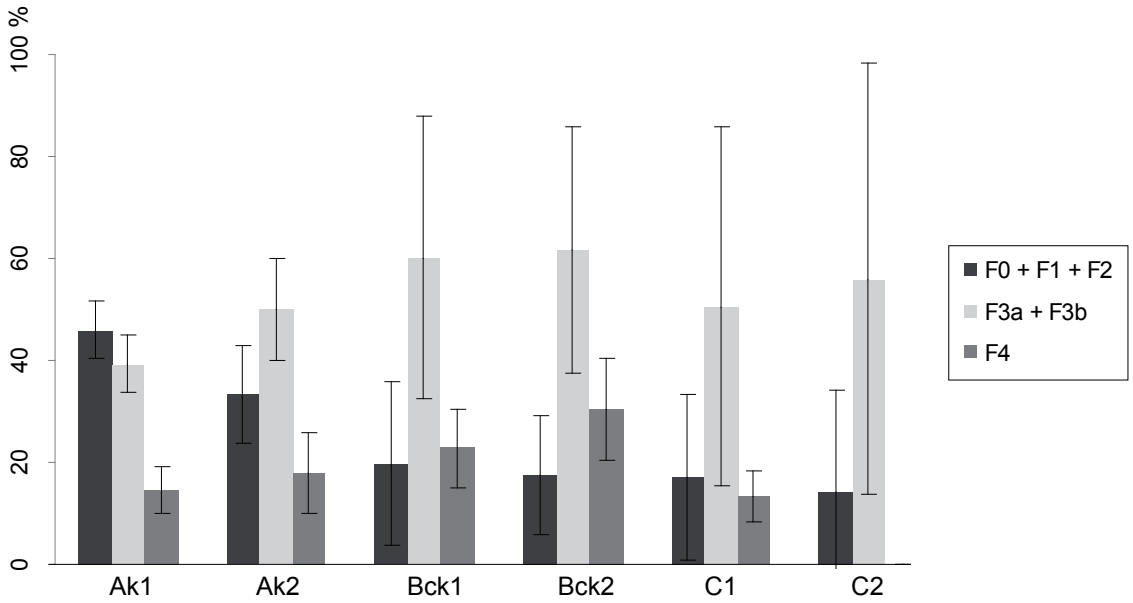


Fig. 4.15- Results from mathematical deconvolution of 64 soil samples (A to C layers) from Burkina Faso. Relationships between bio-molecules (F0 + F1 + F2) - immature geo-molecules (F3a + F3b) - stable/ stabilised geo-molecules (F4).

Consequently, it would be necessary to consider not only the S2 signal, but also the S3 and S4 components, in order to take into account the entire C signals. For "fresh organic material", the S3CO2 graphs are characterized by peaks around 270°C, between 300°C and 400°C, and around 500°C. The signal of CO presence in the S3 curves is weak but reflects the CO_2 curve. The chemical

origin of CO and CO_2 from the organic matter pyrolysis is contentious. The CO_2 could result from cracking of carboxylic, carbonyl, phenolic, hydroxy or methoxyl groups (Gerard-Zaugg 1994), but also from carboxyl or ester groups (Georgakopolous 1984). CO could result from ketone and ether decomposition (Georgakopolous 1984). Another hypothesis, by comparison with infra-red analysis, is that the acidic functions give CO_2 and CO effluents (Copard et al. 2007). CO and CO_2 could also originate from different classes of functional groups freed at known temperatures that change from one organic material to another (Lafargue et al. 1998).

In the oxidation graph (S4 curves), the peak between 400°C and 600°C appear in all the organic samples (Fig. 4.8). The CO_2 peak is associated with CO, confirming the organic origin of the carbon (Lafargue et al. 1998). In fact, this peak is due to the remains of organic carbon that was not bound with oxygen or hydrogen and could not escape during the pyrolysis phase (residual carbon). Except for melanin in the analyzed "fresh organic material", the S4CO2 oxidation graphs show peaks between 650°C and 850°C (Fig. 4.8 and Fig. 4.16), attributed to carbonate decomposition (Lafargue et al. 1998). In Figure 4.17, the dolomite oxidative decomposition shows two characteristic peaks corresponding to the following reactions:

$$CaMg(CO_3)_2 \rightarrow CaCO_3 + MgO + CO_2 \quad (3)$$

and at higher temperatures:

$$CaCO_3 \rightarrow CaO + CO_2 \quad (4)$$

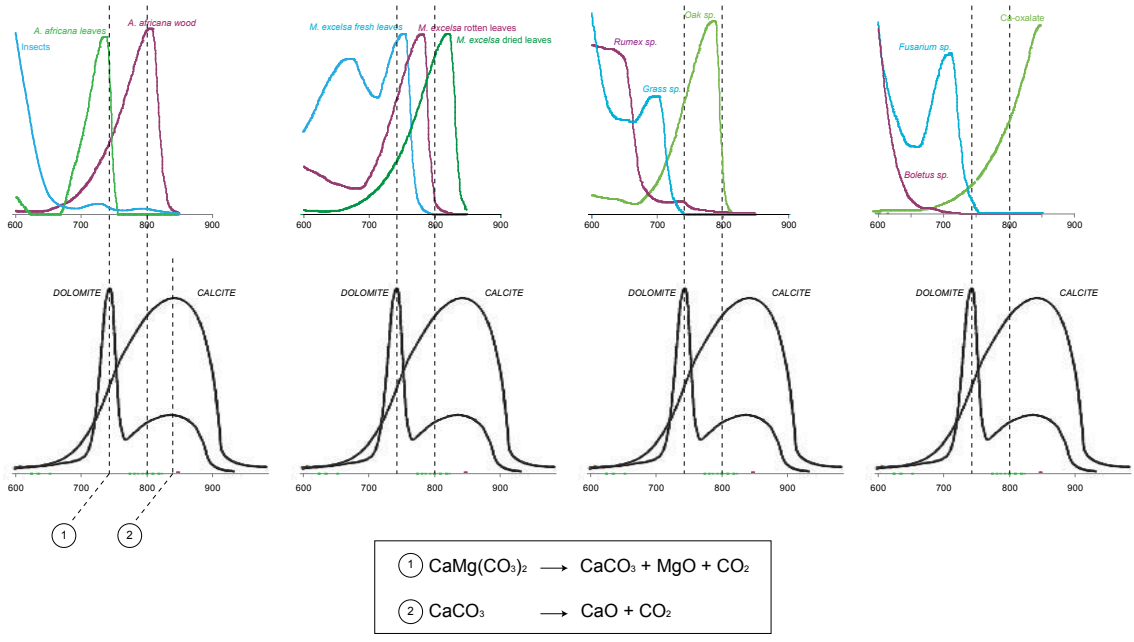


Fig. 4.16- S4CO2 spectra for "fresh organic material" compared to Figure 5 from Lafargue et al. (1998) showing the dolomite and calcite oxidation peaks. 1) and 2) are the two characteristic peak reactions resulting from the dolomite oxidative decomposition.

In contrast, calcite decomposition occurs at about 800°C and is indicated by a single peak, according to equation (4). Between 650°C and 850°C, the analyzed organic material presents five peaks at the following temperatures: 660 ± 20°C (M. *excelsa* fresh leaves, *R. alpinus*, *Oak sp.*, and *Boletus sp.*), 710 ± 10°C (insect, grass, and *Fusarium sp.*), 740 ± 10°C (*A. africana* leaves, *M. excelsa* fresh leaves, and *R. alpinus*), 770°C (M. *excelsa* rotten leaves) and around 800°C (insects, *A. africana* wood, *M. excelsa* dried leaves, *R. alpinus*, and *Oak sp.*).
The last peak emitted from calcium carbonate is also present in the Ca-oxalate oxidation graph, showing the uncertainty in interpretation, if taken alone, for the presence of calcite, Ca-oxalate, or a mix of these two minerals in the original material. A hint for the presence of Ca-oxalate is the S3CO2 peak around 510°C found in *A. africana* leaves, *M. excelsa* rotten and fresh leaves, *Oak sp.* leaves, *Fusarium sp.*, and slightly displaced in *R. alpinus*. These results corroborate X-ray diffraction patterns (Fig. 4.17), carbonate titration, and oxalate measurements. The first peak emitted from dolomite (± 740°C) is present in the S4CO2 oxidation graph from *A. africana* leaves *M. excelsa* rotten leaves, and *R. alpinus*. However, the absence of the second peak might be related to the presence of a carbonate solid solution between Mg and Ca poles. The presence of calcium carbonate crystals in leaf cells is attested in a few families such as Moraceae, Urticaceae, and Acanthaceae (Wu and Kuo-Huang 1997), whereas oxalate, soluble or insoluble, is a common salt present in plants.

In the absence of other analyses on oxalate crystals, such as X-ray diffraction, SEM or Raman spectroscopy, the following points can be stated:

- analyzed “fresh organic material” contains carbonate signatures between Mg and the Ca poles from the dolomite-carbonate solid solution;
- carbonate signature could be the sum of oxalate and carbonate pyrolysis as well as oxidation;
- oxalate could originally be Ca-oxalate or Mg-oxalate, resulting in a calcite or a dolomite signature, respectively;
- carbonate signal could be due to the cracking and recombination in the oven of any organic acid (such as carbonic, oxalic,..) or salt with an oxide (MgO or CaO), and subsequent oxidation.

Moreover so as appears in the oxidation graph the carbonate peak is also present in insect material. In fact was demonstrated that in crab exo-squeletons, among protein (25%), some pigments and lipids, chitin (35%), calcium carbonate (40%) are also present (Hiroyuki Yoshida 2006). Moreover, oxalate decomposing bacteria were isolated from the digestive systems of animals (oribatid mites, earthworms, a springtail, mayfly and a stonefly; Cromak et al. 1977), whereas calcium carbonate and calcium oxalate have been found in oribatid mites (Norton and Behan-Pelletier 1991).

All Rock-Eval6 curve (S2, S3, and S4) shapes from profile P4 (which is located under the living tree; Fig. 4.18) have been interpreted in order to complete C allocation analysis in soils. In P4 profile, the temperature of the maximal compound release in the S3CO2 curve corresponds to

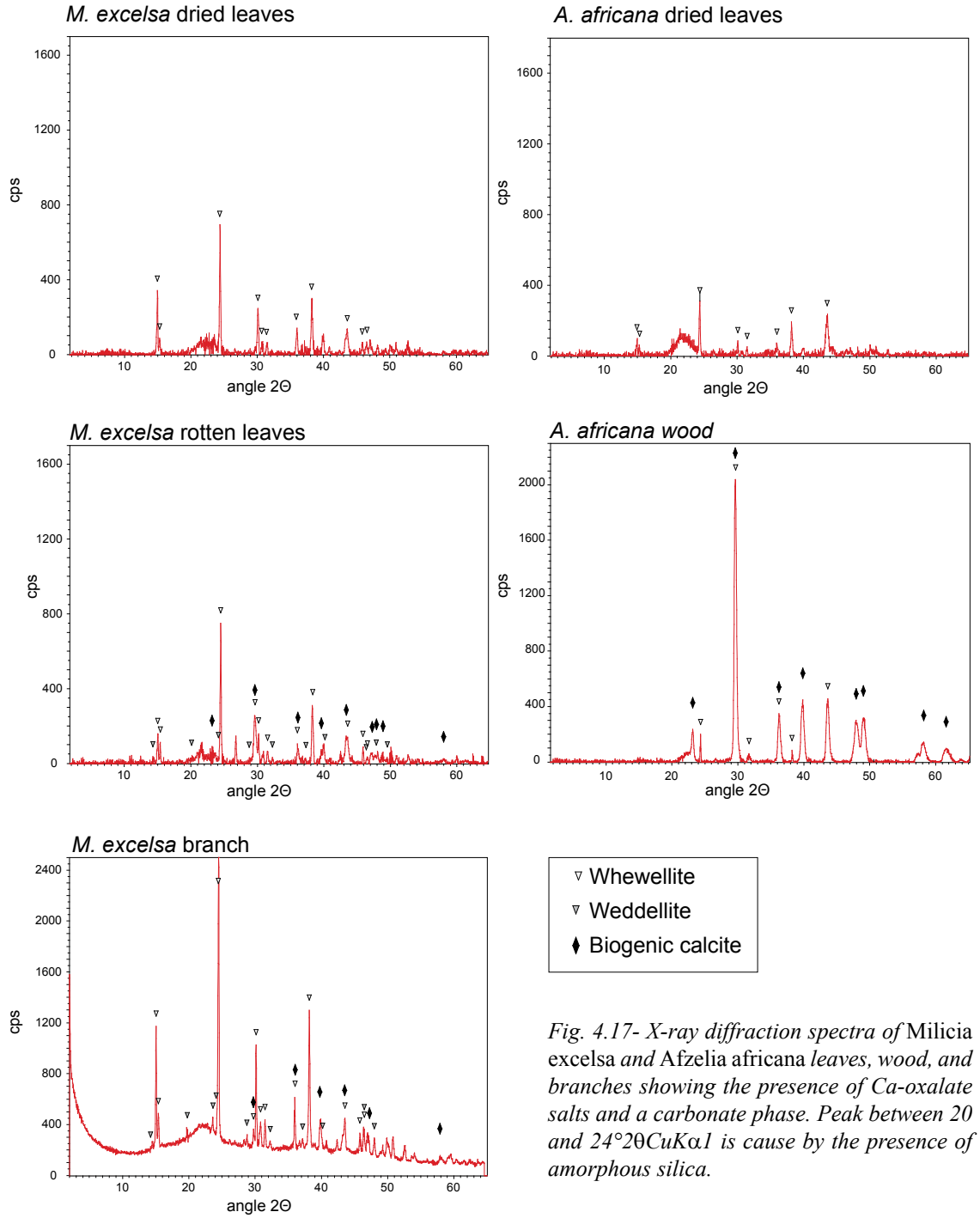


Fig. 4.17- X-ray diffraction spectra of Milicia excelsa *and* Afzelia africana *leaves, wood, and branches showing the presence of Ca-oxalate salts and a carbonate phase. Peak between 20 and 24°2θCuKα1 is cause by the presence of amorphous silica.*

the TpS2. The S3CO2 curve becomes more intense at 15 cm in depth, as well as the S2 curve, indicating an evolution of the C stock from hydrogenate to oxidized material. The S3CO2 curve is also present when the S2 signal is close to 0, indicating that this oxidized organic material is present until 65 cm in depth. The poor hydrogenate nature of this organic material is confirmed by the presence of a peak between 400 and 600°C in the S4CO2 curve. The S3CO shape is not discussed because of its low intensity and irregular shape.

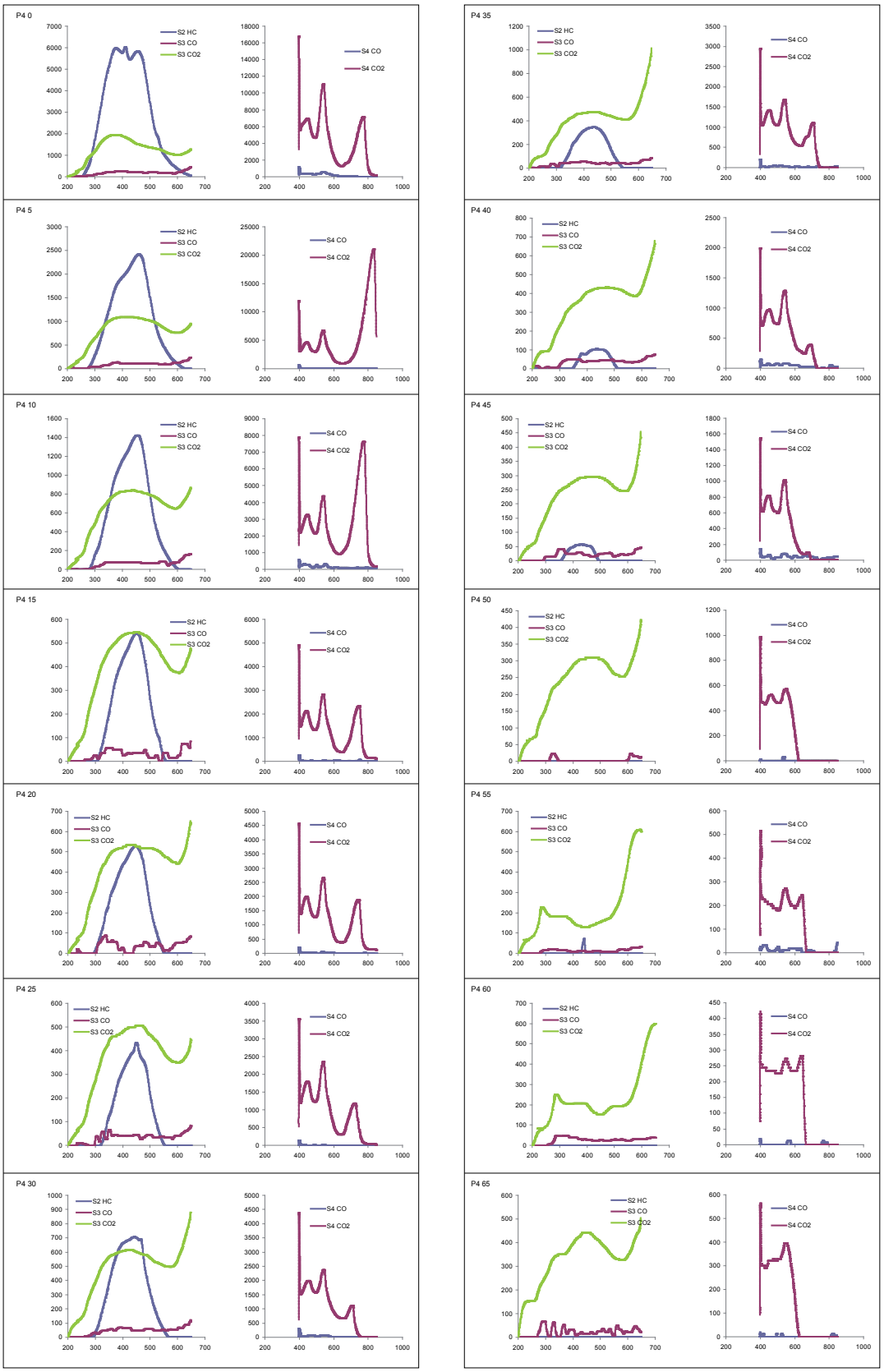


Fig. 4.18- Total Rock-Eval6 diagrams (S2, S3, and S4) for profile P4 (at 4.5 m from a living M. excelsa *tree). X-axis: oven temperature (°C); Y-axis: relative intensity of released compounds.*

The mineral signal of the S4CO2 curve shows clearly the presence of a carbonate phase from 0 to 30 cm deep confirming the carbonate titration results. The Tpeak is located between the dolomite and the calcite analysed by Lafargue et al. (1998) and is confirmed in this study by X-ray diffraction analysis (Fig. 4.17). At 35 cm, 40 cm, and 45 cm, the peak appears at slightly lower temperatures than the dolomite peak, indicating that analysed carbonates contained slightly more magnesium than the one analysed by Lafargue et al. (1998). In a complex medium, such as soils it is impossible to detect oxalate present at levels around 50 mg/kg. However, as demonstrated by the Ca-oxalate pyrolysis graph, a small peak present in P4 0 samples (i.e. at 0 cm) could indicate the presence of oxalate.

In Salina soil samples, the F0 component is always absent (Table 4.2), with the exception at the surface of the reference soil. This could probably be due to the presence of grass. Under the cactus, F1, F2, F3a, F3b, and F4 Gaussian contributions are fairly constant until a depth of 30 cm. Disappearance of the hydrocarbon signal takes place at 45 cm with the exception at 55 cm, where the amount of 558 mg HC / g^{-1} TOC gives a S2 signal that can be divided into five Gaussian components. The hydrocarbonaceous stock is also present until 45 cm deep, associated with molecules with four different thermal resistances ranging from 330°C to 470°C.

In the Salina reference soil (PC2), the S2 signals smoothen with depth (Annex 6). Moreover, Gaussian contributions disappear gradually from 0 to 50 cm, where only the F2 signal remains. Again, at a depth of 60 cm, a S2 signal is still present. When compared to the PC1 profile, enrichment in hydrocarbon material at 55/60 cm in depth is suspected.

4.7 Conclusions

The multi-modal shape of S peaks indicates that the organic matter cracking is not uniform. For complex mixing, each signal corresponds to an assemblage of organic constituents of heterogeneous nature, where chemical bonds break at the same temperature, liberating HC. About 75% of “fresh organic material” cracks at temperatures < 380°C in three distinct temperature ranges typical for biological products. Each class of analysed organic matter showed distinct S2 pyrogram shapes. For fungal material, the dominant signal is at low temperatures (270°C). This is also the dominant peak for herbaceous plants, such as grass and *R. alpinus*. For higher plants, such as *A. africana*, *M. excelsa*, and *Oak sp.*, the dominant signal is at a temperature of 360°C, as well as for wood and insects. For fungal and insect material, an important release of hydrocarbon takes place at the same temperature range than for pure lignin and cellulose pyrolysis, indicating a possible implication in chitin cracking. The degradation state (ex. fresh material vs. dried material) influences the relative S2 peak intensit .
Burkina Faso and Salina soils are very poor in organic carbon (< to 3%). The hydrocarbonaceous carbon stock can be subdivided in six classes of defined cracking temperatures and, therefore, of specifically thermal resistance and maturity. The organic carbon stock is concentrated in the

first 10 cm of soil (first two horizons) and is related to bio-molecules, whereas geo-molecules are already predominant from the second horizon downwards.

To study carbon dynamics in tropical soils, the analysis of S2 curves is not sufficient. For a more complete image of the carbon stocks, S3 and S4 signals have also to be analysed. Moreover, different sampling periods are necessary to have a complete image of the carbon stocks from analysed soils. Our conclusions are only based on soils sampled during November 2005.

Finally, the Rock-Eval6 method could indirectly, by the study of S3CO2 and S4CO2 curves, gives quick information on the eventual presence of calcium or magnesium oxalates. The Rock-Eval6 analysis remains a powerful and pertinent preliminary method to study thermal resistance of organic matter in soils but is not the best solution to characterise and quantify the whole soil constituents. The Rock-Eval6 method remains, at this stage, a black box. Almost nothing is known about the way molecular recombination can take place and causes interference with the original signal.

Chapter 5 OXALATE QUANTIFICATION

Analysis of two oxalate sources: plants oxalate and fungal oxalate

5.1 Introduction

This chapter is principally dedicated to the quantification of oxalate in plants, fungi, and soils from Burkina Faso, with a quick view at a soil from Salina (Italy) associated with *Opuntia sp*. The following main hypotheses have been tested:

- the carbonates present in soils under *M. excelsa* and *A. africana* trees result from the oxalate-carbonate pathway;
- the first oxalate source is the litter from these oxalogenic trees
- oxalogenic fungi are present in the soil and constitutes a second source of oxalate;
- despite these two oxalate sources, no oxalate accumulation is present in soils under a 70 year-old tree because of its oxidation into carbonate.

We used the modified enzymatic method after Trinity Biotech, USA (method n°591) to quantify the oxalate. The quantificati n of oxalate in leaves from plants is complementary to the previous observations made on shape of Ca-oxalate crystals in *M. excelsa* trees from Cameroon and Ivory Coast (Braissant et al. 2002; Braissant et al. 2003; Braissant et al. 2004; Braissant 2005). Burkina Faso soil oxalate is also compared to the one from Cameroon and Ivory Coast soils. These results will be used later to calculate a carbon balance of the studied system. Some cultivable oxalogenic fungi were found after isolation of strains on Malt-Agar from soil samples. The isolation and culture of oxalogenic fungi in wood, on Malt-Agar, and Ca-added medium (gypsum) allows plant and fungal crystals, as well as hyphae-oxalate relationships (with natural light and SEM), to be compared.

The objectives of this chapter are:

1) the quantifica ion of oxalate in leaves from *M. excelsa*, *A. africana*, *Opuntia sp.,* and *A. africana* wood. For comparison, we added also analyses on *Rumex alpinus* and grass (see Chapter 2 for more information about this);
2) the demonstration that in Burkina Faso soils, an oxalogenic fungal community is present. As an initial step, we will determine whether the isolated fungi from Burkina Faso are calcium oxalate producers under laboratory conditions;
3) the quantification of oxalate present in soils
4) the examination of Ca-oxalate distribution in soils related to *M. excelsa*, *A. africana*, and *Opuntia sp.*;
5) the assessment of their implication in biogeochemical Ca and carbon cycles in Burkina Faso and Salina soils.

5.2 Results and discussion

In order to facilitate the reading of this chapter, results regarding plants, fungi and soils, as well as discussion and conclusions, are given in three distinct paragraphs.

5.2.1 Results: oxalate and plants

The total oxalate contents in the foliage of various plant species found in the literature, as well as in this study, are presented in Table 5.1 (Chandler 1937; Vickery 1955; Zarembski and Hodgkinson 1962; Suvachittanont et al. 1973; Valyasevi and Dhanamitta 1974; Ciba-Geigy 1977; Kasidas and Rose 1980; Schelstraete and Kennedy 1980; Haytowicz and Matthews 1984; Ogawa et al. 1984; Awadalia et al. 1985; Souci et al. 1986; Elmadfa et al. 1992/1993; Massey et al. 1993; Guil et al. 1996; Guil-Guerrero et al. 1998; Noonan and Savage 1999; Nakata and McConn 2000; Savage et al. 2000; Perez et al. 2001; Sotomayor et al. 2001; Hönow and Hesse 2002; Kamchan et al. 2004; Kmiecik et al. 2004; Siener et al. 2006; Nakata and McConn 2007). In dry material, the total oxalate content is low in *A. africana* wood (15 mg/100 g), middle in *M. excelsa* leaves (93 ± 21 mg/100 g), high in *A. africana* leaves (278 mg/100 g) and in *Opuntia sp.* cladodes in advanced degradation state (319 mg/100 g; Fig. 5.1), and very high in fresh (frosted directly after sampling; Fig. 5.1) cladodes (844 mg/100 g) and *Rumex alpinus* (1356 mg/100 g). There are no data available for the amount of total oxalic acid in the cited plants.

To complete this study, X-ray diffraction spectra demonstrate that the oxalate present in *M. excelsa* and *A. africana* leaves is principally whewellite (Fig. 4.17). X-ray diffraction on *A. africana* wood emphasizes the presence of whewellite and a carbonate phase, detected during field excursion. Degraded organic matter such as branches and leaves of *M. excelsa,* are characterised by two kinds of Ca-oxalates with a different hydration state: whewellite and weddellite.

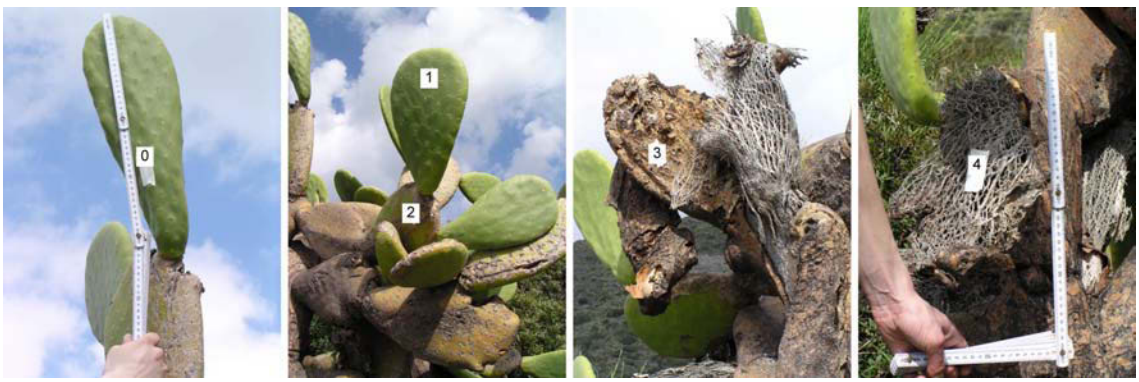


Fig. 5.1- Degradation states (from 0 to 4) of cladodes in the studied Opuntia sp. *(Salina, Italy).*

Vernacular name	Latin name	Family	Total oxalate mg / 100 g	Soil	Origin	Source
Lettuce	*Lactuca sativa*	Asteraceae	0	n.s.	n.s.	
Lettuce	*Valeriana locusta*	Valerianaceae	1	n.s.	n.s.	1
Lettuce	*Lactuca sativa*	Asteraceae	2	n.s.	n.s.	2
Lettuce	*Lactuca sativa*	Asteraceae	2	n.s.	n.s.	3
Parsley	*Petroselinum sativum*	Apiaceae	6	n.s.	n.s.	4
White pine	*Pinus strobus*	Pinaceae	7	Mesic Glossic Hapludalfs	USA, NY, Dunkirk	5
Sauerkraut	*Brassica oleracea*	Brassicaceae	7	n.s.	n.s.	1
Coriander	*Coriandrum sativum*	Apiaceae	10	n.s.	n.s.	6
Lettuce	*Lactuca sativa*	Asteraceae	11	n.s.	n.s.	7
Red oak	*Quercus borealis var. max.*	Fagaceae	11	Mesic Typic Dystrudepts	USA, NY, Lordstown	5
Lettuce	*Lactuca sativa*	Asteraceae	12	n.s.	n.s.	8
Miner's lettuce	*Montia perfoliata*	Portulacaceae	14	n.s.	n.s.	9
Chestnut oak	*Quercus montana*	Fagaceae	14	Mesic Typic Dystrudepts	USA, NY, Lordstown	5
African oak wood	*Afzelia africana*	Fabaceae	15	Ferralsol	BF, Niangoloko	T.s.
Barrel Medic	*Medicago truncata*	Fabaceae	16	Agar plate	n.s.	10
Kale	*Brassica oleracea*	Brassicaceae	20	n.s.	n.s.	6
Yellow birch	*Betula lutea*	Betulaceae	20	Mesic Typic Dystrudepts	USA, NY, Lordstown	5
Barrel Medic	*Medicago truncata*	Fabaceae	21	Greenhouse conditions	USA, TX, Houston	11
Sugar maple	*Acer saccharum*	Aceraceae	21	Mesic Typic Dystrudepts	USA, NY, Lordstown	5
White ash	*Fraxinus americana*	Oleaceae	25	Mesic Typic Dystrudepts	USA, NY, Lordstown	5
Trembling aspen	*Populus tremuloides*	Salicaceae	26	Mesic Typic Dystrudepts	USA, NY, Lordstown	5
Lemon balm	*Melissa officinalis*	Lamiaceae	27	n.s.	n.s.	1
White cedar	*Thuja occidentalis*	Cupressaceae	27	Mesic Glossic Hapludalfs	USA, NY, Dunkirk	5
Trembling aspen	*Populus tremuloides*	Salicaceae	29	Mesic Glossic Hapludalfs	USA, NY, Dunkirk	5
Basswood	*Tilia americana*	Tilaceae	49	Mesic Typic Dystrudepts	USA, NY, Lordstown	5
Rock samphire	*Crithmum maritimum*	Apiaceae	53	Anthropogenic soil	SE of Spain	12
Savory	*Satureja hortensis*	Lamiaceae	55	n.s.	n.s.	1
Peppermint	*Mentha piperita*	Lamiaceae	56	n.s.	n.s.	1
Pignut hickory	*Hicoria glabra*	Juglandaceae	57	Mesic Typic Dystrudepts	USA, NY, Lordstown	5
Cabbage	*Brassica oleracea*	Brassicaceae	60	n.s.	n.s.	8
Red cedar	*Juniperus virginiana*	Cupressaceae	61	Mesic Glossic Hapludalfs	USA, NY, Dunkirk	5
Sow-tistle-of-the-wall	*Sonchus tenerrimus*	Asteraceae	64	Anthropogenic soil	SE of Spain	12
Plantain	*Plantago major*	Plantaginaceae	67	Anthropogenic soil	SE of Spain	12
Pignut hickory	*Hicoria glabra*	Juglandaceae	73	Mesic Typic Dystrudepts	USA, NY, Lordstown	5
Sage	*Salvia officinalis*	Lamiaceae	85	n.s.	n.s.	1
Shepherd's Purse	*Capsella bursa-pastoris*	Brassicaceae	89	n.s.	S, Almeria	13
Rock-elm	*Milicia excelsa*	Moraceae	93	Ferralsol	BF, Nyanmiango	T.s.
Parsley	*Petroselinum sativum*	Apiaceae	100	n.s.	n.s.	14
Cabbage	*Brassica oleracea*	Brassicaceae	100	n.s.	n.s.	6
Lettuce	*Lactuca sativa*	Asteraceae	105	n.s.	n.s.	15
Endive	*Cichorium intybus foliosum*	Asteraceae	110	n.s.	n.s.	6
Parsley	*Petroselinum sativum*	Apiaceae	111	n.s.	n.s.	16
Chicory	*Cichorium intybus*	Asteraceae	121	n.s.	n.s.	6
Garlic Mustard	*Alliaria petiolata*	Brassicaceae	132	n.s.	S, Almeria	13
Parsley	*Petroselinum sativum*	Apiaceae	136	n.s.	n.s.	1
Hedge Mustard	*Sisymbrium irio*	Brassicaceae	138	n.s.	S, Almeria	13
Hedge mustard	*Sisymbrium irio*	Brassicaceae	140	Anthropogenic soil	SE of Spain	12

Table 5.1- Oxalate content of some plant species found in literature completed with results from this study. Results are expressed in milligrams of total oxalate per 100 grams of oven-dried material. The plant species are listed in order of increasing oxalate content. n.s.: not specified; .s.: this study.
References: 1. Hönow and Hesse, 2002; 2. Ogawa et al., 1994; 3. Ciba-Geigy, 1977; 4. Elmadfa et al., 1992/1993; 5. Chandler, 1937; 6. Haytowicz and Matthews, 1984; 7. Souci et al., 1986; 8. Noonan and Savage, 1999; 9. Schelstraete and Kennedy 1980; 10. Nakata and McConn, 2007; 11. Nakata and McConn, 2000; 12. Guil et al., 1996; 13. Guil-Guerrero et al., 1998; 14. Kasidas and Rose, 1980; 15. Suvachittantont et al., 1973; 16. Awadalia et al., 1985 ; 17. Kmiecik et al .2004; 18. Vickery, 1955; 19. Zarembski and Hodgkinson, 1962; 20. Massey et al., 1993; 21. Perez et al., 2001; 22. Savage et al., 2000; 23. Sotomayor et al., 2001; 24. Valyasevi, 1974 ; 25. Kamchan et al., 2006; 26. Siener et al., 2006.

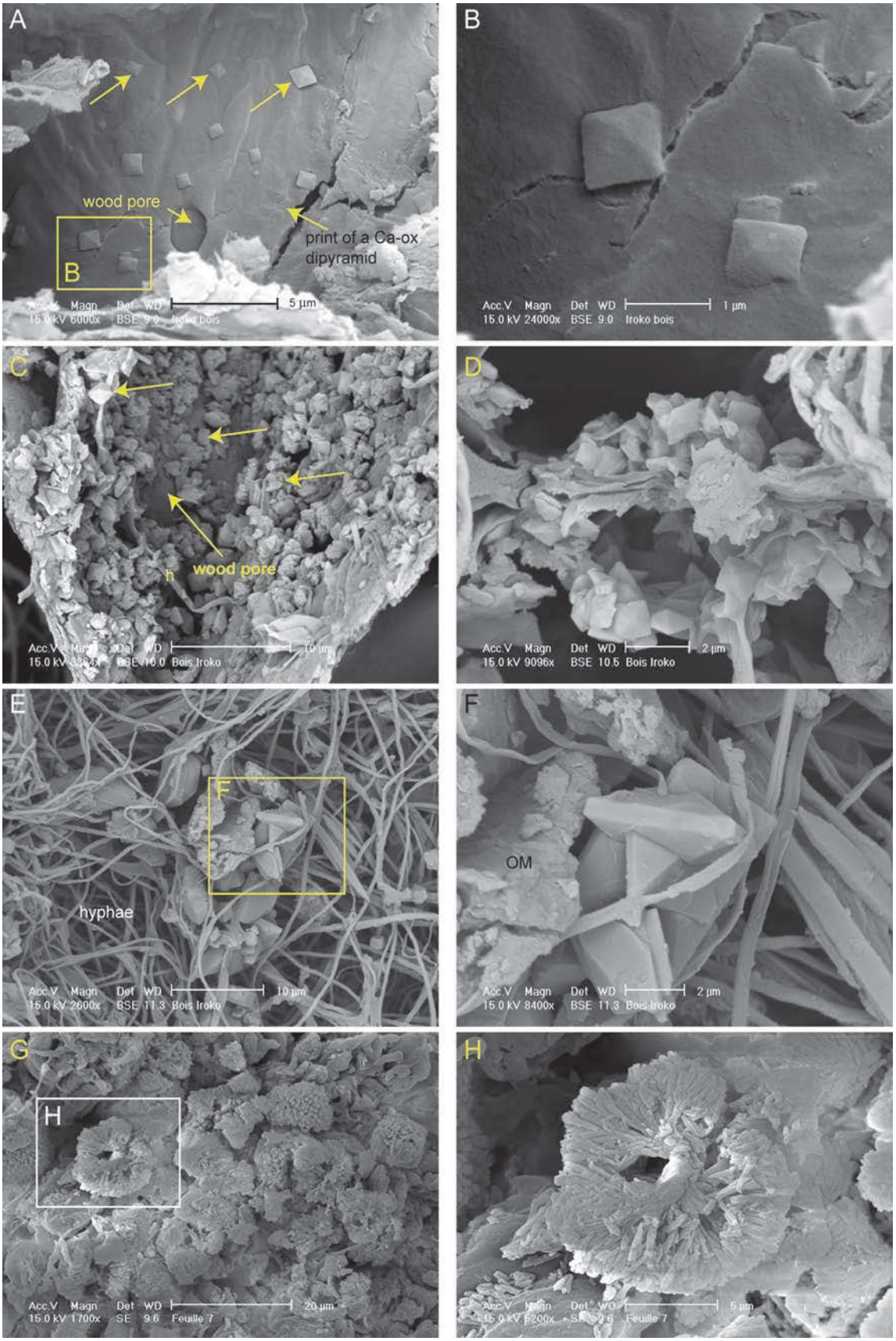
Vernacular name	Latin name	Family	Total oxalate mg / 100 g	Soil	Origin	Source
Dill	*Anethum graveolens*	Apiaceae	144	Brown soil, loess formations	PL, Krakow	17
Dill	*Anethum graveolens*	Apiaceae	159	n.s.	n.s.	1
Tobacco	*Nicotiana tabacum*	Solanaceae	160	n.s.	USA, CT, New Haven	18
Parsley	*Petroselinum sativum*	Apiaceae	166	n.s.	n.s.	19
Parsley	*Petroselinum sativum*	Apiaceae	170	n.s.	n.s.	20
Parsley	*Petroselinum sativum*	Apiaceae	170	n.s.	n.s.	8
Sea rocket	*Cakile maritima*	Brassicaceae	178	n.s.	S, Almeria	13
Celery	*Apium graveolens*	Apiaceae	190	n.s.	n.s.	6
Spinach	*Spinacia oleracea*	Chenopodiaceae	198	n.s.	n.s.	21
Beet	*Beta vulgaris*	Chenopodiaceae	275	n.s.	n.s.	8
African oak	*Afzelia africana*	Fabaceae	278	Ferralsol	BF, Niangoloko	T.s.
Watercress	*Nasturtium officinale*	Brassicaceae	310	n.s.	n.s.	6
Barbary-fig	*Opuntia ficus-indica*	Cactaceae	319	Andosol	I, Salina	T.s.
Spinach	*Spinacia oleracea*	Chenopodiaceae	330	Supermarkets	NZ, Christchurch	22
Lettuce	*Lactuca sativa*	Asteraceae	330	n.s.	n.s.	6
Lettuce	*Lactuca sativa*	Asteraceae	330	n.s.	n.s.	20
Chickweed	*Stellaria media*	Caryophyllaceae	367	Anthropogenic soil	SE of Spain	12
Collards	*Brassica oleracea*	Brassicaceae	450	n.s.	n.s.	6
common sorrel	*Rumex acetosa*	Polygonaceae	500	n.s.	n.s.	8
Garden sorrel	*Rumex patientia*	Polygonaceae	500	n.s.	n.s.	8
Silverbeet	*Beta vulgaris v. cicla*	Chenopodiaceae	526	Supermarkets	NZ, Christchurch	22
Red cedar	*Juniperus virginiana*	Cupressaceae	29	Mesic Glossic Hapludalfs	USA, NY, Dunkirk	5
Ironwood	*Ostrya virginiana*	Betulaceae	38	Mesic Typic Dystrudepts	USA, NY, Lordstown	5
White cedar	*Thuja occidentalis*	Cupressaceae	38	Mesic Glossic Hapludalfs	USA, NY, Dunkirk	5
Parsnip	*Pastinaca sativa*	Apiaceae	40	n.s.	n.s.	6
Spinach	*Spinacia oleracea*	Chenopodiaceae	580	Grocery stores	BR, Campinas	23
Spinach	*Spinacia oleracea*	Chenopodiaceae	582	n.s.	n.s.	21
Spinach	*Spinacia oleracea*	Chenopodiaceae	602	n.s.	BR, Campinas	23
Beet	*Beta vulgaris*	Chenopodiaceae	610	n.s.	n.s.	6
Beet	*Beta vulgaris v. cicla*	Chenopodiaceae	610	n.s.	n.s.	8
Spinach	*Spinacia oleracea*	Chenopodiaceae	610	Grocery stores	BR, Campinas	23
Spinach	*Spinacia oleracea*	Chenopodiaceae	615	Grocery stores	BR, Campinas	23
Curly dock	*Rumex crispus*	Polygonaceae	620	Anthropogenic soil	SE of Spain	12
Spinach	*Spinacia oleracea*	Chenopodiaceae	622	n.s.	n.s.	21
Manioc	*Manihot esculenta*	Euphorbiaceae	635	n.s.	THA, Ubol	24
Spinach	*Spinacia oleracea*	Chenopodiaceae	670	Grocery stores	BR, Campinas	23
Wild betal	*Piper sarmentosum*	Piperaceae	700	markets in Bangkok	THA	25
Spinach	*Spinacia oleracea*	Chenopodiaceae	704	n.s.	n.s.	21
Spinach	*Spinacia oleracea*	Chenopodiaceae	735	Grocery stores	BR, Campinas	23
Barbary-fig	*Opuntia ficus-indica*	Cactaceae	844	Andosol	S Italy, Salina	T.s.
Mangold	*Beta vulgaris ssp.*	Chenopodiaceae	874	n.s.	n.s.	26
NZ spinach	*Tetragonia expansa*	Aizoaceae	890	n.s.	n.s.	8
Garden orach	*Atriplex hortensis*	Chenopodiaceae	900	n.s.	n.s.	8
Amaranth	*Amaranthus viridis*	Amaranthaceae	960	Anthropogenic soil	SE of Spain	12
Spinach	*Spinacia oleracea*	Chenopodiaceae	970	n.s.	n.s.	6
Spinach	*Spinacia oleracea*	Chenopodiaceae	970	n.s.	n.s.	8
Amaranth	*Amaranthus viridis*	Amaranthaceae	1090	n.s.	n.s.	6
Goosefoot	*Chenopodium album*	Chenopodiaceae	1100	Anthropogenic soil	SE of Spain	12
Big spinach	*Chenopodium* spp.	Chenopodiaceae	1100	n.s.	n.s.	8
Purslane	*Portulaca oleracea*	Portulacaceae	1294	n.s.	n.s.	8
Purslane	*Portulaca oleracea*	Portulacaceae	1310	n.s.	n.s.	6
Alpine dock	*Rumex alpinus*	Polygonaceae	1356	Saturated brunisols	CH, Val Piora	T.s.
Sorrel	*Rumex acetosa var. hort.*	Polygonaceae	1391	n.s.	n.s.	26
Chives	*Allium schoenoprasum*	Liliaceae	1480	n.s.	n.s.	6
Parsley	*Petroselinum sativum*	Apiaceae	1700	n.s.	n.s.	6
New Zealand spinach	*Tetragonia expansa*	Aizoaceae	1765	Supermarkets	NZ, Christchurch	22
Spinach	*Spinacia oleracea*	Chenopodiaceae	1959	n.s.	n.s.	26
Elephant-head amaranth	*Amaranthus gangeticus*	Amaranthaceae	3349	n.s.	THL, Ubol	24
Grass	*Grass sp.*		3675	n.s.	CH, Neuchâtel	T.s.
Taro	*Colocasia antiquorum*	Araceae	3789	n.s.	THA, Ubol	24
Cha phlu	*Piper sarmentosum*	Piperaceae	3887	n.s.	THA, Ubol	24
Vietnamese coriander	*Polygonum odoratum*	Polygonaceae	4195	n.s.	THA, Ubol	24

Table 5.1- Continued

5.2.2 Discussion: oxalate and plants

The applied enzymatic methods measured all the oxalate present: oxalic acid, soluble and insoluble oxalate salt. With this method it is impossible to quantify the different oxalate species. Nevertheless, the amount of oxalate measured in *M. excelsa* and *A. africana* leaves is considerable and sufficient to enhance the oxalate-carbonate pathway in soils, as well as in litters (Fig. 4.17, *M. excelsa* rotten leaves). Nevertheless, as pointed out in Table 5.1, the oxalate measurements in a same plant species could result in various values. This is, for example, the case for parsley (*Petroselinum sativum*) where values range from 6 to 1700 mg of oxalate/100 g of dried material (Ciba-Geigy 1977; Haytowicz and Matthews 1984). The differences could be of diverse origins, among which: 1) the sample preparation, 2) the soil quality, 3) the climate, 4) the different state of fruit ripeness, or 5) the tree age (Chandler 1937; Libert and Franceschi 1987; Zindler-Frank et al. 2001; Hönow and Hesse 2002).

Although, oxalic acid is supposed to be present, the only oxalate salts observed in *M. excelsa* tree is Ca-oxalate. Whewellite (Ca-oxalate monohydrate) is mainly associated with the living plant tissues, whereas weddellite (Ca-oxalate dihydrate) is generally related to decaying wood resulting from fungal activity (Arnott 1995; Braissant et al. 2004). In wood, calcium oxalate occupies some idioblasts, forming euhedral crystals, often occurring as chains inside neighbouring cells. Bipyramids are also disposed irregularly on wood tissues (Fig. 5.2). These crystals have different size and do not exceed 1 μm. In roots, calcium oxalate forms a mineral network of crystals between the inner root and the thin cuticle constituting the outer part of the root (Braissant et al. 2004).
As found in *M. excelsa* trees (Braissant et al. 2004), oxalate is also present in wood of *A. africana* (Fig. 4.17). The presence of carbonate on trunks may suggest that oxalogenic communities are already present on the trees themselves and not only in the soil (Pr. Aragno pers. comm.).
The analyzed leaves of *A. africana* contain three times more oxalate than in *M. excelsa,* which could be even more interesting in the context of the carbon dioxide-oxalate-carbonate pathway in terms of a more efficient pump than *M. excelsa* trees, allowing carbon storage in soil. More analyses are necessary to confirm that *A. africana* produce effectively more oxalate than *M. excelsa.* In our case, the analyzed leaves are from trees of about the same age but at 100 km distance from each other, causing changes in soil intrinsic parameters and probably in oxalate results.
Total oxalate content in Salina *Opuntia sp.* is not in accordance with values found in the literature. *Opuntia* nopales collected in a Texas market contain 61 mg/ 100 g of soluble oxalate and 3450 mg/100 g of insoluble oxalate (McConn and Nakata 2004). Another example is the two year old *Opuntia ficus indica* from Jebibina (Central Tunisia), which contains 13100 mg/100g total oxalate (Ben Salem et al. 2002). However, without soil type information, a comparison of the data will be hazardous, because the oxalate content in plants is related to metals available in soils, such as Ca (Wolfson and Sears 1989; Monje and Baran 2002). Hypotheses for the low total oxalate content of Salina *Opuntia sp.*, compared with the literature data, are the low concentration of available Ca in Salina volcanic soils, the higher accumulation of calcium oxalate in preferential cladodes


A
wood pore
print of a Ca-ox dipyramid
B
5 µm
B
1 µm
C
wood pore
h
D
2 µm
E
F
hyphae
10 µm
F
OM
2 µm
G
H
20 µm
H
5 µm

parts, such in a subepidermal layer (our observations), and old cladodes (Sepúlveda et al. 2007). In the case of cacti studied in Salina, the Ca amount was not measured, but the decrease of oxalate amount from fresh to degraded cladodes can be imputable to 1) the transformation of oxalate into carbonate or 2) a reabsorption of Ca-oxalate in order to cover a calcium requirement, 3) an oxalate accumulation in different plant parts, or 4) a mechanical oxalate loss due to the state of the cladode and/or sampling.

Different hydration states of calcium oxalate can accumulate in Opuntioedeae subfamily members (Monje and Baran 2002). In cacti, typical crystal habits are druses, raphides and styloids (Rivera and Smith 1979), and tiny individual crystallites similar to crystals, and individual prisms are also observed (Monje and Baran 2002; Cailleau 2005). In cladodes of *O. ficus-indic* , oxalate crystals are present in parenchyma and chlorenchyma cells (Malainine et al. 2003). Analysis of *Rumex acetosa* var. *hortensis* (Siener et al. 2006) gives the same oxalate content as found in this study in *R. alpinus*.

5.2.3 Partial conclusions: oxalate and plants

- *M. excelsa* is not the only oxalogenic tree present in Burkina Faso.
- *A. africana* leaves contain more oxalate than *M. excelsa* and could display a better pathway for carbon storage in soil.
- Oxalate amount in plant material can only be interpreted with care, due to the different parameters playing a role in oxalate accumulation.
- The enzymatic method applied is adapted for the measurement of oxalate in plant material but is long, expensive, and does not allow the different oxalate species (oxalic acid, soluble and insoluble oxalate salt) to be discriminated.

5.2.4 Results: oxalate and fungi

Fungal strains isolated on Malt-Agar and antibiotic medium have been determined by Dr. Daniel Job (University of Neuchâtel). Unfortunately the fungal isolation is not representatives from the true mycological flora. Sampling, preservation and sample preparation may destroy the delicate mycelium from significant species such those from Basidiomycota. The fungal community is entirely composed of moulds. The dominant isolated genus is Aspergillus. The observed oxalogenic and non oxalogenic strains on Malt-Agar medium are given in Table 5.2. Tests of selected strains in medium supplemented with a high Ca source (gypsum) result in different scenarios: gypsum does or does not improve crystal formation (Table 5.3). The shapes of Ca-oxalate crystals from fungi

Front page: Fig. 5.2- Scanning electron microscope (SEM) micrographs of M. excelsa *wood and leaves; arrows show Ca-oxalate crystals; h: fungal hyphae. A: Ca-oxalate crystals on* M. excelsa *wood surface. B: details from picture A. C:* M. excelsa *wood colonized by fungi. Ca-oxalates are of vegetal and fungal origin. D: Ca-oxalate crystal associated to fungal hyphae (cf. Fig. 5.4-N). E:* M. excelsa *wood colonized by a thick fungal hyphae or actinobacteria. Ca-oxalate crystals are associated to hyphae and are observed near organic matter (OM). F: Detail from picture E (cf. Fig. 5.3). G: Ca-oxalate prisms clustered (druses) in fascicles arranged in the shape of a spiral observed on* M. excelsa *rotten leaves. H: detail from G.*

	P4	P3	P2	P1	L2	F3
OXALOGENIC STRAINS	*Aspergillus sp.*	*Aspergillus sp.*	*Aspergillus sp.*	*Aspergillus sp.*	*Aspergillus sp.*	*Aspergillus sp.*
	A. niger	*A. niger*	*A. niger*	*A. niger*	*A. niger*	*A. niger*
	A. type *niger*	*A.* type *niger*	*A.* type *niger*	*A.* type *niger*	*A.* type *niger*	*A.* type *niger*
	Mucor sp.	*Mucor sp.*	*Mucor sp.*	*Mucor sp.*	*Mucor sp.*	*Mucor sp.*
	Fusarium sp.	*Fusarium sp.*	*Fusarium sp.*	*Fusarium sp.*	*Fusarium sp.*	-
	Penicillium sp.	*Penicillium sp.*	-	-	-	-
	A. ochraceus	-	-	*A.* type *ochraceus*	-	-
	Chalaropsis sp.	-	-	-	*Chalaropsis sp.*	-
	Stilbum sp.	-	-	-	-	-
	Mycelia sterilia	-	-	-	-	-
	-	*A. penicillioides*	-	-	-	-
	-	*Doratomyces sp.*	-	-	-	-
	-	-	*A. alliaceus*	-	-	-
	-	-	-	-	-	*Gliocladium sp.*
	-	-	-	-	-	*Plectomyces sp.*
	-	-	-	-	-	*Sphaeropsis sp.*
	-	-	-	-	-	*Stilbum sp.*
	-	-	-	-	-	*Ascomycota*
NON OXALOGENIC STRAINS	*Aspergillus sp.*	*Aspergillus*	*Aspergillus sp.*	*Aspergillus sp.*	*Aspergillus sp.*	*Aspergillus sp.*
	Trichoderma sp.	*Trichoderma sp.*	*Trichoderma sp.*	*Trichoderma sp.*	*Trichoderma sp.*	*Trichoderma sp.*
	Fusarium sp.	*Fusarium sp.*	*Fusarium sp.*	*Fusarium sp.*	*Fusarium sp.*	-
	Penicillium sp.	*Penicillium sp.*	*Penicillium sp.*	*Penicillium sp.*	-	-
	Dematiaceae	-	-	-	-	*Dematiaceae*
	-	*Aureobasidium sp.*	-	-	-	-
	-	*Cladosporium sp.*	-	-	-	-
	-	-	*A. flavus*	-	-	-
	-	-	-	*Sphaeropsis sp.*	-	-
	-	-	-	-	-	-
	-	-	-	-	-	*Pyrenomycetes*
	-	-	-	-	-	*Sordariales*

Table 5.2- Oxalogenic and non-oxalogenic strains isolated from Burkina Faso soils. P4, P3, P2, and P1 are soils related to M. excelsa *oxalogenic tree. L2 is a soil situated under an* A. africana *stump, and F3 is the Burkina Faso reference soil.*

cultivated on Malt-Agar medium are preferentially bipyramids, whereas in Malt-Agar medium supplemented with gypsum the preferential crystal shape are tablets (Fig. 5.3 and Fig. 5.4).

5.2.5 Discussion: oxalate and fungi

An oxalogenic fungal community is well present in soil. Unfortunately only 5-10% of fungi can be cultured artificially (Manoharachary et al. 2005), and even less with the technique applied in this study. The amount of oxalate produced by fungi depends on the fungal species, the cultural medium, and the environmental conditions. For example, 1) not all the *Aspergillus* and *Fusarium* strains produce oxalate in the same laboratory conditions, 2) cultural media supplemented with calcium improve and trigger the oxalate formation, 3) fungal oxalates are not always present as simple oxalate crystals but they can also be present as twins and complex assemblages, forming a sheath around the fungal hyphae (Fig. 5.2, 5.3 and 5.4). Bipyramids and tablets are found associated to fungal hyphae. Contrary to bipyramids, found in Malt-Agar and litter, tablets develop only in the gypsum medium (Fig. 5.4). Various hypotheses could be proposed (discussion with Prof. E. Verrecchia): 1) the presence of gypsum and the associated solutions modify the ionic strength and

Strain	Occurrence	Culture medium	Ca-oxalate presence	Inoculations time (days)
Aspergillus sp.	P1	MA	-	68
		MA	+	125
		MA + 50 g/l gypsum	-	110
A. flavus	Ubiquitus	MA	-	127
		MA + 50 g/l gypsum	+	180
A. type *ochraceus*	P4	MA	+	7
		MA + 50 g/l gypsum	+	110
A. niger	Ubiquitus	MA	++	3
		MA + 5 g/l gypsum	+++	180
Trichoderma sp.	Ubiquitus	MA	-	125
		MA + 5 g/l gypsum	-	135
		MA + 50 g/l gypsum	-	135

Table 5.3- Oxalate presence on some fungal strains cultivated on Malt-Agar (MA) added with gypsum.

thus, the diffusion property of the ionized elements compared to simple Malt-Agar, 2) the crystal habitus strongly depends on the ion concentrations used in the solid solution, 3) crystal shapes are more regular in less concentrated solutions, and finally 4) the influence of organic material on crystallogenesis remains unknown.

The roles of fungi in this sub-carbon cycle are multiple and imply carbon but also Ca binding with oxalate. Main roles include: 1) plant oxalate release (Gadd 1999), 2) oxalate production (Graustein et al. 1977), 3) carbonate dissolution (Gadd 2007), release of Ca, and diminution of a long term stock, 4) silicate dissolution (Gadd 2007), and release of Ca, 5) Ca-oxalate dissolution and oxidation (Guggiari et al. 2010), 6) translocation of Ca (Wilcoxson and Sudia 1968), pumping Ca into the tree-soil system, and 7) carbonate precipitation (Rautaray et al. 2004; Gadd 2007).

We demonstrated that free-living fungi produce Ca-oxalate crystals rapidly, but this capacity is also attributed to plant symbiotic fungi (Dutton and Evans 1996; Gharieb et al. 1998; Gadd 1999). We have not observed mycorrhizal fungi in studied plants but they are present associated with *A. africana* from a Burkina Faso and Cameroon trees (Sanon et al. 1997; Onguene and Kuyper 2001) as so as associated with *M. excelsa* tree from Cameroon (Onguene and Kuyper 2001). Additionally to Deuteromycotina found in this study, putative ectomycorrhizal fungi were collected under a *A. africana* tree from Burkina Faso (Sanon et al. 1997). This fungi belong to the Agaricales, Aphyllophorales, Boletales, Cantharellales, Hymenogastrales, Russulales, and Sclerodermatales division (Sanon et al. 1997).

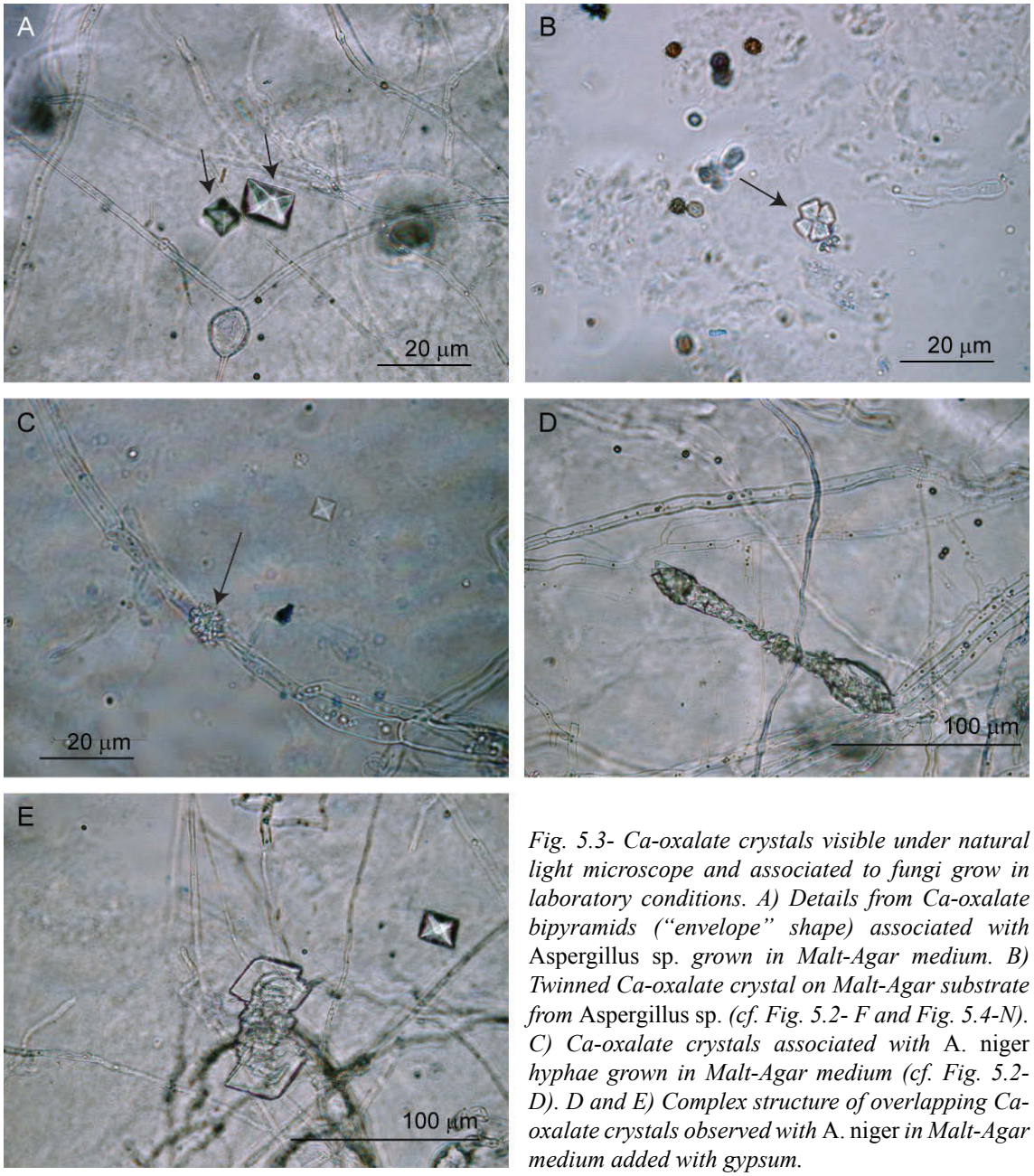


Fig. 5.3- Ca-oxalate crystals visible under natural light microscope and associated to fungi grow in laboratory conditions. A) Details from Ca-oxalate bipyramids ("envelope" shape) associated with Aspergillus sp. *grown in Malt-Agar medium. B) Twinned Ca-oxalate crystal on Malt-Agar substrate from* Aspergillus sp. *(cf. Fig. 5.2- F and Fig. 5.4-N). C) Ca-oxalate crystals associated with* A. niger *hyphae grown in Malt-Agar medium (cf. Fig. 5.2-D). D and E) Complex structure of overlapping Ca-oxalate crystals observed with* A. niger *in Malt-Agar medium added with gypsum.*

5.2.6 Partial conclusions: oxalate and fungi

- Based on cultivable fungi, it result that *Aspergillus sp.*, *Mucor sp.,* and *Fusarium sp.* are the dominant oxalogenic genera isolated in the soil under oxalogenic trees and beyond the oxalogenic tree influence
- The amount of calcium present in the environment and/or translocated seems to play a role in calcium oxalate shape, and disposition on the fungal hyphae.
- This can also influence the infilling of soil pores by carbonate after oxalate oxidation driven by oxalotrophic bacteria.
- *M. excelsa* wood colonisation by fungi is characterised by the presence of weddellite.

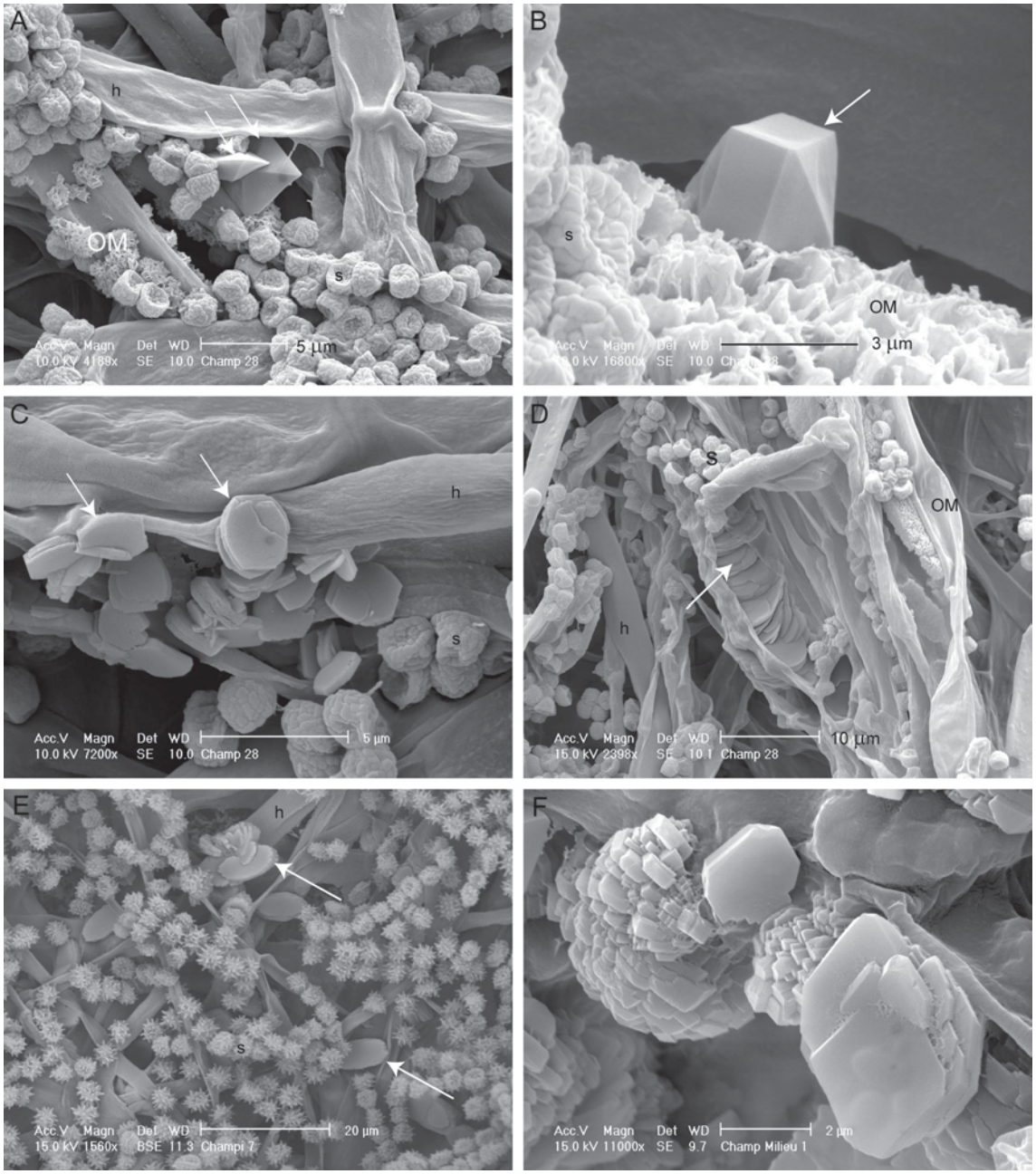


Fig. 5.4- From A to L: scanning electron microscope (SEM) micrographs of Ca-oxalate crystals found associated with fungi grown in Malt-Agar and gypsum (50 g/l) medium; arrow indicate Ca-oxalate crystals; OM: organic matter; h: fungal hyphae; s: fungal spore. A, B, C, and D: Aspergillus type ochraceus*; E, F, G, H, I, and L:* A. niger. *A and B: Ca-oxalate dipyramids (cf. N and Fig. 5.3- A, B, and C); C and D: Ca-oxalate tablets (cf. N and Fig. 5.3- I); E, F, I, and L: complex structures of Ca-oxalate tablets (twinned crystals); G: Ca-oxalate crystals develop around a fungal hyphae; H: detail from G. M: EDS chemical element spectrum of a Ca-oxalate crystal. N: Fig. 38 from Khan (1995).*

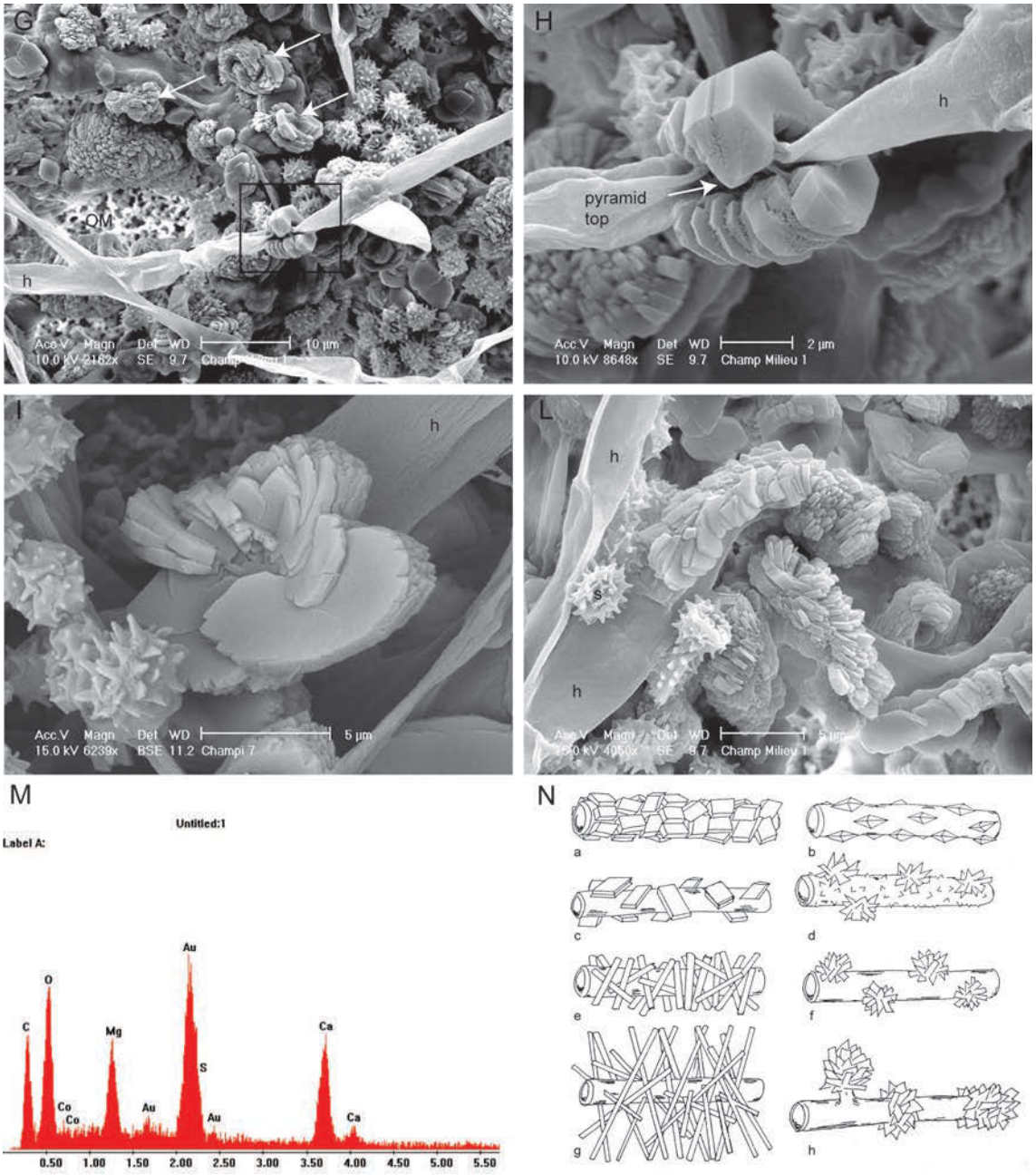


Fig. 5.4- Continued

5.2.7 Results: oxalate and soil

Total oxalate measured in soils profiles each 5 cm are given in Figure 5.5 and the Annex 10. Results are expressed in milligrams of total oxalate per 1 kg of soil (mg/kg). The oxalate concentration in the analysed profiles varies greatly. Burkina Faso reference soil (F3) shows the lowest concentrations of total oxalate. Maximal value is at the surface: 4.3 mg/kg. Under the living *M. excelsa* tree (P4 profile) the oxalate content in the 10 first centimetres varies between 47.2 and 13.3 mg/kg. That

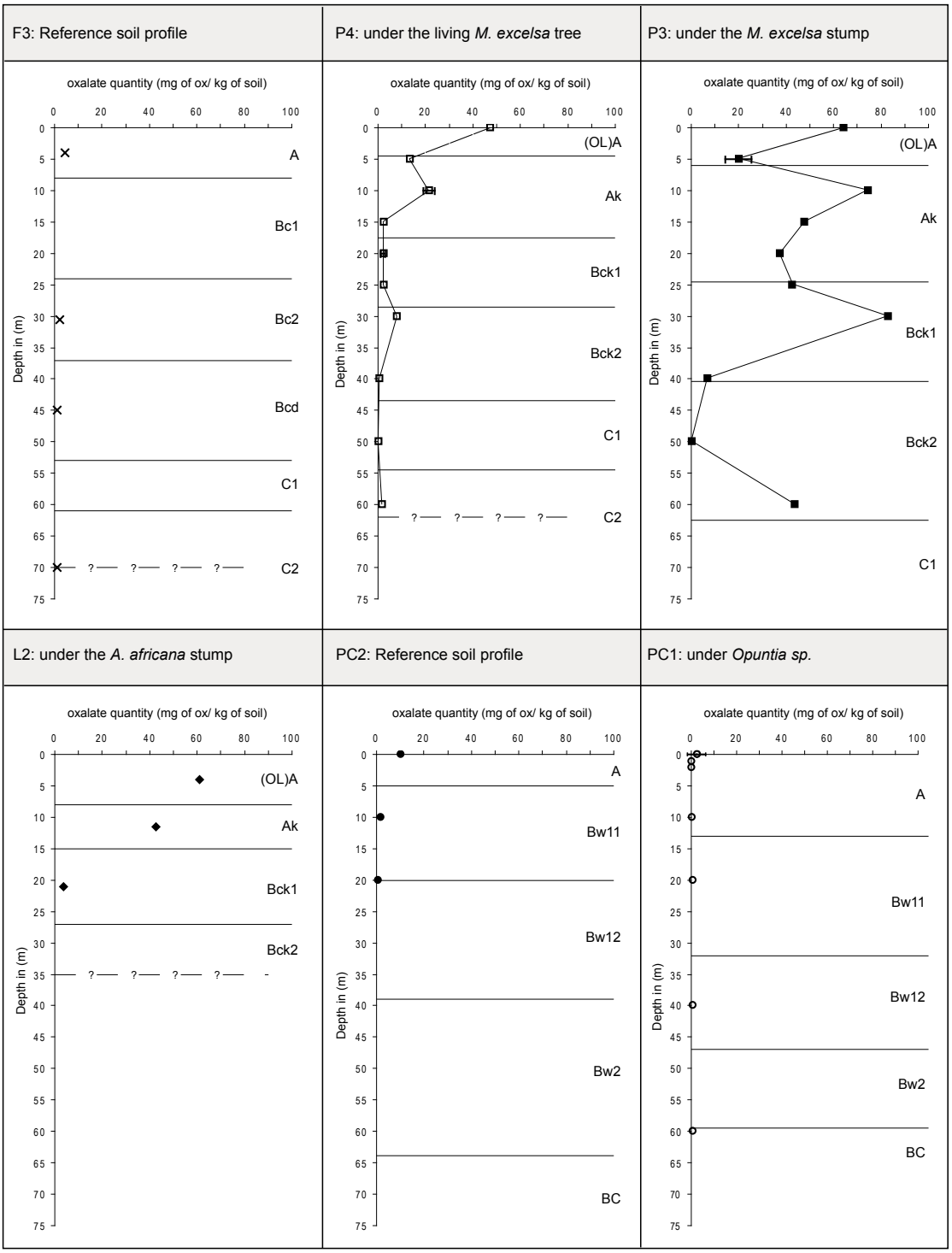


Fig. 5.5- Oxalate profiles measured in soils. F3, P3, P4 and L2 are Burkina Faso soils, PC1 and PC2 are Salina (Italy) soils.

represents more than 80% of the oxalate present in this profile (from 0 to 60 cm). In the following layers, the quantity is constant (2.3 ± 2.6 mg/kg). Two peaks are present at the surface and 10 cm in depth. Under the *M. excelsa* stump (P3 profile) total oxalate varies irregularly with depth with a mean of 41.8 ± 27.4 mg/kg. P3 and P4 soil profiles show a similar trend in the oxalate amount

in the first 10 cm with a decreasing peak at 5 cm. In these soils, Ca-oxalate crystals are observed (Fig. 5.6) 1) in plant material (wood and roots), 2) soil peds, and 3) dispersed in soil pores. Under the *A. africana* stump in the three first soil layers the oxalate content is: 60.9 mg/kg, 42.6 mg/kg and 3.7 mg/kg. Under the *M. excelsa* trees the oxalate crystals are found in the three mentioned cases (Fig. 5.6. E). Maximal oxalate concentration in Salina soils is measured at the surface, and in the reference profile (PC2), beyond the influence of a cactus, with a value of 10.0 mg/kg (Fig. 5.5). This result is questionable because it is a mean of two measurements: 0.0 mg/kg and 20.0 mg/kg. At least one ulterior measurement is necessary.

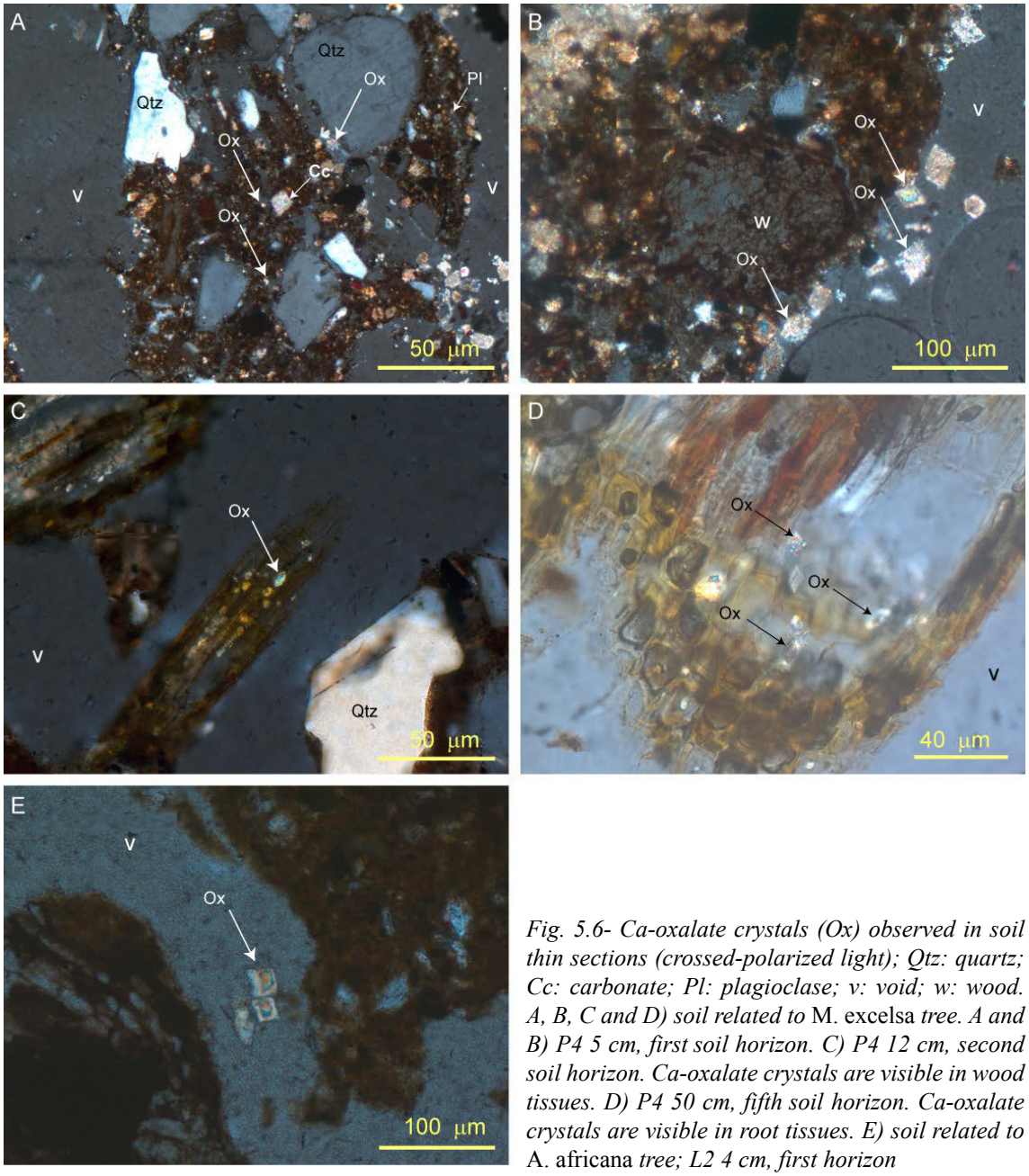


Fig. 5.6- Ca-oxalate crystals (Ox) observed in soil thin sections (crossed-polarized light); Qtz: quartz; Cc: carbonate; Pl: plagioclase; v: void; w: wood. A, B, C and D) soil related to M. excelsa *tree. A and B) P4 5 cm, first soil horizon. C) P4 12 cm, second soil horizon. Ca-oxalate crystals are visible in wood tissues. D) P4 50 cm, fifth soil horizon. Ca-oxalate crystals are visible in root tissues. E) soil related to* A. africana *tree; L2 4 cm, first horizon*

5.2.8 Discussion: oxalate and soil

Oxalate found in studied soils is produced by plants, fungi, and possibly by bacteria. We did not measure the oxalate from the rhizospheric soil but oxalic acid excretion by roots is common in plants (Fox and Comerford 1990). The release of plant metal-oxalate in soil environments depends on biological attacks: physical, such as by insects, or chemical, promoted by organic acids, enzymes, and metabolites from fungi (Gadd 2004) and bacteria (Hodgkinson 1977). Ca-oxalate of microbial origin derives from fungal and bacterial excretions of oxalic acid that binds with an ion to form an oxalate salt, normally Ca-oxalate. We consider that the oxalate measured with the applied enzymatic method may have these different origins: plant, fungal, and bacterial. The oxalate content in Burkina Faso and Salina soils are in the same order of magnitude as those found in other ecosystems. For example, in Tuscany forest soils under *Abies alba*, the amounts of oxalate range from > 200 mg/kg in the topsoil horizons to 1-15 mg/kg in the deepest ones (Certini et al. 2000), but no carbonate content has been measured in this case. Closer to the studied system are the Ivory Coast and Cameroon *M. excelsa* ecosystems studied by Cailleau and Braissant (Braissant et al. 2002; Braissant et al. 2003; Braissant et al. 2004; Cailleau et al. 2004; Braissant 2005; Cailleau 2005; Cailleau et al. 2005). These authors studied the soil profiles under hollow trunks of *M. excelsa* stumps and found that the average oxalate content is respectively inferior to 29 mg/kg in soils of Ivory Coast trees, and 71 mg/kg under Cameroon trees (Cailleau, 2005). The oxalate content is distributed irregularly in these profiles. Maximal oxalate concentration reaches 255 mg/kg and is found at 1.3 m from the hollow Biga trunk at 40 cm in depth (Cailleau, 2005). Nevertheless, the oxalate content associated to *M. excelsa* tree at Cameroon or Ivory Coast contains two times more oxalate than in Burkina Faso (Fig. 5.7). Reasons of this difference can be attributed to: 1) the sampling period, 2) the age of the studied ecosystem, 3) the tree state, alive (in Burkina Faso) or in decomposition, and/or 4) the soil properties, which are sandier in Burkina Faso and present different Ca availability.

The presence of oxalate in the Burkina Faso reference soil (< 4 mg/kg), although very low, can be due to different factors

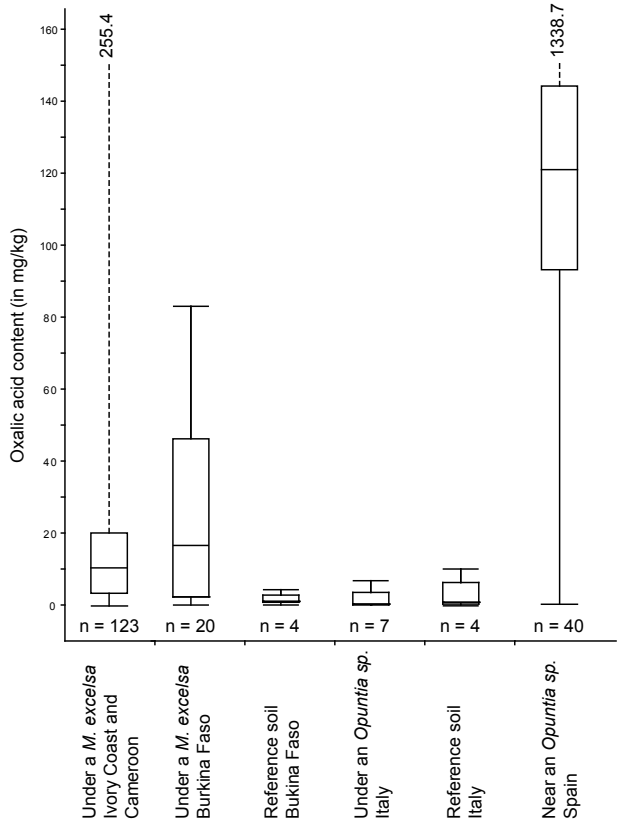


Fig. 5.7- Box plots of oxalate content in studied soils (Burkina Faso and Italy) compared to similar systems studied in Cameroon and Spain (Cailleau 2005). n*: number of samples.*

1) a contamination by *M. excelsa* leaves located at 38 m from this profile, 2) colonies of oxalogenic fungi, whose presence was confirmed by the development of oxalogenic strains on Malt-Agar medium from soil samples coming from this profile, and 3) a certain grass type containing oxalate. Oxalate in grass is common. It has been demonstrated that tropical hair grass (*Setaria sphacelata*) could contain until 5% of oxalate (Jarrige and Ruckebusch 1995). Moreover, we found that grass collected in Neuchâtel (Switzerland) contained 3675 mg of oxalate/100 g of dried material. This is not surprising because in the soil the calcium in not a limiting. But in Africa the observed low level of oxalate is not sufficient to trigger an accumulation of Ca-carbonate in this soil profile (Chapter 6).

The negative correlation between oxalate concentration and depth is explained by a predominant source of oxalate derived from oxalogenic litter degradation and the decrease of fungal oxalate with depth due to the decrease of organic matter concentrations (Chapter 4). Moreover, the soil porosity decreases drastically with increasing depth, constituting an unfavourable environment for organisms.

The irregular distribution of oxalate under the *M. excelsa* stump is probably due to the activity of termites and ants that mix large quantities of material such as soil particles and OM containing oxalate. The high oxalate content measured under the stump (Fig. 5.7) is due either to the presence of a great amount of wood containing oxalate or to the presence of saprophytic oxalogenic fungi degrading the *M. excelsa* stump. Moreover, the activity of ants and termites, together with fungi, improves the oxalate release in the soil environment, accelerating the oxalate-carbonate pathway. The same reasoning is made for the soil under the *A. africana* stump.

The oxalate peak at 5 cm in depth indicates an area of strong oxalate consumption but also a separation between the area in which oxalate derives from leave degradation and the area in which oxalate derives from degradation of more resistant material, such as wood or fungi. Saprophytic fungi and insects rapidly decay litter containing oxalate (oxalic acid, oxalate salts) deposited on the soil surface. More precise studies might resolve this point, but, compared with the carbonate profile, the first hypothesis seems to be the most likely solutio

5.2.9 Partial conclusions: oxalate and soil

- Clear evidence of the impact of the *M. excelsa* tree on the oxalate content in soil is showed.
- Burkina Faso oxalate values are in the same order of magnitude as the ones found under *M. excelsa* stumps from Ivory Coast and Cameroon (Cailleau 2005).
- In all the examined soils, the concentration of oxalate was most important in the first horizon, where the biological activity is more efficient
- At 5 cm deep, lower values in oxalate content could indicate a major area of oxalate consumption (oxalotrophy).
- In the reference soil the oxalate amount is not sufficient to form a carbonate stock
- Despite the high quantities of oxalate present in *Opuntia sp.* cladodes, the soil contains the same amount of oxalate as the soil beyond the influence of the oxalogenic tree. The

low oxalate level in soil does not exclude a high oxalotrophic flux. In fact the oxalate concentration is transitory between its production and its consummation and the reaction speed is regulated by the bacterial affinity for this substratum. The formed carbonate ions are leached and the sink is the ocean and not the soil so as in Africa studied system.

5.3 General conclusions

- The new studied tree *A. africana* seems to be a more powerful oxalate producer than *M. excelsa*.
- An oxalogenic fungal community is present in the soil and is able to produce Ca-oxalate salt in laboratory conditions.
- Despite the presence of a litter containing oxalate, no oxalate accumulates in the soil under a 70 year-old oxalogenic tree.
- The oxalate carbonate pathway takes already place in the litter and is present until a depth of 15 cm.

Chapter 6 CARBONATE QUANTIFICATION

The soil, a reservoir of inorganic carbon

6.1 Introduction

In the previous chapters, the amount of organic carbon and oxalate present in the considered system has been measured and discussed. This chapter is dedicated to the study of mineral carbon, more precisely calcium carbonate, related to the *Milicia excelsa* and the *Afzelia africana* trees found in Burkina Faso. The aim of this chapter is to confirm that the tropical soil is an efficient atmospheric carbon pump and an important carbon reservoir with a residence time of an order of magnitude of millennia.

This study is motivated by the evidence that CO_2 in the air is increasing rapidly since the industrial era. Due to its greenhouse effect and the impact on human life, the challenge is to decrease, or at least to slow down emissions (Lal 2004). A solution would be to value, protect, and promote natural ecosystems able to create efficient natural carbon sinks. An example is the *Milicia excelsa* tree with its related soil (Carozzi 1967; Braissant et al. 2002; Braissant et al. 2003; Braissant et al. 2004; Cailleau et al. 2004; Braissant 2005; Cailleau 2005; Cailleau et al. 2005; Verrecchia et al. 2006). As demonstrated in previous works (Carozzi 1967; Braissant et al. 2002; Braissant et al. 2003; Braissant et al. 2004; Cailleau et al. 2004; Braissant 2005; Cailleau 2005; Cailleau et al. 2005; Verrecchia et al. 2006) and in this thesis, the *M. excelsa* trees from Ivory Coast, Cameroon, Uganda, and Burkina Faso, contain oxalate salts in their leaves and trunk. However, this is not the only oxalogenic tree of Africa, since the *Afzelia africana* trees have also an appreciable amount of oxalate in their leaves that can be potentially transformed into carbonate in soils.

Is the carbon content of Burkina Faso soils comparable to those found in Ivory Coast or Cameroon? Is the carbonate distribution the same? The main hypothesis to be tested in this chapter is if the soil under an oxalogenic tree constitutes a long term carbon sink.

In this chapter, the following points are going to be addressed:

- the oxalate-carbonate pathway is a common process present in different African regions and related to different trees species;
- the distribution of carbonate under *M. excelsa* trees of different ages and a stump;
- the quantification of the carbonate content in the *M. excelsa* rhizosphere;
- the qualificati n of the carbonate content: is the carbonate the product of an *in situ* dissolution/re-precipitation process, has it a detritical or a biogenic origin?
- a leaching rate and a residence time of carbonate resulting from the oxalate-carbonate pathway: could tropical soils be a long term carbon sink?
- the carbonate accumulation under *M. excelsa* in different African regions: is there an emergent factor determining carbonate accumulation?
- sources of calcium (and magnesium) that allow catching soil carbon under its inorganic form. What are the sources of these ions?

The main tool used in this chapter is the carbonate titration (Pauwels et al. 1992), which allows carbonate quantification and was successfully applied in a previous work (Cailleau 2005). The pH value was measured as it is an important parameter in the oxalate-carbonate pathway, managing the calcite precipitation. Soil thin sections helped to define the relationship between oxalate and carbonate, and the distribution of calcite crystals in the soil profile. The type of carbonate has been determined using X-ray diffraction analyses. Ca and Mg, as limiting factors, have been quantified with ICP-MS. Following the oxalotrophic equation, it appears that another limiting factor is the nitrogen availability, which has been measured using a CHN analyser. Moreover, in order to estimate the relative accumulation of alkaline cations under oxalogenic trees, the CEC has been calculated. Finally, the water regime conditions have been defined using grain-size distributions and residual humidity.

6.2 Results

In Burkina Faso, the reference soil (F3) does not contain any carbonate, while soils associated with oxalogenic trees always contain carbonate (Annex 11). No blocks have been found in the opened soil profiles, but a carbonate accumulation of 1 cm x 7 cm x 7 cm has been observed between the bark and the wood from the root of the *M. excelsa* stump. Maximal carbonate contents are found on the soil surface under the *M. excelsa* stump (P3), where it reaches 145.7 ± 2.5 g of carbonate/kg of soil (14.5%). In the four soil profiles associated with the trees, a preferential carbonate accumulation is observed in the first 15 cm. Values remain fairly homogenous after 15 cm in depth (11.2 ± 4.7 g of carbonate/kg of soil). The pH is 5.8 ± 0.2 in the reference soil (F3), and ranges from 6.9 to 9.0, with an average of 8.1 ± 0.6, in soils influenced by oxalogenic African trees (Fig. 6.1, Fig. 6.2 and Annex 11). The conditions of maximal alkalinity, present at a depth comprised between 10 and 30 cm (Ak and Bck1 horizons), are not correlated with the highest carbonate accumulations (Fig. 6.2). Moreover, the pH is higher in deeper layers, where the carbonate concentration is low compared to the surface. Under the cut *A. africana* tree (profile L2) the carbonate content decreases from 5.4% at 4 cm to 0.9% at 21 cm. X-ray diffraction analyses on Burkina Faso soil fractions and *M. excelsa* wood show that carbonate is constituted by low magnesian

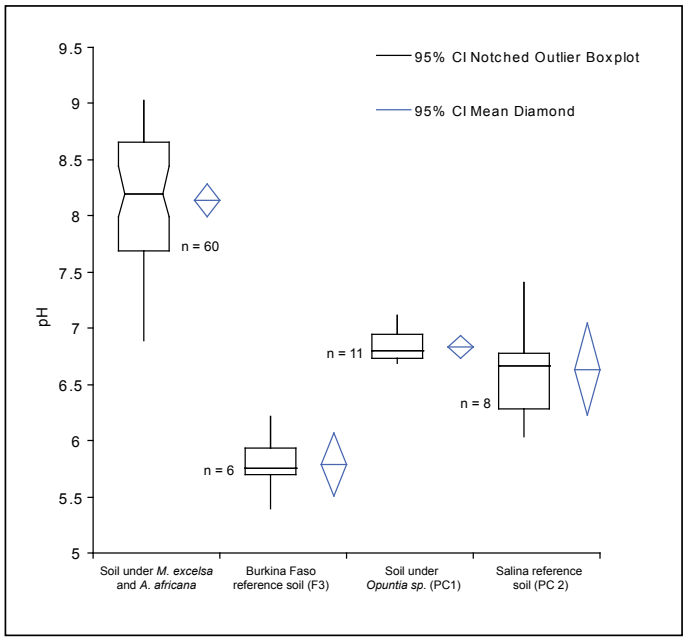


Fig. 6.1- Box plots of pH_{H2O} found in the studied soils. n *is the number of soil pH measurements.*

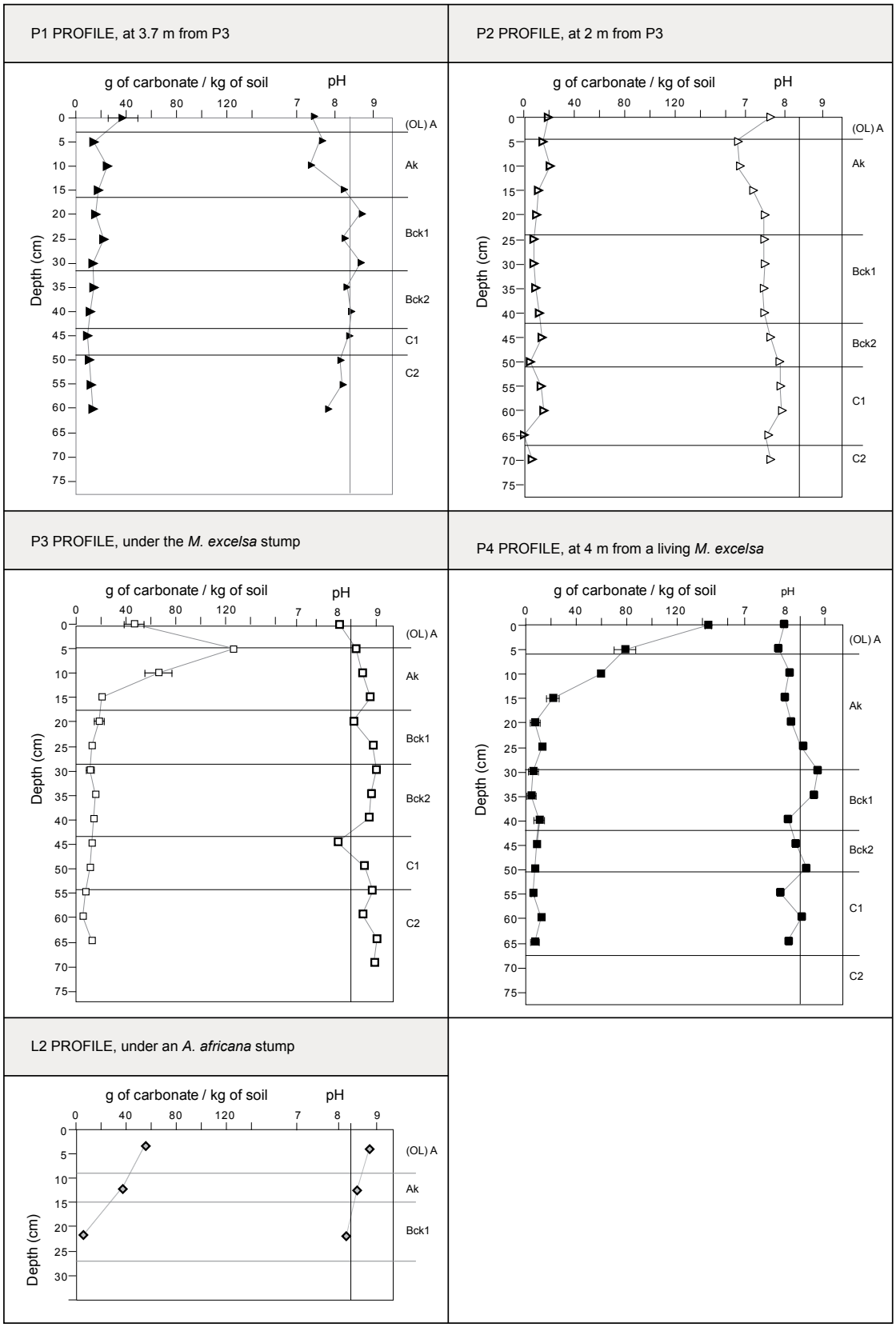


Fig. 6.2- Carbonate content and pH values in function of depth in the different studied soil profiles

calcite, with various concentrations of Mg, from pure calcite (0% $MgCO_3$) to high magnesian calcite (max 8% $MgCO_3$; Fig. 6.3). Magnesian calcite is also found in *A. africana* wood (Fig. 6.4).

Carbonate in African soils can be expressed as various soil features (Fig. 6.5, Fig. 6.6, and Fig. 6.7): 1) cell infillings in wood and roots (biomorphosis), mainly as sparite (> 16 µm), 2) sparitic crystal assemblage in peds, or free in soil pores, being able to form flowe -shaped structures, 3) micritic (< 16 µm) peds, composed mostly either by carbonate, mixed with amorphous organic matter, or mixed with organic matter and silicates. High concentrations of carbonate are found at 5 cm under the living *M. excelsa* tree. Oxalate crystals associated with carbonate are still present. 4) Carbonate coatings on peds are also found in the deeper soil layers. In the soil first layers, all the described features are found. Carbonate, as wood or roots cells pseudomorphoses, is only present in the first layers, whereas carbonate in peds (as micrite) is found in all the soil layers.

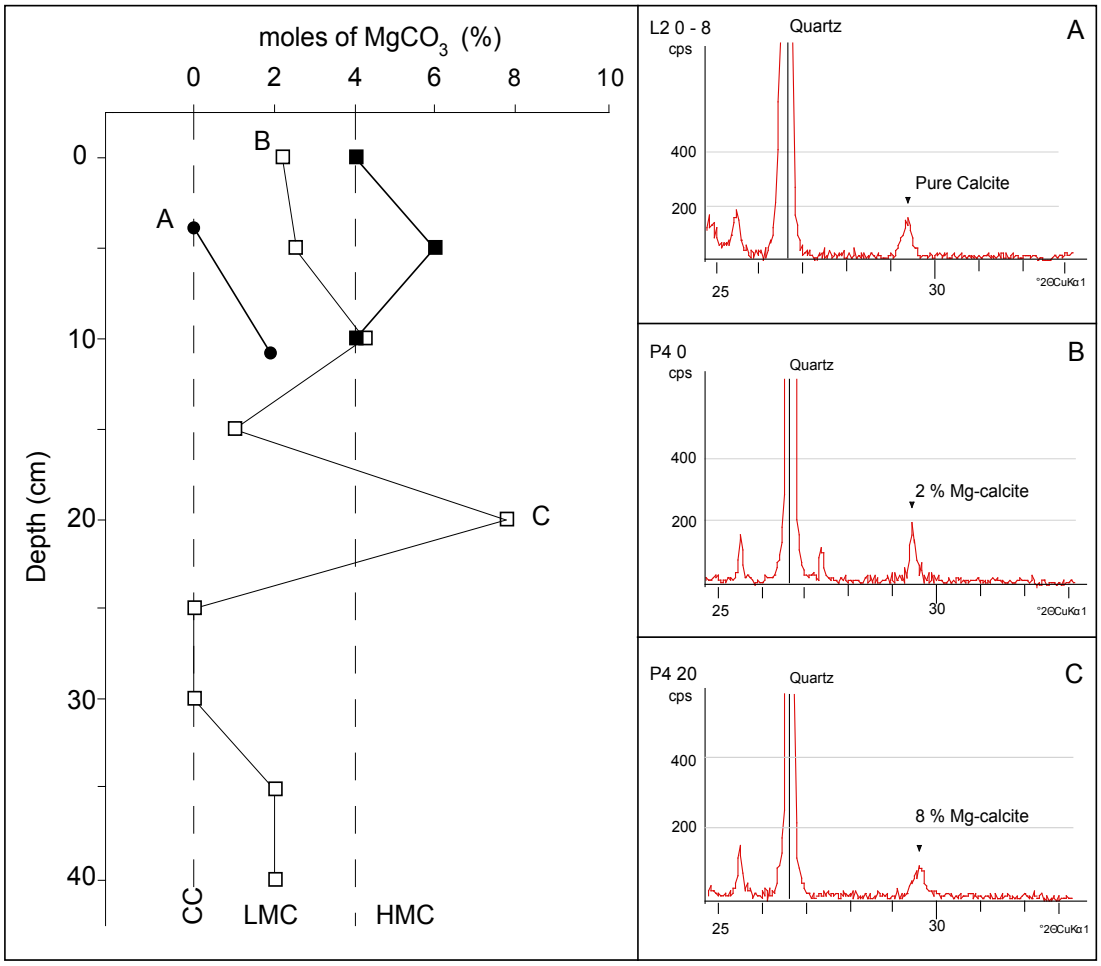


Fig. 6.3- Percentage of magnesian calcite in the profile under the A. africana *tree (black circle) with the respective XR diffraction spectra (L2 0-8), at 4 cm deep showing a pure calcite component (A). White square indicate the magnesium percentage found for the profile under the living* M. excelsa *tree (P4) and black square the values calculated for the soil under the* M. excelsa *stump. B and C are XR spectra from P4 profile at 0 cm and 20 cm deep respectively. CC: Calcium carbonate; LMC: Low magnesian calcite; HMC: high magnesium calcite.*

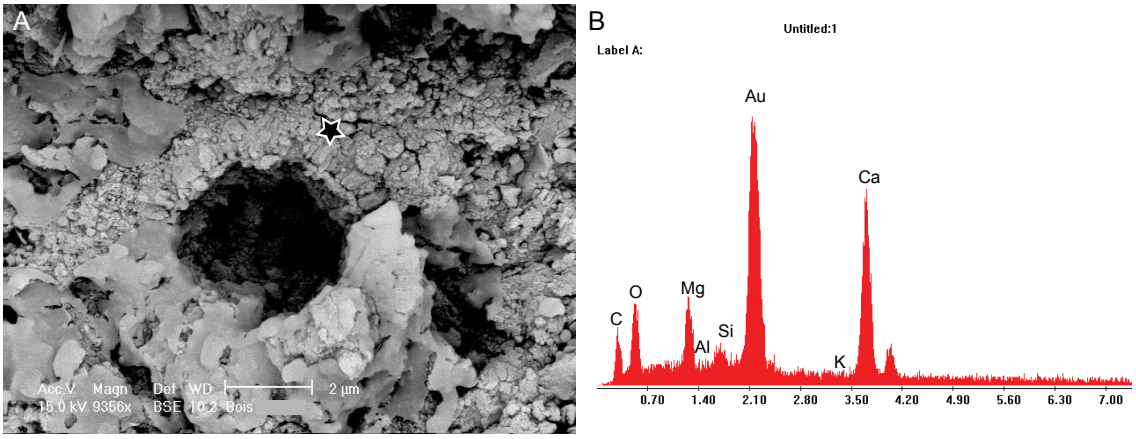


Fig. 6.4- SEM view of a pore in A. africana *wood. The border cells are partially mineralised (star symbol). EDS signal indicates a magnesian carbonate content ("Mg", "Ca", "C", and "O" peaks). "Au" peak is due to gold coating, whereas the "Si" and "Al" (silicon and aluminium) peaks are probably clay mineral contamination.*

Sparite crystals could result from mineralized wood and are present in the soil first layers. Micrite coatings are the predominant features in deeper layers. Carbonates under the *M. excelsa* and the *A. africana* stumps are mainly present as cells pseudomorphoses (sparite) of wood and roots, and only in the soil first three layers. Soils are sandy (Fig. 6.8) with a residual water content comprised between 0 and 0.8% (Annex 11). Granitoid bedrock contains, for 1 kg of rock, the following quantity of alkaline cations: 2.57 g of Ca, 7.24 g of Mg, 0.04 g of K and 0 g of Na (Annex 12). The reference soil exhibits a clear leaching of these cations, whereas an obvious accumulation is measured in soils related to oxalogenic trees (Annex 11 and Annex 12). The quantity of cations analysed in water (well waters and backwater) is in the same order of magnitude of a few mg for 1L of water (Annex 13).

6.3 Qualification of the carbonate state in soil profiles related to *M. excelsa* and *A. africana* trees

Carbonates are only found associated to oxalogenic trees where the pH is always alkaline. The carbonate amount, as a function of depth, has not the same trend than pH distribution (Fig. 6.2). The maximal carbonate amount is found in A horizons whereas a minimal and constant level is maintained all along the deeper horizons (B and C). The presence of some local peaks can partly be explained by the presence of roots, which create a zone where carbonate concentration is important (Fig. 3.7). Organic acid exudation and root respiration are common processes allowing carbonate formation in the rhizosphere (Nguyen 2003; Kuzyakov et al. 2006; Tu et al. 2007). The pH is more alkaline in deeper horizons than in those where carbonate is more abundant. Moreover, an alkaline pH peak is detected between 10 and 30 cm and thus shifted when compared to the overlying carbonate peak. The absence of correlation between the carbonate accumulation and pH alkalinity was already observed in similar ecosystems (Cailleau 2005). Consequently,

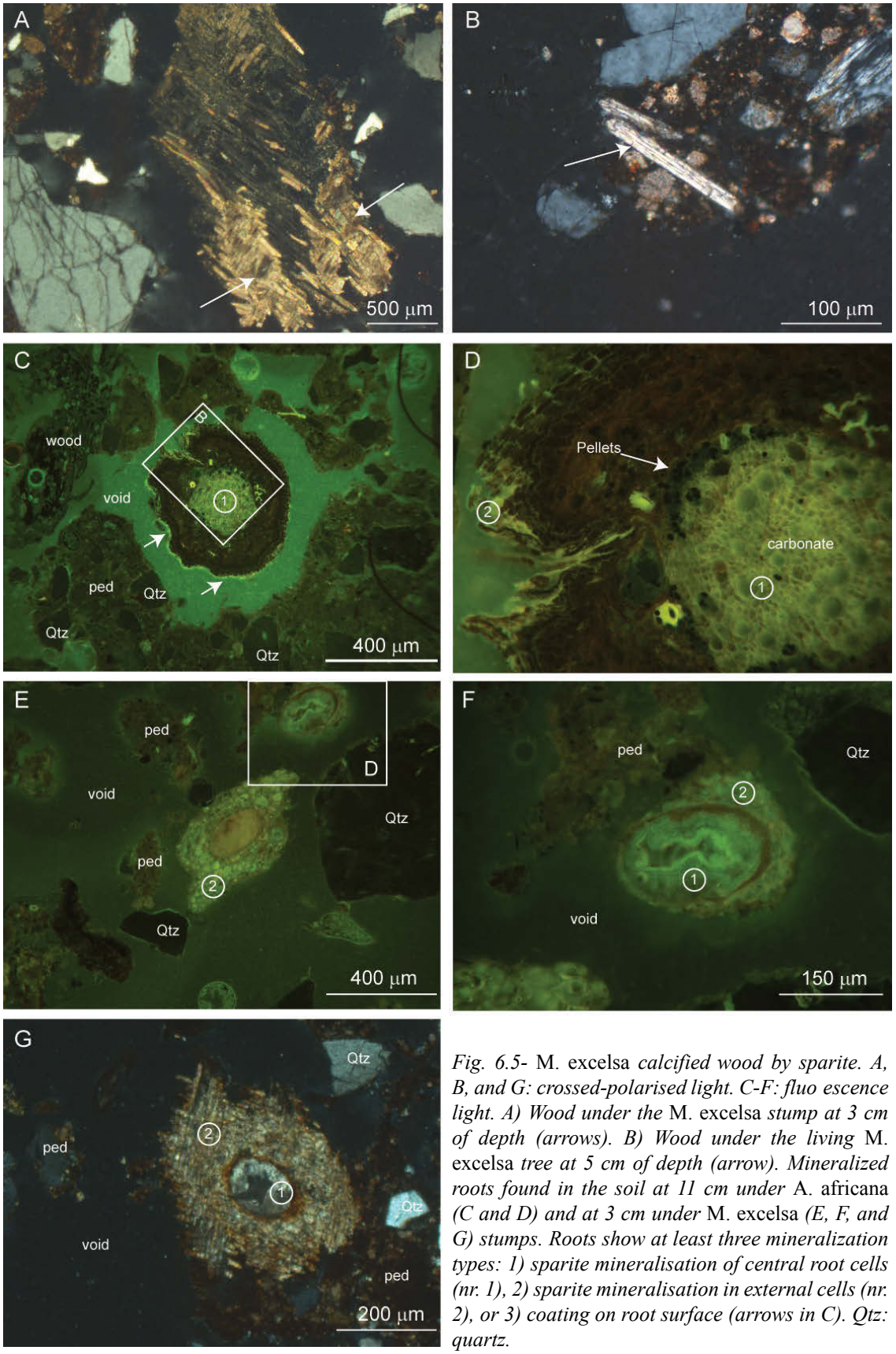


Fig. 6.5- M. excelsa *calcified wood by sparite. A, B, and G: crossed-polarised light. C-F: fluo escence light. A) Wood under the* M. excelsa *stump at 3 cm of depth (arrows). B) Wood under the living* M. excelsa *tree at 5 cm of depth (arrow). Mineralized roots found in the soil at 11 cm under* A. africana *(C and D) and at 3 cm under* M. excelsa *(E, F, and G) stumps. Roots show at least three mineralization types: 1) sparite mineralisation of central root cells (nr. 1), 2) sparite mineralisation in external cells (nr. 2), or 3) coating on root surface (arrows in C). Qtz: quartz.*

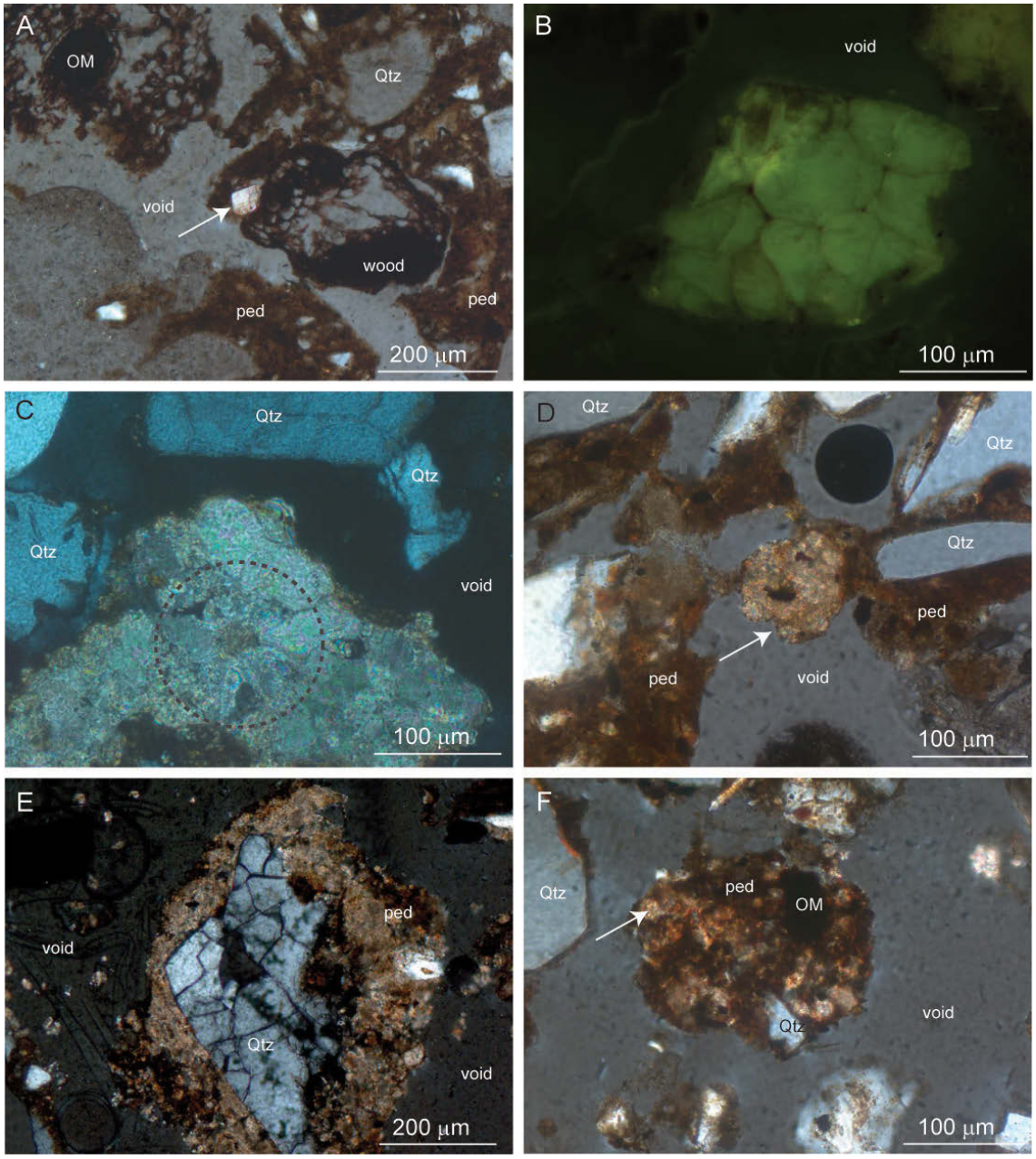


Fig. 6.6- A) Carbonate features found in soils surrounding A. africana *(A) and* M. excelsa *trees (from B to F). A) sparite crystals present at 11 cm under* A. africana *(arrow); OM: organic matter; Qtz: quartz crystal. B) sparite crystals found at 3 cm under* M. excelsa *stump. C) sparite assemblage at 3 cm under the* M. excelsa *stump. A flowe -shaped structure with a dark centre is visible in the dashed lined circle. D) Micritic ped (arrow) at 7 cm under the* M. excelsa *stump. E) Ped composed of carbonate and organic matter including a quartz crystal present at 5 cm under the living* M. excelsa *tree (PL). F) Ped composed of carbonate, organic matter, and quartz found at 12 cm under the living* M. excelsa *tree. A: natural light; B: fluo escence light; C-F: crossed-polarized light.*

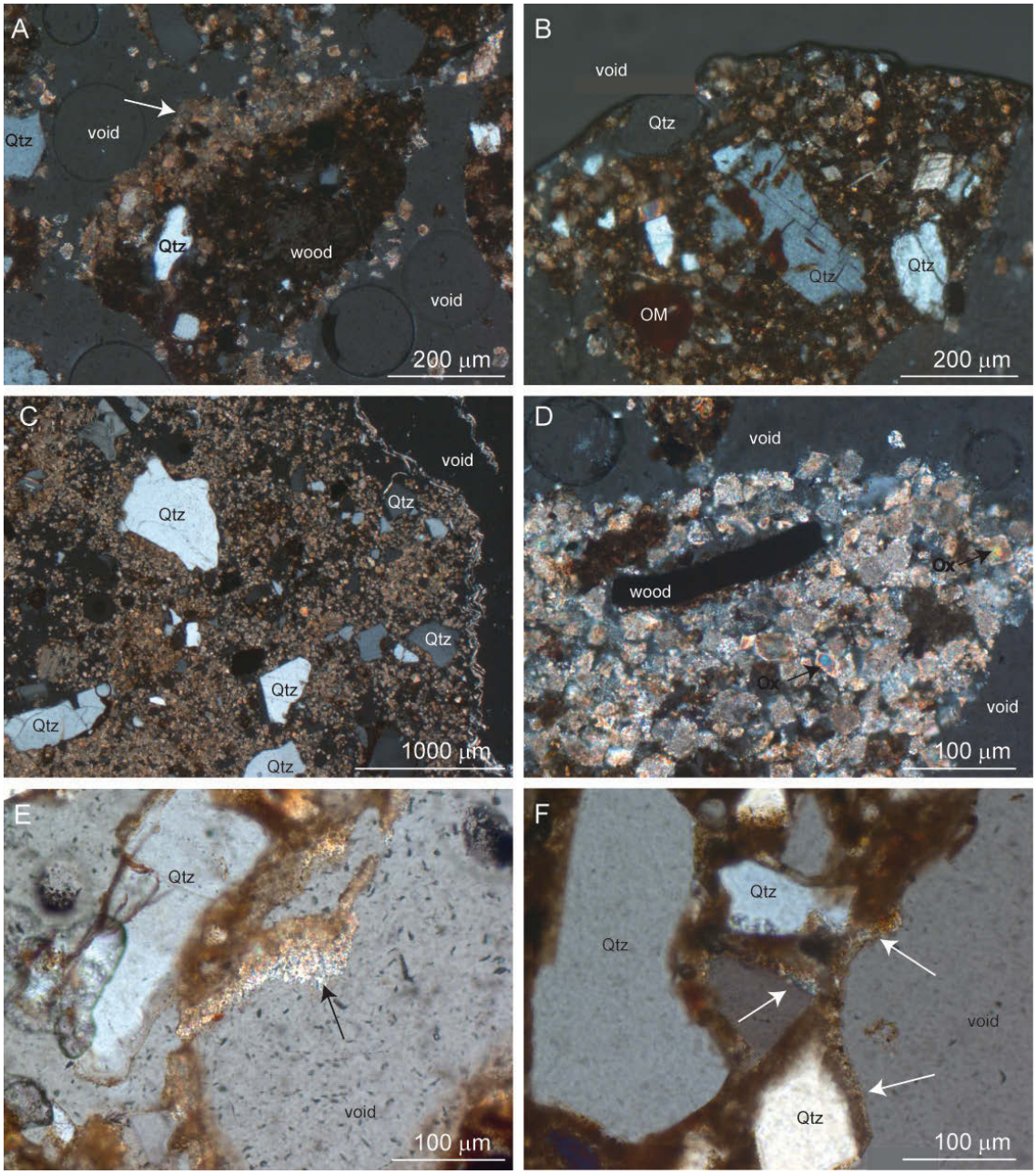


Fig. 6.7- Carbonate features (crossed-polarised light) found in soils surrounding M. excelsa *trees. A) Carbonate and oxalate accumulation around a wood remain found at 5 cm under the living* M. excelsa *tree. B) Ped composed of quartz, carbonate, oxalate, and organic matter present at 5 cm under the living* M. excelsa *tree. C and D) Carbonate and oxalate crystals including silicate and organic matter at 5 cm under the living* M. excelsa *tree. E and F) carbonate coatings (arrows) at 40 cm and 50 cm under the living* M. excelsa *tree.*

alkaline pH conditions are not due to the presence of calcite only. The process that manages pH alkalinity and carbonate precipitation is bacterial oxalate consumption (Braissant 2005; Cailleau 2005). Oxalotrophy modifies ion species and concentrations present in the soil solution, influencing pH conditions. Water percolation in the soil leaches carbonate ions in deeper layers where, if calcium is lacking, they remain in the solution and contribute and probably maintain an

alkaline pH environment. Calcite field stability, depending on pH conditions, is in turn strictly depending on temperature, pCO_2, and ion concentrations. Moreover, a minimal level of water is necessary, because phase equilibrium takes place in solutions. To have an approximation of the equilibrium taking place in an open system, *i.e.* soils, parameters such as temperature, pCO_2, ion and water concentrations are kept constant, reflecting an instantaneous equilibrium (Verrecchia et al. 2006). However, the reality is certainly more complex. Instantaneous equilibria are present in a kinetic environment. Images of these kinetic equilibria are carbonate cements composed of different possible seasonal layers found in Ivory Coast (Carozzi 1967; Cailleau 2005). In tropical systems, conditions of super-saturation or dilution are imposed by rain periods, alternating with dry periods, that in turns manage periods of intense and low biological activity, influencing the pCO_2 in the soil pores and carbonate precipitation.

Litter containing oxalate (oxalic acid, oxalate salt) deposited on the soil surface is rapidly decayed by saprophytic fungi and insects. Oxalate is thus released in the soil environment and available for bacteria that use it as carbon and electron sources, resulting in carbonate precipitation. Previous studies have shown that the highest concentration of oxalotrophic bacteria lies between the surface and 30 cm in depth, and consequently, constitutes the maximal potential for oxalate consumption (Braissant 2005; Khammar et al. 2009). Flower-shaped structures found previously in Petri dishes associated with *Ralstonia eutropha* bacteria (Braissant 2005; Cailleau 2005) are present in the studied soils, supporting the idea of a possible involvement of bacteria in carbonate precipitation (Fig. 6.6 C).

In the mineral horizons, the constant carbonate value can also be the result of the dissolution of the carbonate formed in the upper horizon, leached by water and re-precipitated in the deeper layers, forming coatings. Because the studied soils are sandy (Fig. 6.8), acid rains lasting six

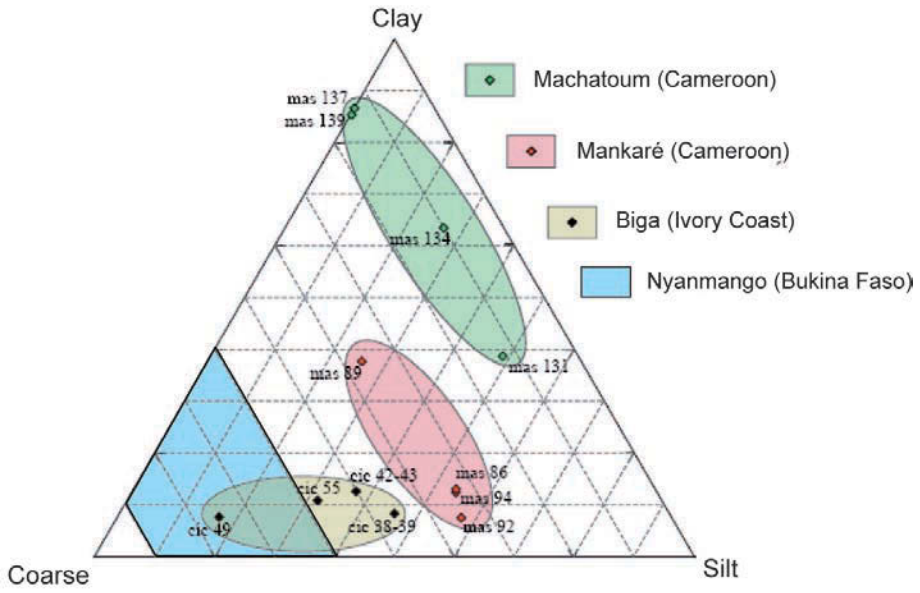


Fig. 6.8- Grain size ternary diagram of Burkina Faso soils compared to soils surrounding M. excelsa *from Cameroon and Ivory Coast (Cailleau, 2005).*

months favour the local carbonate dissolution in the soil surface and the leaching of carbonate ions in depth, where local supersaturation conditions can allow re-crystallisation. In the case of a sloping system, carbonate ions can also be leached away, reaching streams, which eventually will bring them to the oceans, where a biologically carbonate precipitation can take place.
In addition, in the soil, sawdust is present and likely results from wood cut and action of termites. One consequence is the release of carbonate crystals and oxalate salts from wood tissues, increasing the carbonate content in the soil first centimetres. Moreover, the stump wood is partially burnt, accelerating the oxalate transformation into carbonate. Micromorphology confirms the presence of highest carbonate concentrations in smithereens of wood tissues. Charcoal is present in soils as well (Fig. 6.9) evidencing savannah burning, a current practice providing quick and fresh growing for cattle of nomadic people (Peul ethnic group; Lerebours-Pigeonnière and Ménager 2001).

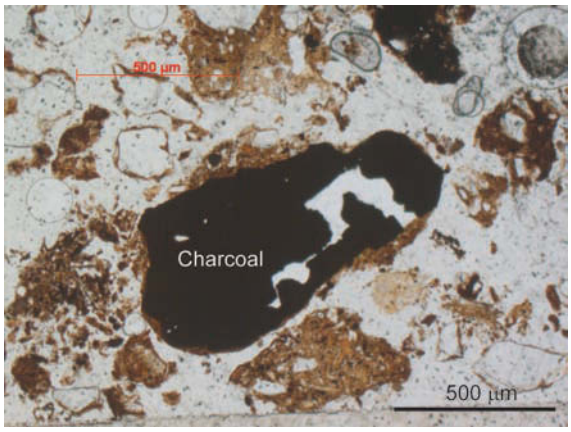


Fig. 6.9- Thin section detail (natural light), showing burned wood tissues present in the soil surrounding A. africana *stump probably resulting from the bush-fi e practice.*

The transformation of oxalate crystals into carbonate during combustion is carried out when the temperature exceeds 470°C (Canti 2003; see Chapter 4). This process affects the soil first centimetres and resulting carbonate crystals retain the calcium oxalate habit and can therefore be considered as a calcium carbonate pseudomorphosis on Ca-oxalate (Cailleau 2005). The same characteristics and processes observed in the *M. excelsa* stump are also present in the *A. africana* stump. There is a high carbonate amount in the soil first layers, with a regular decrease with depth.
The carbonate found has low magnesium-calcite mineralogy, and is present in wood as well as in the soil. Oxalotrophic bacteria were found on wood surface from oxalogenic Indian (Pr. Aragno personal communication) and Bolivian trees (M. Mota, pers. com.). Low magnesium-calcite has also been found in Cameroon and Ivory Coast soils surrounding oxalogenic trees (Cailleau 2005). Precipitation of this kind of low magnesium carbonate could be the result of a pure physicochemical process (e.g. supersaturation), or driven by microorganisms (Kübler 1992; Braissant 2005; Dupraz et al. 2009). Because carbonate formation is in this case the consequence of the oxalate-carbonate pathway, it is possible that the oxalate involved is a magnesium oxalate, such as glushinskite [$Mg(C_2O_4) \cdot 2\ H_2O$], which is commonly associated with plants (Cowgill 1989; Garvie 2003; Monje and Baran 2005), fungi (Adamo and Violante 2000; Kolo and Claeys 2005; Gadd 2007), or lichens (Wilson et al. 1980; Adamo and Violante 2000; Burford et al. 2003). In fact, magnesium is present in the bedrock and soils (Annex 12). Moreover, fungi and bacteria can influence the cationic species of carbonate during biochemical processes (Braissant 2005). Magnesium is preferentially associated with fungal hyphae because fungi are metalophile. The

ionic difference in carbonate species can be the result of the oxalate consumption by different oxalotrophic bacteria due to their different affinity for a specific cation (Braissant 2005). This affinity can depend on the available links associated to the cell wall as well as the chemical nature of the link sites (Braissant 2005). Nevertheless, there is no doubt that the oxalate-carbonate pathway allows the accumulation of alkali cations. This accumulation is the end-product of an immobilisation of Ca and Mg related to the carbonate precipitation.

6.4 Quantification of carbonate in the rhizosphere of *M. excelsa* trees and the *A. africana* stump from Burkina Faso

On the basis of core sampling, sieving, and carbonate titration we estimated the carbonate present in the soil volume under the living *M. excelsa* tree foliar crown as well as in the soil surrounding the *M. excelsa* stump cut 18 years before sampling. Results under the *A. africana* stump being available, we compared the carbonate content under these two different tree stumps. In this estimation, we have neither measured the mineralised wood nor the carbonate present in the coarse fraction (> 2 mm).

Complete results and calculations are given in Annex 14). The carbonate present under the living *M. excelsa* tree foliar crown, until 60 cm in depth, is estimated at ~ 50 kg for m^3 of soil (that is 6 kg of mineral carbon for m^3 of soil). Under the *M. excelsa* stump, it is **~** 30 kg of carbonate for m^3 of soil, and in the *A. africana* stump soil the value is **~** 20 kg/m^3.

The different carbonate accumulations between the two stumps can be explained, by the different diameters for both stumps (80 cm for *A. africana* versus 92 cm for *M. excelsa*) or the sampling strategy, as well as the intrinsic soil parameters. Moreover, nor the age of the *A. africana* stump, neither the date of the cut, are known with certainty. The carbonate content in the soil surrounding *M. excelsa* and *A. africana* trees is in the same order of magnitude than the one measured by Cailleau (2005) in non-sieved soil, who found a value of 128 kg carbonate/m^3 of soil under a stump 170 years old.

The carbonate content in these systems is underestimated because neither the carbonate present in the mineralised wood nor the carbonate remaining in the fraction > 2 mm, are considered. We have the carbonate quantity present in the soil of a living tree and a stump cut 18 years ago. Because the trees have the same trunk diameter and assuming that each tree system has worked under the same conditions, producing equal carbonate amount for a given time, we are now able to calculate a carbonate leaching ratio vs. time, and an approximation of the carbon residence time in Burkina Faso soils, and by analogy, in Cameroon soils.
The age of the tree is necessary to give an accumulation rate. Lacking a precise dating method, such as ^{14}C or dendrochronology, we estimate the tree age on the basis of a *M. excelsa* stump of Machatoum (Cameroon) of 2.3 m in diameter which has been dated with ^{14}C as 170 ± 30 year

old (Cailleau 2005). With the assumption that the trunk growth is linear (Durrieu De Madron 2003), the Burkina Faso trees, with a 0.9 m in diameter should have an age of about 70 years. This estimation is in agreement with the age estimation given by a Mangodara man present at the plantation. Supposing, as a first approximation, that the accumulation is linear in time, the accumulation is about 120 kg of carbonate per year that is equivalent to a sequestration 50 kg y^{-1} of atmospheric CO_2.

6.5 Carbonate leaching rate and carbon residence time in tropical soils under a *M. excelsa* tree

Is the *M. excelsa* ecosystem a long-term carbon sink? The order of magnitude of the residence time for soil organic carbon (SOC) ranges from 10 till 1'000 years (Prentice et al. 2001), whereas for mineral carbon, the residence time can be even 100'000 times longer, with an estimation of 10^2 to 10^6 years (Retallack 1990). Is this estimation applicable to the inorganic carbon from the tropical *M. excelsa* soil? If the living tree is cut now, how long will the carbonate remain in the soil? To answer this question, the soils under a living *M. excelsa* tree and a stump with the same diameter cut 18 years ago are compared. Using the previous results, it is possible to estimate a potential carbonate residence time and a carbonate leaching rate for the studied Burkina Faso system.

To simplify, we assume that, in the *M. excelsa* ecosystem, only rain dissolves carbonate. In fact, pH of rain is about 5.6 and thus, rain can act as an acid, attacking carbonates and leading to carbon leaching (Harter 2002). Bicarbonate ions (HCO_3^-) are then carried by the water system towards the oceans, where they play a role in the sea carbonate precipitation ($CaCO_3$). During precipitation reactions, only one mole of bicarbonate (among the two consumed) precipitates, the other one being reintroduced in the atmosphere in the form of CO_2. In this case, the soil acts as a carbon pump between the atmosphere and the hydrosphere.

The difference between the carbonate content between the living tree and the stump can be used to estimate the carbonate leached during 18 years, estimation that leads to a value of 38.5 kg of carbonate loss per year. Thus, assuming to cut the 70 years old tree right now, all its carbonate would be completely dissolved in approximately 210 years, giving a carbonate residence time of 280 years for a 70 years old stump. Observation of carbonate blocks in soil surrounding *M. excelsa* tree of more than 150 years (Campbell and Fisher 1932; Harris 1933; Carozzi 1967; Cailleau 2005) suggests that the residence time of carbonate could easily reach 1000 years.

6.6 Comparison of carbonate content in the soils of *M. excelsa* trees from Burkina Faso, Ivory Coast, and Cameroon

The carbonate content in the rhizosphere of the living Burkina Faso tree is ~ 50 kg/m^3 of soil, while there are 128 kg of carbonate/m^3 of soil around a stump in Biga (Ivory Coast; Cailleau

2005; Table 6.1). Moreover, in the soils related to *M. excelsa* trees from Ivory Coast (Carozzi 1967; Cailleau 2005) and Cameroon (Cailleau 2005), carbonate blocks are present, whereas, no blocks were found in Burkina Faso soils. In the soil under the living *M. excelsa* tree in Ivory Coast, accumulation is so important that carbonate blocks can reach 1.0 to 1.5 m in size (Carozzi 1967). Similarly, in the soil surrounding a stump in Biga, 2 kg of carbonate were found in the first 50 centimetres, and in Mankaré, 48 kg of carbonate were also found in 0.5 m^3 of soil (Cailleau et al. 2005). These three last trees were cut less than one year before the sampling period (Dr. Cailleau pers. comm.).

Tree	Country	Site	State of the tree	Cut period befor sampling	Tree diameter	Basement	Soil type	A.m.s.l.	Sampling period	Ref.
1. M. excelsa	Cameroon	Mankaré	stump	1 year	2.2 m	alluvial deposits	ferralitic	620	2 - 3. 2003	1 & 2
2. M. excelsa	Cameroon	Machatoum	stump	1 year	2.3 m	basalt	ferralitic	770	2 - 3. 2003	1 & 2
3. M. excelsa	Ivory Coast	Biga	stump	1 year	2.5 m	granites & granitoids	ferralitic	280	4. 2002	1 & 2
4. M. excelsa	Burkina Faso	Mangodara	living		0.9 m	granitoids	ferralsol	300	11. 2005	3
5. M. excelsa	Burkina Faso	Mangodara	stump	18 years	0.9 m	granitoids	ferralsol	300	11. 2005	3
6. A. africana	Burkina Faso	Niangoloko	stump	10 years	0.9 m	granitoids	ferralsol	300	11. 2005	3
7. Opuntia sp.	Spain	Tabernas	living			schistes ardoisier	colluviosol isohumique	1000	2 - 3. 2004	1 & 2
8. Opuntia sp.	Italy (Sicily)	Salina	living			pyroclastic deposits	andosols	40	4. 2006	3
Tree	**Site**	**Climate**	**Precipitations mm/year**	**Wet months**	**T°C**	**Situation**	**Ox (mg/kg)**	**Carb. (%)**	**Grain size**	**Ref.**
1. M. excelsa	Mankaré	equatorial	3000 - 5000	4 - 7 & 9 -12	25 ± 2.8	slope (< 5°)	0 - 70	0 - 73	clay to sandy	1 & 2
2. M. excelsa	Machatoum	equatorial	3000 - 5000	4 - 7 & 9 -12	25 ± 2.8	slope (15°)	0 - 175	-	clay to silt	1 & 2
3. M. excelsa	Biga	tropical	2500	3 - 7 & 9 -11	26	plain	0 - 255	0 - 64	silt/sandy	1 & 2
4. M. excelsa	Mangodara	intertropical	1300	4 - 10	16 - 40	plain	0 - 47	0 - 13	sand	3
5. M. excelsa	Mangodara	intertropical	1300	4 - 10	17 - 40	plain	0 - 83	0 - 15	sand	3
6. A. africana	Niangoloko	intertropical	1300	4 - 10	16 - 40	plain	4 - 61	1 - 5	sand	3
7. Opuntia sp.	Tabernas	sub atlantic	200	6 - 9	-5 - 48	slope (15°)	183 ± 253	0 - 1	?	1 & 2
8. Opuntia sp.	Salina	Mediterranean	600	5 - 8	16 - 22	gently slope	0 - 10	1 - 3	sand-silt	3

Table 6.1- Main factors present in M. excelsa, A. africana*, and* Opuntia sp. *ecosystems. A.m.s.l.: above mean sea level. References: 1. Cailleau (2005); 2. Braissant (2005); 3. This study.*

Why is there at least three times less carbonate (per m^3) under the Burkina Faso *M. excelsa* tree than under the Ivory Coast or Cameroon trees? Some hypotheses can be discussed regarding this large difference. In the following paragraphs, we will examine some parameters that could influence the carbonate content such as (1) the age of the tree, (2) the moisture regime, (3) the soil grain size distribution, (4) the calcium/magnesium and nitrogen limiting factors, and (5) the equilibrium conditions. This list is obviously not exhaustive.

The most evident factor that can explain the lower accumulation of carbonate in Burkina Faso soil is the different age of the trees. We previously calculated that the Nyanmiango tree is about 70 years old, whereas the Biga tree, as the Cameroon trees, is 170 ± 30 years old. It is possible that in 100 years the Nyanmango tree will reach a carbonate accumulation similar to that found in

Ivory Coast or Cameroon soils. Carbonate quantification under trees from the same place and of different age would answer this question and further improve the proposed model.

Because it has been demonstrated that the main carbonate formation takes place in biofilms (Braissant 2005), a minimal amount of water in soil pores is essential. Climate of Burkina Faso, Ivory Coast, and Cameroon, differs in terms of rainfall amount. This factor can profoundly influence the intrinsic soil parameters. Rainfall data (Breman and de Ridder 1991) over a period of 80 years (1920- 2000) show that the mean annual value in Burkina Faso is between 800 and 1250 mm, in Ivory Coast between 1250 and 1500 mm, and in Cameroon between 1750 and 2250 mm (Fig. 6.10; http://www.cpc.ncep.noaa.gov/). One consequence on the soil is its moisture regime, which is ustic (dry in some or all parts for 90 or more cumulative days per year) in Burkina Faso, ustic to udic in Ivory Coast, and udic (dry in all parts for less than 45 consecutive days) in Cameroon (NRCS 2007; http://www.soilinfo.psu.edu/). Moreover, in Burkina Faso and Cameroon, there is only one rainy season, whereas in the Biga site there are two. Consequently, two carbonate supersaturation periods can occur. The alternation of dry and moist periods are attested in Biga soils by laminated cements with contrasted isotopic signatures (Cailleau 2005). In Burkina Faso, the longer duration of dry conditions (from May to October) decreases the biological activity period, the oxalate consumption, the carbonate formation, and the subsequent carbonate accumulation.

In addition, soil texture influences water and ions retention. Nyanmiango soils are mainly sandy (Fig. 6.8) and the low content in organic matter and clay also results in residual water content < 1% (Annex 11). If clayed layers can acts as permeability barriers supporting lateral flux (Cailleau 2005), sandy layers can also act in the same manner. Carbonate ions are leached to the river

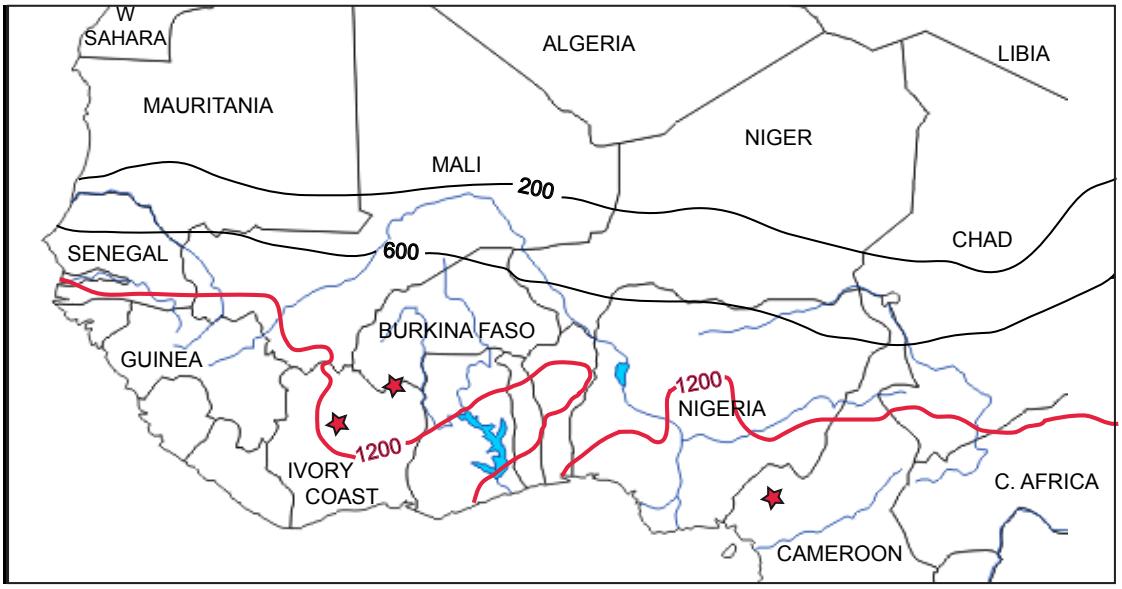


Fig. 6.10- West African average annual rainfall isohyetes in mm/yr (Breman and de Ridder 1991). Stars indicate sites of studied M. excelsa *trees. Burkina Faso: this study; Cameroon and Ivory Coast: Cailleau (2005) and Braissant (2005).*

system, and then to the ocean, where they can precipitate via biomineralization. Nevertheless, in this system, carbonates fill progressively the soil pores, diminishing gradually the hydric regime and water circulation.

A further hypothesis of the lower content in calcium carbonate is that the environment for carbonate formation is not stable enough so that the conditions are insufficiently alkaline. The carbonate stability field, at 25°C and 1 atm, starts at pH 8.4. Nyanmango soils influenced by *M. excelsa* tree have a mean pH of 8.1 ± 0.6 (Fig. 6.2). Below 8.4, bicarbonate ions (HCO_3^-) are dominant (Fig. 1.3) and calcite crystallisation does not take place spontaneously. Nevertheless, micro-environments with a pH > = 8.4, and situations of supersaturation would allow calcite precipitation.

One limiting factor that manages the carbon immobilization is calcium (Ca), and to a lesser extent, magnesium (Mg) availability. Primary Ca and Mg sources are silicates (Fig. 1.4) that show, in the analyzed soil profiles, dissolution gulfs (Fig. 6.11). Silicate dissolution factors are discussed in Chapter 1. Once released from silicates, Ca and Mg are 1) incorporated in the biomass, 2) complexed with oxalic acids (or other organic ligands), 3) precipitated with CO_3^{2-} to

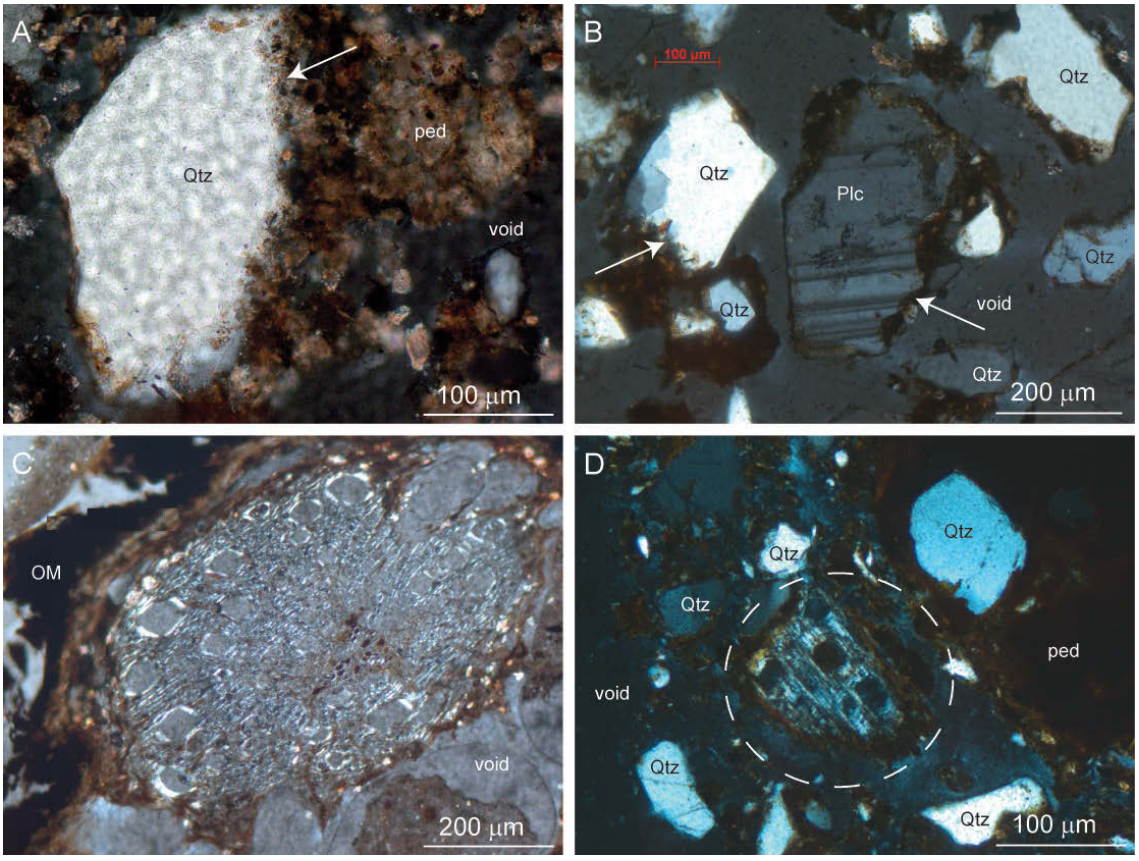


Fig. 6.11- A and B) Thin section details (crossed-polarized light) of soil under a living M. excelsa *tree showing quartz (A) and plagioclase (B) with corrosion gulfs (arrows). Plagioclase remains attest the calcium origin from silicate minerals. C and D) Silicified wood remains in soil under* A. africana *stump (C) and* M. excelsa *stump (D).*

form carbonate, 4) leached in river systems, 5) carried by wind or 6) dust or 7) incorporated and translocated by fungal hyphae. Second carbon sources (recycled) calcium/magnesium sources are 1) organic matter, 2) oxalate salts, and 3) carbonate.

For the studied system, the Ca and Mg contribution can be calculated, or estimated, either by means of previous literature data or with results achieved with this study. The Ca and Mg content from leucocratic granitoidic bedrock are respectively of 2.57 and 7.24 g/kg of rock (Annex 12). The amount of released Ca and Mg from granitoid can be estimated as 0.030 to 0.352 kg/ha/year for Ca and as 0.006 to 0.344 kg/ha/year for Mg (Boeglin and Probst 1998; Doumbia et al. 1998; Bierman and Caffee 2001; Cailleau 2005). The fraction carried by the wind (Harmattan) into the organic matter, is estimated as 3.5 kg/ha/year for Ca and of 0.4 kg/ha/year for Mg (Stoorvogel et al. 1997). The rainfall contribution, containing Ca and Mg in ionic state (Ca^{2+} and Mg^{2+}), is 2.5 to 4.6 kg/ha/year for Ca and of 0.6 kg/ha/year for Mg. Thus, from silicate weathering, wind, and rainfall, the total Ca and Mg inputs are of about 10 kg/ha/year and 1 kg/ha/years respectively (Fig. 6.12).

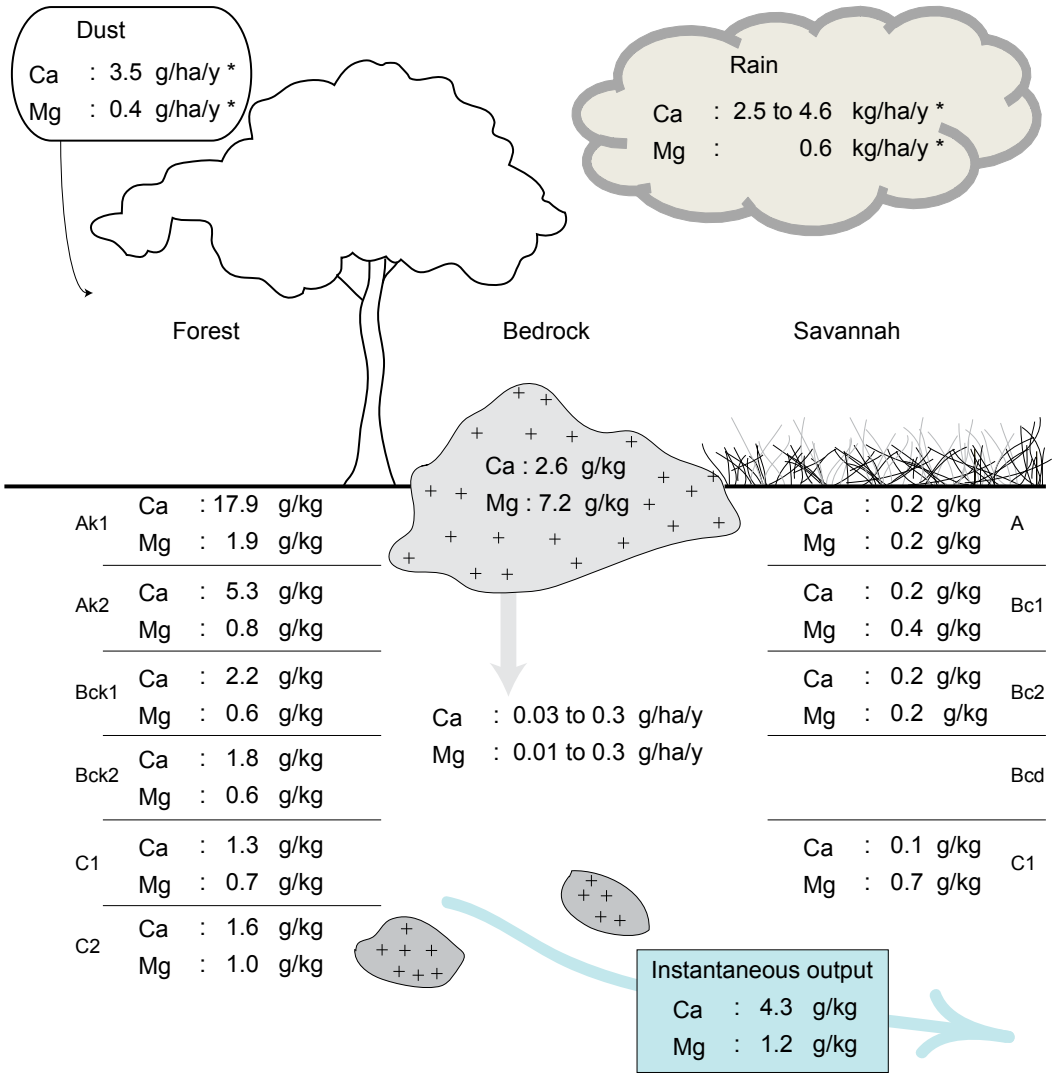


Fig. 6.12- Calcium and magnesium balance from literature (*) and this study.

Organic matter, organic acids, and carbonates present under the oxalogenic tree, promote an unusual accumulation of Ca and Mg, compared to other tropical soils. If in the reference soil (F3), the Ca and the Mg are leached, by comparison with the bedrock, soils implicated in the oxalate-carbonate pathway clearly show a Ca (and in minor part a Mg) enrichment, especially in the first 15 cm (Fig. 6.12). This accumulation is associated with an increase of the pH values and the cation exchange capacity (Annex 11) reaching levels, in the surficial layers, comparable to those of the Burkina Faso compost (Zosso 2007). Loss of Ca and Mg induced by river systems is very low, with an instantaneous measurement of ~ 4 ppm of Ca and 1 ppm of Mg (Annex 13).

6.7 A particular case: the Salina ecosystem

The study of an ecosystem composed of *Opuntia sp.* in a Mediterranean environment was motivated by the high content of oxalate normally measured in cacti (Garvie 2003). Results would have been useful in order to calibrate the parameters necessary for the formation of this carbon sink.

The carbonate content in Salina soils (PC1 and PC2) and the pH values do not vary either with depth or the presence of *Opuntia sp.* plants (Annex 11), contrary to what has been observed in Africa. Values are of 27.5 ± 4.5 g of carbonate/kg of soil and the pH is 6.8 ± 0.3. On the other hand, dust material sampled in Salina Island clearly shows a magnesium rich carbonate exogenous source (Fig. 6.13), probably carried by Sahara dust storms (Goudie and Middleton 2001).
The fact that these values do not vary with the depth, and the presence of similar carbonate contents in the reference soil and the soil under the cactus, challenges the proposed oxalate-carbonate pathway. Nevertheless, the acid tests clearly show the high presence of carbonate on decayed cladodes (Fig. 3.11), rich in oxalate druses. Moreover, the absence of oxalate accumulation in these soils indicates that oxalotrophy must take place. So what does happen? A hypothesis is that the oxalate-carbonate pathway takes place anyway in the degraded cladodes still attached to the plant, and/or the carbonate carried by the wind hides the carbonate characteristic curve. If carbonate precipitates in the soil or carbonate ions are formed as a result of the oxalate-carbonate pathway, during rainfall periods, carbonate leaching is facilitated by the fairly steep topography (see Chapter 3). As a result, the carbonate in the soil surface remains constant. In any event, if this soil cannot be considered as a sink, it acts as a carbon pump from the atmosphere to the hydrosphere and constitutes a support for organisms involved in the oxalate-carbonate pathway.

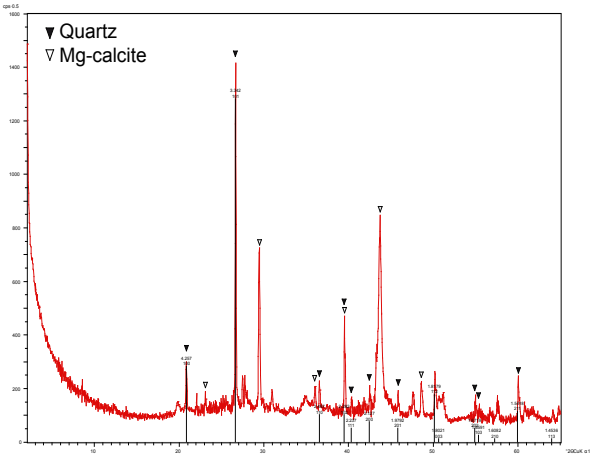


Fig. 6.13- X-ray spectrum of Salina dust showing a magnesium component of 5%.

6.8 Summary

- The oxalate-carbonate pathway studied in Ivory Coast and Cameroon takes also place in Burkina Faso where climatic conditions are drier.
- As previously supposed, *Milicia excelsa* is not the only tree able to generate the oxalate-carbonate pathway. The African trees *Afzelia africana* (and *Bombax costatum*) have been proven to be able to stock carbon (in its carbonate form) in the soil.
- The pH values and the carbonate presence in soils under oxalogenic African trees clearly prove the tree (litter) influence on soil chemistr .
- The distribution of carbonate in Burkina Faso soils shows the impact of *M. excelsa* and *A. africana* trees on the oxalate-carbonate pathway. *A. africana* is a potential and confirmed soil carbon sink driver. More analyses under a living tree would allow the potentiality of this tree to be compared to *M. excelsa*. Despite the high oxalate content in *Opuntia sp.*, the carbonate curve in the soil is different from the one found under African oxalogenic trees.
- Various factors influence carbonate accumulations in soils: intrinsic soil properties (grain size, calcium availability), system maturity (age of the tree, carbonate infilling soil pores), external factors (topography, climate), bioturbation (termite and ants).
- Supersaturation conditions, soil humidity, and alternation of dry and moist conditions are important to attain significant carbonate accumulations
- Carbon residence time in soils is of several hundred years. Dissolution of this pedogenic carbonate allows the carbonate ions to enter the hydrosphere where carbonate can re-precipitate. In this case, the oxalogenic tree ecosystem works like a carbon pump from the atmosphere pool to the ocean reservoir.
- This first and rough model of carbonate accumulation in tropical soils demonstrates that the *M. excelsa* oxalogenic tree is an effective, fast, and powerful pump driving CO_2 from the atmosphere to the soil. Availability of more data would allow the establishment of a more accurate model. It could be run in a STELLA software application, able to create and visualize dynamic systems such as the oxalate-carbonate pathway.
- Discovery of *M. excelsa* trees in Burkina Faso and another tree ecosystem, the *A. africana* tree, showing a potential capacity to initiate the oxalate-carbonate pathway, encourages and confirms that African soils constitute a carbon sink.
- These results confirm previous researches on the importance and occurrence of soil inorganic carbon formed in tropical soils (Braissant et al. 2003; Braissant et al. 2004; Cailleau et al. 2004; Braissant 2005; Cailleau 2005; Cailleau et al. 2005; Verrecchia et al. 2006) for the global carbon balance in terrestrial ecosystems. Soil inorganic carbon plays an important role in soils of dry regions (Lal 2004), but it seems now clear that tropical regions have also to be taken into account.

Chapter 7 CONCLUSIONS

The carbon balance

Results of this study, together with works presented by Cailleau (2005), Braissant (2005), and Khammar (2009), have considerably enhanced our knowledge about the oxalate-carbonate pathway, which is now known to be able to induce the formation of an important mineral carbon (and calcium) stock in tropical soils. In this thesis, we tried to give an answer to the following question: what is the concentration of carbon present in three different forms, i.e. as part of organic matter, as oxalate, and as carbonate, both in the considered tree and in its related soil? Once this question answered, we propose a carbon balance. The main conclusions can be summarized as follows.

7.1 Carbon in its organic form

By means of Rock-Eval pyrolysis, it has been found that, in Burkina Faso soils, the total organic carbon (TOC) does not exceed 3% of the total soil mass and is present in six different hydrocarbonaceous compounds. These carbon pools are present until 60 cm in depth. At the depth of 10 cm, the bio-molecule signals decrease and the geo-molecule signals become dominant, suggesting that, with increasing depth, the carbon stock is present in oxygenated material rather than hydrocarbonaceous compounds. New thermal S2 intervals have been defined based on about 110 sampled soils and 10 reference organic materials. It clearly appears that the S2 curve shapes can be completed with the analysis of S3 and S4 curves for the characterization of the carbon present in the bulk soil. For the first time, the Rock-Eval6 spectra of chitin (a structure molecule), fungal material, insects, and calcium oxalate salt (Ca-ox) have been analyzed. In addition, Rock-Eval6 results are supported by thin sections observations.

7.2 Carbon in oxalate form

The enzymatic protocol used for the urinary oxalate quantification was adapted for both plant and soil materials in order to measure their respective concentrations in oxalic acid. Leaves of *Milicia excelsa* trees from Southern Burkina Faso contain about 90 mg of oxalic acid/100 g of dry material. This quantity is sufficient for a 70 year-old tree to accumulate inorganic carbon in soil. Moreover, it turned out that *Afzelia africana* trees, which contain oxalic acid in leaves (280 mg/100 g) as well as in wood (15 mg/100g), could potentially be even a more powerful atmospheric carbon pump than *M. excelsa* tree.

Furthermore, a second source of oxalate has been investigated, i.e. Fungi. The developed and determined fungal community is entirely composed of moulds (*Aspergillus sp.*, *Mucor sp.*, and *Fusarium sp.*). This result confirms the fact that, in the studied soils, there is a flora, probably very rich and still underestimated, of fungi that secrete oxalic acid. Since only these two sources

have been taken into account in the present work, it is important to mention that at least two other sources have not been measured, but only discussed: excretion of oxalic acid by plant-roots and by bacteria. Being stable at atmospheric conditions, oxalate salts should accumulate in soils and be found in the geological record, or at least in old soils. The quantity of oxalate in soils, associated with oxalogenic trees, showed that, even on the soil surface, the concentration of oxalate does not exceed few ‰, i.e. 100 times less than in leaves. The process which quickly mineralizes oxalate is the bacterial oxalotrophy (Khammar et al. 2009).

7.3 Carbon in carbonate form

An indirect consequence of bacterial oxalotrophy is carbonate precipitation, which occurs not only in soil pores, but can start from the litter as well, and probably already on the trunk. Because calcium comes from silicate weathering, dust, and rain, pedogenic carbonate is considered to act as a carbon sink. In Burkina Faso, under a 70 year-old tree, the carbonate content reaches a maximum of 15% of the soil mass and, as opposite to older ecosystems (Ivory Coast, Cameroon, and Uganda), no carbonate blocks have been found. This information led us to briefly discuss some factor influencing this mineral accumulation. The main factors that maintain and improve the carbonate accumulation are the age of the tree, the alternation of dry and rainy periods, and the availability of calcium.

7.4 Distribution of carbon forms in Burkina Faso and Ivory Coast ecosystems

A carbon balance of the studied ecosystem is calculated in order to show the potential of a tropical tree-soil system to pump carbon dioxide from the atmosphere to the soil and to demonstrate its ability to form a long-term carbon sink. This system is similar, but non-equal, to those studied by Cailleau (2005) in Ivory Coast (Fig. 7.1). The main differences are the ages of the trees (70 years vs. 170 years), the state of the tree (living tree vs. stump), and the dynamics of the oxalate-carbonate pathway itself. In Burkina Faso ecosystems, the TOC diminishes drastically from the initial surface until 15 cm in depth. After this limit, however, the values become constant. This distribution is regulated by the tree litter fall. Oxalate and carbonate are present from the soil surface. Oxalate is present in leaves, and once on the soil surface, the carbonate is formed as a result of the microbial oxalate oxidation. In the litter, plant and fungal oxalates are mixed. At 5 cm in depth, a positive carbonate peak and a negative oxalate peak is observed, could indicate an optimum of oxalate consumption. The maximal carbonate precipitation is therefore located in the very first soil centimetres, just under the soil surface. A further oxalate peak can be observed at 10 cm in depth, where the influence of fungal, root exudates, and root degradation is not negligible. Finally, a TOC and an oxalate peaks are also observed at 30 cm in depth. These two peaks can be explained by either the presence of tree roots, which actively release oxalic acid, by root senescence, or by biodegraded roots, releasing passively oxalate salts.

In comparison, the distribution of carbon under a hollow stump of *M. excelsa* in Ivory Coast

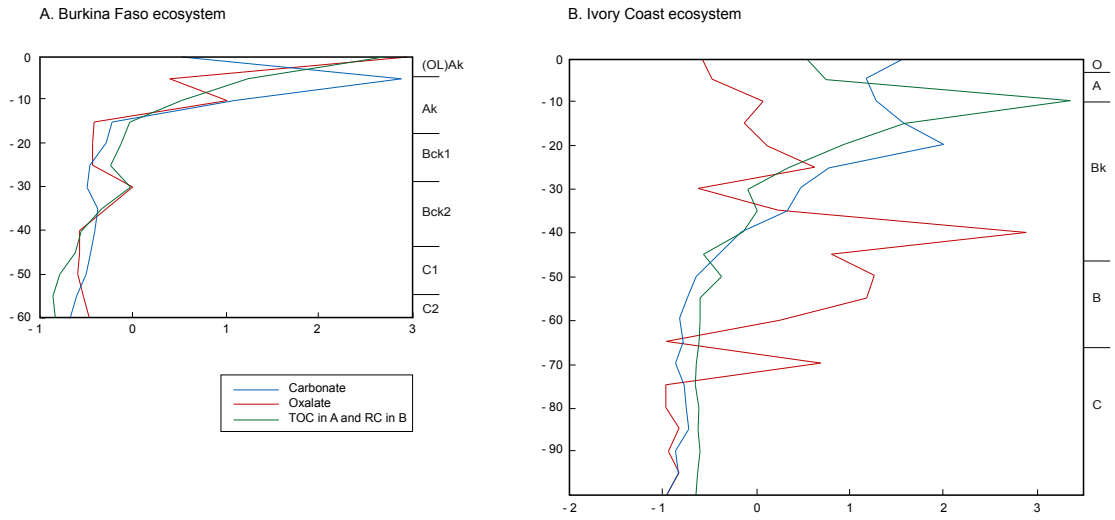


Fig. 7.1- Distribution of total organic carbon (TOC) Burkina Faso (A) and residual carbon (RC) Ivory Coast (B; Cailleau 2005), carbon in oxalate form and carbon in carbonate form in the soil related to a M. excelsa *tree. Values are standardized. The Burkina Faso* M. excelsa *tree is a living tree, having an estimated age of about 70 years, whereas the Ivory Coast* M. excelsa *tree is the stump of a 170 year-old tree.*

(Cailleau 2005) is slightly different. The plant organic matter that contains oxalate is the wood (more recalcitrant material than leaves) and the oxalate release rate is, in this case, determined by termite activity (stump degradation). In this ecosystem, termites are essential for oxalate release from wood tissues to the soil environment. In addition, saprophytic fungi improve oxalate availability, by both their wood degradation and oxalate production. The maximum carbonate accumulation is, as in Burkina Faso soils, located in the second horizon (the organo-mineral layer). There is also an oxalate peak concomitant to this carbonate peak. The author explains the presence of these oxalate and carbonate peaks by a release of oxalate present in the OM and by the bacterial oxalogenic activity that results in carbonate ion formation and precipitation. Additionally, since saprophytic fungi are present, the release of carbonate present in wood is increased as well. In Burkina Faso, similarly as in Ivory Coast, there is a peak of oxalate at a depth of 40 cm and another one at 70 cm, both probably caused by root exudations.

Burkina Faso and Ivory Coast are two similar systems but at two different maturity steps. In Burkina Faso the system is young, with a process regulated by a carbon flux starting from the foliar crown and ending at the soil surface, whereas in Ivory Coast, the system is old regulated by diffusion processes, probably being much less sensitive to the foliar crown input. The Burkina Faso soil can be subdivided into two dynamic compartments, regulated by two different processes: the accumulation in the first 10 cm and the diffusion between 10 and 60 cm. In Ivory Coast the system work in the same way but it is older so that the wood input due to termite activity is bigger so as evidenced in hollow trunks.

7.5 The Burkina Faso reservoir capacity

In Burkina Faso, the largest carbon accumulation is located at the soil surface, where 85% of the carbon is present (Fig. 7.2). It is assumed that no carbon is present in the layer between 60 cm and 1 m in order to compare the carbon stock with values found in the literature (Table 7.1; Prentice et al. 2001). These results show that the total carbon stock present under an about 70 year-old oxalogenic tree is 60% more important than those estimated for tropical soils (forest, savannahs, and grassland soils). Consequently, the studied ecosystem forms carbon stocks that are comparable to the ones of the temperate grasslands and shrub lands.

A model can be proposed with the former results, completed by means of additional literature data. Carbon reservoir capacities and residence times in Burkina Faso ecosystems can be estimated (Fig. 7.3). The *M. excelsa* tree and its related soil are divided into the following reservoirs: atmosphere (infinite pool), leaves, wood, and soil. The latter is composed of three functional layers: from 0 to 10 cm in depth, from 10 to 60 cm, and from 60 to 100 cm. Compared to the preindustrial era, the concentration of CO_2 in the atmosphere increased about 25%, from 280 to more than 370 ppm (Janzen 2004). Residence time of a CO_2 molecule in the air is fixed at 5 years. Photosynthesis captures atmospheric CO_2 into leaves. TOC constitutes about 40% of leaves and wood tissues. The *M. excelsa* tree is a deciduous African tree. The maximal litter fall occur during May (Fig. 7.4), so the residence time of TOC in leaves is never longer than one year. Oxalate crystals carried by leaves reach the soil, providing a new oxalate

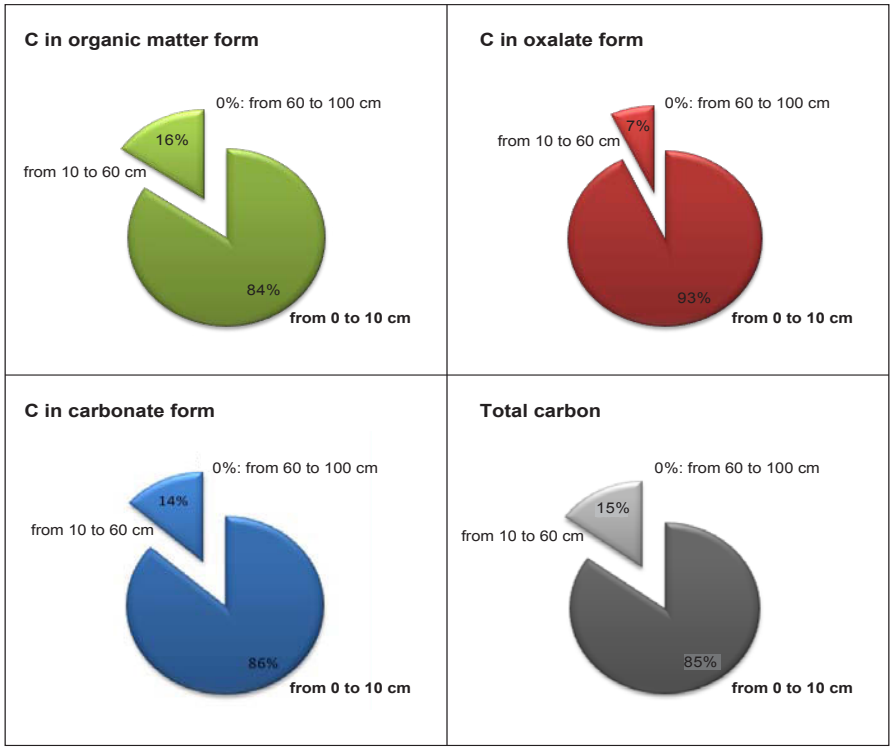


Fig. 7.2- Amounts of carbon forms present in the 3 soil layers under a living M. excelsa *tree from Burkina Faso.*

		Global C stock (g/m^3)	
	Biome	**Plants**	**Soil**
	Wetlands	4286	64286
	Boreal forests	6423	34380
	Temperate grasslands and scrub lands	720	23600
	Tundra	632	12737
	Tropical forest	**12045**	**12273**
	Tropical savannas and grasslands	**2933**	**11733**
	Temperate forests	**5673**	**9615**
	Croplands	188	8000
	Deserts and semi-deserts	176	4198

	Under an oxalogenic tree		C g/m^3
C-organic	in the first 10 cm		**15270**
	from 10 to 60 cm		2804
	from 65 to 100 cm		0
C-oxalate	in the first 10 cm		**29**
	from 10 to 60 cm		2
	from 65 to 100 cm		0
C-carbonate	in the first 10 cm		**5062**
	from 10 to 60 cm		797
	from 65 to 100 cm		0
	Total C in the first 10 cm		**20361**
	Total C from 15 to 60 cm		**3604**
	Total C from 65 to 100 cm		**0**
			kg/m3
	In wood	TOC = 37.9%	246.35
	wood density = 650 kg/m3	C-carbonate = 9.8 %	63.61
		C-oxalate = 0.015 %	0.10
		Total C in wood	**310**

Table 7.1- Estimates of soil organic carbon pools found in literature (Prentice 2001) compared to those calculated under a living M. excelsa *tree from Burkina Faso.*

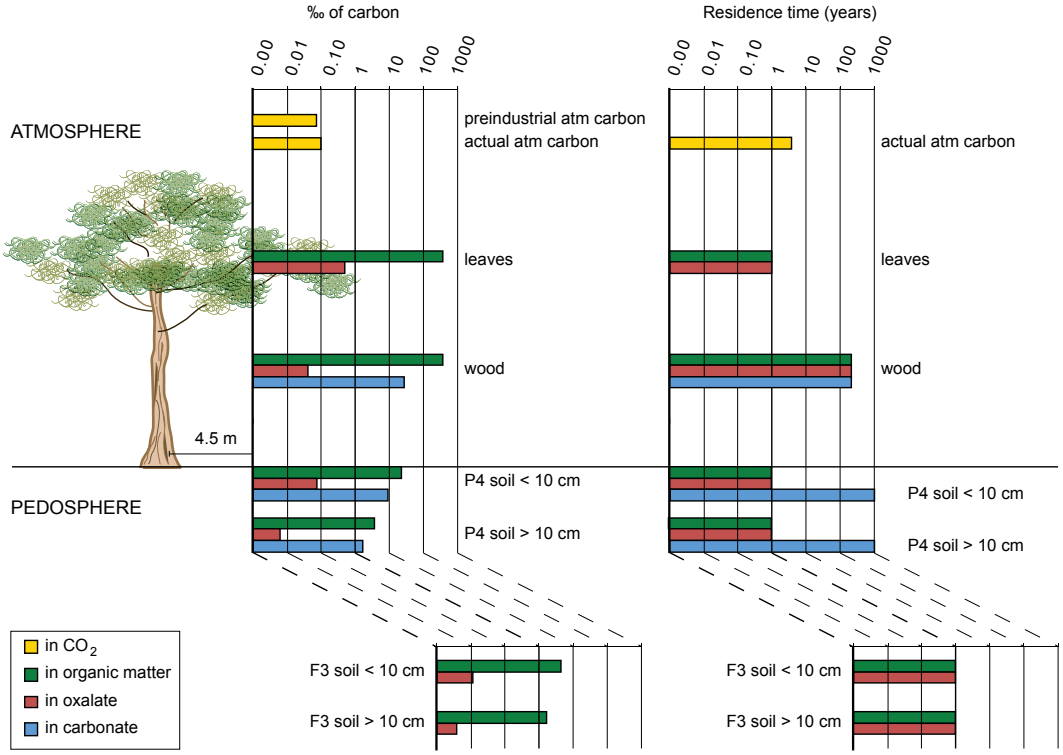


Fig. 7.3- Carbon stocks and residence times in the studied M. excelsa *tree ecosystem.*

contribution every year. Branches and wood represent a C-organic stock with a residence time that can be at the maximum in the order of magnitude of the tree age. Although the maximum lifetime of a *M. excelsa* tree is unknown, trees of about 250 years are frequently cited or studied in the Central African Republic (Durrieu De Madron 2003). Oxalate and carbonate are also present in wood tissues. This carbonate does not result from *in situ* bacterial oxalotrophy, but is likely the result of carbonate ion root uptake from the soil, followed by a precipitation in wood tissues (Cailleau 2005). Normally, *M. excelsa* stumps remain in place after the tree is cut, as a result of deforestation and wood trade. Their biodegradation is difficult, due to the intrinsic properties of lignin and the high carbonate content of wood, which makes it practically impenetrable to normal chainsaws. Nevertheless, termites are able to grind *M. excelsa* stumps (Cailleau 2005), allowing the release of oxalate and carbonate into the soil environment. The residence time of carbon stock present in wood is difficult to estimate, but it is admitted that it can reach an order of magnitude of centuries. On the contrary, soil fauna in tropical environments rapidly degrades litter, so oxalotrophic organisms quickly consume C-oxalate stock. Since the oxalate is rapidly degraded, its quantity present in the soil at a given time is extremely low, representing a very poor stock of carbon (< ‰). In fact, despite the annual aerial litter fall on the topsoil, the TOC and the oxalate salts do not accumulate. This implies a consumption of this carbon by-product (mineralization) and a powerful oxalate oxidation. According to the calculations and estimation made in the former paragraph, the residence time of the carbonate stock in *M. excelsa* system is in the order of magnitude of a millennium of years, therefore representing a non-negligible C-stock.

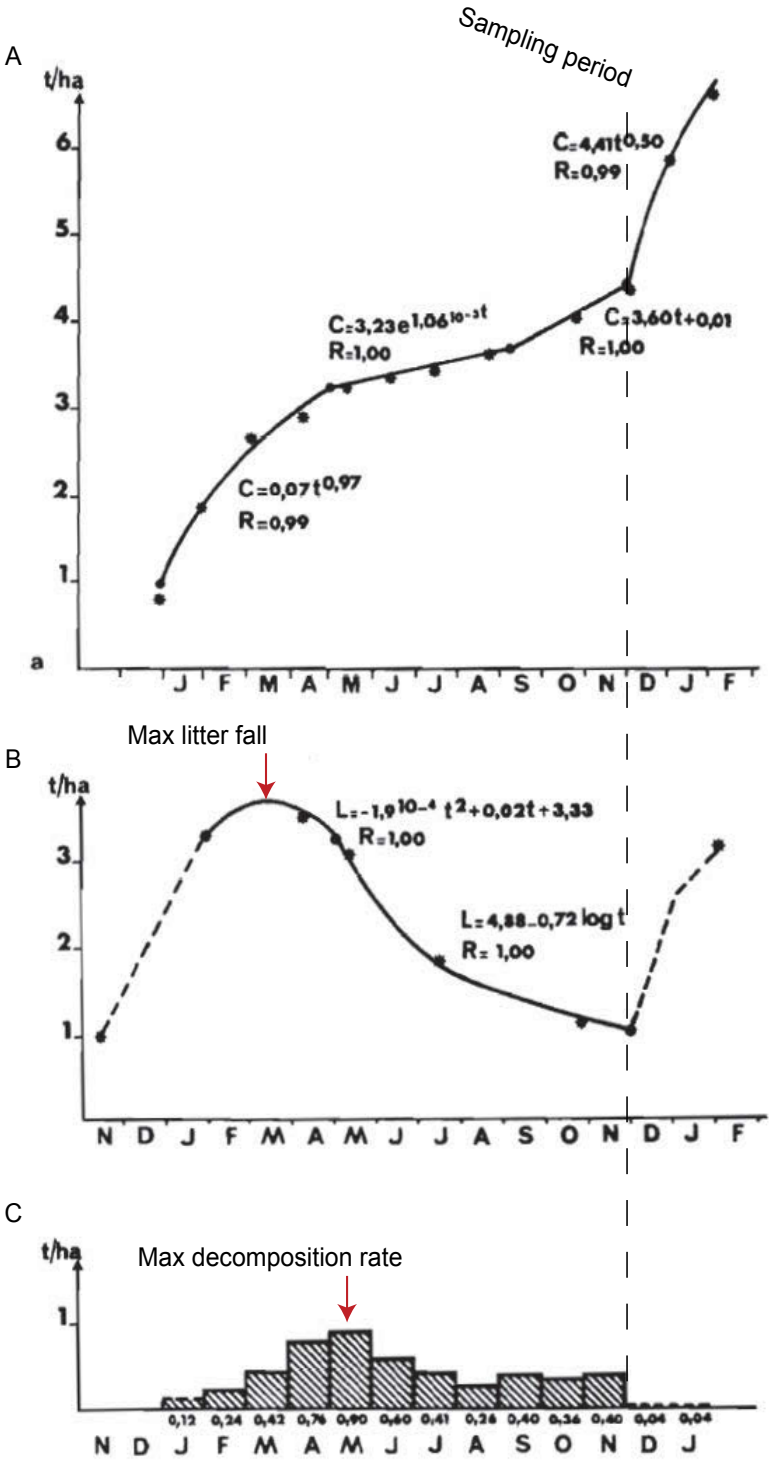


Fig. 7.4- Seasonal evolution of the litter in a dense Celtis *semi-evergreen forest at Ivory Coast. A: leaves fall (cumulative distribution function). B: Evolution of the litter weight on soil. C: Monthly values calculated for the absolute rate of decomposition (adapted from Devineau 1982).*

7.6 A carbon flux estimatio

An oxalate-carbonate pump efficienc , or the carbon flux from litter to hydrosphere, can be approximated (Fig. 7.5, Annex 15). TOC, as well as carbon contents in oxalate and in carbonate, are given in paragraph above. Rates of litter fall are taken from literature (Devineau 1982). From the oxalate metabolism equation (Chapter 1), it results that, for every 200 molecules of carbon present in the oxalate salt, 93.6 are transformed into calcite and 93.6 are released as CO_2 (Verrecchia et al. 2006). Consequently, the carbonate production derived from litter oxalate can be calculated. In each stage of this pathway, there is a carbon loss in CO_2 form (organic matter mineralization). However, in spite of this loss, the carbon balance is still positive in terms of trapping.

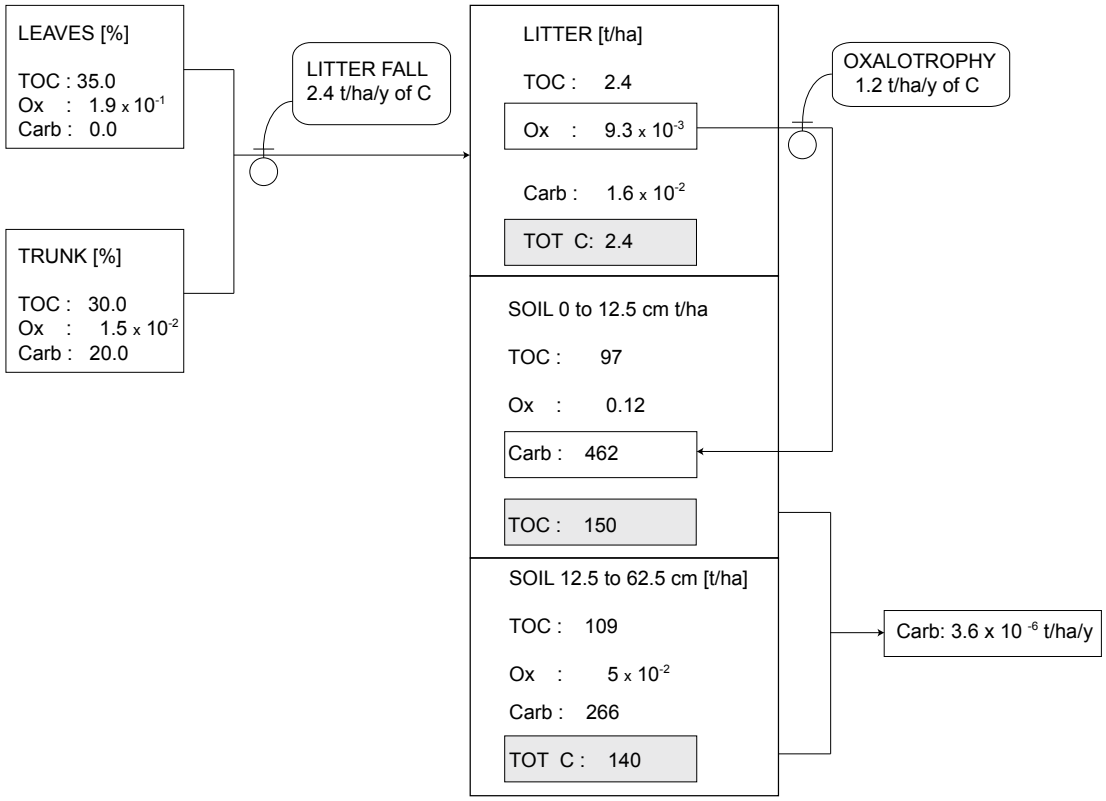


Fig. 7.5- Carbon fluxes in the studied M. excelsa *tree ecosystem. Only calculated fluxes are shown (see Annex 15). TOC : Total organic carbon ; Ox : measured oxalic acid ; Carb: carbonate; TOT C: total carbon. This last is calculated as follow: carbon represent 26.68 % in oxalate and 12 % in carbonate.*

Chapter 8 OUTLOOKS

The use of Rock-Eval6 pyrolysis for soil studies can be improved by a choice of better-suited standards. Spectra of elementary components can be of interest for the attribution of particular pyrogramme signals. A standardized protocol, adapted for soils and recent material, would definitely be helpful for data comparisons. A first attempt has been recently conducted demonstrating its huge potential in biochemical studies (Carrie et al. 2012).

It would be interesting to explore the implications of roots in the oxalate-carbonate pathway, the relationship between fungi, and bacteria, and the investigation of the role of fungi (saprophytes, oxalogenic and symbiotic) in this mineralization process. Similarly to what has been conducted for bacteria (Khammar et al. 2009), it would be useful to find a molecular marker allowing the characterization of the abundance and the diversity of fungi producing oxalate. In addition, the fungal function in respect to the oxalate dissolution has still to be investigated as well.

So, as demonstrated in this study with the discovery of carbonate in soils related to another oxalogenic tropical tree, *A. africana*, the oxalate - carbonate pathway can be more widespread than initially suspected. Surveys of the occurrence of similar systems under different pedological factors could result in great outcomes on global carbon quantification and implication

Chemical changes in soils due to the oxalate - carbonate pathway indicate a pH increase and an accumulation of alkaline cations (Ca and Mg), which can improve soil fertility. Consequently, plantations of biomineralizing plants would not only enhance CO_2 retention and capture in soils but also increase agronomical productivity.

Finally, by exploring the oxalate-carbonate pathway in other ecosystems, parameters tuning the mineral carbon accumulation could be more accurately defined in order to increase the outputs of this natural and powerful CO_2-pump.

REFERENCES

Adamo P, Violante P (2000). Weathering of rocks and neogenesis of minerals associated with lichen activity. Appl Clay Sci 16:229-256.

Ajah PO, Madubuike FN (1997). The proximate composition of some tropical legume seeds grown in two states in Nigeria. Food Chem 59 (3):361-365.

Albuzio A, Ferrari G (1989). Modulation of the molecular size of humic sub-stances by organic acids of the root exudates. Plant Soil 113 (2):237-241.

Allison MJ, Daniel SL, Cornick NA (1995). Oxalate degrading bacteria. In: Calcium oxalate in biological systems. Khan R (ed), pp 131-168. CRC Press, Boca Raton, FL.

Amundson R (2001). The carbon budget in soils. Ann Rev Earth Pl Sc 29:535-562.

Andersen CB (2002). Understanding carbonate equilibria by measuring alkalinity in experimental and natural systems. J. Geosci Education 50:389-403.

Arnott H (1995). Calcium oxalate in fungi. In Calcium Oxalatein Biology Systems (ed. Khan SR). CRC Press, London, pp. 73-111.

Arnott HJ (1976). Calcification in higher plants. pp 55-78. In: Watabe N. and Wilbur K. M. (eds). The mechanisms of mineralization in the invertebrates and plants. University of South Carolina Press, Columbia, S. C.

Arnott HJ, Pautard FGE (1970). Calcification in plants. In: Biological calcification, pp 375-476. Edited by Schraer H. Amsterdam: North-Holland Publishing Company.

Aubréville A (1970). Légumineuses (Césalpinioïdées). Flore du Cameroun. Volume 9. Muséum National d'Histoire Naturelle, Paris, France. 143 pp.

Awadalia MZ, Bassily NS, Saba NA (1985). Oxalate content of some Egyptian foodstuffs. J Egypt Public Health Assoc 60 (3):41-51.

Barca D, Ventura G (1991). Evoluzione vulcano-tettonica dell'isola di Salina (Arcipelago delle Eolie). Mem Soc Geol It 47:401-415.

Bationo BA, Ouedraogo SJ, Boussim IJ (2000). *Afzelia africana* Sm. (Caesalpiniaceae): étude de la prédation des graines dans une savane boisée du Burkina Faso. Bois des forêts des tropiques 264 (2):55-56.

Bell M, Lawrence D (2009). Soil carbon sequestration - myths and mysteries. The State of Queensland. Department of Primary Industries and Fisheries. 9 pp.

Ben Salem H, Nefzaoui A, Ben Salem L (2002). Supplementation of *Acacia cyanophylla* Lindl. foliage-based diets with barley or shrubs from arid areas (*Opuntia ficus-indica f. inermis* and *Atriplex nummularia L.*) on growth and digestibility in lambs. Anim Feed Sci Technol 96 (1-2):15-30.

Bierman P, Caffee M (2001). Slow rates of rock surface erosion and sediment production across the Namib Desert and escarpment, Southern Africa. Am J Sci 301:326-358.

Blackmore MA, Quayle JR (1970). Microbial growth on oxalate by a route not involving glyoxylate carboligase. Biochem J 118:53-59.

Boeglin J-L, Probst J-L (1998). Physical and chemical weathering rates and CO_2 consumption in a tropical environment: the upper Niger basin. Chem Geol 148:137-156.

Bonaventura MPD, Gallo MD, Cacchio P, Ercole C, Lepidi A (1999). Microbial formation of oxalate films on monument surfaces: Bioprotection or biodeterioration? Geomicrobiol J 16:55-64.

Bosi E (1996-1997). Le ragioni della conservazione e le esigenze dello sviluppo nella progettazione delle Riserve Naturali dell'Arcipelago Eoliano. Università degli studi di Parma, Parma.

Bosu PP, Cobbinah JR, Nichols JD, Nkrumah EE, Wagner MR (2006). Survival and growth of mixed plantations of *Milicia excelsa* and *Terminalia superba* 9 years after planting in Ghana. Forest Ecol Manag 233 (2-3):352-357.

Bot A, Benites J (2005). The importance of soil organic matter. Key to drought-resistant soil and sustained food production. FAO Soils Bulletin 80. 95 pp.

Braissant O (2005). Carbonatogénèse bactérienne liée au cycle biogéochimique oxalate-carbonate. Université de Neuchâtel. 214 pp.

Braissant O, Cailleau G, Aragno M, Verrecchia EP (2004). Biologically induced mineralization in the tree *Milicia excelsa* (Moraceae): its causes and consequences to the environment. Geobiology 2 (1):59-66.

Braissant O, Cailleau G, Dupraz C, Verrecchia EP (2003). Bacterially induced mineralization of calcium carbonate in terrestrial environments: the role of exopolysaccharides and amino acids. J Sediment Res 73 (3):485-490.

Braissant O, Verrecchia EP, Aragno M (2002). Is the contribution of bacteria to terrestrial carbon budget greatly underestimated? Naturwissenschaften 89 (8):366-370.

Breman H, de Ridder N (1991). Manuel sur les pâturages des pays sahéliens. Paris.

Brovkin V, Cherkinsky A, Gorachkin S (2008). Estimating soil carbon turnover using radiocarbon data: a case study for European Russia. Ecol Model 216 (2):178-187.

Buffle J, Greter FL, Haerdi W (1977). Measurement of complexation properties of humic and fulvic acids in natural waters with lead and copper ion-selective electrodes. Anal Chem 49:216-222.

Burford EP, Kierans M, Gadd GM (2003). Geomycology: fungi in mineral substrata. Mycologist 17 (3):98-107.

Cailleau G (2005). Cycle du carbone et biominéralisation carbonatée en milieu continentale: la diagenèse des phases oxalate-carbonate. Université de Neuchâtel. 254 pp.

Cailleau G, Braissant O, Dupraz C, Aragno M, Verrecchia EP (2005). Biologically induced accumulations of $CaCO_3$ in orthox soils of Biga, Ivory Coast. Catena 59:1-17.

Cailleau G, Braissant O, Verrecchia EP (2004). Biomineralization in plants as a long-term carbon sink. Naturwissenschaften 91 (4):191-194.

Callot G (1999). La Truffe, la Terre, la Vie, INRA (Paris). 210 pp.

Callot G, Chamayou H, Maertens C, Salsac L (1982). Les interactions sol- racine. Incidence sur la nutrition minérale INRA Paris.

Callot G, Mousain D, Plassard C (1985). Inter-relation entre les aiguilles de calcite et hyphes mycéliens. Agronomie 5 (3):209-216.

Campbell WG, Fisher RC (1932). The composition and origin of “stone” in Iroko wood (*Chlorophora excelsa*, Benth. and Hook. f.). Emp For J 11:244-245.

Canti MG (2003). Aspect of the chemical and microscopic characteristics of plant ashes found in archaeological soils. Catena 54:339-361.

Carozzi AV (1967). Recent calcite-cemented sandstone generated by the equatorial tree Iroko (*Chlorophora excelsa*), Daloa, Ivory Coast. J Sediment Petrol 37 (2):597-600.

Carvalho S, de Oliveira F, Vaz H (2004). Situation des ressources génétiques forestières de la République démocratique de Sao Tomé-et-Principe. Service de la mise en valeur des ressources forestières; Document de travail FGR/63F; Division des ressources forestières FAO, Rome, Italie. 42 pp.

Castanier S, Le Metayer-Levrel G, Orial G, Loubière J-F, Perthuisot J-P (2000). Bacterial carbonatogenesis and application to preservation and restoration of historic property. In: Sciences (ed) Of Microbes and Art: the role of microbial communities in the degradation and protection of cultural heritage. Florence, Italy, Ciferri O, Tiano, P and Mastromei, G, pp 203-218.

Castanier S, Le Métayer-Levrel G, Perthuisot J-P (1999). Ca-carbonates precipitation and limestone genesis - the microbiogeologist point of view. Sediment Geol 126 (1-4):9-23.

Certini G, Corti G, Ugolini FC (2000). Vertical trends of oxalate concentration in two soils under *Abies alba* from Tuscany (Italy). J Plant Nutr Soil Sc 163 (2):173-177.

Chalumeau L (2003). Méthodologie des analyses granulométriques. Laboratory of Geodynamic of the Biosphere; Institute of Geology, Neuchâtel. 5 pp.

Chandler RF (1937). Certain relationships between the calcium and oxalate content of foliage of certain forest trees. J Agric Res 55 (5):393-396.

Chandra T, Shethna Y (1975). Oxalate and formate metabolism in Alcaligenes and Pseudomonas species. Antonie van Leeuwenhoek 41 (1):465-477.

Chang C-C, Beevers H (1968). Biogenesis of oxalate in plant tissues. Plant Physiol 43 (11):1821-1828.

Cheavin WHS (1938). The crystals and cystolites found in plant cells. Part 1: Crystals. Microscope 2.155-158.

Ciba-Geigy A (1977). Wissenschaftliche Tabellen Geigy: Teilband Körperflüssigkeiten. Aufl, Ciba-Geigy, B, vol 8. Basel.

Cobbinah JR, Wagner MR (1995). Phenotypic variation in *Milicia excelsa* to attack by *Phytolyma lata* (Psyllidae). Forest Ecol Manag 75 (1-3):147-153.

Copard Y, Amiotte-Suchet P, Di-Giovanni C (2007). Storage and release of fossil organic carbon related to weathering of sedimentary rocks. Earth Planet Sc Lett 258 (1-2):345-357.

Cowgill UM (1989). A naturally occurring alpha magnesium oxalate dihydrate from the northern Jordan Valley (Israel). Mineral Mag 53 (4):505-507.

Cromack K, Sollis P, Todd RL, Fogel R, Todd AW, Fender WM, Crossley ME, Crossley DA (1977). The role of oxalic acid and bicarbonate in calcium cycling by fungi and bacteria: some possible implications for soil animals. Ecol Bull 25:246-252.

Dart RC, Barovich KM, Chittleborough DJ, Hill SM (2007). Calcium in regolith carbonates of central and Southern Australia: Its source and implications for the global carbon cycle. Palaeogeogr Palaeocl 249 (3-4):322-334.

De Rosa R, Donato P, Ventura G (2002). Fractal analysis of mingled/mixed magmas: an example from the Upper Pollara eruption (Salina Island, Southern Tyrrhenian Sea, Italy). Lithos 65:299-311.

Devineau J-L (1976). Données préliminaires sur la litière et la chute des feuilles dans quelques formations forestières semi-décidues de moyenne Côte-d'Ivoire. Oecol Plant 11 (4):375-395.

Devineau JL (1982). Etude pondérale des litières d'arbre dans deux types de forêts tropophiles en Côte d'Ivoire. Ann Univ Abidjan, Série É (Écologie), tome XV:27-62.

Diedhiou AG, Verpillot F, Gueye O, Dreyfus B, Duponnois R, Bâ AM (2004). Do concentrations of glucose and fungal inoculum influence the competitiveness of two early-stage ectomycorrhizal fungi in *Afzelia africana* seedlings? Forest Ecol Manag 203 (1-3):187-194.

Disnar J-R, Jacob J, Morched-Issa M, Lottier N, Arnaud F (2008). Assessment of peat quality by molecular and bulk geochemical analysis: Application to the Holocene record of the Chautagne marsh (Haute Savoie, France). Chem Geol 254 (1-2):101-112.

Disnar JR, Guilleta B, Keravisa D, Di-Giovanni C, Sebag D (2003). Soil organic matter (SOM) characterization by Rock-Eval pyrolysis: scope and limitations. Org Geochem 34 (3):327-343.

Doumbia S, Pouclet A, Kouamelan A, Peucat JJ, Vidal M, Delor C (1998). Petrogenesis of juvenile-type Birimian (Paleoproterozoic) granitoids in Central Côte-d'Ivoire, West Africa: geochemistry and geochronology. Precambrian Res 87 (1-2):33-63.

Dupraz C, Reid RP, Braissant O, Decho AW, Norman RS, Visscher PT (2009). Processes of carbonate precipitation in modern microbial mats. Earth-Science Rev 96:141-162.

Durrieu De Madron L (2003). Accroissement diamétrique du bété et de l'iroko. Bois des forêts des tropiques 275 (1):83-87.

Dutton MV, Evans CS (1996). Oxalate production by fungi: its role in pathogenicity and ecology in the soil environment. Can J Microbiol 42 (9):881-895.

Dutton MV, Evans CS, Atkey PT, Wood DA (1993). Oxalate production by Basidiomycetes, including the white-rot species *Coriolus versicolor* and *Phanerochaete chrysosporium*. Appl Microbiol Biotechnol 39 (1):5-10.

Elmadfa I, Aign W, Muskat E, Frutzsche D, Cremer DH (1992/1993). Die große GU Nährwerttabelle. Gräfe und Unzer, München.64 pp.

Espitalié J, Deroo G, Marquis F (1985). La pyrolyse Rock-Eval et ses applications; première partie. Rev I Fr Pétrol 40 (5):563-579.

Espitalié J, Laporte JL, Madec M, Marquis F, Leplat P, Paulet J, Boutefeu A (1977). Méthode rapide de caractérisation des roches mères, de leur potentiel pétrolier et de leur degré d'évolution. Rev I Fr Pétrol 32 (23-42).

Eswaran H, Reich PF, Kimble JM, Beinroth FH, Padmanabhan E, Moncharoen P (2000). Global carbon stocks. pp 15-25. In: Global climate change and pedogenic carbonates. Lal R, Kimble JM, Eswaran H, and Stewart BA (eds), Lewis Publishers, Boca Raton, FL.

Fox TR, Comerford NB (1990). Low-molecular-weight organic acids in selected forest soils of the Southeastern USA. Soil Sci Soc Am J 54 (4):1139-1144.

Franceschi V (2001). Calcium oxalate in plants. Trends Plant Sci 6 (7):331.

Franceschi VR, Horner HT (1980). Calcium oxalate crystals in plants. Bot Rev 46 (4):361-427.

Franceschi VR, Loewus FA (1995). Oxalate biosynthesis and function in plants. In: Khan SR (ed) Calcium Oxalate in Biological Systems. CRC Press, Boca Raton, FL, pp 113-130.

Franceschi VR, Nakata PA (2005). Calcium oxalate in plants: Formation and function. Annu Rev Plant Biol 56:41-71.

Gadd GM (1999). Fungal production of citric and oxalic acid: Importance in metal speciation, physiology and biogeochemical processes. Adv in Microb Physiol 41:47-92.

Gadd GM (2004). Mycotransformation of organic and inorganic substrates. Mycologist 18 (2):60-70.

Gadd GM (2007). Geomycology: biogeochemical transformations of rocks, minerals, metals and radionuclides by fungi, bioweathering and bioremediation. Mycol Res 111 (1):3-49.

Garvie LAJ (2003). Decay-induced biomineralization of the saguaro cactus (*Carnegiea gigantea*). Am Min 88:1879-1888.

Georgakopolous A (1984). Contribution à l'analyse des sédiments récents par la pyrolyse de type Rock-Eval. Université de Paris Sud. 136 pp.

Gerard-Zaugg L (1994). Effets de la maturation thermique sur les processus d'oxydation des charbons. Université de Nancy. 242 pp.

Gessner MO, Schmitt AL (1996). Use of solid-phase extraction to determine ergosterol concentrations in plant tissue colonized by fungi. Appl Environ Microbiol 62 (2):415-419.

Gharieb MM, Sayer JA, Gadd GM (1998). Solubilization of natural gypsum ($CaSO_4.2H_2O$) and the formation of calcium oxalate by *Aspergillus niger* and *Serpula himantioides*. Mycol Res 102 (7):825-830.

Gobat J-M, Aragno M, Matthey W (2010). Le sol vivant. PPUR, Lausanne. 820 pp.

Gobat J-M, Vadi G, Weber G (2005). Protocole de description des sols. Neuchâtel, Laboratoire d'écologie végétale et de phytosociologie. Institut de botanique, Université de Neuchâtel.

Golubyatnikov LL, Svirezhev YM (2008). Life-cycle model of terrestrial carbon exchange. Ecol Model 213 (2):202-208.

Goudie AS, Middleton NJ (2001). Saharan dust storms: nature and consequences. Earth-Science Rev 56 (1â€“4):179-204.

Graustein WC, Cromack KJ, Sollins P (1977). Calcium oxalate: occurrence in soils and effect on nutrient and geochemical cycles. Science 198:1252-1254.

Guggiari M, Bloque R, Aragno M, Verrecchia EP, Job D (2010). Role and dynamics of calcium oxalate production by selected Fungi. Bull. Bodenkd. Ges. Schweiz 30:123-126.

Guil-Guerrero JL, Gimenez Martinez JJ, Torija Isasa ME (1998). Mineral nutrient composition of edible wild plants. J Food Comp Anal 11 (4):322-328.

Guil JL, Torija ME, Gimenez JJ, Rodriguez-Garcia I, Gimenez A (1996). Oxalic acid and calcium determination in wild edible plants. J Agric Res 44 (7):1821-1823.

Hamel R, Levasseur R, Appanna V (1999). Oxalic acid production and aluminium tolerance in *Pseudomonas fluo escens*. J Inorg Biochem 76:99-104.

Harris CM (1933). Stone in *Chlorophora excelsa* B. and H., Iroko. Emp For J 12:229-238.

Harter RD (2002). Acid soils of the tropics; North Ft. Myers. 11 pp.

Hawthorne WD (1995). Ecological profiles of Ghanaian forest trees. Oxford Forestry Institute: Oxford. 345 pp.

Haytowicz DB, Matthews RH (1984). Composition of foods: Vegetables and vegetable products: raw, processed, prepared. Agriculture handbook. USDA, Human Nutrition Information Service. 502 pp.

Hetényi M, Nyilas T, Tóth TM (2005). Stepwise Rock-Eval pyrolysis as a tool for typing heterogeneous organic matter in soils. J Analand Appl Pyrol 74 (1-2):45-54.

Hodgkinson A (1977). Oxalic acid in biology and medicine. London. Academic Press. 325 pp.

Hönow R, Hesse A (2002). Comparison of extraction methods for the determination of soluble and total oxalate in foods by HPLC-enzyme-reactor. Food Chem 78 (4):511-521.

Houghton RA (2002). Terrestrial carbon sinks-uncertain explanations. Biologist 49 (5):155-160.

Hue NV, Craddock GR, Adams F (1986). Effect of organic acids on aluminum toxicity in subsoils. Soil Sci Soc Am J 50 (1):28-34.

Inngjerdingen K, Nergård CS, Diallo D, Mounkoro PP, Paulsen BS (2004). An ethnopharmacological survey of plants used for wound healing in Dogonland, Mali, West Africa. J Ethnopharmacol 92 (2-3):233-244.

IPCC (2001). Climate Change 2001.

Jansen JWA (1974). Timber trees of Liberia; University of Liberia, Monrovia. UNDP/SF/FAO College of Agriculture and Forestry Project; University of Liberia, Monrovia. 83 pp.

Janzen HH (2004). Carbon cycling in earth systems: A soil science perspective. Agricult Ecosys Environ 104 (3):399-417.

Jarrige R, Ruckebusch Y (1995). Nutrition des ruminants domestiques: ingestion et digestion. Publié par Editions Quae. 922 pp.

Kadiri AB, Olowokudejo J-D (2008). Comparative foliar epidermal morphology of the West African species of the genus Afzelia Smith (Leguminosae: Caesalpinioideae). Estudio comparativo de la epidermis de la hoja de especies del genero Afzelia Smith (Leguminosae: Caesalpinioideae) de Africa occidental. Gayana Bot 65 (1):84-92.

Kamchan A, Puwastien P, Sirichakwal PP, Kongkachuichai R (2004). *In vitro* calcium bioavailability of vegetables, legumes, and seeds. J Food Comp Anal 17 (3-4):311-320.

Kasidas GP, Rose GA (1980). Oxalate contents of some common foods: determination by an enzymatic method. J Hum Nutr 34 (4):255-266.

Khammar N, Martin G, Ferro K, Job D, Aragno M, Verrecchia E (2009). Use of the frc gene as a molecular marker to characterize oxalate-oxidizing bacterial abundance and diversity structure in soil. J Microbiol Meth 76 (2):120-127.

Khan SR (1995). Calcium oxalate in biological systems, edited by Saheed Khan, 400 pp.

Kmiecik W, Lisiewska Z, Slupski J (2004). Effects of freezing and storing of frozen products on the content of nitrates, nitrites, and oxalates in dill (*Anethum graveolens L.*). Food Chem 86 (1):105-111.

Knight R (1980). Origin and world importance of tropical and subtropical fruit crops. In: Nagy S. and Shaw P.E. (eds). Tropical and subtropical fruits. Composition, properties and uses. AVI, Westport, CT. 120 pp.

Kögel-Knabner I (2002). The macromolecular organic composition of plant and microbial residues as inputs to soil organic matter. Soil Biol Biochem 34 (2):139-162.

Kolo K, Claeys P (2005). In vitro formation of Ca-oxalates and the mineral glushinskite by fungal interaction with carbonate substrates and seawater. Biogeosciences Discuss 2 (2):451-497.

Kraimer RA, Monger HC, Steiner RL (2005). Mineralogical distinctions of carbonates in desert soils. Soil Sci Soc Am J 69 (6):1773-1781.

Kübler B (1992). Calcites magnésiennes. Identification et dosage par diffraction X de $MgCO_3$ dans la solution solide. Cahiers de l'Institut de Géologie, Laboratoire de Minéralogie, Pétrographie et Géochimie; Université de Neuchâtel, Institut de Géologie série AX, N.22, 15 pp.

Kuzyakov Y, Shevtzova E, Pustovoytov K (2006). Carbonate re-crystallization in soil revealed by ^{14}C labeling: Experiment, model and significance for paleo-environmental reconstructions. Geoderma 131:45-58.

Lafargue E, Marquis F, Pillot D (1998). Les applications du Rock-Eval 6 dans l'exploration et la production des hydrocarbures, et dans les études de contamination des sols; Rock-Eval 6 Applications in Hydrocarbon Exploration, Production, and Soil Contamination Studies Oil Gas Sci Technol 53 (4):421-437.

Lal R (2004). Soil carbon sequestration impacts on global climate change and food security. Science 304 (5677):1623-1627.

Lerebours-Pigeonnière A, Ménager M-T (2001). Les atlas de l'Afrique: Burkina Faso: Groupe Jeune Afrique: les éditions du Jaguar. 62 pp.

Libert B, Franceschi VR (1987). Oxalate in crop plants. J Agric Food Chem 35 (6):926-938.

Liebezeit G, Wiesner MG (1990). Pyrolysis of recent marine sediments. I. Biopolymers. Org Geochem 16 (4-6):1179-1185.

Lindner M, Karjalainen T (2007). Carbon inventory methods and carbon mitigation potentials of forests in Europe: a short review of recent progress. Eur J For Res 126 (2):149-156.

Lowenstam HA, Weiner S (1989). On Biomineralization: Oxford University Press, New York, 324 pp.

Magassouba FB, Diallo A, Kouyaté M, Mara F, Mara O, Bangoura O, Camara A, Traoré S, Diallo AK, Zaoro M, Lamah K, Diallo S, Camara G, Kéita A, Camara MK, Barry R, Kéita S, Oularé K, Barry MS, Donzo M, Camara K, Toté K, Berghe DV, Totté J, Pieters L, Vlietinck AJ, Baldé AM (2007). Ethnobotanical survey and antibacterial activity of some plants used in Guinean traditional medicine. J Ethnopharmacol 114 (1):44-53.

Malainine ME, Dufresne A, Dupeyre D, Mahrouz M, Vuong R, Vignon MR (2003). Structure and morphology of cladodes and spines of *Opuntia ficus-indic* . Cellulose extraction and characterisation. Carbohydr Polymers 51 (1):77-83.

Manoharachary C, Sridhar K, Singh R, Adholeya A, Suryanarayanan TS, Rawat S, Johri BN (2005). Fungal biodiversity: Distribution, conservation and prospecting of fungi from

India. Curr Sci 89 (1):58-71.

Marchand C, Lallier-Vergès E, Disnar JR, Kéravis D (2008). Organic carbon sources and transformations in mangrove sediments: A Rock-Eval pyrolysis approach. Org Geochem 39 (4):408-421.

Massey LK, Roman-Smith H, Sutton RAL (1993). Effect of dietary oxalate and calcium on urinary oxalate and risk of formation of calcium oxalate kidney stones. J Am Diet Assoc 93 (8):901-906.

McConn MM, Nakata PA (2004). Oxalate reduces calcium availability in the pads of the prickly pear cactus through formation of calcium oxalate crystals. J Agric Food Chem 52 (5):1371-1374.

McKeague JA, Cline MG (1963). Silica in soils. Adv Agron:339-396.

Messini A, Favilli F (1990). Calcium oxalate decomposing microorganisms; a microbial group of the rhizosphere of forest plants. Ann di Microbiol Enzim 40:93-102.

Millot G, Nahon D, Paquet H, Ruellan A, Tardy Y (1977). L'épigenie calcaire des roches silicatées dans les encroûtements carbonatés en pays subaride antiatlas. Maroc. Sci Géo Bull 30 (3):129-152.

Monje PV, Baran EJ (2002). Characterization of calcium oxalates generated as biominerals in cacti. Plant Physiol 128 (2):707-713.

Monje PV, Baran EJ (2005). Evidence of formation of glushinskite as a biomineral in a Cactaceae species. Phytochemistry 66 (5):611-614.

Mulas M, Mulas G (2004). Potentialités d'utilisation stratégique des plantes des genres Atriplex et Opuntia dans la lutte contre la désertification. Rapport d'activité du groupe de recherche sur la désertification, université Sassari. 61 pp

Naba S, Lompo M, Debat P, Bouchez JL, Béziat D (2004). Structure and emplacement model for late-orogenic Paleoproterozoic granitoids: the Tenkodogo–Yamba elongate pluton (Eastern Burkina Faso). J Afr Earth Sc 38 (1):41-57.

Nakata PA (2003). Advances in our understanding of calcium oxalate crystal formation and function in plants. Plant Sci 164 (6):901-909.

Nakata PA, McConn MM (2000). Isolation of *Medicago truncatula* mutants defective in calcium oxalate crystal formation. Plant Physiol 124 (3):1097-1104.

Nakata PA, McConn MM (2007). Calcium oxalate content affects the nutritional availability of calcium from *Medicago truncatula* leaves. Plant Sci 172 (5):958-961.

Nguyen C (2003). Rhizodeposition of organic C by plants: mechanisms and controls. Agronomie 23 (5-6):375-396.

Nichols JD, Wagner MR, Agyeman VK, Paul B, Cobbinah JR (1998). Influence of artificial gaps in tropical forest on survival, growth, and *Phytolyma lata* attack on *Milicia excelsa*. Forest Ecol Manag 110 (1-3):353-362.

Noonan SC, Savage GP (1999). Oxalate content of foods and its effect on humans. Asia Pac J Clin Nutr 8 (1):64-74.

Norton RA, Behan-Pelletier VM (1991). Calcium carbonate and calcium oxalate as cuticular hardening agents in oribatid mites (Acari: Oribatida). Can J Zool 69 (6):1504-1511.

Ofori DA, Cobbinah JR (2007). Integrated approach for conservation and management of genetic resources of Milicia species in West Africa. Forest Ecol Manag 238 (1-3):1-6.

Ofori DA, Newton AC, Leakey RRB, Grace J (1996). Vegetative propagation of *Milicia excelsa* by leafy stem cuttings: effects of auxin concentration, leaf area and rooting medium. Forest Ecol Manag 84 (1-3):39-48.

Ogawa Y, Takahashi S, Kitagawa R (1984). Oxalate content in common Japanese foods. Acta Urol Japonica. Hinyokika Kiyo 30 (3):305-310.

Onana J, Devineau J-L (2002). *Afzelia africana* Smith ex Persoon dans le Nord-Cameroun. Etat actuel des peuplements et utilisation pastorale. Rev Elev Méd Vét des Pay 55 (1):39-45.

Onguene NA, Kuyper TW (2001). Mycorrhizal associations in the rain forest of South Cameroon. Forest Ecol Manag 140 (2-3):277-287.

Ouédraogo-Koné S, Kaboré-Zoungrana CY, Ledin I (2006). Behaviour of goats, sheep and cattle on natural pasture in the sub-humid zone of West Africa. Livestock Science 105 (1-3):244-252.

Ouinsavi C, Sokpon N, Bada O (2005). Utilization and traditional strategies of *in situ* conservation of iroko (*Milicia excelsa* Welw. C.C. Berg) in Benin. Forest Ecol Manag 207 (3):341-350.

Palache C, Berman H, Frondel C (1951). Dana's system of mineralogy, (7th edition), v. II, 1101-1102.

Pauwels JM, Van Ranst E, Verloo M, Mvondo ZE (1992). Manuel de laboratoire de pédologie: méthodes d'analyses des sols et des plantes; équipements, gestion des stocks de verrerie et de produits chimiques. Centre Universitaire de Dschang. AGCD: Publications agricoles. Vol 28. 265 pp.

Perez EF, Neto GO, Kubota LT (2001). Bi-enzymatic amperometric biosensor for oxalate. Sens

Actua 72 (1):80-85.

Pohlmann AA, McColl JG (1988). Soluble organics from forest litter and their role in metal dissolution. Soil Sci Soc Am J 52 (1):265-271.

Pottier J-C (1969). Carte pédologique de reconnaissance de la république de Haute Volta: Ouest-Sud. Service Cartographique de l'O.R.S.T.O.M de Dakar.

Prentice IC, Farquhar GD, Fasham MJR, Goulden ML, Heimann M, Jaramillo VJ, Kheshgi HS, Le Quéré C, Scholes RJ (2001). The Carbon Cycle and Atmospheric Carbon Dioxide. In: Climate Change 2001: The Scientific Basis. Contribution of Working Group I to the Third Assessment Report of the Intergovernmental Panel on Climate Change. [Houghton JT, Ding Y, Griggs DJ, Noguer M, van der Linden PJ, Dai X, Maskell K, and Johnson CA, (eds)]. Cambridge University Press, Cambridge, United Kingdom and New York, NY, USA, 881 pp.

Prior J, Cutler D (1992). Trees to fuel Africa's fires: Trees are a vital source of firewood in rural Africa, but the wrong ones turn savannas into desert. New Sci 135:35-39.

Quayle J, Keech D, Taylor G (1961). Carbon assimilation by *Pseudomonas oxalaticus* (OXI). 4. Metabolism of oxalate in cell-free extracts of the organism grown on oxalate. Biochem J 78:225-236.

Quayle JR (1963). Carbon assimilation by *Pseudomonas oxalaticus* (OX1). 6. Reactions of oxalyl-coenzyme A. Biochem J 87:368-373.

Rasmussen C (2006). Distribution of soil organic and inorganic carbon pools by biome and soil taxa in Arizona. Soil Sci Soc Am J 70 (1):256-265.

Rautaray D, Ahmad A, Sastry M (2004). Biological synthesis of metal carbonate minerals using fungi and actinomycetes. J Mater Chem 14:2333-2340.

Ren Y, Picout DR, Ellis PR, Ross-Murphy SB, Reid JSG (2005). A novel xyloglucan from seeds of *Afzelia africana* Se. Pers. extraction, characterization, and conformational properties. Carbohydr Res 340 (5):997-1005.

Retallack GJ (1990). Soil of the past. An introduction to paleopedology. Unwin Hyman Ltd, London. 512 pp.

Retamal N, Duran JM, Fernandez J (1987). Seasonal variations of chemical composition in prickly pear (*Opuntia ficus-indica* (L.) Miller). J Sci Food Agric 38:303-311.

Rivera ER, Smith BN (1979). Crystal morphology and ^{13}Carbon/^{12}Carbon composition of solid oxalate in cacti. Plant Physiol 64 (6):966-970.

Sahin N (2003). Oxalotrophic bacteria. Res Microbiol 154 (6):399-407.

Sanon KB, Bâ AM, Dexheimer J (1997). Mycorrhizal status of some fungi fruiting beneath indigenous trees in Burkina Faso. Forest Ecol Manag 98 (1):61-69.

Savage GP, Vanhanen L, Mason SM, Ross AB (2000). Effect of cooking on the soluble and insoluble oxalate content of some New Zealand foods. J Food Comp Anal 13 (3):201-206.

Schelstraete M, Kennedy BM (1980). Composition of miner's lettuce (*Montia perfoliata*). J Am Diet Assoc 77 (1):21-25.

Schimel DS (1995). Terrestrial ecosystems and the carbon cycle; Global Change Biology, 1.77-91.

Sebag D, Disnar JR, Guillet B, Di-Giovanni C, Verrecchia EP, Durand A (2006). Monitoring organic matter dynamics in soil profiles by Rock Eval pyrolysis: bulk characterization and quantification of degradation. Eur J Soil Sci 57 (3):344-355

Seneviratne G (2003). Global warming and terrestrial carbon sequestration. J Biosci 28 (6):653-655.

Sepúlveda E, Sáenz C, Aliaga E, Aceituno C (2007). Extraction and characterization of mucilage in *Opuntia spp.* J Arid Environ 68 (4):534-545.

Siener R, Hönow R, Seidler A, Voss S, Hesse A (2006). Oxalate contents of species of the Polygonaceae, Amaranthaceae and Chenopodiaceae families. Food Chem 98 (2):220-224.

Soon YK, Abboud S (1993). Cadmium, chromium, lead, and nickel. In: Carter MR (eds). Soil sampling and methods of analysis. Canadian Society of Soil Science. pp 101-107.

Sotomayor MDPT, Raimundo IM, Oliveira Neto G, Kubota LT (2001). Bi-enzymatic optode detection system for oxalate determination based on a natural source of enzyme. Anal Chim Acta 447 (1-2):33-40.

Souci SW, Fachmann W, Kraut H (1986). Die Zusammensetzung der Lebensmittel, Nährwerttabellen 1986/87. In Deutsche Forschungsanstalt für Lebensmittelchemie (eds), Garching bei München 3. H. von Scherz, G. Kloos, F. Senser (eds), Stuttgart: Wissenschaftliche Verlags-gesellschaft mbH.86 pp.

Sposito G (1994). Chemical equilibrium and kinetics in soils. New. York, Oxford University Press, 288 pp.

Stevenson FJ (1982). Humus chemistry genesis, composition, reactions.

Stoorvogel JJ, Van Breemen N, Janssen BH (1997). The nutrient input by Harmattan dust to a forest ecosystem in Côte d›Ivoire, Africa Biogeochemistry 37 (2):145-157.

Sulpizio R, De Rosa R, Donatob P (2008). The influence of variable topography on the depositional behaviour of pyroclastic density currents: The examples of the Upper Pollara eruption (Salina Island, Southern Italy). J Volcanol Geoth Res 175 (3):367-385.

Suvachittanont O, Meksongsee L, Dhanamitta S, Valyasevi A (1973). The oxalic acid content of some vegetables in Thailand, its possible relationship with the bladder stone disease. J Med Assoc Thai 56 (11):645-653.

Tait K, Sayer JA, Gharieb MM, Gadd GM (1999). Fungal production of calcium oxalate in leaf litter microcosms. Soil Biol Biochem 31 (8):1189-1192.

Tamer A, Aragno M (1980). Isolement, caractérisation et essai d'identification de bactéries capables d'utiliser l'oxalate comme seule source de carbone et d'énergie. Bull Soc Neuchâtel Sci Nat 103:91-104.

Tanner A, Bornemann S (2000). *Bacillus subtilis* YvrK is an acid-induced oxalate decarboxylase. J Bacteriol 182:5271-5273.

Tappan G, McGahuey M (2007). Tracking environmental dynamics and agricultural intensification in Southern Mali. Agr Syst 94 (1):38-51.

Tous J, Ferguson L (1996). Mediterranean fruits. In: Janick J (ed), Progress in new crops. ASHS Press, Arlington, VA. pp 416-430.

Trumbore SE (1997). Potential responses of soil organic carbon to global environmental change. Proc Natl Acad Sci USA 94 (16):8284-8291.

Tu S, Guo Z, Sun J (2007). Effect of oxalic acid on potassium release from typical chinese soils and minerals. Pedosphere 17 (4):457-466.

Urey HC (1952). The planets: their origin and development. Yale University Press. S.Miller, Science, 245 pp.

Valyasevi A, Dhanamitta S (1974). Studies of bladder stone disease in Thailand. XVII. Effect of exogenous source of oxalate on crystalluria. Am J Clin Nutr 27:877-882.

van Parijs FRD, Morreel K, Ralph J, Boerjan W, Merks RMH (2010). Modeling Lignin Polymerization. I. Simulation Model of Dehydrogenation Polymers. Plant Physiology 153 (3):1332-1344. doi:10.1104/pp.110.154468.

Verrecchia EP (2002). Géodynamique du carbonate de calcium à la surface des continents. In: Géopré E (ed) J.-C. Miskovsky (ed) Géologie de la Préhistoire: méthodes, techniques, applications. Paris, pp 233-258.

Verrecchia EP (2004). Invitation à la géochimie des carbonates. Université de Neuchâtel, Master en Biogéosciences; Version 1.0, novembre 2004. 22 pp.

Verrecchia EP, Braissant O, Cailleau G, Aragno M (2006). The oxalate-carbonate pathway in soil carbon storage: the role of fungi and oxalotrophic bacteria. In: Fungi in biogeochemical cycles, Gadd GM (ed). Cambridge University Press. pp 289-310.

Verrecchia EP, Dumont J-L, Verrecchia KE (1993). Role of calcium oxalate biomineralization by fungi in the formation of calcretes; a case study from Nazareth, Israel. J Sediment Res 63 (5):1000-1006.

Vickery HB (1955). The metabolism of the organic acids of tobacco leaves. IX. Effect of culture of excised leaves in solutions of oxalate and succinate in the presence of cyanide. J Biol Chem 217 (1):83-94.

Villenave C, Duponnois R (2002). Interactions between ectomycorrhizal fungi, plant-parasitic and free-living nematodes and their effects on seedlings of the hardwood *Afzelia africana* Sm. Pedobiologia 46 (2):176-187.

Wakao N, Yasuda T, Jojima Y, Yamanaka S, Hiraishi A (2002). Enhanced growth of *Acidocella facilis* and related acidophilic bacteria at high concentrations of aluminium. Microbes and Environ 17 (2):98-104.

Webb MA (1999). Cell-mediated crystallization of calcium oxalate in plants. Plant Cell 11 (4):751-761.

Wilcoxson R, Sudia T (1968). Translocation in fungi. The Botanical Review 34 (1):32-50.

Wilson MJ, Jones D, Russell JD (1980). Glushinskite, a naturally occurring magnesium oxalate. Mineral Mag 43:837-840.

Wolfson R, Sears BB (1989). A reduction in the abundance of calcium oxalate crystals in Oenothera improves the yield of intact chloroplasts. Plant Cell Environ 12 (1):109-112.

Wu C-C, Kuo-Huang L-L (1997). Calcium crystals in the leaves of some species of Moraceae. Bot Bull Acad Sin 38:97-104.

Zarembski PM, Hodgkinson A (1962). The oxalic acid content of English diets. Brit J Nutr 16:627-634.

Zindler-Frank E, Hönow R, Hesse A (2001). Calcium and oxalate content of the leaves of *Phaseolus vulgaris* at different calcium supply in relation to calcium oxalate crystal formation. J Plant Physiol 158 (2):139-144.

Zosso A (2007). Incorporation de la matière organique en fonction de techniques culturales différentes sur des sols agricoles de Léo, centre-sud du Burkina Faso. 77 pp. Diplôme.

ANNEXES

Annex 1. Protocol for S2 curves deconvolution with PeakFit program

1) Copy the .S00 file in Excel. There are the PYRO CURVES followed by the OXI CURVES. The five columns from the PYRO CURVES correspond to: 1° the number of the steps, 2° the temperature, 3° the S2 pyrograms, 4° the S3CO pyrogram, and 5° the S3CO2 pyrogram. The four oxi columns correspond to: 1° the number of the steps, 2° the temperature, 3° the SCO pyrogram, and 4° the S4CO2 pyrogram.

2) For S2 curve deconvolution with Peak-Fit program take the column 2 and 3 from the PYRO CURVE, temperature and intensity respectively. Cancel the intensity of 0 value and all the data when the temperature decrease (around 648°C). Save the file

3) Open the file with the Peak-Fit program. Select column: x for Temperature and y for Intensity.

4) Click “AutoFit and Subtract Baseline”, and confirm the Baseline subtraction

5) Choose “Auto fit Peaks I residuals” (blue Gaussian curve)

6) The program shows any curves.

7) Unlock “Vary Widths” and delete all the proposed peaks in the second graph. Now the aim is to minimize the residual signal from the third graph, and chose the best r2 with the minimal Gaussian contribution.

8) Click in the residual graphic (third curve) on the highest intensity record and lock the peak. For doing this click on the peak of the Gaussian curve and “Lock” the temperature.

9) Click on the “Fast peak Fit with numerical Update”. Click on Review peak, and note the r^2 value.

10) Click on OK and delete the previous peak.

11) Create two new Gaussian curves on the maximal intensity of the residual graph and lock, so as previously, the temperatures. Click on the “Fast peak Fit with numerical Update”, and note the r^2 value.

12) Repeat the same procedure until the r^2 value does not vary anymore (7-8 peak are sufficient for soil tests). Restoration rates of initial S2 signals depend on the number of elementary Gaussian distributions (Sebag et al. 2006).

13) If the r^2 does not change considerably anymore as a new Gaussian curve is added, the iteration should be finished

14) Click on Numeric taste and the Peak summary is shown.

Annex 2. Oxalate quantificatio

The present protocol is an enzymatic method that allows the calculation of total (soluble and insoluble) oxalate concentrations in a soil or leaf sample. This is an adapted version of the Trinity Biotech, method n°591, established for urinary oxalate quantification (http://www.trinitybiotech.com/data/Products/Insert/046-141A%20Rev%2007-09.pdf)
The analyses require two days. Day 1: preparation of samples: grinding, weighting, and 12h (1 night) acidific tion. Day 2: analysis. 9h are necessary for 20 samples (1 blank, 1 standard and 18 samples).
The enzymatic method described below is based on the oxidation of oxalate by oxalate oxidase followed by measurement of hydrogen peroxide (H_2O_2) produced during the reaction by a peroxidase-catalysed reaction (Trinity-Biotech Procedure No 591).

Equipment and glassworks
- 20 Falcon ™ tubes 50 ml
- 20 falcon ™ tubes 15 ml
- 20 filters 0.45 µ
- 1 x 25 ml graduated pipette
- 1 x 10 ml graduated pipette
- 40 sterile Eppendorf
- 40 sterile Tips 1ml
- 40 sterile Tips 0.5 ml
- pH paper
- agitation table
- centrifuge
- vacuum pump
- vortex
- spectrophotometer

Reagents
- 20 ml of deionised sterile water
- Trinity Biotech OXALATE KIT: Reactive A, Reactive B, Standard 0.5 mmol/l
- HCl 0.5 N
- HCl 5 N
- HCl and NaOH of different normality (ex: 0.5 N, 1 N, 2,5 N)

Procedure
Day 1:
1) Put 10 g of dry soil in a 50 ml falcon tube. For leaves containing oxalate put only 0.5 g of soil material.

2) Add 25 ml of HCl 0.5 N. Create a blank that contains only HCl. If the sample contains more than 10-15 % carbonate, take HCl 1N in order to degas all CO_2 present in the sample.
3) Put on an agitation table 12h (one night).

Day 2:

1- Check the pH (pH paper). Total oxalate solubilisation requires a pH inferior to 2. If not the case add HCl. Measure precisely the added HCl.
2- Centrifuge the samples.
3- Filter the samples at 0.45 µm with a vacuum pump.
4- Collect exactly 10 ml of the filtrate and put them in a 15 ml Falcon tube
5- Weigh the samples in their Falcon tube.
6- Adjust the sample pH between 5 and 7. Attention: the pH function is logarithmic and changes drastically around 5 with the addition of HCl.
7- Weight the samples in their Falcon tube again.
8- For ten samples: reconstitute the Oxalate Reagent A and Oxalate Reagent B in sterile conditions. Reconstitute the Oxalate Reagent A with 10 ml of deionised water. Cork and mix by gentle inversion.
9- Reconstitute the Oxalate Reagent B with 2 ml of deionised water. Cork and return carefully until dissolution. Sample Diluent is not necessary.

STORAGE AND STABILITY: Store the dry reagents refrigerated (2-8°C). Reagents are stable until the expiration date indicated on the labels. Store the sample purifier tubes at room temperature (18-26°C). Reconstituted Oxalate Reagent A is stable for 1 day at ambient temperature (18-26°C) and 1 month when stored refrigerated (2-8°C).
Reconstituted Oxalate Reagent B should be used immediately upon reconstitution. Alternatively, it can be stored for 2 days at 2-8°C or aliquoted and stored at -20°C for 28 days. Each aliquot can be used once and not refrozen. NOTE: warm Oxalate Reagent B to approximately 37°C in order to dissolve any crystalline material which may form during storage in the refrigerator (Trinity-Biotech Procedure No 591).

10) Set up a series of sample purifier tubes for samples and Controls (Trinity-Biotech Procedure No 591);
11) pipette 2 ml of each of the 10 ml mixture from above in the purifier tubes. Vortex and mix for approximately 5 minutes by intermittent mixing (Trinity-Biotech Procedure No 591);
12) centrifuge the tubes for 10 minutes at 1200 rpm (1500xg).

Determination of Oxalate (Trinity-Biotech Procedure No 591)

1) Warm oxalate reagents to assay temperature (any temperature between ambient and 37°C);
2) label Eppendorfs for: 1 blank + 1 Standard + 18 samples;

3) pipette 1 ml Oxalate Reagent A into each Eppendorf;
4) pipette 50 µl of Supernatants or Filtrates (derived from Step 11), to respective Eppendorf;
5) pipette 0.1 ml of Oxalate Reagent B into each tube and immediately mix by gentle inversion;
6) incubate the tubes at desired temperature (18 - 37°C) for 5 min;
7) 15 min before use turn on the spectrophotometer;
8) regulate the spectrophotometer to 590 nm;
9) put deionised water in the sample carrier and press “Backcorr” to tare the zero;
10) read absorbance of blank, standard, and soil sample at 590 nm according to the order in which they were prepared;

Calculation
Known parameters:
- Optical Density (OD) of the sample
- OD of the blank
- OD of the standard

Mmol of oxalate per litre:
Oxalate (mmol/l) = [(OD sample – OD blank)/(OD standard – OD blank)] * 0.5 (mmol/l)
Where: 0.5 = oxalate concentration (mmol/l) in the standard.

Example:
Weight of dried soil sample: 10.3374 g
OD standard = 0.628
OD blank = 0.066
OD soil sample = 0.277

mmol/l oxalate = [(0.277 – 0.066)/(0.628 – 0.066)] * 0.5 = 0.18772242 mmol/l

Tinning correction: during the pH adjustment, to the starting 10 ml were added X ml of HCl and/or NaOH. The difference between the weight before and after this adding makes it possible to calculate the tinning correction of each sample and to correct the mmol/l oxalate.
Example:
- Weight of the sample before the pH correction: 17.22 g (= weight of the tube + 10 ml of filtrate)
- Weight of the sample after the pH adjustment of = 17.83 g (= weight of the tube + 10 ml of filtrate + ml of volume added to adjust the pH)

Thus: grams added to balance the pH: 17.83 g - 17.22 g = 0.61 g or ml
Thus: 0.18772242 mmol/l oxalate in 10.61 ml; what means that the OD is lower than the 10 ml OD, because the sample was diluted.

Thus: 0.18772242 mmol/l oxalate/10 ml = x mmol/l oxalate/10.61 ml
x = 0.199173488 mmol/l

In 10.3374 g of soil there was added 25 ml of HCl. Thus:
0.199173488 mmol/l oxalate /1000 ml = x mmol oxalate/25 ml; or 0.199173488/40
x = 0.004979337 mmol oxalate in 10.3374 g of soil

In 1 kg of soil there is:
0.004979337 mmol /10.3374 g = x mmol/1000 g = 0.481681758 mmol of oxalate in 1 kg of soil.

To transform mmol/l en mg /kg:
1 mole of oxalic acid: ($C_2H_2O_4$ = 12.011 * 2 + 1.0079 * 2 + 15.9994 * 4) = 90.0354 g/moles

Thus: 0.481681758 mmol * 90.0354 g/moles = 43.368409754 mg oxalate in 1 kg of soil (= 0.043368409754 g oxalate/ kg of soil = 0.0043468 %)

Source: Trinity-Biotech (Procedure No 591). Oxalate. Ireland

Annex 3. Some vegetation found in the studied forest with the *Milicia excelsa* trees near Njanmiango:

- *Achyranthes aspera*
- *Blepharis maderaspatensis*
- *Bridelia ferruginea*
- *Desmodium gangeticum*
- *Digitaria horizontalis*
- *Diospyros mespiliformis*
- *Holarrhena floribund*
- *Hyptis suaveolens, Lamiaceae*
- *Leptadenia hastate*
- *Opilia celtidifolia*

These species were determined by Mr. Ouedrago P. Alassane, Engineer of water forests and member of the Institute of water and forest from Bobo Diulasso.

Annex 4. Rock-Eval6 parameters for Burkina Faso (F3, P1, P2, P3, P4, and L2), and Rock-Eval 6 parameters for Salina soils.

Sample	Horizon	PC [%]	RC [%]	TOC [%]	MINC [%]	HI [mg HC/g TOC]	OI [mg CO2/g TOC]	Quant [mg]	File
F3 Hs	A	0.04	0.39	0.43	0.08	36	224	61.8	1586_26.r00
F3 A1	Bc1	0.02	0.22	0.24	0.05	0	343	61.3	1586_27.r00
F3 A1	Bc1	0.02	0.22	0.24	0.05	17	319	70.9	1586D22.r00
F3 A2	Bc2	0.02	0.18	0.20	0.05	0	365	63.2	1586_28.r00
F3 A2	Bc2	0.02	0.13	0.15	0.05	0	544	65.4	1586D23.r00
F3 A3	Bcd	0.02	0.16	0.18	0.06	0	477	68.3	1586_29.r00
F3 A3	Bcd	0.02	0.11	0.13	0.06	0	550	64.0	1586D24.r00
F3 A4	C1	0.03	0.12	0.14	0.07	18	636	57.8	1586_30.r00
F3 A5	C2	0.03	0.11	0.13	0.06	0	750	59.1	1586_31.r00
F3 A5	C2	0.02	0.07	0.10	0.05	0	892	69.7	1586D25.r00
P1 0	(OL)A	1.31	3.87	5.18	0.48	241	163	51.0	1700B12.r00
P1 5	Ak	0.02	0.10	0.11	0.01	111	166	68.9	1586B13.r00
P1 10	Ak	0.02	0.16	0.18	0.04	85	149	66.3	1586B14.r00
P1 15	Ak	0.01	0.14	0.15	0.04	48	168	69.1	1586B15.r00
P1 20	Bck1	0.02	0.20	0.22	0.05	48	148	71.2	1586B16.r00
P1 25	Bck1	0.01	0.19	0.20	0.03	33	166	82.6	1586B17.r00
P1 30	Bck1	-	-	-	-	-	-	-	-
P1 35	Bck2	0.01	0.16	0.17	0.03	8	184	61.3	1586B18.r00
P1 35	Bck2	0.04	0.38	0.42	0.12	12	347	71.0	1586D12.r00
P1 40	Bck2	0.01	0.17	0.19	0.03	7	200	63.7	1586B19.r00
P1 45	C1	0.01	0.18	0.19	0.03	10	202	73.6	1586B20.r00
P1 50	C1	0.02	0.19	0.21	0.04	27	254	66.9	1586B21.r00
P1 50	C1	0.04	0.38	0.42	0.10	14	318	51.9	1700B13.r00
P1 55	C2	0.05	0.38	0.42	0.09	30	328	55.0	1700B14.r00
P1 60	C2	0.03	0.28	0.30	0.06	25	244	59.3	1586B23.r00
P2 0	(OL)A	0.58	2.25	2.84	0.23	202	143	62.9	1586B24.r00
P2 5	Ak	0.20	1.23	1.44	0.12	120	155	71.0	1586B25.r00
P2 10	Ak	0.26	1.53	1.80	0.13	111	192	55.7	1700B15.r00
P2 15	Ak	0.16	1.24	1.40	0.11	77	190	51.6	1700B16.r00
P2 20	Bck1	0.16	1.14	1.31	0.12	83	201	51.6	1700B17.r00
P2 25	Bck1	0.05	0.63	0.68	0.07	20	191	50.4	1700B18.r00
P2 30	Bck1	0.04	0.54	0.57	0.07	2	220	50.9	1700B19.r00
P2 35	Bck2	0.03	0.46	0.49	0.06	2	214	54.7	1700B20.r00
P2 35	Bck2	0.04	0.43	0.47	0.10	7	284	61.1	1586D13.r00
P2 40	Bck2	0.03	0.49	0.51	0.06	2	182	50.4	1700B21.r00
P2 40	Bck2	0.03	0.37	0.40	0.07	0	274	54.1	1850A29.r00
P2 45	C1	0.04	0.47	0.51	0.06	27	207	55.4	1700B22.r00
P2 50	C2	0.04	0.37	0.40	0.11	5	303	70.3	1586D14.r00
P2 50	C2	0.03	0.35	0.38	0.06	0	297	54.8	1700B23.r00
P2 55	C2	0.04	0.37	0.40	0.09	9	321	51.6	1700B24.r00
P2 60	C2	0.05	0.41	0.47	0.11	27	336	51.9	1700B25.r00
P2 65	C2	0.04	0.22	0.26	0.11	0	573	61.3	1586D15.r00
P2 65	C2	0.03	0.27	0.30	0.08	0	420	53.9	1700B26.r00
P2 70	C2	0.03	0.22	0.25	0.09	4	489	70.3	1586D16.r00
P2 70	C2	0.03	0.24	0.27	0.06	0	386	55.0	1700B27.r00

Annex 4. Continued. Rock-Eval6 parameters for soils.

Sample	Horizon	PC [%]	RC [%]	TOC [%]	MINC [%]	HI [mg HC/g TOC]	OI [mg CO2/g TOC]	Quant [mg]	File
P3 0	(OL)A	1.22	5.99	7.21	2.02	140	167	51.0	1700d20.r00
P3 5	(OL)A	0.40	1.96	2.36	1.06	134	205	50.4	1700c16.r00
P3 10	Ak	0.22	0.91	1.13	0.84	139	291	51.8	1700c17.r00
P3 15	Ak	0.06	0.54	0.60	0.18	44	236	50.2	1700c18.r00
P3 20	Ak	0.04	0.26	0.30	0.08	36	411	53.6	1700c19.r00
P3 20	Ak	0.05	0.47	0.52	0.09	25	255	58.0	1700d21.r00
P3 25	Bck1	0.03	0.35	0.38	0.07	3	295	52.5	1700c20.r00
P3 30	Bck1	0.09	0.56	0.65	0.09	89	219	55.7	1700d22.r00
P3 35	Bck1	0.04	0.40	0.44	0.08	21	285	50.6	1700d23.r00
P3 40	Bck1	0.03	0.25	0.28	0.07	0	337	65.1	1586D17.r00
P3 40	Bck1	0.02	0.27	0.29	0.05	0	310	54.2	1700c23.r00
P3 45	Bck2	0.03	0.19	0.22	0.05	22	415	52.7	1700c24.r00
P3 50	Bck2	0.03	0.28	0.31	0.07	10	313	67.8	1586D18.r00
P3 50	Bck2	0.03	0.40	0.42	0.19	2	221	55.2	1700c25.r00
P3 55	Bck2	0.07	0.52	0.59	0.07	66	228	52.0	1700c26.r00
P3 60	Bck2	0.04	0.35	0.39	0.09	8	315	63.1	1586D19.r00
P3 65	C1	0.03	0.20	0.22	0.05	0	418	53.8	1700c27.r00
P4 0	(OL)A	0.60	2.34	2.94	0.81	177	204	70.7	1586_12.r00
P4 0	(OL)A	0.64	2.46	3.09	0.68	180	171	57.9	1700d12.r00
P4 5	Ak	0.25	1.59	1.84	1.77	101	190	66.8	1586_13.r00
P4 10	Ak	0.16	1.10	1.26	0.81	83	211	66.2	1586_14.r00
P4 15	Ak	0.08	0.73	0.81	0.32	45	217	63.8	1586_15.r00
P4 20	Bck1	0.07	0.65	0.73	0.27	46	231	68.8	1586_16.r00
P4 25	Bck1	0.06	0.57	0.64	0.19	39	238	68.7	1586_17.r00
P4 30	Bck1	0.10	0.72	0.82	0.21	60	256	68.0	1586_18.r00
P4 35	Bck1	0.06	0.50	0.56	0.21	40	292	65.9	1586_19.r00
P4 40	Bck1	0.04	0.34	0.38	0.13	14	342	68.5	1586_20.r00
P4 45	Bck2	0.03	0.30	0.33	0.09	8	305	60.2	1586_21.r00
P4 50	Bck2	0.03	0.19	0.21	0.08	0	454	66.0	1586_22.r00
P4 50	Bck2	0.03	0.17	0.20	0.08	0	492	51.1	1700d13.r00
P4 55	C1	0.03	0.10	0.13	0.08	0	826	71.1	1586D20.r00
P4 55	C1	0.03	0.12	0.15	0.09	0	786	60.6	1586_23.r00
P4 60	C1	0.04	0.11	0.14	0.09	0	929	63.7	1586D21.r00
P4 60	C1	0.03	0.14	0.18	0.08	0	693	69.9	1586_24.r00
P4 65	C1	0.05	0.13	0.17	0.11	0	990	61.5	1586_25.r00
P4 65	C1	0.04	0.10	0.14	0.11	0	1053	55.0	1700d14.r00
L2 0-8	(OL)A	0.53	3.07	3.60	0.88	106	213	61.7	1586D26.r00
L2 8-15	Ak	1.08	4.22	5.31	0.82	163	252	63.6	1586D27.r00
L215-27	Bck1	0.23	0.64	0.88	0.25	151	511	62.6	1586D28.r00

Annex 4. Continued. Rock-Eval6 parameters for soils.

Sample	Horizon	PC [%]	RC [%]	TOC [%]	MINC [%]	HI [mg HC/g TOC]	OI [mg CO2/g TOC]	Quant [mg]	File
PC1 0.00	H1	0.41	1.35	1.76	0.14	203	227	51.0	1700A21.r00
PC1 0.01	H1	0.61	1.72	2.33	0.16	246	209	59.2	1700A22.r00
PC1 0.02	H1	0.42	1.39	1.82	0.14	206	228	55.5	1700A23.r00
PC1 0.10	H1	0.19	0.84	1.04	0.12	137	273	57.3	1700A24.r00
PC1 0.20	H2	0.12	0.63	0.75	0.10	109	249	54.7	1700A25.r00
PC1 0.30	H2	0.07	0.52	0.59	0.09	47	279	57.9	1700A26.r00
PC1 0.35	H3	0.05	0.02	0.06	0.09	128	2362	57.5	1700A27.r00
PC1 0.40	H3	0.04	0.11	0.15	0.08	32	784	59.9	1700A28.r00
PC1 0.45	H3	0.03	0.00	0.03	0.07	0	3667	57.5	1700A29.r00
PC1 0.50	H4	0.03	0.02	0.05	0.08	0	2475	50.8	1700A30.r00
PC1 0.55	H4	0.12	0.00	0.13	0.12	588	1769	53.4	1700A31.r00
PC1 0.60	H5	0.04	0.08	0.12	0.09	0	1240	71.3	1586D38.r00
PC1 0.60	H5	0.03	0.10	0.12	0.06	0	776	52.2	1700c12.r00
PC1 0.60	H5	0.03	0.27	0.30	0.06	0	368	52.6	1700d19.r00
PC1 0.65	H5	0.03	0.34	0.36	0.06	0	260	51.8	1700c13.r00
PC1 0.70	H5	0.03	0.37	0.39	0.05	0	249	52.7	1700c14.r00
PC1 0.70	H5	0.05	0.32	0.37	0.10	0	477	73.6	1586D36.r00
PC2 0.00	H1	0.76	1.87	2.63	0.16	279	216	58.4	1700A12.r00
PC2 0.05	H1	0.09	0.56	0.65	0.09	73	277	52.0	1700A13.r00
PC2 0.10	H2	0.06	0.38	0.43	0.07	45	334	56.9	1700A14.r00
PC2 0.20	H2	0.03	0.30	0.33	0.07	6	339	51.6	1700A15.r00
PC2 0.30	H3	0.04	0.36	0.40	0.07	9	309	57.3	1700A16.r00
PC2 0.40	H4	0.04	0.32	0.36	0.07	0	360	50.5	1700A17.r00
PC2 0.50	H4	0.03	0.27	0.29	0.06	0	361	57.2	1700A18.r00
PC2 0.60	H4	0.06	0.58	0.64	0.09	19	268	55.5	1700A19.r00
PC2 0.70	H5	0.05	0.46	0.51	0.08	17	307	50.2	1700A20.r00

Annex 5. CHN values of Burkina Faso (F3, P1, P2, P3, P4, and L2) and Salina (PC1 and PC2) soils.

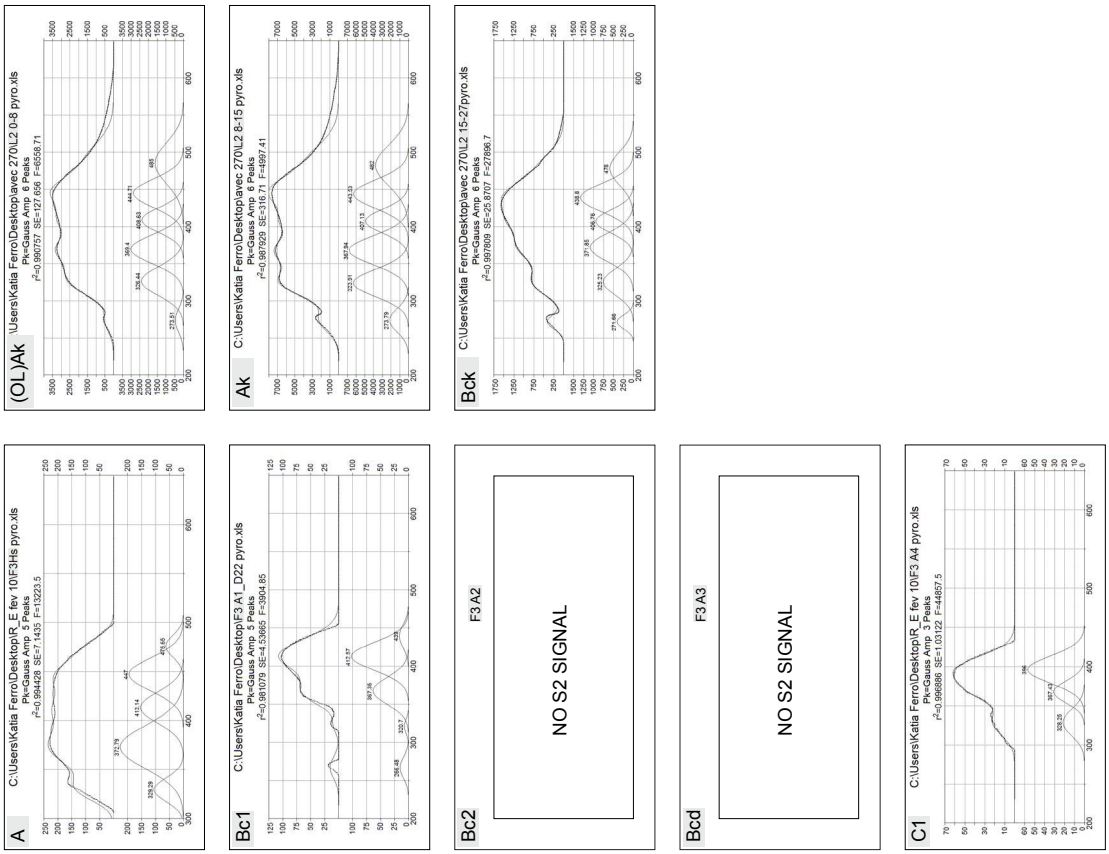
Sample	C	H	N	C/N	Weight
		[%]			[mg]
F3 Hs	0.5	0.1	0.0	18	20.89
F3 A1	0.3	0.1	0.0	20	20.62
F3 A2	0.2	0.1	0.0	17	21.40
F3 A3	0.2	0.2	0.0	16	21.40
F3 A4	0.1	0.2	0.0	11	20.39
F3 A5	0.2	0.4	0.0	14	19.36
P1 0	6.8	1.2	0.5	14	21.08
P1 5	2.0	0.4	0.1	14	19.27
P1 5	2.0	0.4	0.1	14	17.04
P1 5	1.9	0.4	0.1	13	20.68
P1 10	1.6	0.4	0.1	14	22.27
P1 15	1.1	0.3	0.1	18	21.25
P1 20	1.0	0.2	0.1	17	21.09
P1 25	0.8	0.2	0.0	20	22.85
P1 30	0.6	0.2	0.0	19	20.68
P1 35	0.6	0.2	0.0	22	22.47
P1 40	0.5	0.2	0.0	22	22.55
P1 45	0.4	0.2	0.0	22	21.47
P1 50	0.6	0.3	0.0	20	21.45
P1 55	0.5	0.3	0.0	20	18.83
P1 60	0.5	0.4	0.0	18	19.33
P2 0	3.4	0.6	0.2	14	21.31
P2 5	1.9	0.4	0.1	13	22.36
P2 10	1.6	0.4	0.1	14	20.10
P2 15	1.2	0.3	0.1	14	18.40
P2 20	1.2	0.3	0.1	16	19.69
P2 25	0.7	0.2	0.0	20	21.17
P2 30	0.6	0.2	0.0	22	19.30
P2 35	0.5	0.2	0.0	24	20.21
P2 40	0.4	0.2	0.0	25	20.68
P2 45	0.7	0.2	0.0	28	20.06
P2 50	0.5	0.2	0.0	25	18.20
P2 55	0.5	0.3	0.0	22	19.51
P2 60	0.6	0.5	0.0	20	19.04
P2 65	0.4	0.3	0.0	21	16.66
P2 70	0.4	0.3	0.0	21	22.01
P3 0	8.9	1.5	0.5	18	18.52
P3 5	2.9	0.6	0.2	17	22.92
P3 10	2.2	0.4	0.1	19	18.15
P3 15	0.7	0.2	0.0	19	19.97
P3 20	0.6	0.2	0.0	18	20.99
P3 25	0.5	0.2	0.0	19	19.63
P3 30	0.8	0.2	0.0	22	18.15
P3 35	0.5	0.2	0.0	22	21.86
P3 40	0.3	0.1	0.0	21	20.03
P3 45	0.3	0.1	0.0	22	19.26
P3 50	0.4	0.2	0.0	25	20.86
P3 55	0.6	0.2	0.0	35	18.84
P3 60	0.5	0.2	0.0	24	19.49
P3 65	0.3	0.2	0.0	15	20.97

Sample	C	H	N	C/N	Weight
		[%]			[mg]
P4 0	3.6	0.6	0.3	14	12.30
P4 5	3.4	0.5	0.2	21	22.55
P4 10	1.9	0.3	0.1	18	19.80
P4 10	1.9	0.3	0.1	20	18.44
P4 10	1.9	0.4	0.1	19	18.72
P4 15	1.0	0.2	0.1	17	18.03
P4 20	1.0	0.3	0.1	16	21.96
P4 25	0.8	0.3	0.0	19	22.81
P4 30	1.0	0.3	0.1	17	19.48
P4 35	0.8	0.2	0.0	17	19.23
P4 40	0.5	0.2	0.0	21	18.44
P4 45	0.4	0.2	0.0	21	19.61
P4 50	0.3	0.2	0.0	18	18.54
P4 55	0.2	0.3	0.0	12	19.12
P4 60	0.2	0.3	0.0	14	18.39
P4 65	0.3	0.5	0.0	16	23.65
L2 0-8	4.3	1.0	0.2	18	18.41
L2 15-27	1.7	0.8	0.1	17	19.46
L2 8-15	5.8	1.5	0.3	18	19.69
PC1 0.00	1.8	0.9	0.1	19	19.87
PC1 0.01	2.3	0.9	0.1	18	19.03
PC1 0.02	2.1	1.0	0.1	14	21.72
PC1 0.10	1.1	0.7	0.1	15	21.72
PC1 0.20	0.8	0.7	0.0	18	19.95
PC1 0.30	0.7	0.6	0.0	15	19.99
PC1 0.30	0.7	0.7	0.0	15	20.85
PC1 0.30	0.7	0.7	0.0	17	19.06
PC1 0.35	0.6	0.7	0.0	14	21.15
PC1 0.40	0.5	0.6	0.0	18	19.27
PC1 0.45	0.4	0.5	0.0	15	20.29
PC1 0.50	0.4	0.6	0.0	18	20.75
PC1 0.55	1.0	0.7	0.1	16	19.58
PC1 0.60	0.3	0.6	0.0	18	19.27
PC1 0.65	0.4	0.6	0.0	17	21.10
PC1 0.70	0.4	0.7	0.0	17	19.49
PC2 0.00	3.1	1.1	0.2	17	19.33
PC2 0.05	0.6	0.6	0.0	17	20.08
PC2 0.10	0.6	0.6	0.0	16	21.60
PC2 0.20	0.4	0.6	0.0	16	19.02
PC2 0.30	0.5	0.6	0.0	16	20.53
PC2 0.40	0.4	0.6	0.0	19	18.78
PC2 0.50	0.4	0.6	0.0	18	20.37
PC2 0.60	0.7	0.8	0.0	21	19.13
PC2 0.70	0.7	0.7	0.0	16	18.84

Annex 6. Deconvolution of the multilobed S2 pyrograms from Burkina Faso (P1, P2, P3, P4, P5, F3, and L2) and Salina (PC1 and PC2; Italy) soil profiles

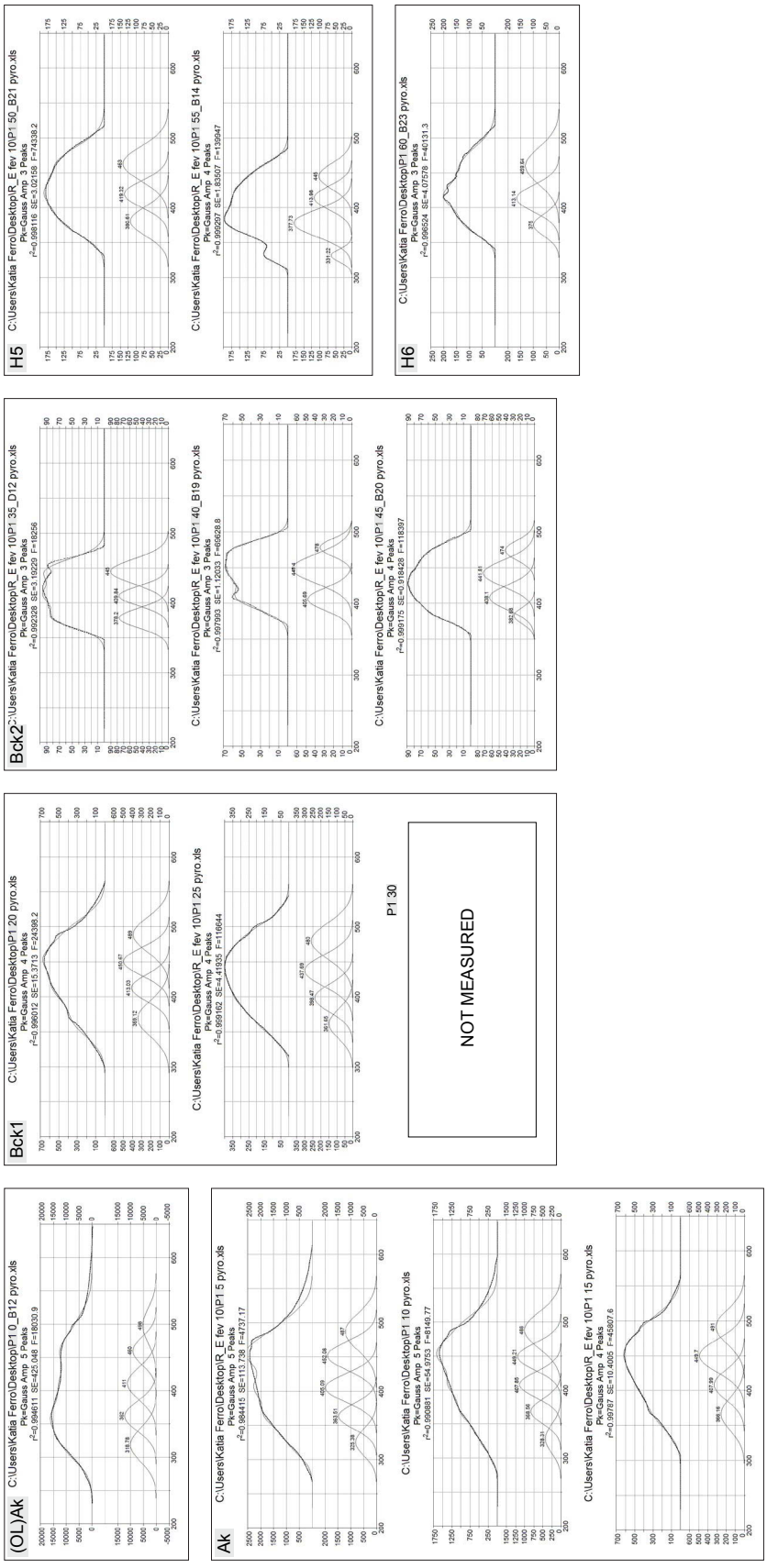
F3: Reference soil from *M. excelsa* system.

L2: *A. africana* soil.



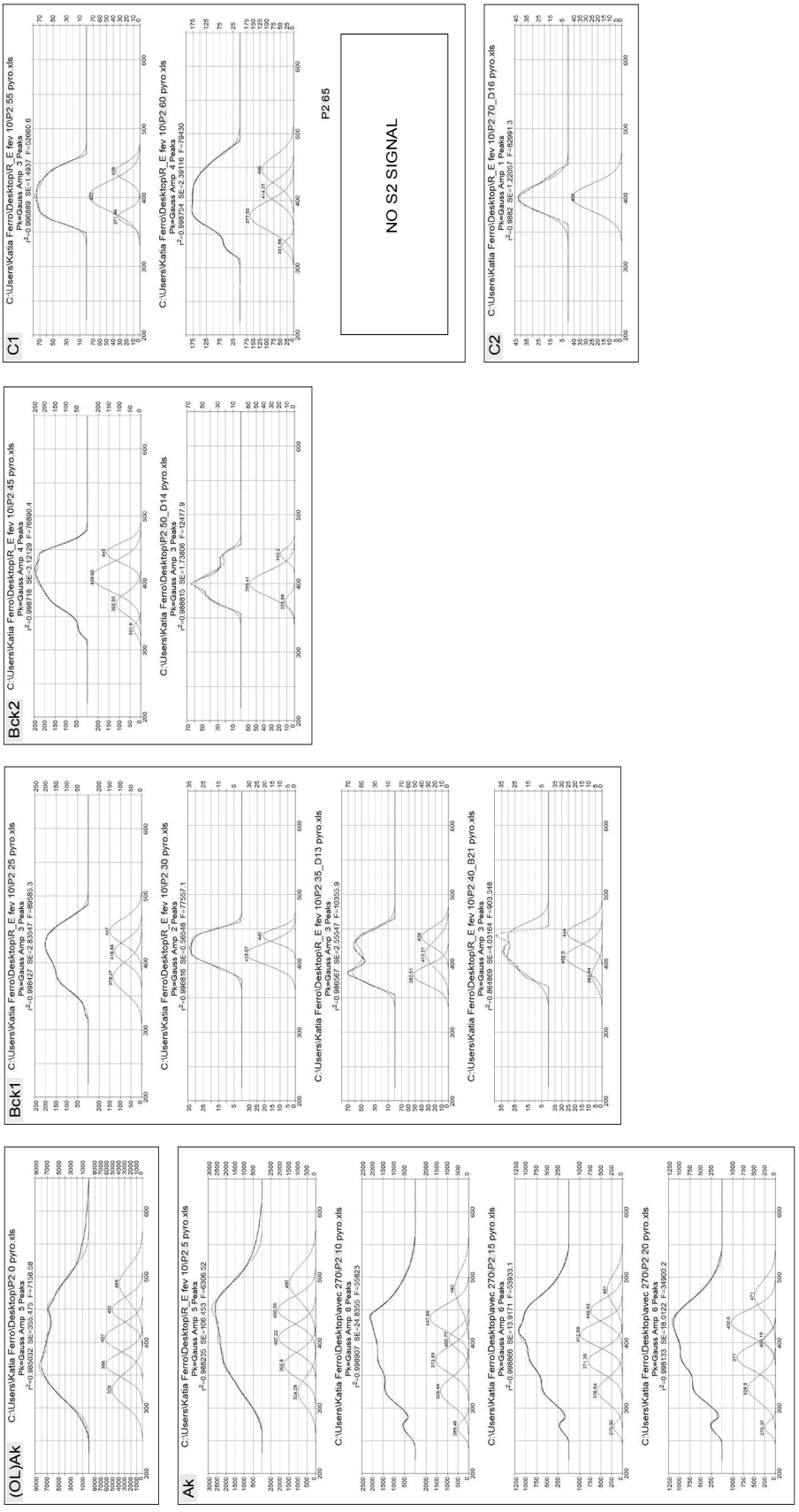
Annex 6. Continued. Deconvolution of S2 curves.

P1: Soil located at 2.0 m from a *M. excelsa* stump.



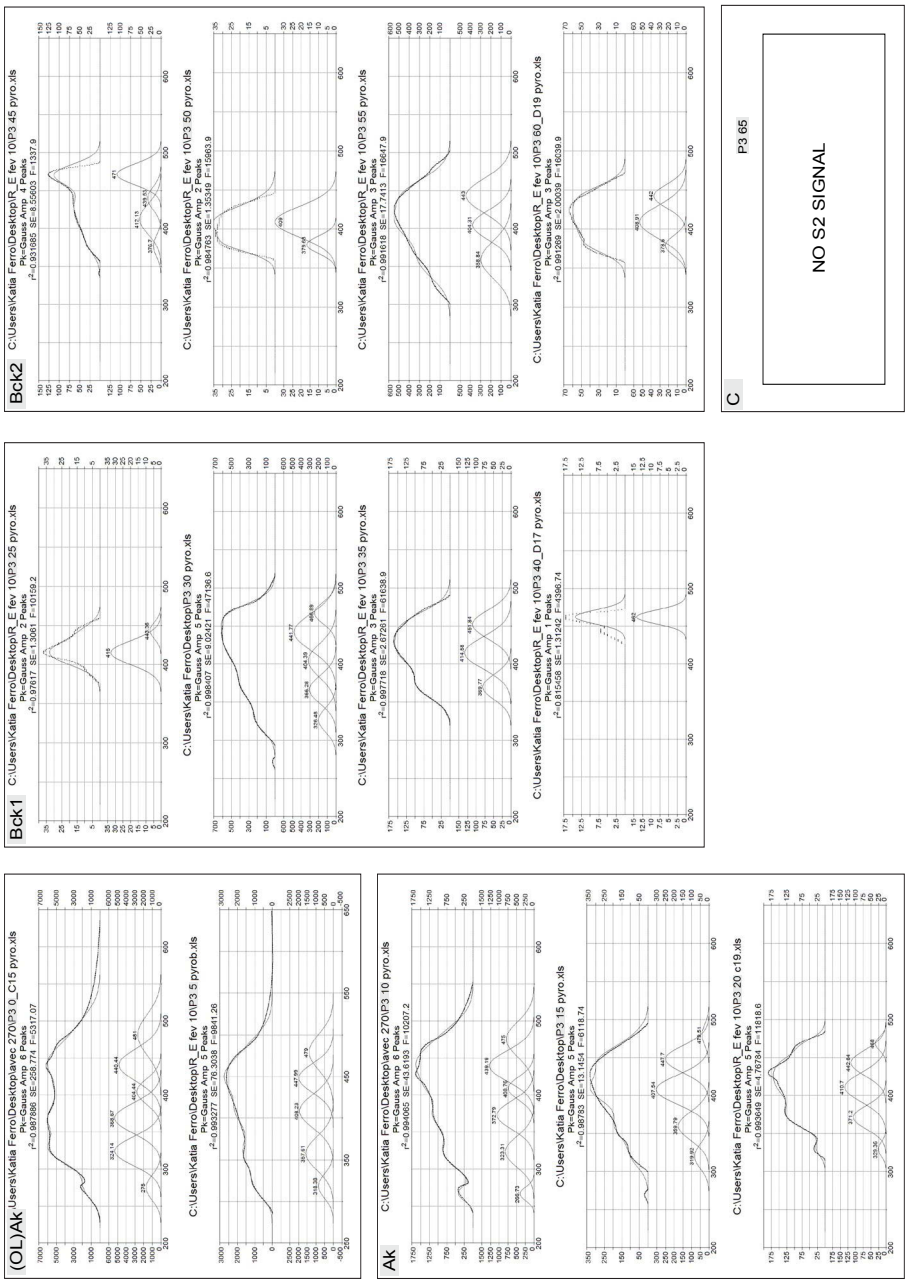
Annex 6. Continued. Deconvolution of S2 curves.

P2: Soil located at 3.4 m from a *M. excelsa* stump.



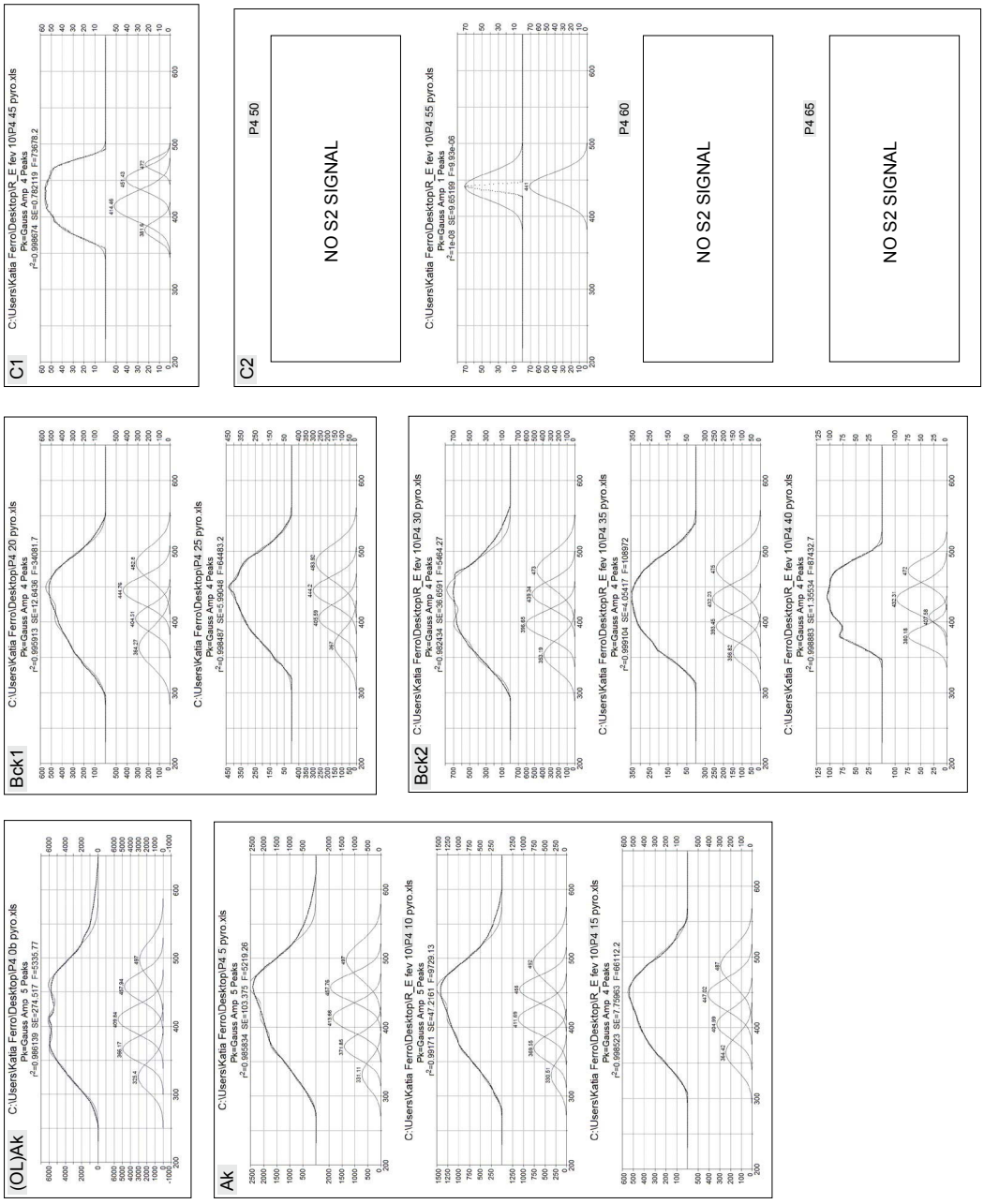
Annex 6. Continued. Deconvolution of S2 curves.

P3: Soil located under a *M. excelsa* stump.



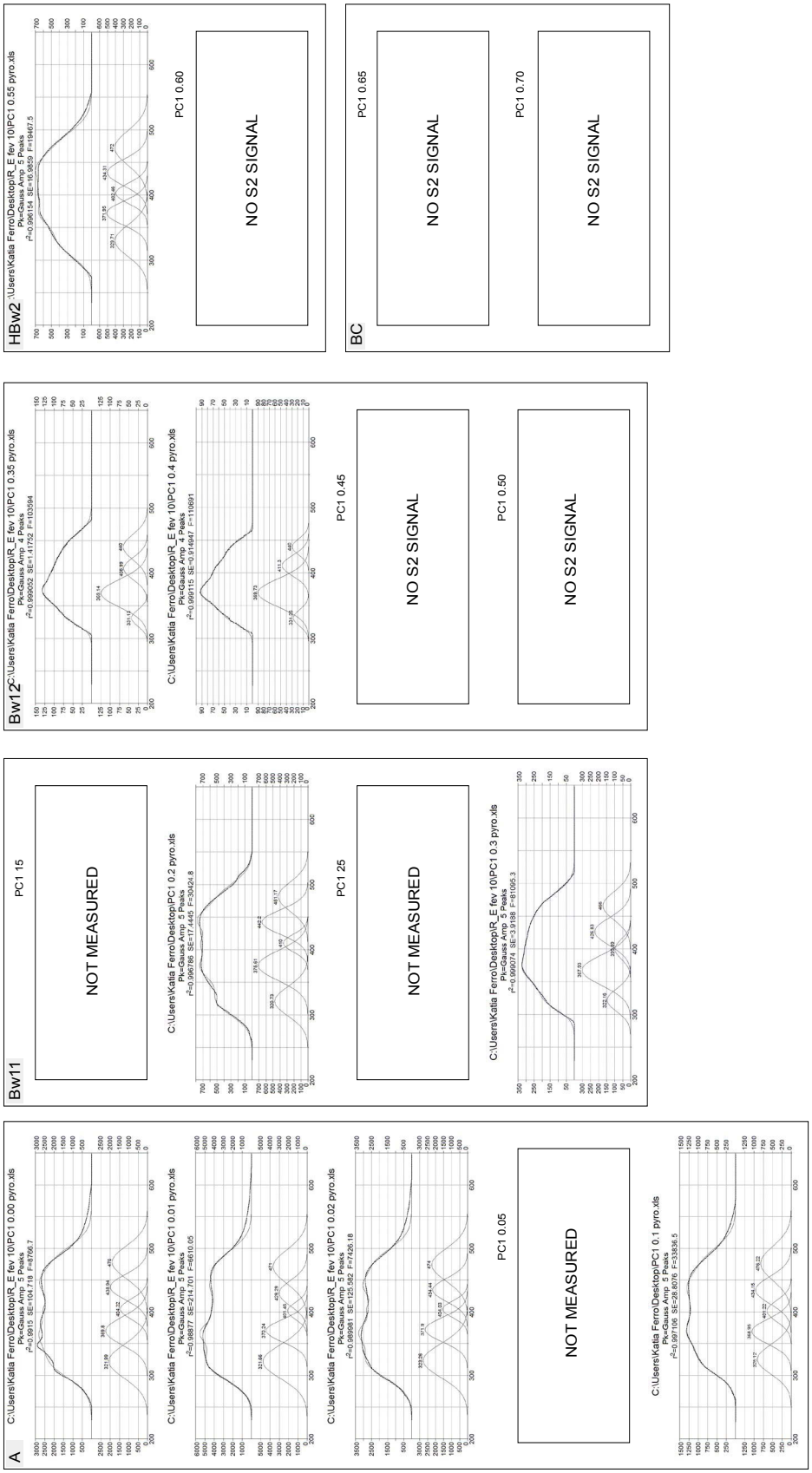
Annex 6. Continued. Deconvolution of S2 curves.

P4: Soil at 4.5 m from the trunk of a living *M. excelsa* tree



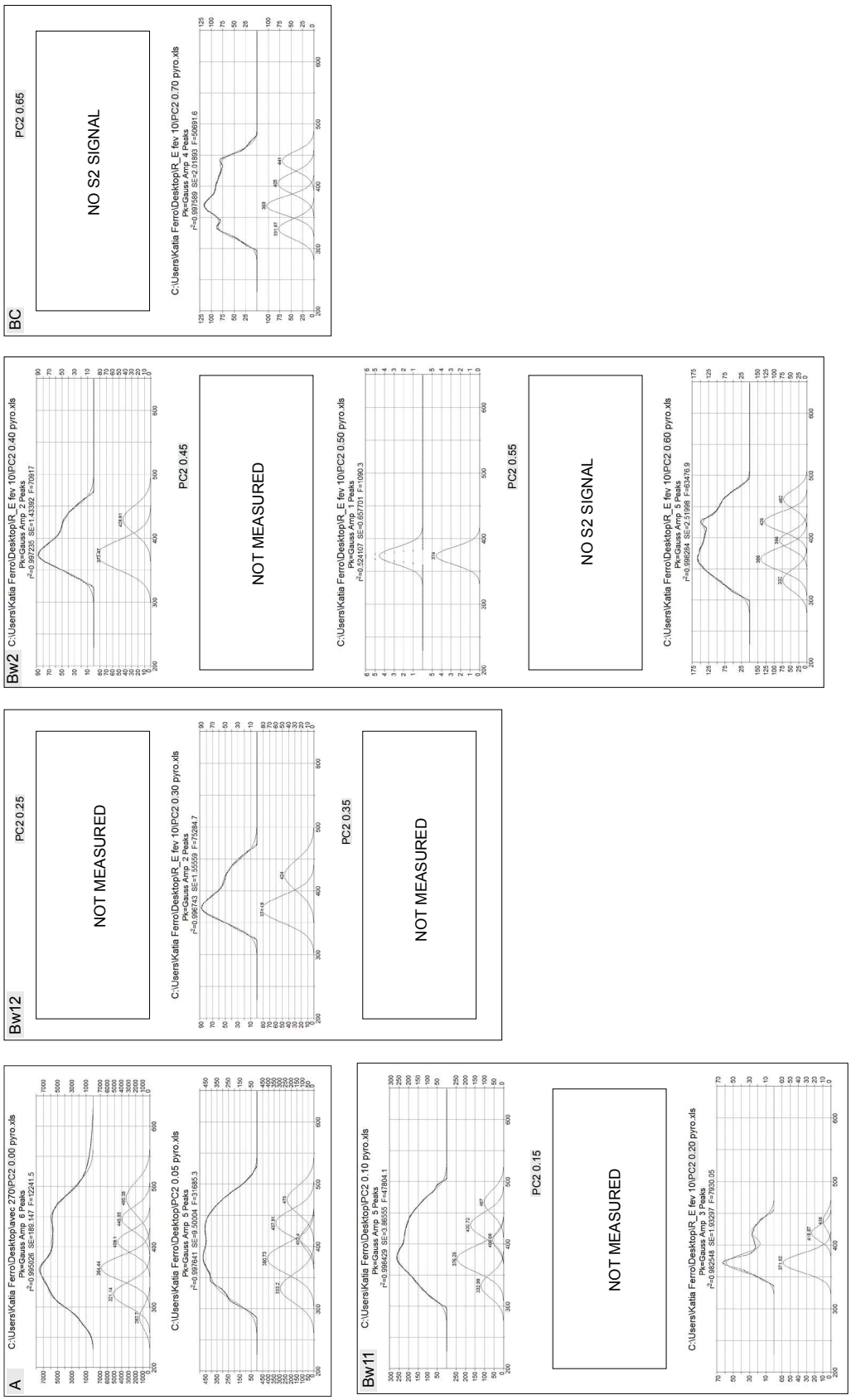
Annex 6. Continued. Deconvolution of S2 curves.

PC1: Salina soil under an *Opuntia sp.* cactus.



Annex 6. Continued. Deconvolution of S2 curves.

PC2: Salina reference soil.



Annex 7. Results of temperature intervals and area contributions resulting from mathematical deconvolution of S2 pyrograms performed on "fresh organic material". F0, F1, F2, F3a, F3b, and F4 are elementary Gaussian components and TpS2 is the highest peak from S2 pyrogram.

		Peak temperature (°C)					
Samples	TpS2	F0	F1	F2	F3a	F3b	F4
Boletus sp.	317	267	317	366	415	456	496
Fusarium sp.	272	272	313	367	420	463	503
Melanin	270	270	310	366	419	454	494
A. africana wood	361	270	319	361	420	458	500
A. africana leaves	361	279	323	361	410	457	498
M. excelsa dried leaves	360	270	319	360	418	460	503
M. excelsa rotten leaves	331	264	331	377	427	468	508
M. excelsa fresh leaves	264	264	325	370	422	465	504
Oak sp. leaves	356	266	318	356	409	450	495
Grass leaves	273	273	334	368	415	456	502
R. alpinus leaves	315	258	315	371	421	463	504
Insects	376	272	329	376	433	474	518
Mean		269	321	367	419	460	502
S.d.		5	7	6	7	7	7
Minimum		258	310	356	409	450	494
Maximum		279	334	376	433	474	518

	Area contribution (%)					
Samples	F0	F1	F2	F3a	F3b	F4
Boletus sp.	34	24	21	8	9	4
Fusarium sp.	34	27	16	11	7	5
Melanin	30	20	21	13	7	8
A. africana wood	11	21	53	6	4	4
A. africana leaves	12	14	37	17	13	7
M. excelsa dried leaves	11	21	51	9	4	4
M. excelsa rotten leaves	19	38	20	14	5	5
M. excelsa fresh leaves	21	24	22	16	12	6
Oak sp. leaves	21	16	33	17	8	4
Grass leaves	31	31	13	14	7	5
R. alpinus leaves	30	22	19	16	7	6
Insects	13	31	36	13	4	3
Mean	22	24	28	13	7	5
S.d.	9	7	13	4	3	1
Minimum	11	14	13	6	4	2
Maximum	34	38	53	17	13	8

Annex 8. Average values of T_{peak} (°C) and area contribution (%) of the elementary Gaussian components resulting from mathematical deconvolution of S2 pyrograms performed on "fresh organic material" and soils.

		Tpeak of the six elementary Gaussian components / °C					
	Nr of samples	**F0**	**F1**	**F2**	**F3a**	**F3b**	**F4**
"Fresh organic material"	12						
Mean		**269**	**321**	**367**	**419**	**460**	**502**
S. d.		6	8	6	7	7	7
Minimum		258	310	356	409	450	494
Maximum		279	334	376	433	474	518
Burkina Faso soils	64						
Mean		**271**	**326**	**371**	**408**	**446**	**482**
S. d.		3	4	7	6	7	8
Minimum		266	318	353	393	431	467
Maximum		275	333	383	419	463	498
Salina soils	23						
Mean		**283**	**327**	**371**	**406**	**435**	**473**
S. d.		-	5	4	6	6	6
Minimum		283	321	364	408	429	475
Maximum			333	374	419	446	480

	Contribution area of the six elementary Gaussian components / %					
	F0	**F1**	**F2**	**F3a**	**F3b**	**F4**
"Fresh organic material"						
Mean	**22**	**24**	**28**	**13**	**7**	**5**
S. d.	9	7	13	4	3	1
Minimum	11	14	13	6	4	3
Maximum	34	38	53	17	13	8
Burkina Faso soils						
Mean	**5**	**14**	**22**	**33**	**31**	**20**
S. d.	1	7	8	21	16	9
Minimum	0	0	0	0	0	0
Maximum	6	23	44	100	100	45
Salina soils						
Mean	**5**	**21**	**39**	**15**	**22**	**19**
S. d.	-	7	23	13	7	5
Minimum	0	0	0	0	0	0
Maximum	5	33	100	57	39	25

Annex 9. Deconvolution results of the S2 FID signal found in literature data.

	F0	F1			F2			F3			F4	F5
Sebag et al., 2006												
Mean of 119 soil samples	**280**	**307**			**371**			**436**			**481**	**560**
Disnar et al., 2003												
PODZOL												
OL		304			363			424			480	
OF		308			370			439			482	
OH		309			368			434			481	
A1		308			370			434			438	
B21h		309			375			455			503	
B22h		302			379			454			503	
SPODIC CAMBISOL												
OF		306			375			432			476	
OH		290			361			439			480	
A11		309			369			437			478	
A12		308			371			436			474	
A13		305			369			439			481	
A1-Bw		309			372			438			481	
DISTRIC FERRALSOL												
OF-OH	284		338		376			431			480	
A11	281		330		381			434			480	555
A12	281		336		380			434			487	558
Hetényi et al., 2006												
Sieved sample		293	331	359	383	403	417	431	444	446	480	607
Lipid-free sample		295	342		374	401		427	434		480	602
Humin before TFA/HCl treatment		309	352			389		427	441	449		590
Humin after TFA/HCL treatment		314				390		428			486	623
Macromolecular organic matter (marsh soil)			342					425	435		505	625
TOTAL	282	305	339	359	373	396	417	435	439	448	482	590
S.D.	2	6	8		6	7		8	5	2	14	29
Total means	**271**		**325**		**370**		**408**	**445**			**480**	
Total s.d.	6		6		8		8	11			9	

Annex 10. Results of oxalate measured by enzymatic method in soils.

Sample	mg of soil /kg ox	s. d.	Sample	mg of soil /kg ox	s. d.
F3 Hs	4.3		PC1 0.00	6.7	3.4
F3 A1	-		PC1 0.01	5.5	
F3 A2	2.1		PC1 0.02	0.0	
F3 A3	1.0		PC1 0.05	-	
F3 A4	-		PC1 0.10	0.0	
F3 A5	1.1		PC1 0.15	-	
			PC1 0.20	0.2	
L2 0 -8	60.9		PC1 0.25	-	
L2 8 -15	42.6		PC1 0.30	-	
L2 15 -27	3.7		PC1 0.35	-	
			PC1 0.40	0.2	
P3 0	64.1		PC1 0.45	-	
P3 5	19.8	5.6	PC1 0.50	-	
P3 10	74.3		PC1 0.55	-	
P3 15	47.3		PC1 0.60	0.5	
P3 20	37.2				
P3 25	42.1		PC2 0.00	20.0	
P3 30	82.9		PC2 0.00	0.0	
P3 35	*n. m.*		PC2 0.10	1.3	
P3 40	6.7		PC2 0.20	0.4	
P3 45	*n. m.*				
P3 50	0.0				
P3 55	*n. m.*				
P3 60	43.4				
P4 0	47.2				
P4 5	13.3				
P4 10	21.3	2.4			
P4 15	2.3				
P4 20	2.0	0.8			
P4 25	2.1				
P4 30	7.8				
P4 35	-				
P4 40	0.3				
P4 45	-				
P4 50	0.0				
P4 55	-				
P4 60	1.5				

Annex 11. Results on carbonate titration (% carb), pH_{H2O} and pH_{KCl} measurements, residual water content (R.w.), base saturation (S méq/100 g of soil), exchange acidity (AE méq/100 g of soil), cation exchange capacity (CEC), and base cation saturation ratio (V%) of Burkina Faso (F3, P1, P2, P3, P4, and L2) and Salina soils (PC1 under the cactus, and PC2). S.d.: standard deviation.

Sample	carb [%]	s.d.	pH_{H2O}	pH_{KCl}	R.w.	S méq / 100 g of soil	AE	CEC	V [%]
M. excelsa w.	24.01								
A. africana w.	20.50								
F3 Hs	0.00		5.76	4.60	0.0	0.4	1.4	2	23
F3 A1	0.00		5.74	4.55	-	1.3	1.7	3	43
F3 A2	-		6.21	5.12	0.0				
F3 A3	-		5.91	5.20	0.1	0.6	1.9	2	22
F3 A4	-		5.72	4.94	-				
F3 A5	0.00		5.39	4.67	0.1	1.9	2.3	4	46
P1 0	3.72	1.18	7.47	7.10	-				
P1 5	1.46		7.68	7.25	-				
P1 10	2.47		7.39	-	-				
P1 15	1.82		8.25	7.90	-				
P1 20	1.58		8.72	7.57	-				
P1 25	2.24		8.27	7.57	-				
P1 30	1.32		8.69	8.54	-				
P1 35	1.43		8.32	7.90	-				
P1 40	1.12		8.44	7.71	-				
P1 45	0.91		8.39	7.67	-				
P1 50	1.07		8.16	7.53	-				
P1 55	1.19		8.22	7.92	-				
P1 60	1.36		7.84	7.79	-				
P2 0	1.97		7.53	7.32	-				
P2 5	1.53		6.89	6.87	-				
P2 10	2.08		6.93	6.58	-				
P2 15	1.15		7.19	6.82	-				
P2 20	1.00		7.42	7.18	-				
P2 25	0.80		7.41	7.02	-				
P2 30	0.81	0.19	7.42	7.22	-				
P2 35	0.90		7.40	7.15	-				
P2 40	1.25		7.41	7.10	-				
P2 45	1.43		7.53	7.21	-				
P2 50	0.48	0.09	7.71	7.69	-				
P2 55	1.37		7.73	7.73	-				
P2 60	1.57		7.76	7.54	-				
P2 65	0.00		7.49	7.48	-				
P2 70	0.62		7.53	7.51	-				
P3 0	14.57	0.25	8.07	7.51	0.8	99.7	4.3	128	78
P3 5	7.94	0.87	8.50	7.82	-				
P3 10	5.96		8.65	8.03	0.2	116.0	3.7	140	83
P3 15	2.16	0.52	8.85	8.06	-				
P3 20	0.73	0.39	8.44	8.16	0.1	11.8	2.9	30	39
P3 25	1.29		8.92	7.89	-				
P3 30	0.59	0.32	9.00	8.16	0.1	3.8	3.0	23	16
P3 35	0.41	0.28	8.88	-	-				
P3 40	1.05	0.40	8.83	7.91	0.0	3.0	4.6	33	9
P3 45	0.85		8.04	7.74	-				
P3 50	0.72		8.72	7.56	0.1	3.2	3.5	26	12
P3 55	0.58	0.12	8.90	7.61	-				
P3 60	1.20		8.67	7.96	0.1	7.3	3.1	28	26
P3 65	0.71	0.31	9.03	7.69	-				
P3 70	-		8.97	7.77	-				

Sample	carb [%]	s.d.	pH_{H2O}	pH_{KCl}	R.w.	S méq /
P4 0	4.63	0.81	7.99	7.34	-	76.2
P4 5	12.65	0.12	7.82	7.67	-	137.3
P4 10	6.57	1.07	8.11	7.67	-	
P4 15	2.05		8.00	7.68	-	
P4 20	1.83	0.41	8.15	7.43	0.1	18.9
P4 25	1.21		8.46	7.56	-	10.6
P4 30	1.10	0.30	8.84	7.24	-	21.6
P4 35	1.50		8.74	8.24	-	15.0
P4 40	1.39		8.07	7.65	0.1	1.5
P4 45	1.24		8.28	7.80	-	1.0
P4 50	1.09		8.54	7.65	-	
P4 55	0.73		7.89	7.40	-	
P4 60	0.50		8.43	7.41	0.1	0.0
P4 65	1.24		8.09	7.51	-	0.0
L2 0-8	5.44	0.03	8.85	7.61	0.4	68.7
L2 8-15	3.78		8.50	7.49	-	61.2
L2 15-27	0.87		8.22	7.05	0.3	10.2
PC1 0.00	2.58	0.69	6.73	6.23	0.4	
PC1 0.005	3.33		-	-	-	
PC1 0.01	2.74	0.50	7.00	6.60	-	
PC1 0.02	2.81		7.12	6.63	-	
PC1 0.10	2.12	0.70	6.84	6.24	0.4	
PC1 0.15	3.18		-	-	-	
PC1 0.20	2.73		6.94	6.33	-	
PC1 0.25	-		-	-	-	
PC1 0.30	2.69	1.07	6.85	6.24	0.3	
PC1 0.35	2.77		-	-	-	
PC1 0.40	2.42		6.73	6.12	-	
PC1 0.45	1.74		-	-	-	
PC1 0.50	3.48		6.70	6.04	-	
PC1 0.55	2.52		-	-	-	
PC1 0.60	2.45		6.75	6.02	0.3	
PC1 0.65	2.99		-	-	-	
PC1 0.70	3.42		6.69	5.94	-	
PC2 0.00	2.88	0.71	6.03	5.16	-	
PC2 0.05	3.33	0.17	6.58	6.25	-	
PC2 0.10	3.34		6.66	6.08	0.3	
PC2 0.20	2.36		7.41	-	-	
PC2 0.30	2.78		6.76	5.94	0.3	
PC2 0.40	-		-	6.04	-	
PC2 0.50	2.43		6.78	6.00	-	
PC2 0.60	2.76		.	5.88	0.5	
PC2 0.70	2.16		6.22	6.17	-	

Annex 12. ICP-MS results of bedrock and soils (values are in ppb).

Samples	Ca	Mg	K	Na	Li	Be	Al	Sc	Ti	V	Cr	Mn	Fe	Co	Ni	Cu	Zn
Granitoid	2'574'023	7'243'159	39'610			2'667	160'953		1'987	828'722	94	3'910'970	8'851'418	158'245	16'191	13	38'229
F3 Hs	248'006	208'343	1'548		43'201	4'667	41'124		162	197'431	155	690'596	2'805'027	25'477	5'311	15	8'046
F3 A1	160'450	389'903	548'618	0	3'004	0	3'609'052	1'084	163'030	13'140	27'917	87'587	5'943'615	2'379	5'081	4'493	10'627
F3 A2	193'337	224'104	1'629		43'401	2'667	34'347		200	170'645	142	814'899	2'607'149	32'628	5'074	17	6'773
F3 A4	73'919	659'524	951'538	43'577	6'443	0	5'449'887	129	28'880	30'202	57'806	173'992	13'636'048	5'523	10'599	9'531	22'487
L2 0-8	18'034'049	1'362'685	1'125'646	0	540	631	16'338'923	3'672	91'548	48'929	24'406	329'892	21'743'226	4'727	7'758	13'030	25'149
L2 8-15	6'792'160	359'623	1'527		30'400	2'000	101'032		798	393'837	59	2'097'532	6'201'408	42'855	6'018	33	17'910
L2 15-27	1'650'949	379'149	2'356		79'602	6'667	231'720		1'255	880'779	171	2'804'234	13'115'097	66'287	10'415	61	22'455
P1 0	10'040'902	1'374'021	1'530'608	820	4'475	196	4'707'634	40	17'851	23'717	45'073	189'167	11'208'845	4'527	11'012	11'589	47'264
P1 5	3'608'992	967'205	1'080'685	1'947	5'071	535	5'998'918	106	22'682	30'339	54'360	203'200	14'270'867	5'215	11'153	11'439	45'212
P1 10	7'857'784	1'037'342	1'115'443	4'355	6'707	306	6'345'893	125	24'368	32'148	61'080	230'460	14'492'704	5'782	18'898	13'362	42'363
P1 20	4'751'755	743'323	777'222	0	3'779	360	4'253'254	90	20'005	25'750	44'401	174'027	12'102'193	4'721	9'718	10'290	29'951
P1 30	2'207'919	740'156	933'461	11'074	5'677	269	5'504'999	148	25'983	32'168	49'757	192'579	13'409'441	6'641	10'943	11'954	19'852
P1 40	1'186'068	608'141	802'411	0	4'819	282	5'140'039	111	24'650	31'284	50'283	174'062	13'466'481	5'481	10'765	11'354	15'612
P1 60	2'133'475	1'183'716	1'497'699	12'738	10'489	459	10'764'602	339	37'031	48'698	86'824	210'151	22'709'229	8'545	20'452	18'545	31'839
P2 0	6'384'397	1'310'490	1'150'315	0	316	388	3'903'276	1'500	146'094	28'534	52'587	173'685	12'893'943	3'863	6'660	11'312	42'264
P2 5	2'413'191	771'306	858'543	4'788	5'614	395	5'597'023	110	21'318	26'843	56'432	189'257	11'771'951	5'521	12'426	13'016	35'977
P2 10	2'305'392	723'649	771'286	266	4'343	193	4'838'990	84	19'881	26'583	39'704	176'624	12'383'758	4'105	10'056	10'576	27'760
P2 15	2'034'675	784'099	718'502	0	1'804	418	4'291'248	1'305	155'518	25'263	48'344	173'684	11'684'958	4'167	8'714	8'860	30'494
P2 20	2'567'990	988'785	955'655	0	3'798	132	5'850'734	2'342	188'064	27'691	45'528	235'838	13'006'816	7'484	10'601	11'069	35'020
P2 30	1'100'897	537'799	603'976	0	3'418	0	4'226'192	122	19'464	27'591	52'868	159'822	12'435'967	4'739	9'581	13'431	23'663
P2 40	788'141	570'559	696'322	7'216	3'548	188	4'338'934	76	20'952	28'029	45'000	193'292	12'393'023	5'636	8'383	9'898	23'450
P2 50	981'633	563'778	614'722	8'651	3'742	201	3'391'468	56	18'682	26'599	39'537	167'962	12'013'504	4'806	8'191	12'042	19'897
P2 60	2'658'746	1'307'744	1'531'271	8'286	10'453	425	8'413'936	375	33'578	43'314	71'564	259'552	20'235'362	10'278	21'963	19'165	33'848
P2 70	1'017'129	827'062	901'235	7'470	6'142	393	6'038'298	179	27'348	40'096	70'896	200'415	17'624'659	8'011	16'302	13'560	29'962
P3 0	36'827'728	3'841'065	1'399'016	3'374	4'057	0	3'652'290	21	18'713	16'614	26'124	276'693	8'842'846	5'781	8'054	9'974	49'044
P3 20	1'896'518	776'744	815'269	89'385	3'350	289	3'937'008	19	19'696	24'170	50'188	155'570	11'325'521	5'164	8'478	8'398	20'722
P3 30	1'266'963	548'993	682'532	0	2'165	116	2'093'855	0	13'770	17'778	31'613	153'290	8'158'828	4'273	6'045	7'784	16'826
P3 40	545'920	438'341	672'483	0	2'766	112	3'504'847	0	19'563	27'096	43'311	165'358	11'459'166	5'228	7'915	6'935	16'646
P3 50	416'647	529'931	885'614	0	3'208	421	4'014'712	67	22'046	26'268	37'680	171'834	11'671'165	5'156	8'028	8'337	16'401
P3 60	1'195'499	576'183	796'263	54'431	2'400	101	2'701'571	0	16'327	23'124	34'713	144'298	9'856'872	4'542	7'179	7'397	20'915
P4 0	18'451'936	1'416'530	868'028	0	2'265	408	3'679'351	1'174	139'083	19'786	28'177	159'739	9'129'254	3'422	8'575	9'809	48'357
P4 10	18'237'345	1'083'340	737'328	0	2'980	101	3'475'939	34	17'834	20'831	34'430	158'474	10'108'450	4'150	8'157	9'743	34'190
P4 20	4'547'810	598'977	634'001	0	3'212	0	3'493'542	9	16'449	22'124	30'558	138'781	9'958'718	4'339	8'711	8'718	13'434
P4 20	2'778'805	452'898	2'534		70'402	1'333	55'084		374	248'279	103	1'060'646	3'849'614	53'758	9'143	30	11'727
P4 30	4'538'324	689'585	969'224	0	3'550	212	3'749'054	0	17'644	22'632	25'818	148'321	9'782'500	4'032	7'589	8'799	16'513
P4 40	2'305'172	545'694	676'913	22'102	2'305	309	2'980'455	39	17'624	22'012	36'132	121'607	9'574'846	3'325	5'611	7'190	17'153
P4 50	1'187'933	593'459	824'234	41'655	4'828	194	5'529'212	129	26'137	30'832	38'499	180'408	13'779'370	8'344	9'162	9'932	25'853
P4 50 a	735'389	437'097	3'005		83'202	4'667	60'674		608	333'122	117	1'433'486	4'982'106	103'630	10'864	27	10'500
P4 50 b	696'049	395'382	2'760		83'602	667	60'642		485	307'404	107	1'322'518	4'649'391	93'750	10'238	29	9'909
PC1 0.00	11'174'669	6'499'842	2'184'624	2'311'186	5'079	0	22'290'571	3'347	659'345	58'278	6'645	450'271	16'382'889	10'284	11'331	41'058	44'088
PC1 0.01	10'684'234	6'753'135	2'551'257	2'425'130	5'314	431	22'335'240	3'556	666'468	57'832	6'714	521'987	16'660'452	10'671	13'556	44'322	55'005
PC1 0.015	13'861'211	7'069'773	2'361'237	2'884'208	5'208	545	23'634'266	3'217	651'325	58'437	6'677	422'464	16'461'705	10'561	11'367	42'323	46'245
PC1 0.02	12'462'831	6'945'616	2'781'773	3'006'336	5'927	267	25'302'196	3'482	783'099	70'930	7'252	479'245	18'654'056	10'806	12'688	46'031	64'103
PC1 0.10	11'338'556	5'594'739	2'070'866	2'279'925	7'554	253	24'956'903	3'709	736'036	60'012	7'425	359'393	18'069'860	9'144	12'653	41'725	37'703
PC1 0.20	12'827'091	5'180'465	2'226'573	2'778'739	6'135	257	26'178'270	3'916	832'510	69'148	7'693	318'047	19'095'536	9'583	10'748	36'675	44'528
PC1 0.30	12'754'029	5'498'971	2'514'224	2'968'970	7'728	755	29'176'343	4'458	976'690	76'168	8'240	377'923	21'830'520	10'197	11'322	45'456	42'070
PC1 0.40	11'549'131	5'033'496	2'234'209	2'476'022	7'753	519	27'762'822	4'209	929'344	73'405	7'745	376'552	20'648'629	9'753	9'397	40'766	49'384
PC1 0.50	12'722'015	5'572'982	2'391'844	2'875'754	8'382	546	30'927'190	4'366	1'124'803	88'579	9'782	409'107	24'087'987	10'871	11'785	44'521	55'544
PC1 0.60	11'088'142	4'527'272	2'180'392	2'381'844	7'024	465	26'793'224	4'362	894'060	74'265	8'658	401'274	20'658'918	10'518	10'981	45'557	47'917
PC1 0.70	11'111'517	4'852'607	2'435'653	2'855'569	8'346	977	27'666'309	4'322	934'121	77'024	9'731	439'057	21'986'275	11'148	11'815	47'794	47'605
PC2 0.60	9'173'032	4'574'949	2'468'764	3'182'628	10'208	412	26'298'058	5'263	839'634	67'777	9'911	514'626	21'768'517	11'608	11'851	60'881	47'260

Annex 12. Continued. ICP-MS results of bedrock and soils (values are in ppb).

Samples	Ga	As	Br	Rb	Sr	Mo	Ag	Cd	In
Granitoid	473'278	2		237'613	125'907	0	1'116	0	
F3 Hs	100'204	1		25'519	22'661	1	10'200	0	
F3 A1	1'630	294	0	9'987	3'521	0	0	0	3
F3 A2	86'203	1		27'965	14'018	1	2'603	0	
F3 A4	3'338	0	42'435	19'651	4'029	110	128	0	0
L2 0-8	7'709	504	0	10'840	230'407	0	347	0	15
L2 8-15	291'830	3		21'969	414'703	0	2'600	0	
L2 15-27	555'483	6		33'187	39'462	1	5'000	0	
P1 0	2'962	132	42'980	12'804	450'402	375	17	0	0
P1 5	3'489	192	34'015	15'235	146'763	314	28	0	19
P1 10	4'058	550	45'059	15'945	175'881	182	71	11	0
P1 20	2'627	121	45'800	13'459	96'910	166	109	0	0
P1 30	3'417	161	42'946	17'024	43'221	171	171	0	4
P1 40	3'124	591	39'102	16'403	22'967	167	9	0	8
P1 60	6'046	620	40'537	26'830	26'617	311	88	0	0
P2 0	2'483	0	0	11'845	234'493	0	249	0	12
P2 5	3'072	222	45'573	15'051	93'171	218	455	0	0
P2 10	2'849	434	39'942	13'696	94'821	179	8	0	0
P2 15	2'174	409	0	11'815	61'440	270	118	0	5
P2 20	3'319	486	0	15'446	81'424	0	205	0	7
P2 30	2'854	421	37'467	12'784	34'183	229	227	0	2
P2 40	2'993	254	45'295	15'628	27'831	251	718	0	0
P2 50	2'560	498	46'430	14'810	21'133	385	292	0	0

Annex 13. Cations and anions from sampled waters analysed with ICP-MS. Water samples in Burkina Faso (E) were collected in November 2005. The following samples have been analysed by ICP-MS:

- Sample E1: water from a well 25 m deep located 1 km east from the *M. excelsa* site.
- Sample E2: water from a well located in the Farakorosso village, about 1 km far from the *M. excelsa* forest. The water is pumped at 102 m deep in the granitic layer.
- Sample E3: water from a well 100 m deep located near Sirakorosso village.
- Sample E4: water from a backwater located near Diomanidougou.
- Rainwater from Salina was collected in April 2006.

Note: the nitrate quantities present in two samples (E2 and E3) exceed the values accepted for potable water (Mellet and Guinkot 2009). High values of chlorine, sulphate, and nitrate detected in Salina rainwater are due to the sea influence

Sample	Na	K	Mg	Ca	Cl	SO_4^-	NO_3^-
				ppm			
E1	11.45	5.35	16.59	28.23	0.03	0.26	-
E2	24.86	2.27	2.72	23.56	12.70	1.28	68.36
E3	14.77	4.54	5.99	28.54	1.29	3.25	16.74
E4	10.00	1.92	1.34	4.29	0.05	0.12	-
Salina rain water	7.76	1.31	2.12	5.81	10.69	5.85	3.57
Water on a cactus	10.63	7.74	3.68	19.14	18.15	17.82	11.81

Annex 14. Carbonate content under a living and an old stump of *Milicia excelsa* tree

Calculation of the carbonate content present in the soil under the foliar crown of a living *Milicia excelsa* tree is presented here. The carbon present in the soil associated with a *M. excelsa* tree cut 18 years ago is calculated in the same manner. The two trunks have the same diameter (0.9 m) at 1 m height from the ground.

Carbonate content under a living *M. excelsa* tree (P4 profile

Soil samples were taken at 4.5 m from the trunk, each 5 cm from the soil surface (0 cm) to 60 cm deep. The percentage of carbonate measured each 5 cm in the fraction < 2 mm is given in Annex Table 14.1. Under the tree foliar crown the carbonate is present in a cylinder of radius 9 m (foliar crown projection; Fig. 14.1) to a depth of 60 cm for a total volume of 152.7 m^3. If we consider a density of 2.4 g/cm^3 for the soil, the amount of carbonate present in this volume is of about 8040 kg (52.7 kg/m^3).

Sample	Fraction		Total (g)		carb	% carb /
	< 2mm (g)	> 2mm (g)			[%]	fraction < 2mm
P1 0	108.77	12.44	121.21	q	3.72	4.05
P1 5	112.94	10.94	123.88	0.50	1.46	1.65
P1 10	117.38	11.35	128.73	0.51	2.47	2.90
P1 15	158.24	18.36	176.60	0.71	1.82	2.87
P1 20	149.65	21.92	171.57	0.69	1.58	2.37
P1 25	134.37	21.62	155.99	0.62	2.24	3.02
P1 30	173.29	38.81	212.10	0.85	1.32	2.29
P1 35	159.47	17.55	177.02	0.71	1.43	2.28
P1 40	157.13	38.66	195.79	0.78	1.12	1.76
P1 45	122.98	30.75	153.73	0.61	0.91	1.12
P1 50	105.35	27.57	132.92	0.53	1.07	1.13
P1 55	101.55	41.76	143.31	0.57	1.19	1.20
P1 60	88.29	77.05	165.34	0.66	1.36	1.20
	sum	sum	sum		mean	sum
	1689.41	368.78	2058.19		1.67	**27.85**
P3 0	76.53	4.66	81.19		14.57	11.15
P3 5	140.54	14.91	155.45		7.94	11.16
P3 10	156.43	15.80	172.23		5.96	9.33
P3 15	125.71	26.46	152.17		2.16	2.72
P3 20	153.05	31.70	184.75		0.73	1.12
P3 25	146.92	41.03	187.95		1.29	1.89
P3 30	142.22	35.81	178.03		0.59	0.84
P3 35	167.39	41.80	209.19		0.41	0.69
P3 40	154.42	40.90	195.32		1.05	1.63
P3 45	116.42	24.31	140.73		0.85	0.99
P3 50	146.50	45.19	191.69		0.72	1.06
P3 55	128.86	25.60	154.46		0.58	0.75
P3 60	111.46	37.70	149.16		1.20	1.34
	sum	sum	sum		mean	sum
	1766.45	385.87	2152.32		2.93	**44.67**
L2 0-8	53.35	13.80	67.15		5.40	2.88
L2 8-15	62.96	5.32	68.28		3.80	2.39
L215-27	63.35	24.32	87.67		0.90	0.57
	sum	sum	sum		mean	sum
	179.66	**43.44**	**223.10**		3.37	1.95

Sample name	Fraction		Total (g)	carb	% carb /
	< 2mm (g)	> 2mm (g)		[%]	fraction < 2mm
P2 0	171.83	16.81	188.64	1.97	3.39
P2 5	133.61	19.38	152.99	1.53	2.04
P2 10	140.55	12.40	152.95	2.08	2.92
P2 15	143.12	22.18	165.30	1.15	1.65
P2 20	160.98	13.34	174.32	1.00	1.61
P2 25	154.18	26.40	180.58	0.80	1.24
P2 30	170.18	22.90	193.08	0.81	1.37
P2 35	135.85	23.44	159.29	0.90	1.23
P2 40	161.49	33.43	194.92	1.25	2.01
P2 45	139.96	41.07	181.03	1.43	2.00
P2 50	160.30	29.19	189.49	0.48	0.76
P2 55	122.87	39.71	162.58	1.37	1.68
P2 60	99.18	39.39	138.57	1.57	1.56
	sum	sum	sum	mean	sum
	1894.10	339.64	2233.74	1.26	**23.47**
P4 0	120.18	3.54	123.72	4.63	5.57
P4 5	133.79	7.90	141.69	12.65	16.93
P4 10	139.06	12.43	151.49	6.57	9.14
P4 15	172.58	17.44	190.02	2.05	3.54
P4 20	169.74	20.31	190.05	1.83	3.11
P4 25	164.07	19.77	183.84	1.21	1.99
P4 30	152.96	12.26	165.22	1.10	1.68
P4 35	147.96	18.66	166.62	1.50	2.21
P4 40	118.17	84.40	202.57	1.39	1.65
P4 45	121.39	85.85	207.24	1.24	1.51
P4 50	43.39	109.53	152.92	1.09	0.47
P4 55	39.15	134.58	173.73	0.73	0.28
P4 60	33.18	116.10	149.28	0.50	0.16
	sum	sum	sum	mean	sum
	1555.62	642.77	2198.39	2.81	**48.25**

Table 14.1- Results of two size fractions of soils and their carbonate content found at 4.5 m from the trunk of a living M. excelsa *tree (P4 soil), under an old stump of* M. excelsa *tree (P3 soil), at 2m from P3 (P2 soil), and at 3.4 m from P3 (P2 soil).*

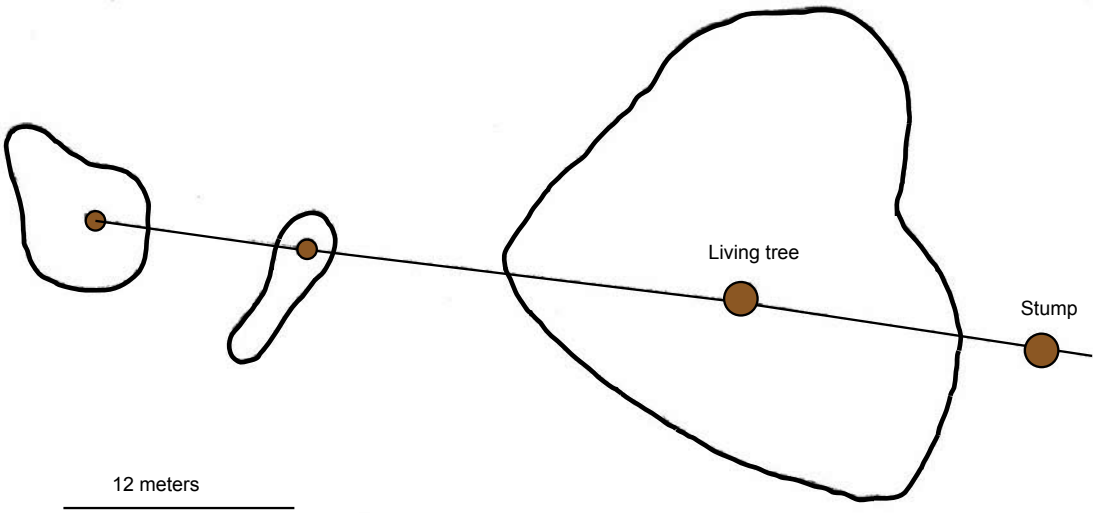


Fig. 14.1- Foliar crow projection of the living M. excelsa *trees and stump from Njanmango.*

Carbonate under a *M. excelsa* and an *A. africana* stump

In this case, the total cylinder is composed of three parts, *A* with the related profile P1, *B* with the related profile P2, and *C* with the related profile P3 (Fig. 14.2). This subdivision is performed because we get 3 profiles at different distance from the stump: P3 under the trunk, P2 at 2 m from the trunk, and P1 at 3.4 m from the trunk. Results of sieving and carbonate titration in the different layers and profiles are presented in Table 14.1.

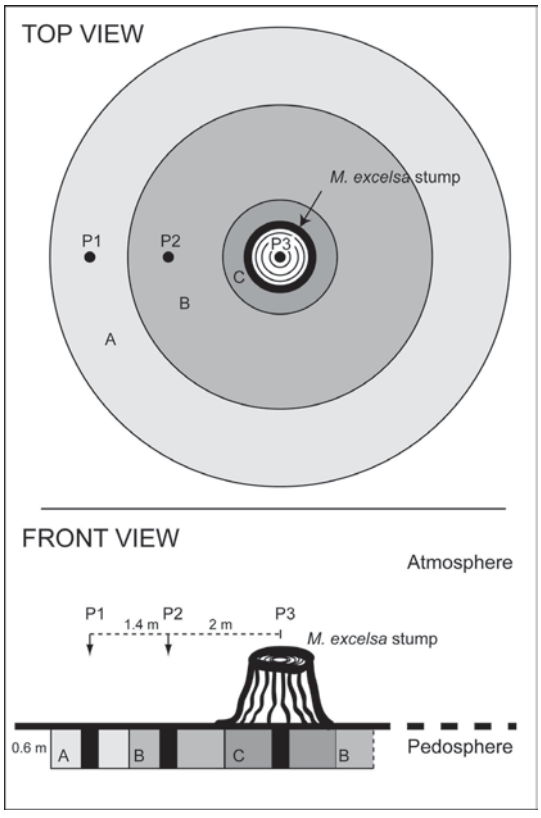


Fig. 14.2- Top view and front view from the 3 cylinders (A, B, and C) as considerate for the calculation of carbonate content in the soil surrounding a M. excelsa *stump.*

The cylinders A, B and C have a volume of 17.9 m^3, 11.9 m^3, and 1.9 m^3 respectively. The total carbonate calculated in a volume of 31.7 m^3 is about 975 kg (30.8 kg/m^3).

Under the *A. africana* stump, the carbonate content is measured in the middle of the first three horizons. The taken volume is 0.85 m^3 (1 m x 1 m x 27 cm) and the carbonate distribution is considered as homogeneous. It results under the stump a carbonate accumulation of 17.7 kg, 20.9 kg of carbonate/m^3 of soil.

Annex 15. Calculation of the total carbon present in the litter of *M. excelsa* (See Fig. 7.5)
From this study result that:

		TOC	Oxalate [%]	Carbonate	TOTAL C
M. excelsa	Leaves	33.73	0.09	0.00	33.76
	Wood			24.01	2.88
P4 profile	Soil between 0 and 10 cm	2.04	2.73E-03	7.95	2.99
	Soil between 10 and 60 cm	0.47	7.60E-05	1.26	0.63
A. africana	Leaves	39.78	0.28	0.00	39.86
	Wood	31.38	0.02	20.50	33.84

Devineau (1982) calculated that in a *Celtis* forest in Lamto (Ivory Coast), with *M. excelsa* trees, in 1980 th (Pauwels et al. 1992)e litter was composed of (t/ha):

Petioles	Leaves	Bark	Fruit	Wood	TOTAL	
4.76	0.18	0.92	0.01	0.07	5.94	t/ha
80.13	3.03	15.49	0.17	1.18		%

In this study the analyses have been made on the whole leaves: petioles and leaves. To have an order of magnitude of the total organic carbon (TOC) and the oxalate present in the wood of *M. excelsa* tree, there are taken the quantities measured in the *A. africana* wood. Cailleau (2005) observed that oxalate is present in bark but not carbonate. The oxalate amount present in the bark is considered the same than thus measured in the wood. In contrast oxalate and carbonate are present in wood tissues. Assuming that the litter under the *M. excelsa* tree is constituted of 100 % of *M. excelsa* products it results that the litter contains:

	TOC	Oxalate	Carbonate	
Leaves + petioles	1.81580	0.00917	0.00000	
Bark	0.28868	0.00014	0.00000	
Wood	0.28868	0.00001	0.01558	
TOTAL [t/ha]	2.39315	0.00932	0.01558	
				TOTAL C [t/ha]
TOTAL CARBON	2.39315	0.00249	0.00187	2.40

Paper project 1

Carbon dynamics in a tropical soil influenced by *M. excelsa* oxalogenic tree

Abstract

An oxalogenic tree constitutes a powerful system able to catch and immobilize atmospheric CO_2 in soils for several hundred years. Conversion of atmospheric CO_2 into calcium carbonate results from bacterial oxalate consumption that transforms rapidly oxalic acid into carbonic acid. As calcium comes from silicate weathering, the carbonate accumulation can be considered as a net carbon sink. This accumulation is so important that in systems older than 100 years, the soil can be partly cemented and carbonate blocks can form. In order to evaluate and quantify the carbon budget of such a system in southern Burkina Faso, trees and soil profiles have been studied using Rock-Eval technique, oxalate enzymatic digestion, and carbonate titration. The resulting carbon budget shows that the system composed of *Milicia excelsa* (Moraceae) oxalogenic tree and its associated soil is able to accumulate more than 60 % of carbon than conventional tropical soils described in the literature. The aim of this paper is (1) to describe the carbon dynamics in a soil influenced by the *M. excelsa* tree, (2) to evaluate the carbon budget, and (3) to show that the carbonate stock has a residence time of several hundred years. This study demonstrates that the carbon balance in a soil related to a *M. excelsa* tree is still positive in terms of trapping. The Burkina Faso soil can be subdivided into two dynamic compartments, regulated by two different processes: the accumulation in the first 10 cm and the diffusion between 10 and 60 cm. The total carbon stock present under an about 70 year-old oxalogenic tree is 60% more important than those estimated for tropical soils (forest, savannas, and grassland soils). Moreover, the residence time of the carbonate stock in *M. excelsa* system is in the order of magnitude of a millennium of years, therefore representing a non-negligible C-stock.

1. Introduction

The importance of carbonate accumulation in soils surrounding the tropical oxalogenic tree *M. excelsa* has already been highlighted (Braissant et al. 2004; Cailleau et al. 2004; Cailleau 2005; Cailleau et al. 2005). Indeed, these authors found that this oxalogenic tree-soil system runs like a pump, driving carbon from the atmosphere to the hydrosphere through the pedosphere and, therefore, inscribes it in the global carbon cycle. In the global carbon cycle, the major pools are (Table 1): the ocean, carbonate rocks, terrestrial ecosystems, and the atmosphere (Trumbore 1997; Eswaran et al. 2000; Amundson 2001; IPCC 2001; Prentice et al. 2001; Janzen 2004; Lal 2004; Rasmussen 2006; Dart et al. 2007; Brovkin et al. 2008). Inland organic carbon is present in living phytomass, necromass, and soil organic matter (Golubyatnikov and Svirezhev 2008), whereas carbon in living vegetation is estimated at 466 PgC (Lal 2004) to 610 PgC (Schimel 1995).

Reservoirs	Amount in billions of metric tons (Pg of C)
Marine sediments and sedimentary rocks	66'000'000 to 100'000'000
Ocean	38'000 to 39'000
Fossil fuel reserves and combustible	27'000
Soil organic matter to 1m depth	1500 to 2000
Soil inorganic carbon	930 to 1738
Soil carbonate	940
Atmosphere	750 to 785 as CO_2
Terrestrial plants	470 to 660
Biota	400 to 600
Ocean biomass	3

Table 1.1- Estimated major reservoirs of carbon on the Earth.

Accumulation of carbon in soils varies with soil depth and latitude (climate). At a depth of 1 m, it contains about 1500 - 2000 PgC in various organic forms, from recent plant litter to charcoal and very old humified compounds (Amundson 2001; Prentice et al. 2001). Soil layers deeper than 1 m contain several hundreds of PgC in the form of peat in Northern ecosystems and organic carbon in moist tropical forest soils (Trumbore 1997). Additionally, about 950 PgC are stored in inorganic (carbonate) form, predominantly in dry lands (Eswaran et al. 2000; Lal 2004). Soil carbonate is the major form of soil inorganic carbon (SIC). SIC forms an estimated reservoir ranging from 930 PgC to 1738 PgC (Rasmussen 2006), surpassing the atmospheric reservoir (Lal 2004). The ability of pedogenic carbonate to sequester atmospheric C depends on the source of calcium (Ca) present during carbonate pedogenesis (Kraimer et al. 2005). A net carbon sink is a system where the carbonate accumulation involves only atmospheric CO_2 and Ca from Ca-carbonate-free sources (Cailleau et al. 2004).

A missing carbon sink results from global carbon budget estimations (Schimel 1995; Prentice et al. 2001; Houghton 2002; Janzen 2004; Lal 2004) and is suspected to be present in terrestrial ecosystems ("residual terrestrial sink"). It is evaluated at ± 3 PgC / y (Schimel 1995; Houghton 2002). In terms of fluxes, the residual terrestrial sink has been evaluated as 1.9 ± 1.3 PgC / y during the 80's and 2.3 ± 1.3 PgC / y during the 90's (Retallack 1990; Prentice et al. 2001).

Carbon of soil organic matter (SOM) has a turnover time going from a second (e.g. it is rapidly consumed when released as sugars or root exudates) to several hundred years (as stable or recalcitrant substances; Trumbore 1997; Prentice et al. 2001; Seneviratne 2003; Lal 2004). In contrast, soil inorganic carbon has potentially a residence time of 1'000'000 years (Retallack 1990; Prentice et al. 2001), which makes interesting the serach of a system forming rapidly carbonate and able to maintain this carbonate accumulation during many years. Carbonate precipitation can occur according to abiotic or biotic processes (Lowenstam and Weiner 1989; Sposito 1994; Callot 1999; Castanier et al. 1999; Andersen 2002; Verrecchia 2002; Verrecchia et al. 2006; Dupraz et al. 2009). In studied soils, the main involved process related to carbonate precipitation is the oxalotrophy. Oxalic acid and oxalate salts are widely distributed in the Plant kingdom and are a common metabolic product of fungi, algae, and lichens (Gadd 1999). They are found in some bacterial culture as well (Hodgkinson 1977). Despite plants and microorganisms release these acids continuously in soils, oxalate concentrations range from 10^{-6} to 10^{-3} M (Allison et al. 1995; Khan 1995), and are rare in the geological record (Graustein et al. 1977). Although these acids account for a small fraction of the total dissolved organic carbon, they play an important role in soil genesis, plant physiology, and microorganism metabolism (Graustein et al. 1977; Hue et al. 1986; Pohlmann and McColl 1988; Albuzio and Ferrari 1989).

Ca-oxalate is energetically stable (Kps = $4*10^{-9}$ M^2 in water at pH 7.0). The only known sub-spontaneous diagenetic evolution of Ca-oxalate is a possible transformation of weddellite into whewellite by dehydration (Verrecchia et al. 2006) and solely the activation energy given by bacterial consumption transforms oxalate into carbonic acid (Verrecchia et al. 2006). Bacterial oxalate consumption (oxalotrophy) is performed by oxalotrophic aerobic and anaerobic bacteria (Verrecchia et al. 2006). Heterotrophic bacteria transform oxalate into carbonic acid following this equation, currently named the oxalate - carbonate pathway:

$$1000\ \mathbf{CaC_2O_4}\cdot nH_2O + 372\ O_2 + 32\ NH_4^+ \rightarrow 32\ C_4H_8O_2N^+_{biomass} + 936\ \mathbf{CaCO_3} + 64\ Ca(OH)_{2aq} + ...+ (1000 \cdot (n-2) + 1872)\ H_2O + 936\ CO_2$$

This pathway increases pH values of the soil solution. If the pH reaches carbonate stability conditions (*i.e.* pH > 8.4) and divalent cations (Ca^{2+} or Mg^{2+}) available in the soil solution, complexation with carbonic acid results in carbonate precipitation.

In this study, it is demonstrated that a system composed of an oxalogenic tree and its related soil is an efficient natural

engine to form a long-term carbon sink. For the first time, a carbon budget is proposed for a "Ferralic Calcisol (Arenic)" (according to the WRB classification) formed under a *M. excelsa* tree in southern Burkina Faso.

2. Material and methods

Material: leaves, wood, and soils samples (see thesis).
An oxalogenic tree and its related tropical soil environment constitute the studied model. The main site is located in southern Burkina Faso, in the wooded savannah with a Sudanian trend. The annual rain precipitation is 1300 mm/year. The P4 profile is a soil related to a living 70 year-old *M. excelsa* tree and is situated under its foliar crown, at 4 m distance from the trunk. The P3 soil profile is right under the *M. excelsa* stump. The reference profile is about 30 m from the tree and out of any of its potential influence. In this place, the vegetation is dominated by grass
Sampling: see thesis.
Methods: Rock-Eval technique, oxalate enzymatic digestion, and carbonate titration are the main methods used to quantify the carbon present in organic, oxalate, and carbonate phases, respectively.
Rock-Eval, oxalate enzymatic digestion, and carbonate titration (see thesis). But also: grain size distribution, pH-meter, and thin sections (see thesis).
Fungi: Fungi manipulation and fungi isolation (see thesis).

3. Results and discussion

3.1 Distribution of oxalate, carbonate, and pH in soils and trees

Results on pH, total organic carbon (TOC), oxalate (ox), and carbonate content in the soil influenced by a *M. excelsa* tree (P4 and P3) and a soil out of the tree influence (F3) are present in Table 2. Soil out of *M. excelsa* oxalogenic tree influence is a "Plinthic Ferralsol (Arenic") (WRB classification). This soil profile is acidic, with very low organic carbon content (< 0.5 %). The oxalate amount does not exceed 4 ‰ and there is no carbonate. This soil results from thousands of years of tropical pedogenesis. In contrast, under the *M. excelsa* tree, soils properties are completely different, except for the grain size distribution that remains as sandy. As expected, soil organic carbon contents are higher under the tree influence. In addition, the pH is clearly alkaline and pedogenic carbonates are observed: this is unusual and unexpected on granitoid basements in such climatic conditions. This alkaline pH results from the oxalate consumption, which transforms a strong acid (oxalic acid) in a weak acid (carbonic acid). Moreover, release of OH^- ions, as a result of bacterial oxalate metabolism, contributes to pH increase (Quayle et al. 1961; Quayle 1961,1963; Blackmore and Quayle 1970; Chandra and Shethna 1975; Hodgkinson 1977; Tamer and Aragno 1980; Braissant et al. 2002; Sahin 2003).

Using Rock-Eval pyrolysis, it has been found that, in Burkina Faso soils, the total organic carbon (TOC) does not exceed 3% of the total soil mass and is present in six different hydrocarbonaceous compounds. These carbon pools are present until 60 cm of depth. At a depth of 10 cm, the bio-molecule signal decreases and the geo-molecule signal becomes dominant, suggesting that, with increasing depth, the carbon stock is characterized by oxygenated material rather than hydrocarbonaceous compounds.

Sample	Horizon	pH_{H2O}	TOC [%]	carb [%]	s.d.	ox [‰]	s. d.
P3 0	(OL)A	8.1	7.21	14.57	0.25	64.1	
P3 5	(OL)A	8.5	2.36	7.94	0.87	19.8	5.6
P3 10	Ak	8.7	1.13	5.96		74.3	
P3 15	Ak	8.9	0.60	2.16	0.52	47.3	
P3 20	Ak	8.4	0.30	0.73	0.39	37.2	
P3 20	Ak		0.52				
P3 25	Bck1	8.9	0.38	1.29		42.1	
P3 30	Bck1	9.0	0.65	0.59	0.32	82.9	
P3 35	Bck1	8.9	0.44	0.41	0.28		
P3 40	Bck1	8.8	0.28	1.05	0.40	6.7	
P3 40	Bck1		0.29				
P3 45	Bck2	8.0	0.22	0.85			
P3 50	Bck2	8.7	0.31	0.72		0.0	
P3 50	Bck2		0.42				
P3 55	Bck2	8.9	0.59	0.58	0.12		
P3 60	Bck2	8.7	0.39	1.20		43.4	
P3 65	C1	9.0	0.22	0.71	0.31		
		9.0		-			
P4 0	(OL)A	8.0	2.94	4.63	0.81	47.2	
P4 0	(OL)A		3.09				
P4 5	Ak	7.8	1.84	12.65	0.12	13.3	
P4 10	Ak	8.1	1.26	6.57	1.07	21.3	2.4
P4 15	Ak	8.0	0.81	2.05		2.3	
P4 20	Bck1	8.2	0.73	1.83	0.41	2.0	0.8
P4 25	Bck1	8.5	0.64	1.21		2.1	
P4 30	Bck1	8.8	0.82	1.10	0.30	7.8	
P4 35	Bck1	8.7	0.56	1.50			
P4 40	Bck1	8.1	0.38	1.39		0.3	
P4 45	Bck2	8.3	0.33	1.24			
P4 50	Bck2	8.5	0.21	1.09		0.0	
P4 50	Bck2		0.20				
P4 55	C1	7.9	0.13	0.73			
P4 55	C1		0.15				
P4 60	C1	8.4	0.14	0.50		1.5	
P4 60	C1		0.18				
P4 65	C1	8.1	0.17	1.24			
P4 65	C1		0.14				
F3 Hs	A	5.8	0.43	0.00		4.3	
F3 A1	Bc1	5.7	0.24	0.00			
F3 A1	Bc1		0.24				
F3 A2	Bc2	6.2	0.20	-		2.1	
F3 A2	Bc2		0.15				
F3 A3	Bcd	5.9	0.18	-		1.0	
F3 A3	Bcd		0.13				
F3 A4	C1	5.7	0.14	-			
F3 A5	C2		0.13			1.1	
F3 A5	C2	5.4	0.10	0.00			
M. excelsa wood				24.01			
M. excelsa dried leaves			34			933.4	

Table 2- pH, total organic carbon (TOC), carbonate (carb), and oxalate (ox) values. P3: soil under a M. excelsa *stump, P4: soil under a living* M. excelsa *tree, and F3: reference soil ("Plinthic Ferralsols (Arenic)").*

Leaves of *Milicia excelsa* trees from southern Burkina Faso contain about 90 mg of oxalic acid/100 g of dry material. Furthermore, a second source of oxalate is present: oxalogenic fungi (Fig. 1). The fungal community is entirely composed of moulds (*Aspergillus sp.*, *Mucor sp.*, and *Fusarium sp.*). Oxalic acid is produced in large amounts by species belonging to all classes of Fungi (Dutton and Evans 1996). Ca-oxalate crystals are commonly associated with free-living, pathogenic, and plant symbiotic fungi.

This result confirms the fact that, in the studied soils, there is a flora, probably very rich and still underestimated, of fungi that secrete oxalic acid. Since only these two sources have been taken into account in the present work, it is important to mention that at least two other sources have not been measured, but only discussed: excretion of oxalic acid by plant roots and by bacteria. Being stable at atmospheric conditions, oxalate salts should accumulate in soils and be found in the geological record, or at least in old soils. The quantity of oxalate in soils, associated with oxalogenic trees, showed

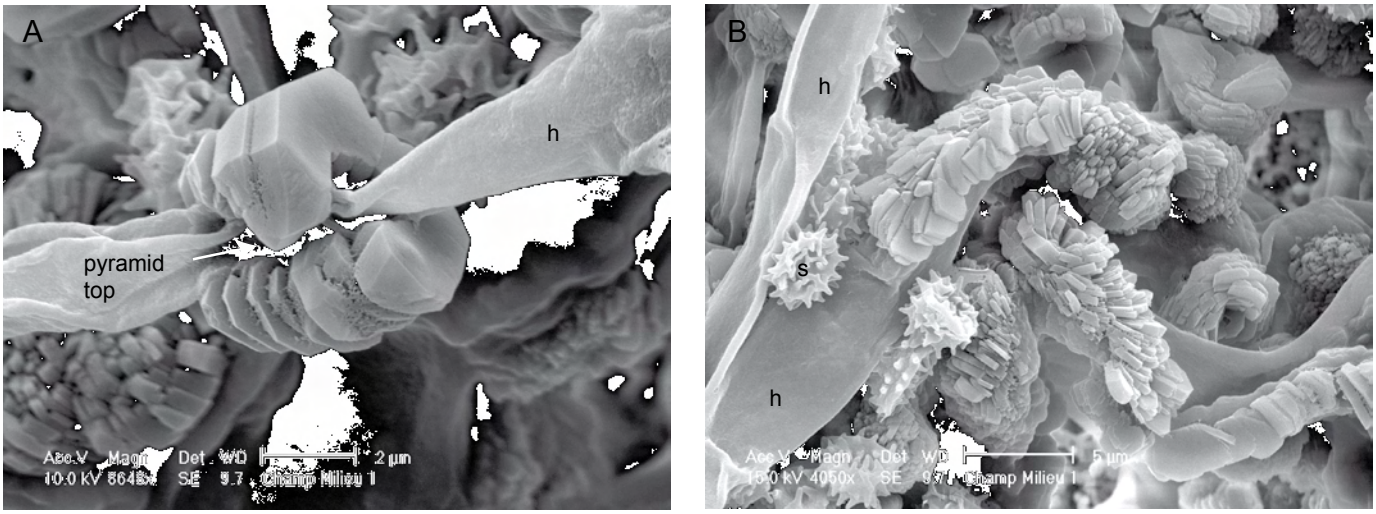


Fig. 1- Scanning electron microscope (SEM) micrographs of Ca-oxalate crystals associated with fungi.

that, even on the soil surface, the concentration of oxalate does not exceed a few ‰, i.e. 100 times less than in leaves, which must imply some oxalotrophic process. In addition, it has been demonstrated that oxalotrophic bacteria are well present in the studied soils (Khammar et al. 2009).

An indirect consequence of bacterial oxalotrophy is carbonate precipitation, which occurs not only in soil pores (Fig. 2), but can start from the litter as well, and probably already on the trunk. Because calcium comes from silicate weathering

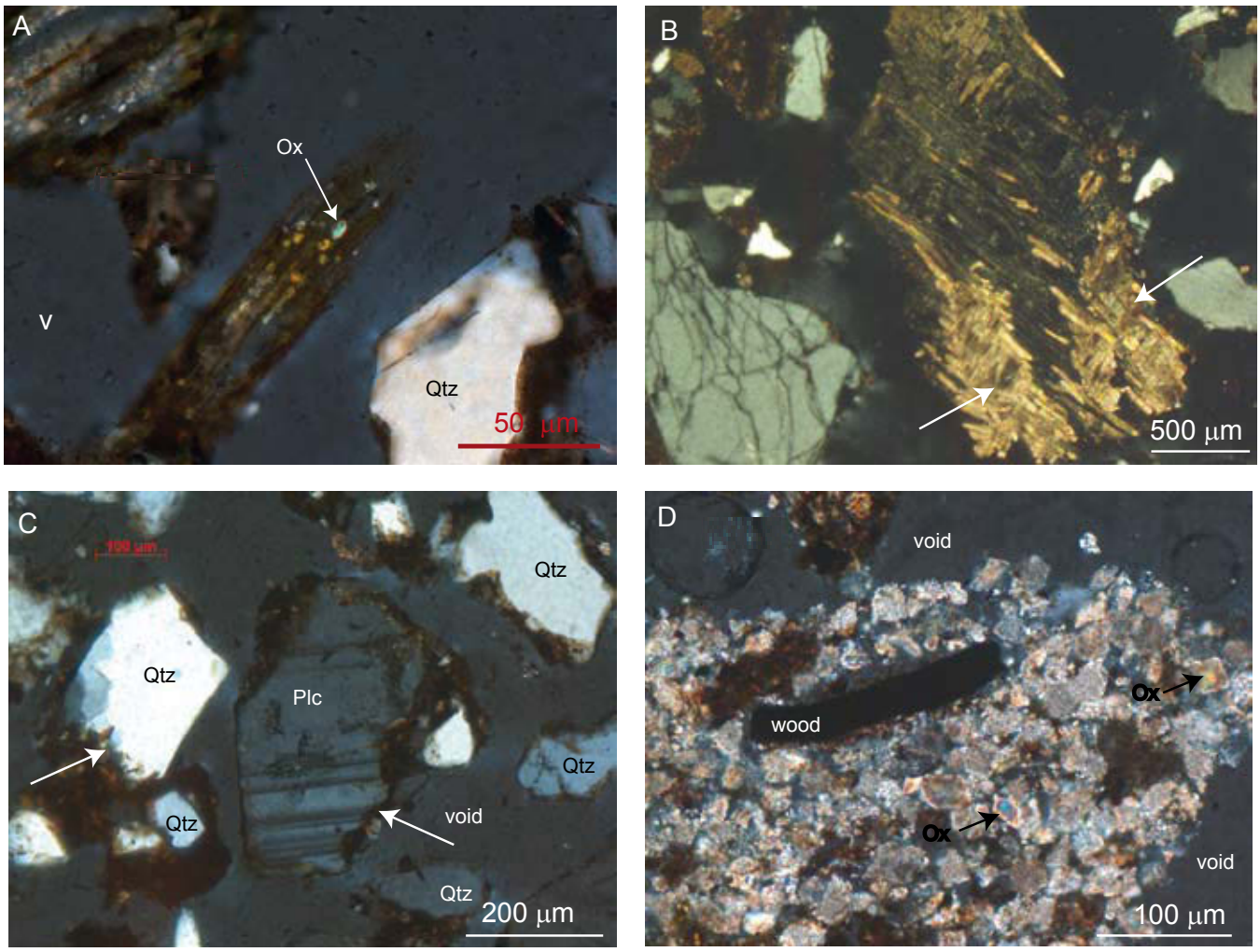


Fig. 2- Thin sections details under light microscopy. A) Ca-oxalate crystals (Ox) and B) calcite crystals observed in M. excelsa *wood tissues. C) Plagioclase crystals present in* M. excelsa *soil showing corrosion gulfs. D) Oxalate and carbonate crystals present at 5 cm under a living* M. excelsa *tree.*

(Fig. 2), dust, and rain, pedogenic carbonate is considered to act as a carbon sink. In Burkina Faso, under a 70 year-old tree, the carbonate content reaches a maximum of 15% of the soil mass and, as opposite to older ecosystems (Ivory Coast, Cameroon, and Uganda) no carbonate blocks have been found. The main factors that maintain and improve the carbonate accumulation are the age of the tree, the alternation of dry and rainy periods, and the availability of calcium.

3.2 Distribution of carbon forms in Burkina Faso and Ivory Coast ecosystems

A carbon balance of the studied ecosystem is calculated in order to show the potential of a tropical tree-soil system to pump carbon dioxide from the atmosphere to the soil and to demonstrate its ability to form a long-term carbon sink. This system is similar, but non-equal, to those studied by Cailleau (2005) in Ivory Coast (Fig. 3). The main differences are the ages of the trees (70 years vs. 170 years), the state of the tree (living tree vs. stump), and the dynamics of the oxalate-carbonate pathway itself. In Burkina Faso ecosystems, the TOC diminishes drastically from the initial surface until 15 cm in depth. After this limit, however, the values become constant. This distribution is regulated by the tree litter fall. Oxalate and carbonate are present from the soil surface. Oxalate is present in leaves, and once on the soil surface, the carbonate is formed as a result of the microbial oxalate oxidation. In the litter, plant and fungal oxalates are mixed. At 5 cm in depth, a positive carbonate peak and a negative oxalate peak is observed and could indicate an optimum of oxalate consumption (Fig. 3). The maximal carbonate precipitation is therefore located in the very first soil centimeters, just under the soil surface. A further oxalate peak can be observed at 10 cm in depth, where the influence of fungal, root exudates, and root degradation is not negligible. Finally, a TOC and an oxalate peaks are also observed at 30 cm in depth. These two peaks can be explained by either the presence of tree roots, which actively release oxalic acid, by root senescence, or by biodegraded roots, releasing passively oxalate salts.

In comparison, the distribution of carbon under an hollow stump of *M. excelsa* in Ivory Coast (Cailleau 2005) is slightly different. The plant organic matter that contains oxalate is the wood (more recalcitrant material than leaves) and the oxalate release rate is, in this case, determined by termite activity (stump degradation). In this ecosystem, termites are essential for oxalate release from wood tissues to the soil environment. In addition, saprophytic fungi improve oxalate availability, by both their wood degradation and oxalate production. The maximum carbonate accumulation is, as in Burkina Faso soils, located in the second horizon (the organo-mineral layer). There is also an oxalate peak concomitant

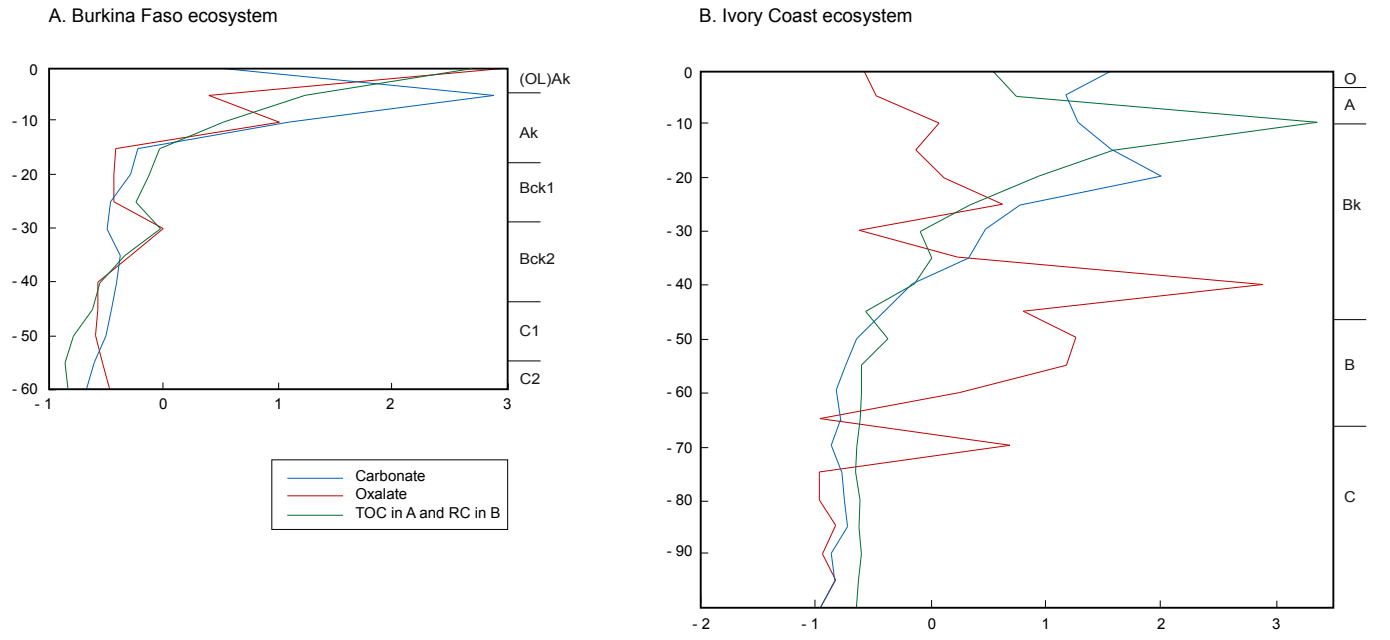


Fig. 3- Distribution of total organic carbon (TOC) Burkina Faso (A) and residual carbon (RC) Ivory Coast (B; Cailleau 2005), carbon in oxalate form and carbon in carbonate form in the soil related to a M. excelsa *tree. Values are standardized. The Burkina Faso* M. excelsa *tree is a living tree, having an estimated age of about 70 years, whereas the Ivory Coast* M. excelsa *tree is the stump of a 170 year-old tree.*

to this carbonate peak. The author explains the presence of these oxalate and carbonate peaks by a release of oxalate present in the OM and by the bacterial oxalogenic activity that results in carbonate ion formation and precipitation. Additionally, since saprophytic fungi are present, the release of carbonate present in wood is increased as well. In Burkina Faso, similarly as in Ivory Coast, there is a peak of oxalate at a depth of 40 cm and another one at 70 cm, both probably caused by root exudations.

Burkina Faso and Ivory Coast are two similar systems but at two different maturity steps. In Burkina Faso the system is young, with a process regulated by a carbon flux starting from the foliar crown and ending at the soil surface, whereas in Ivory Coast, the system is old regulated by diffusion processes, probably being much less sensitive to the foliar crown input. The Burkina Faso soil can be subdivided into two dynamic compartments, regulated by two different processes: the accumulation in the first 10 cm and the di fusion between 10 and 60 cm.

3.3 The Burkina Faso reservoir capacity

It is assumed that no carbon is present in the layer between 60 cm and 1 m in order to compare the carbon stock with values found in the literature (Table 3; Prentice et al. 2001).

		Global C stock (g/m^3)	
	Biome	**Plants**	**Soil**
	Wetlands	4286	64286
	Boreal forests	6423	34380
	Temperate grasslands and scrub lands	720	23600
	Tundra	632	12737
	Tropical forest	**12045**	**12273**
	Tropical savannas and grasslands	**2933**	**11733**
	Temperate forests	**5673**	**9615**
	Croplands	188	8000
	Deserts and semi-deserts	176	4198

	Under an oxalogenic tree		C g/m^3
C-organic	in the first 10 cm		**15270**
	from 10 to 60 cm		2804
	from 65 to 100 cm		0
C-oxalate	in the first 10 cm		**29**
	from 10 to 60 cm		2
	from 65 to 100 cm		0
C-carbonate	in the first 10 cm		**5062**
	from 10 to 60 cm		797
	from 65 to 100 cm		0
	Total C in the first 10 cm		**20361**
	Total C from 15 to 60 cm		**3604**
	Total C from 65 to 100 cm		**0**
			kg/m3
	In wood	TOC = 37.9%	246.35
	wood density = 650 kg/m3	C-carbonate = 9.8 %	63.61
		C-oxalate = 0.015 %	0.10
		Total C in wood	**310**

Table 3- Estimates of soil organic carbon pools found in literature (Prentice 2001) compared to those calculated under a living M. excelsa *tree from Burkina Faso.*

In Burkina Faso, the largest carbon accumulation is located at the soil surface, where 85% of the carbon is present (Fig. 4). These results show that the total carbon stock present under an about 70 year-old oxalogenic tree is 60% more important than those estimated for tropical soils (forest, savannas, and grassland soils). Consequently, the studied ecosystem forms carbon stocks that are comparable to the ones of the temperate grasslands and shrub lands.

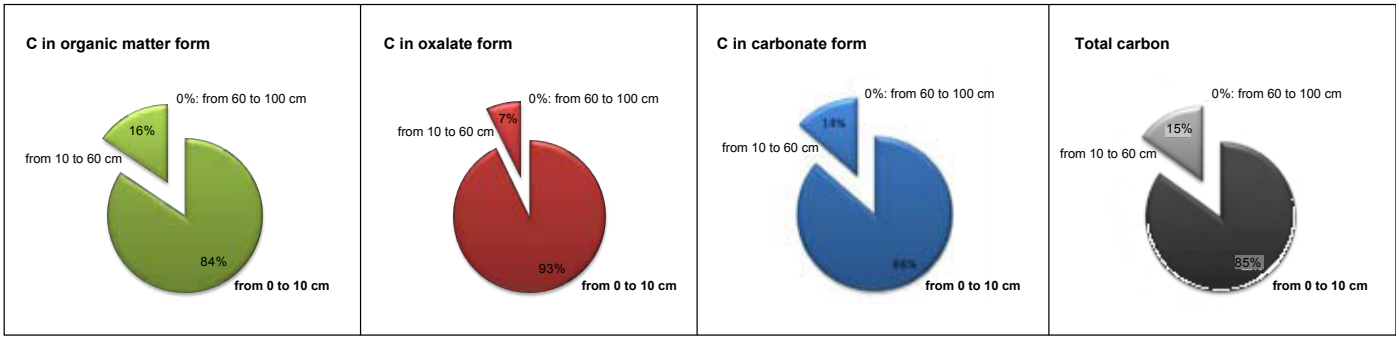


Fig. 4- Amounts of carbon forms present in the 3 soil layers under a living M. excelsa *tree from Burkina Faso.*

A model can be proposed with the former results, completed by means of additional literature data. Carbon reservoir capacities and residence times in Burkina Faso ecosystems can be estimated (Fig. 5). The *M. excelsa* tree and its related soil are divided into the following reservoirs: atmosphere (infinite pool), leaves, wood, and soil. The latter is composed of three functional layers: from 0 to 10 cm in depth, from 10 to 60 cm, and from 60 to 100 cm. Compared to the preindustrial era, the concentration of CO_2 in the atmosphere increased about 25%, from 280 to more than 370 ppm (Janzen 2004). Residence time of a CO_2 molecule in the air is fixed at 5 years. Photosynthesis captures atmospheric CO_2

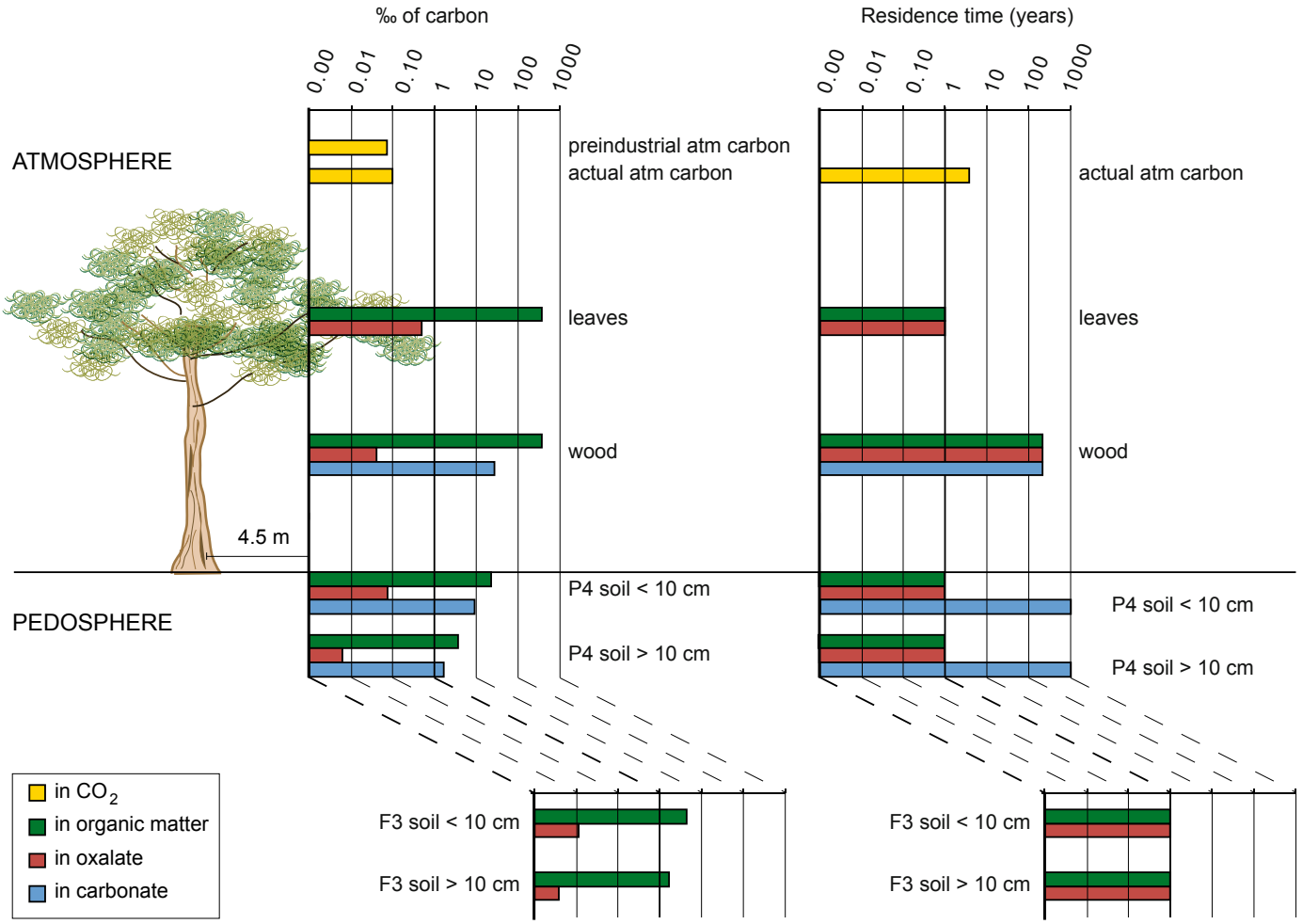


Fig. 5- Carbon stock and residence times in the studied M. excelsa *tree ecosystem.*

into leaves. TOC constitutes about 40% of leaves and wood tissues (Table 2). The *M. excelsa* tree is a deciduous African tree. The maximal litter fall occur during May (Devineau 1982), so the residence time of TOC in leaves is never longer than one year. Oxalate crystals carried by leaves reach the soil, providing a new oxalate contribution every year. Branches and wood represent a C-organic stock with a residence time that can be at the maximum in the order of magnitude of the tree age. Although the maximum lifetime of a *M. excelsa* tree is unknown, trees of about 250 years are frequently cited or studied in the Central African Republic (Durrieu De Madron 2003). Oxalate and carbonate are also present in wood tissues (Fig. 2). This carbonate does not result from *in situ* bacterial oxalotrophy, but is likely the result of carbonate ion root uptake from the soil, followed by a precipitation in wood tissues (Cailleau 2005). Normally, *M. excelsa* stumps remain in place after the tree is cut, as a result of deforestation and wood trade. Their biodegradation is difficult, due to the intrinsic properties of lignin and the high carbonate content of wood, which makes it practically impenetrable to normal chainsaws. Nevertheless, termites are able to grind *M. excelsa* stumps, allowing the release of oxalate and carbonate into the soil environment. The residence time of carbon stock present in wood is difficult to estimate, but it is admitted that it can reach an order of magnitude of centuries. On the contrary, litter is rapidly degraded by soil fauna in tropical environments, so C-oxalate stock is quickly consumed by oxalotrophic organisms. Since the oxalate is rapidly degraded, its quantity present in the soil at a given time, is extremely low, representing a very poor stock of carbon (< ‰). In fact, despite the annual aerial litter fall on the topsoil, the TOC and the oxalate salts do not accumulate. This implies a consumption of this carbon byproduct (mineralization) and a powerful oxalate oxidation. According to the calculations and estimation made in the former paragraph, the residence time of the carbonate stock in *M. excelsa* system is in the order of magnitude of a millennium of years, therefore representing a non-negligible C-stock.

3.4 A carbon flux estimatio

An oxalate-carbonate pump efficienc , or the carbon flux from litter to hydrosphere, can be approximated (Fig. 6). TOC, as well as carbon contents in oxalate and in carbonate, are given in a paragraph above. Rates of litter fall are taken from

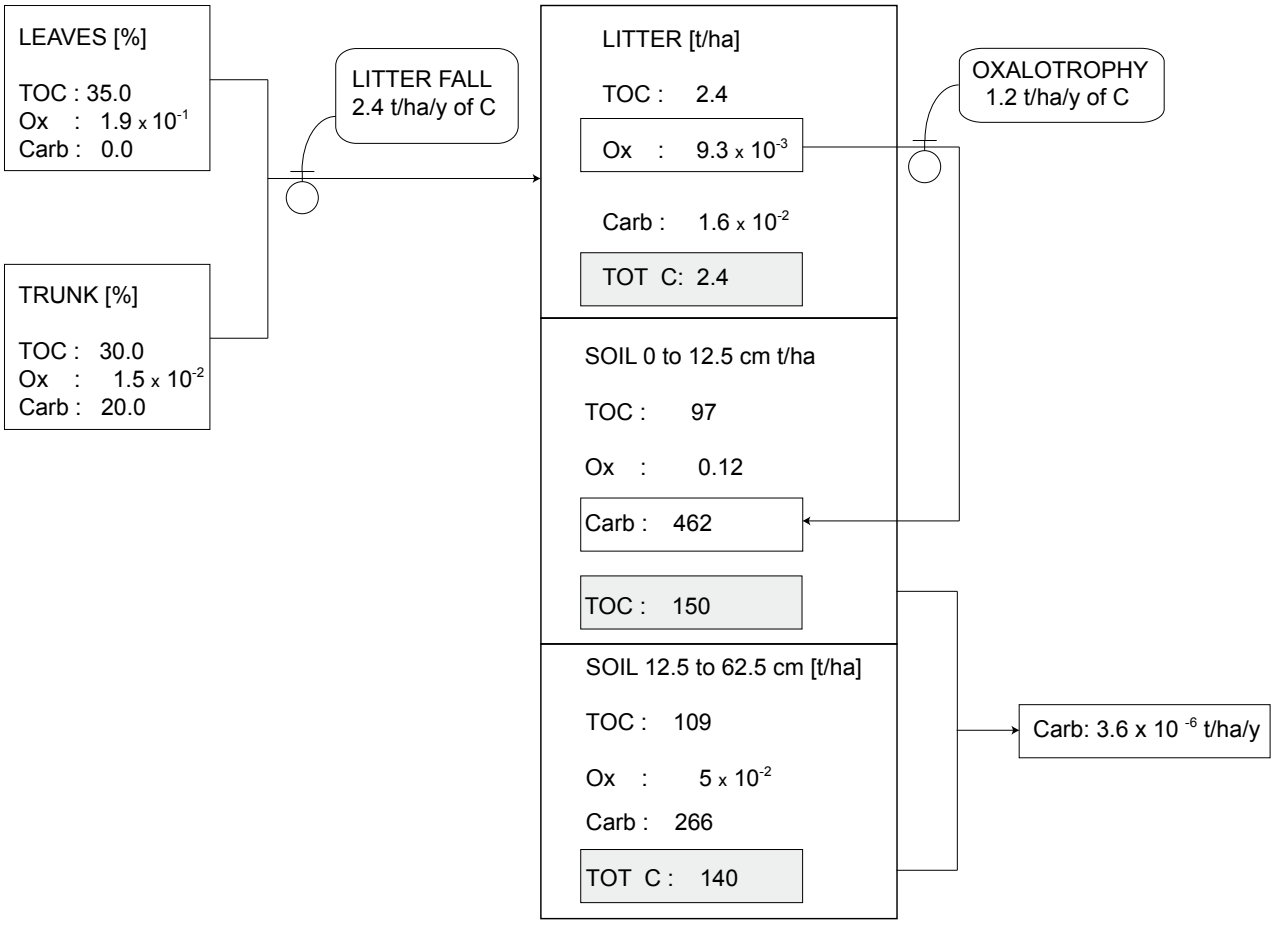


Fig. 6- Carbon fluxes in the studied M. excelsa *tree ecosystem. Only calculated fluxes a e shown.*

literature (Devineau 1982). From the oxalate metabolism equation (see above), it results that, for every 200 molecules of carbon present in the oxalate salt, 93.6 are transformed into calcite and 93.6 are released as CO_2 (Verrecchia et al. 2006). Consequently, the carbonate production derived from litter oxalate can be calculated. In each stage of this pathway, there is a carbon loss in CO_2 form (organic matter mineralization). However, in spite of this loss, the carbon balance is still positive in terms of trapping.

4. Conclusions

Results of this study, together with works presented by Cailleau (2005), Braissant (2005), and Khammar et al. (2009), have considerably enhanced our knowledge about the oxalate-carbonate pathway. This pathway is presently known to be able to induce the formation of an important mineral carbon (and calcium) stock in tropical soils. Calcium carbonate formation in tropical soil is a natural, rapid, powerful, and widespread process allowing a long-term carbon stock in soils. Moreover, the presence of carbonate in a soil normally depleted in basic cation can improve soil fertility by increasing pH and alkaline cation accumulation.

Burkina Faso *M. excelsa* studied trees, with their related soils, is a young system with a process regulated by a carbon flux going from the foliar crown to the soil surface, whereas in Ivory Coast, the system is old and regulated by a diffusion process. Moreover, the Burkina Faso soil can be subdivided into two dynamical compartments, regulated by two different processes: the accumulation in the first 10 cm and the diffusion between 10 and 60 cm. Residence time of the carbonate stock in *M. excelsa* system is in the order of magnitude of a millennium of years, therefore representing a non-negligible C-stock.

References

Albuzio A, Ferrari G (1989). Modulation of the molecular size of humic sub-stances by organic acids of the root exudates. Plant Soil 113 (2):237-241.

Allison MJ, Daniel SL, Cornick NA (1995). Oxalate degrading bacteria. In: Calcium oxalate in biological systems. Khan R (ed), pp 131-168. CRC Press, Boca Raton, FL.

Amundson R (2001). The carbon budget in soils. Ann Rev Earth Pl Sc 29:535-562.

Andersen CB (2002). Understanding carbonate equilibria by measuring alkalinity in experimental and natural systems. J. Geosci Education 50:389-403.

Blackmore MA, Quayle JR (1970). Microbial growth on oxalate by a route not involving glyoxylate carboligase. Biochem J 118:53-59.

Braissant O, Cailleau G, Aragno M, Verrecchia EP (2004). Biologically induced mineralization in the tree Milicia excelsa (Moraceae): its causes and consequences to the environment. Geobiology 2 (1):59-66.

Braissant O, Verrecchia EP, Aragno M (2002). Is the contribution of bacteria to terrestrial carbon budget greatly underestimated? Naturwissenschaften 89 (8):366-370.

Brovkin V, Cherkinsky A, Gorachkin S (2008). Estimating soil carbon turnover using radiocarbon data: a case study for European Russia. Ecol Model 216 (2):178-187.

Cailleau G (2005). Cycle du carbone et biominéralisation carbonatée en milieu continentale: la diagenèse des phases oxalate-carbonate. Université de Neuchâtel. 254 pp.

Cailleau G, Braissant O, Dupraz C, Aragno M, Verrecchia EP (2005). Biologically induced accumulations of $CaCO_3$ in orthox soils of Biga, Ivory Coast. Catena 59:1-17.

Cailleau G, Braissant O, Verrecchia EP (2004). Biomineralization in plants as a long-term carbon sink. Naturwissenschaften 91 (4):191-194.

Callot G (1999). La Truffe, la Terre, la Vie, INRA (Paris). 210 pp.

Castanier S, Le Métayer-Levrel G, Perthuisot J-P (1999). Ca-carbonates precipitation and limestone genesis - the

microbiogeologist point of view. Sediment Geol 126 (1-4):9-23.

Chandra T, Shethna Y (1975). Oxalate and formate metabolism in Alcaligenes and Pseudomonas species. Antonie van Leeuwenhoek 41 (1):465-477.

Dart RC, Barovich KM, Chittleborough DJ, Hill SM (2007). Calcium in regolith carbonates of central and Southern Australia: Its source and implications for the global carbon cycle. Palaeogeogr Palaeocl 249 (3-4):322-334.

Devineau JL (1982). Etude pondérale des litières d'arbre dans deux types de forêts tropophiles en Côte d'Ivoire. Ann Univ Abidjan, Série É (Écologie), tome XV:27-62.

Dupraz C, Reid RP, Braissant O, Decho AW, Norman RS, Visscher PT (2009). Processes of carbonate precipitation in modern microbial mats. Earth-Science Rev 96:141-162.

Durrieu De Madron L (2003). Accroissement diamétrique du bété et de l'iroko. Bois des forêts des tropiques 275 (1):83-87.

Eswaran H, Reich PF, Kimble JM, Beinroth FH, Padmanabhan E, Moncharoen P (2000). Global carbon stocks. pp 15-25. In: Global climate change and pedogenic carbonates. Lal R, Kimble JM, Eswaran H, and Stewart BA (eds), Lewis Publishers, Boca Raton, FL.

Gadd GM (1999). Fungal production of citric and oxalic acid: Importance in metal speciation, physiology and biogeochemical processes. Adv in Microb Physiol 41:47-92.

Golubyatnikov LL, Svirezhev YM (2008). Life-cycle model of terrestrial carbon exchange. Ecol Model 213 (2):202-208.

Graustein WC, Cromack KJ, Sollins P (1977). Calcium oxalate: occurrence in soils and effect on nutrient and geochemical cycles. Science 198:1252-1254.

Hodgkinson A (1977). Oxalic acid in biology and medicine. London. Academic Press. 325 pp.

Houghton RA (2002). Terrestrial carbon sinks-uncertain explanations. Biologist 49 (5):155-160.

Hue NV, Craddock GR, Adams F (1986). Effect of organic acids on aluminum toxicity in subsoils. Soil Sci Soc Am J 50 (1):28-34.

IPCC (2001). Climate Change 2001.

Janzen HH (2004). Carbon cycling in earth systems: A soil science perspective. Agricult Ecosys Environ 104 (3):399-417.

Khan SR (1995). Calcium oxalate in biological systems, edited by Saheed Khan, 400 pp.

Kraimer RA, Monger HC, Steiner RL (2005). Mineralogical distinctions of carbonates in desert soils. Soil Sci Soc Am J 69 (6):1773-1781.

Lal R (2004). Soil carbon sequestration impacts on global climate change and food security. Science 304 (5677):1623-1627.

Lowenstam HA, Weiner S (1989). On Biomineralization: Oxford University Press, New York, 324 pp.

Pohlmann AA, McColl JG (1988). Soluble organics from forest litter and their role in metal dissolution. Soil Sci Soc Am J 52 (1):265-271.

Prentice IC, Farquhar GD, Fasham MJR, Goulden ML, Heimann M, Jaramillo VJ, Kheshgi HS, Le Quéré C, Scholes RJ (2001). The Carbon Cycle and Atmospheric Carbon Dioxide. In: Climate Change 2001: The Scientific Basis. Contribution of Working Group I to the Third Assessment Report of the Intergovernmental Panel on Climate Change. [Houghton JT, Ding Y, Griggs DJ, Noguer M, van der Linden PJ, Dai X, Maskell K, and Johnson CA, (eds)]. Cambridge University Press, Cambridge, United Kingdom and New York, NY, USA, 881 pp.

Quayle J, Keech D, Taylor G (1961). Carbon assimilation by Pseudomonas oxalaticus (OXI). 4. Metabolism of oxalate in cell-free extracts of the organism grown on oxalate. Biochem J 78:225-236.

Quayle JR (1961). Metabolism of C, compounds in autotrophic and heterotrophic microorganisms. Annu Rev Microbiol 15:119-152.

Quayle JR (1963). Carbon assimilation by Pseudomonas oxalaticus (OX1). 6. Reactions of oxalyl-coenzyme A. Biochem J 87:368-373.

Rasmussen C (2006). Distribution of soil organic and inorganic carbon pools by biome and soil taxa in Arizona. Soil Sci

Soc Am J 70 (1):256-265.
Retallack GJ (1990). Soil of the past. An introduction to paleopedology. Unwin Hyman Ltd, London. 512 pp.
Sahin N (2003). Oxalotrophic bacteria. Res Microbiol 154 (6):399-407.
Schimel DS (1995). Terrestrial ecosystems and the carbon cycle; Global Change Biology, 1.77-91.
Sposito G (1994). Chemical equilibrium and kinetics in soils. New. York, Oxford University Press, 288 pp.
Tamer A, Aragno M (1980). Isolement, caractérisation et essai d'identification de bactéries capables d'utiliser l'oxalate comme seule source de carbone et d'énergie. Bull Soc Neuchâtel Sci Nat 103:91-104.
Trumbore SE (1997). Potential responses of soil organic carbon to global environmental change. Proc Natl Acad Sci USA 94 (16):8284-8291.
Verrecchia EP (2002). Géodynamique du carbonate de calcium à la surface des continents. In: Géopré E (ed) J.-C. Miskovsky (ed) Géologie de la Préhistoire: méthodes, techniques, applications. Paris, pp 233-258.
Verrecchia EP, Braissant O, Cailleau G, Aragno M (2006). The oxalate-carbonate pathway in soil carbon storage: the role of fungi and oxalotrophic bacteria. In: Fungi in biogeochemical cycles, Gadd GM (ed). Cambridge University Press. pp 289-310.

Paper project 2

How can calcium carbonate precipitate in West Africa acidic soils? Lessons from micromorphology of a "Ferralic Calcisol"

Abstract

In southern Burkina Faso (Niangoloko), thousands of years of pedogenesis have resulted in "Plinthic Ferralsols (Arenic)" (WRB classification). However, it is observed that under the influence of the oxalogenic tree *Milicia excelsa* (Moraceae), the soil evolves into a "Ferralic Calcisol (Arenic)" in less a millenium. It is proposed that the driving force of this carbonate accumulation is the bacterial oxalotrophy, which generates a carbonate reservoir in the soil. The aim of this paper is to study the various carbon forms and pathways in the soil horizons under a living *M. excelsa* tree of about 70 years old and under a *M. excelsa* stump from a tree of about the same age, and cut 18 years ago. The three main carbon forms present in the soil are: the organic matter, oxalate and carbonate crystals, as well as charcoal material. The use of micromorphology brings clues to the main processes involved in the formation of a long-term carbon stock as carbonate in African soils. If oxalotrophy takes place mainly in the first soil layers (organo-mineral horizons), dissolution and re-precipitation processes occur in deeper horizons, resulting in stable carbonate coatings on peds, forming a long-term oxidized carbon sink.

1. Introduction

1.1. Milicia excelsa *tree*

The *M. excelsa* tree (from Moraceae family) is a large forest tree, with an umbrella-shaped crown (Jansen 1974; Fig. 1). It can easily reach 47 m in height and more than 2.5 m in diameter (Ofori and Cobbinah 2007). The bark is thick and subject to sclerosis, with a dark brown to blackish scaly surface, displaying yellowish lenticels, while its roots are red. In local medicine, the tree is known for its properties (Jansen 1974), as many parts of it are used to heal human diseases (Ouinsavi et al. 2005). Moreover, the *M. excelsa* tree is used to preserve cultural values and it incarnates many divinities (Ouinsavi et al. 2005). Milicia species are deciduous (Devineau 1976) and dioic trees (Jansen 1974) and have long been considered as pioneers (Nichols et al. 1998; Bosu et al. 2006). They prefer well-drained soils, intense light exposition and dry zones (Ofori and Cobbinah 2007). The *M. excelsa*, although essentially a rain forest tree, extends also farther north, into the dried savannah, along stream galleries (Carozzi 1967). It is found starting from the sea level till altitudes of more than 4500 m a.s.l. in Tanzania. Moraceae are well known for their predisposition to siliceous and calcareous secretions (Carozzi 1967). The *M. excelsa* tree is among the most economically important hardwood species in tropical Africa (Bosu et al. 2006), and with a density of 655 kg/m3, it is a moderately hard timber and it is very durable (Carozzi 1967; Jansen 1974). For its over-exploitation, combined with its poor regeneration, the *M. excelsa* tree is currently under threat of extinction (Bosu et al. 2006). All attempts to grow Milicia species in plantations have generally failed due to the attack of gall-forming insects (Cobbinah and Wagner 1995; Ofori et al. 1996; Bosu et al. 2006; Ofori and Cobbinah 2007). Finally, Milicia trees are used as light-cover trees for plantations such as cacao and coffee in Sao Tomé and Príncipe (western equatorial coast of Central Africa(Carvalho et al. 2004).



Fig. 1- A Milicia excelsa *tree and leaves situated in the Mangodara village (South of Burkina Faso), near "Le Commissariat".*

1.2. Mineralization of Milicia excelsa *tree*

Mineralization of the *M. excelsa* tree (former *Chlorophora excelsa*, Harris 1933) has been studied since a long time. e.g. in Uganda (Campbell and Fisher 1932) and Ivory Coast (Carozzi 1967), for its biological interest as well as for its defects involved in timber trade (Carozzi 1967). Crystals in *M. excelsa* tree tissues are made of silica, carbonate, and oxalate.

Carbonate concretion locations in the tree and their nature were first studied in the aerial part of the plant (Harris 1933). First observations led to the conclusions that stones were formed by sap exudation. Calcium is present in the sap in the form of soluble calcium bicarbonate and, at the contact with the atmosphere, carbonate precipitates (following the stalactite principle; Harris 1933). The sap is the vector of the calcitic mineralisation in the bark, as was confirmed isotopically using δ13C (Cailleau 2005).

Tree mineralization takes place under different conditions. The contact with the atmosphere allows carbonate precipitation to take place (similarly to cave stalactite) as the tree can be wounded until the xylem zone (Harris 1933) in which sap contains up to 1.4 % dissolved carbonate. More recently, a theory suggested that wounds are exposed to bacterial contamination and allowing the oxalate-carbonate pathway to take place in the trunk (Braissant 2005). Recent observations in Bolivia (Alto Beni, Amazona) and India seem to confirm the presence of oxalotrophic bacteria on barks of oxalogenic trees. Another possible process involved could be supersaturation in vessels induced by water stress during the dry season (Cailleau 2005). This process leads to carbonate precipitation in wood as well as in roots tissues (Cailleau et al. 2005).

Amorphous silica was detected only in bark tissues of *M. excelsa* tree. It is present associated with oxalate crystals and is abundant in areas where phloem rays are abundant and tightened (Cailleau 2005).

Oxalate crystals in *M. excelsa* tree tissues were observed only recently. Oxalate (oxalic acid or the corresponding soluble and insoluble salts) is a photosynthetic by-product and is commonly found in plants where it can be present in all tissues (Arnott and Pautard 1970; Hodgkinson 1977; Franceschi and Horner 1980; Nakata 2003; Franceschi and Nakata 2005). The most important functions of oxalate present in plants include: 1) calcium regulation, 2) ion balance (Nakata 2003), 3) plant protection against grazing animals (Franceschi and Horner 1980; Franceschi 2001; Nakata 2003), 4) metal (Al, Pb, Sr, Cd, and Cu) or oxalic acid detoxification (Franceschi and Horner 1980; Nakata 2003), 5) storage form for either Ca or oxalate (Franceschi and Horner 1980), 6) tissue support (plant rigidity; Franceschi and Horner 1980; Nakata 2003), 7) light gathering and reflection (Franceschi 2001; Nakata 2003), and 8) combustion retardation (Prior and Cutler 1992).

In *M. excelsa* tissues, only Ca-oxalate monohydrate $Ca(C_2O_4)\cdot(H_2O)$ is observed (Cailleau 2005). In the bark, whewellite crystals are present in the parenchymal cells, sometimes trapped by amorphous silica, whereas in wood tissues, it is observed mainly in 1) small cells or small vessels located around major conducting vessels, 2) in the wood rays, and 3) in the parenchymal cells in the edge of the structures mentioned above. In wounded tree parts, oxalate crystals can present dissolution gulfs and can be found associated with carbonate crystals. Whewellite crystals were also observed in roots tissues (Cailleau 2005). In *M. excelsa* leaves, oxalic acid concentration can reach 900 ‰.

1.3. Carbonate in soils related to Milicia excelsa

Carbonate is also present in soils surrounding *M. excelsa* trees. Carbonate accumulation is so important that, in the root vicinity, carbonate blocks of a size reaching 1.5 m can be observed (Carozzi 1967; Cailleau 2005). These carbonate blocks are constituted of pure calcite (crypto- to microcrystalline) with remains of calco-alkaline granite basement and organic material. Near the roots and the lower part of the trunk, these carbonate concretions can be banded by zones of fibrous calcite. The origin of their formation is the same as proposed previously, i.e. abundant sap exudation infill ng soil pores and cementing the rhizosphere (Carozzi 1967). Recently, the presence of carbonate in acidic soils raises the question of the origin of the carbonate and its implication in the carbon cycle. The hypothesis that soil carbonate is generated by the oxalate-carbonate pathway has then been tested (Braissant et al. 2002; Braissant et al. 2003; Braissant et al. 2004; Cailleau et al. 2004; Cailleau 2005; Cailleau et al. 2005; Verrecchia et al. 2006), and confirmed. Oxalate salts are synthesized by *M. excelsa* and stored as a calcium salt. Release of oxalate in the soil during organic matter degradation, principally performed by saprophytic fungi, initiates the oxalate-carbonate pathway in the presence of oxalotrophic bacteria. Soil solution alkalinisation induced by bacterial oxalotrophy constitutes the starting point. If the pH increases up to 8.4 and, if calcium is present, carbonate precipitates in the soil pores. In contrast, if the pH is lower than 8.4, carbonate ions (CO_3^{2-}) present in the soil solution are pumped by roots in the same way as calcium or other nutrients, and enter in the xylem tissues or are leached out of the soil system. Therefore, generated by the oxalate-carbonate pathway, various carbonate features have been found in the soil associated with a secular *M. excelsa* tree in Ivory Coast (Cailleau et al. 2005). Biologically induced mineralisation in the *M. excelsa* system is observed as calcified wood microstructures such as parenchyma cells and cellulose fibres, different types of rhombohedra, needle fibre calcite, large blocks, micritic aggregates, and hemi-spherulites (Cailleau et al. 2005). Moreover, carbonate associated with *M. excelsa* can also be the product of oxalate combustion (Canti 2003) due to the burning usually applied in Africa for agricultural purposes.

2. Material and methods

Material: thin sections (see thesis).
Sampling: see thesis
Methods: Rock-Eval technique, oxalate enzymatic digestion, carbonate titration, pH, ICP-MS, and X-ray diffraction (see thesis).

3. Results and discussion

Total organic carbon (TOC), oxalate, carbonate, and pH values measured in soil profiles each 5 cm are given in Figure 2 for the living tree and the stump of *M. excelsa*. About 70% of theTOC are present in the first 10 cm: 2.34 ± 1.94% vs. 0.39 ± 0.26% deeper in the soil. Organic carbon features found in soils are wood remains and organic carbon forming peds (Figs. 3-5). This wood is high mineralized in oxalate and carbonate but amorphous silica can also be found (Cailleau 2005).

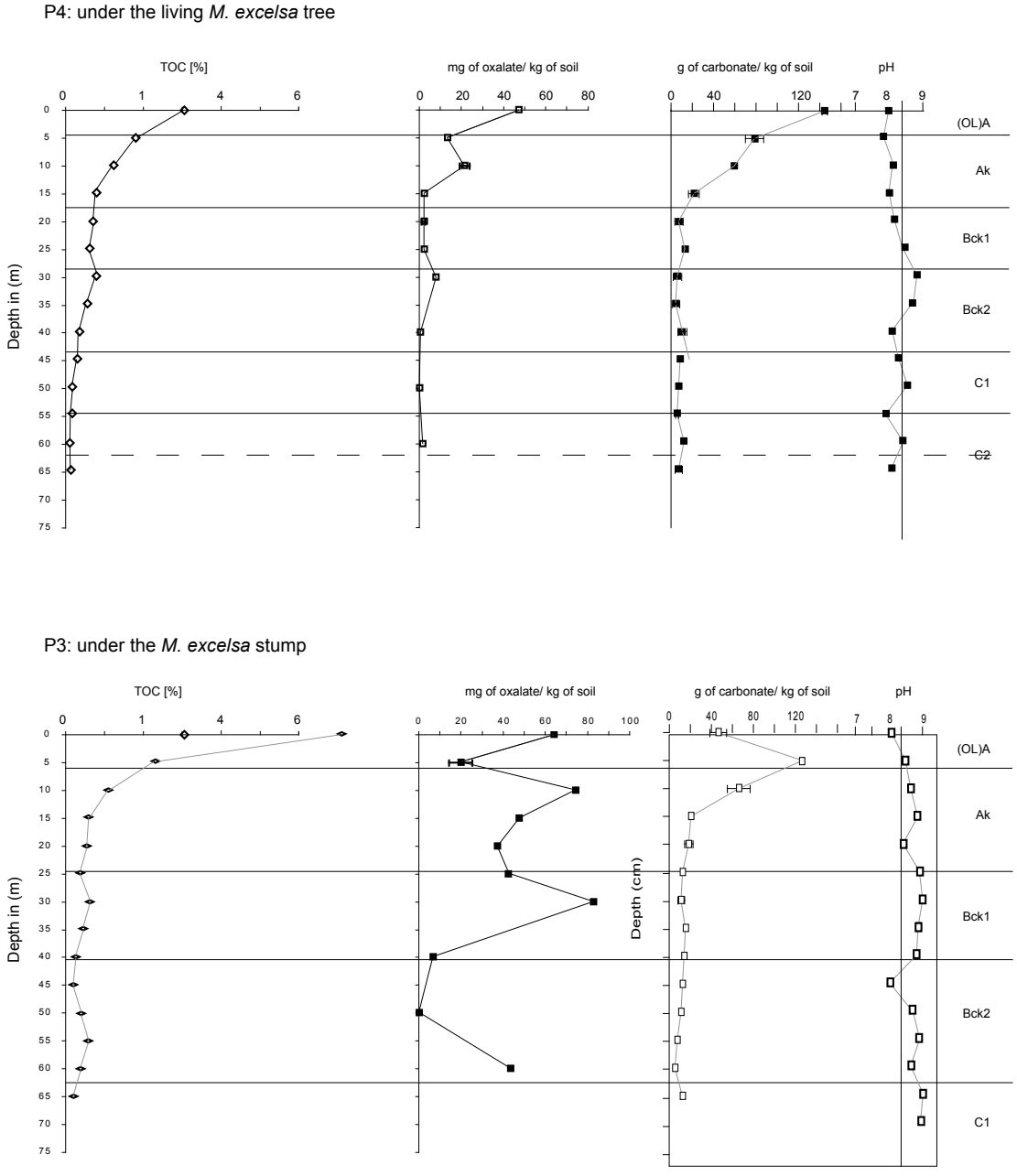


Fig. 2- Total organic carbon (TOC), oxalate, carbonate, and pH profiles in soils related to a living M. excelsa *tree (P4 profile) and a* M. excelsa *stump (P3 profile)*

Oxalate distribution under the living tree and the stump is not the same. Highest values are associated with the *M. excelsa* stump, where concentration can reach 83 mg of oxalate/kg of soil. In this soil profile, the oxalate amount varies irregularly with depth. In contrast, 80 % of the oxalate concentration is in the first 10 cm under the living *M. excelsa* tree (P4 profile). In the deeper layers, the concentration is constant and very low (± 2.3 mg of oxalate / kg of soil). The similarities between these two profiles consist in peaks present at the surface and 10 cm in depth. In these soils, Ca-oxalate crystals are observed (Fig. 3) 1) in plant material (wood and roots), 2) in soil peds, and 3) dispersed in soil pores.

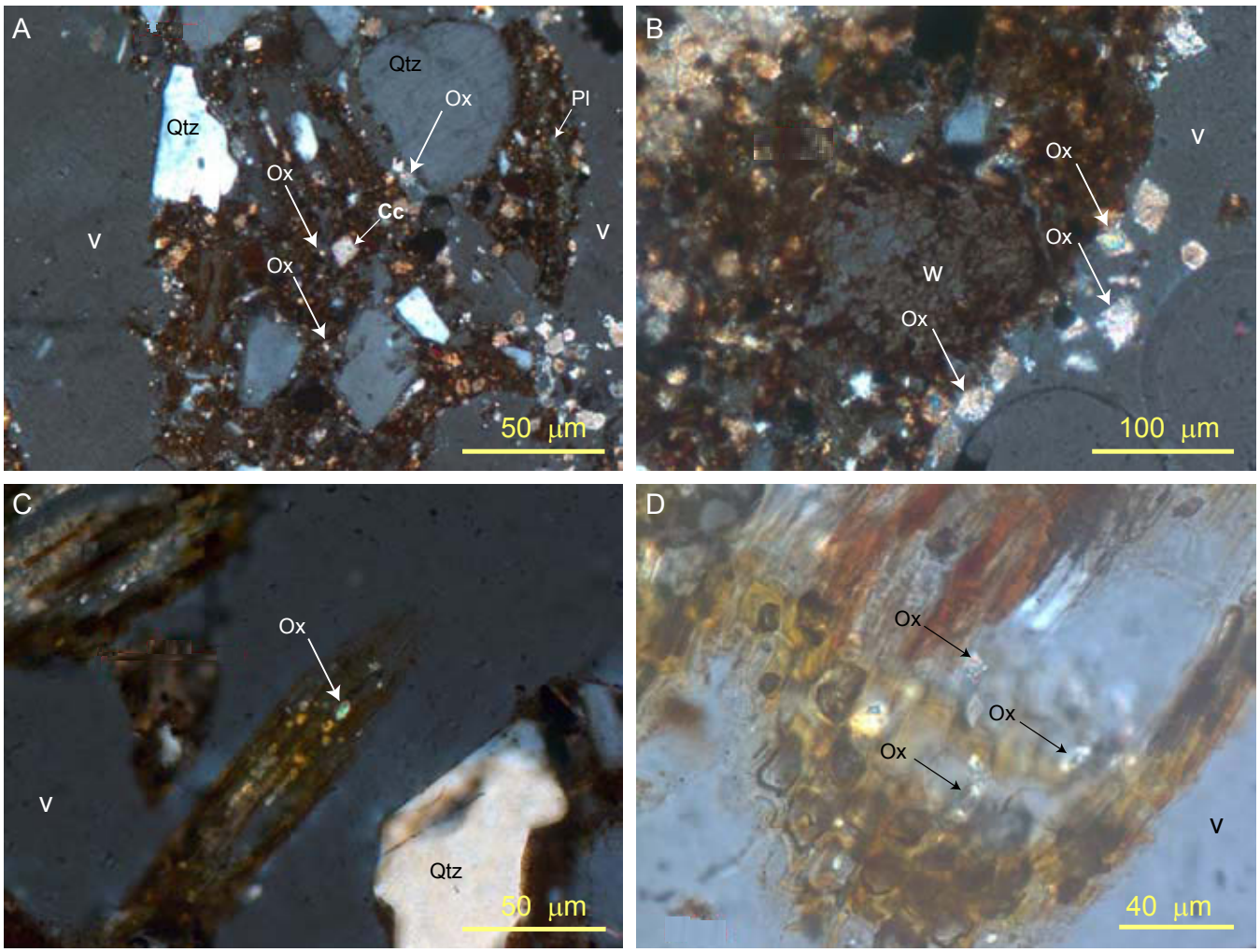


Fig. 3- Ca-oxalate crystals (Ox) observed in soil thin sections under light microscopy; Qtz: quartz; Cc: carbonate; Pl: plagioclase; v: void; w: wood. A, B, C and D) soil related to M. excelsa *tree. A and B) P4 5 cm, first soil horizon. C) P4 12 cm, second soil horizon. Ca-oxalate crystals are visible in wood tissues. D) P4 50 cm, fifth soil horizon. Ca-oxalate crystals a e visible in root tissues.*

The oxalate observed in these soils is produced by plants, fungi, and possibly by bacteria. Oxalate from the rhizospheric soil was not measured, but oxalic acid excretion by roots is common in plants (Fox and Comerford 1990). The release of plant metal-oxalate in soil environments depends on biological attacks: physical, such as by insects, or chemical, promoted by organic acids, enzymes, and metabolites from fungi (Gadd 2004) and bacteria (Hodgkinson 1977). Ca-oxalate of microbial origin derives from fungal and bacterial excretions of oxalic acid that binds with an ion to form an oxalate salt, normally Ca-oxalate. The oxalate content in Burkina Faso is of the same order of magnitude as those found in other ecosystems, such in Tuscany related to Abies alba (Certini et al. 2000) or in Ivory Coast and Cameroon related to *M. excelsa* stumps (Braissant 2005; Cailleau 2005). The negative correlation between oxalate concentration and depth is explained by a predominant source of oxalate derived from oxalogenic litter degradation and the decrease of fungal oxalate with depth due to the decrease of organic matter concentrations. Moreover, the soil porosity decreases drastically with increasing depth, constituting an unfavourable environment for organisms. The irregular distribution of oxalate

under the *M. excels*a stump is probably due to the activity of termites and ants that mix large quantities of material such as soil particles and OM containing oxalate. The high oxalate content measured under the stump is due either to the presence of a great quantity of wood containing oxalate or to the presence of saprophytic oxalogenic fungi degrading the *M. excelsa* stump. Moreover, the activity of ants and termites, together with fungi, improves the oxalate release in the soil environment, accelerating the oxalate-carbonate pathway. The oxalate peak at 5 cm in depth indicates an area of strong oxalate consumption but also a separation between the area in which oxalate derivates from leave degradation and the area in which oxalate derivates from degradation of more resistant material, such as wood or fungi. Saprophytic fungi and insects rapidly decay litter containing oxalate (oxalic acid, oxalate salts) deposited on the soil surface. Oxalate is thus released in the soil environment and available for bacteria that use it as carbon and electron sources, resulting in carbonate precipitation. Previous studies have shown that the highest concentration of oxalotrophic bacteria lies between the surface and 30 cm in depth, and consequently, constitutes the maximal potential for oxalate consumption (Braissant 2005; Khammar et al. 2009). Flower-shaped structures found previously in Petri dishes associated with *Ralstonia eutropha* bacteria (Braissant 2005; Cailleau 2005) are present in the studied soils, supporting the idea of a possible involvement of bacteria in carbonate precipitation (Fig. 4).

Field observations and laboratory data confirm that carbonate is present only in soils affected by *M. excelsa*. Maximal carbonate concentration is found on the soil surface under the *M. excelsa* stump (P3), where it reaches 145.7 ± 2.5 g of carbonate/kg of soil (14.5%). A preferential carbonate accumulation is observed in the first 15 cm (Fig. 2). Values remain fairly homogenous after 15 cm in depth (11.2 ± 4.7 g of carbonate/kg of soil). Carbonate can be expressed as various soil features (Fig. 4, Fig. 5, and Fig. 6): 1) cell infillings in wood and roots (biomorphosis), mainly as sparite (> 16 μm), 2) sparitic crystal assemblage in peds, or free in soil pores, being able to form flowe -shaped structures (Fig. 4), 3) micritic (< 16 μm) peds, composed mostly either by carbonate, mixed with amorphous organic matter, or mixed with organic matter and silicates. Oxalate crystals associated with carbonate are still present (Fig. 6). Carbonate coatings on peds are also found in the deeper soil layers. In the soil first layers, all the described features are found. Carbonate, as wood or roots cells pseudomorphoses, is only present in the first layers, whereas carbonate in peds (as micrite) is found in all the soil layers. Sparite crystals could result from mineralized wood and are present in the soil first layers. Micrite coatings are the predominant features in deeper layers. Carbonates under the *M. excelsa* stumps are mainly present as cells pseudomorphoses (sparite) of wood and roots, and only in the soil first three layers

The pH of soils, far from the tree influence, is of 5.8 ± 0.2, whereas it has an average of 8.1 ± 0.6 in soils influenced by oxalogenic African trees (Fig. 2). The conditions of maximal alkalinity, present at a depth comprised between 10 and 30 cm (Ak and Bck1 horizons), are not correlated with the highest carbonate accumulations. Moreover, the pH is higher in deeper layers, where the carbonate concentration is low compared to the surface. Carbonate is only found associated to oxalogenic trees where the pH is always alkaline. The carbonate quantity, as a function of depth, has not the same trend than pH distribution (Fig. 2). The maximal carbonate amount is found in A horizons whereas a minimal and constant level is maintained all along the deeper horizons (B and C). The presence of some local peaks can partly be explained by the presence of roots, which create a zone where carbonate concentration is important. Organic acid exudation and root respiration are common processes allowing carbonate formation in the rhizosphere (Nguyen 2003; Kuzyakov et al. 2006; Tu et al. 2007). The pH is more alkaline in deeper horizons than in those where carbonate is more abundant. Moreover, an alkaline pH peak is detected between 10 and 30 cm and thus shifted when compared to the overlying carbonate peak. The absence of correlation between the carbonate accumulation and the pH alkalinity was already observed in similar ecosystems (Cailleau 2005). Consequently, alkaline pH conditions are not due to the presence of calcite only. The process that manages pH alkalinity and carbonate precipitation is bacterial oxalate consumption (Braissant 2005; Cailleau 2005). Oxalotrophy modifies ion species and concentrations present in the soil solution, influencing pH conditions. Water percolation in the soil leaches carbonate ions in deeper layers where, if calcium is lacking, they remain in the solution and contribute and probably maintain an alkaline pH environment. Calcite field stability, depending on pH conditions, is in turn strictly depending on temperature, pCO_2, and ion concentrations. Moreover, a minimal level

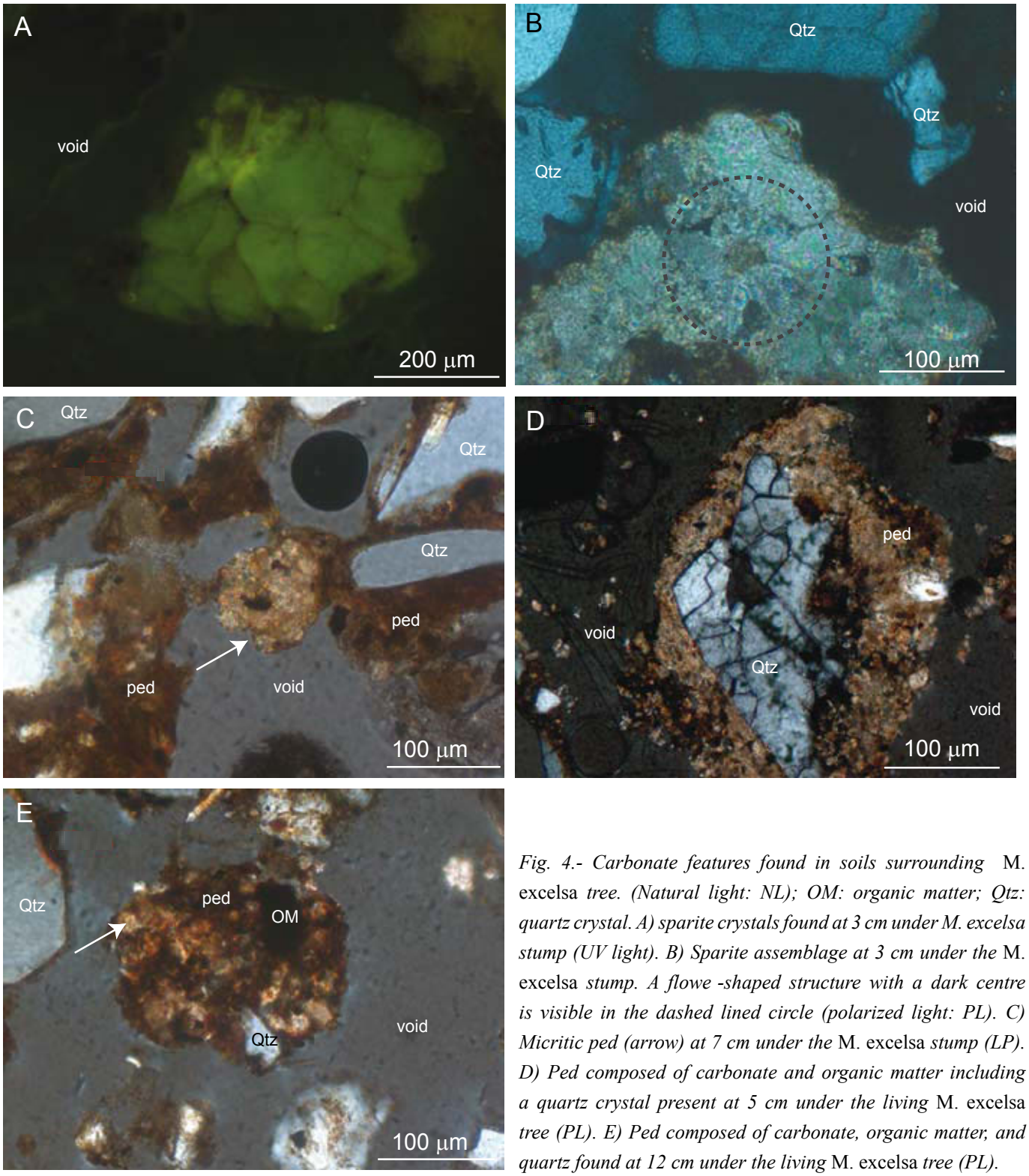


Fig. 4.- Carbonate features found in soils surrounding M. excelsa *tree. (Natural light: NL); OM: organic matter; Qtz: quartz crystal. A) sparite crystals found at 3 cm under M. excelsa stump (UV light). B) Sparite assemblage at 3 cm under the* M. excelsa *stump. A flowe -shaped structure with a dark centre is visible in the dashed lined circle (polarized light: PL). C) Micritic ped (arrow) at 7 cm under the* M. excelsa *stump (LP). D) Ped composed of carbonate and organic matter including a quartz crystal present at 5 cm under the living* M. excelsa *tree (PL). E) Ped composed of carbonate, organic matter, and quartz found at 12 cm under the living* M. excelsa *tree (PL).*

of water is necessary, because phase equilibrium takes place in solutions. To have an approximation of the equilibrium taking place in an open system, i.e. soils, parameters such as temperature, pCO_2, ion and water concentrations are kept constant, reflecting an instantaneous equilibrium (Verrecchia et al. 2006). However, the reality is certainly more complex. Instantaneous equilibria are present in a kinetic environment. Images of these kinetic equilibria are carbonate cements composed of different possible seasonal layers found in Ivory Coast (Carozzi 1967; Cailleau 2005). In tropical systems, conditions of super-saturation or dilution are imposed by rain periods, alternating with dry periods that in turns manage periods of intense and low biological activity, influencing the pCO_2 in the soil pores and carbonate precipitation. In the mineral horizons, the constant carbonate value can also be the result of the dissolution of the carbonate formed in the upper horizon, leached by water and re-precipitated in the deeper layers, forming coatings (Fig. 6). Because the studied soils are sandy, acid rains lasting six months favour the local carbonate dissolution in the soil surface and the

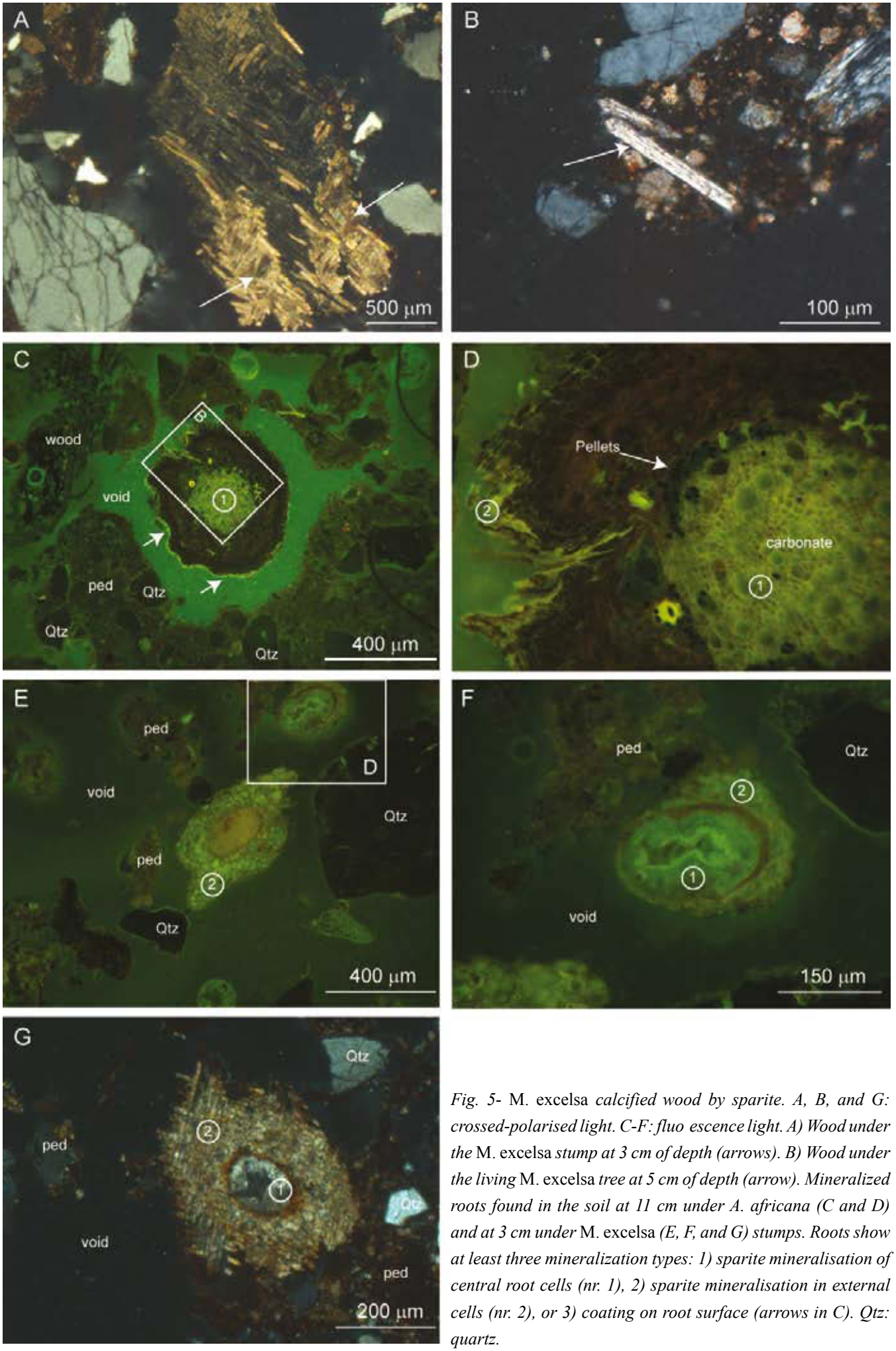


Fig. 5- M. excelsa *calcified wood by sparite. A, B, and G: crossed-polarised light. C-F: fluo escence light. A) Wood under the* M. excelsa *stump at 3 cm of depth (arrows). B) Wood under the living* M. excelsa *tree at 5 cm of depth (arrow). Mineralized roots found in the soil at 11 cm under A. africana (C and D) and at 3 cm under* M. excelsa *(E, F, and G) stumps. Roots show at least three mineralization types: 1) sparite mineralisation of central root cells (nr. 1), 2) sparite mineralisation in external cells (nr. 2), or 3) coating on root surface (arrows in C). Qtz: quartz.*

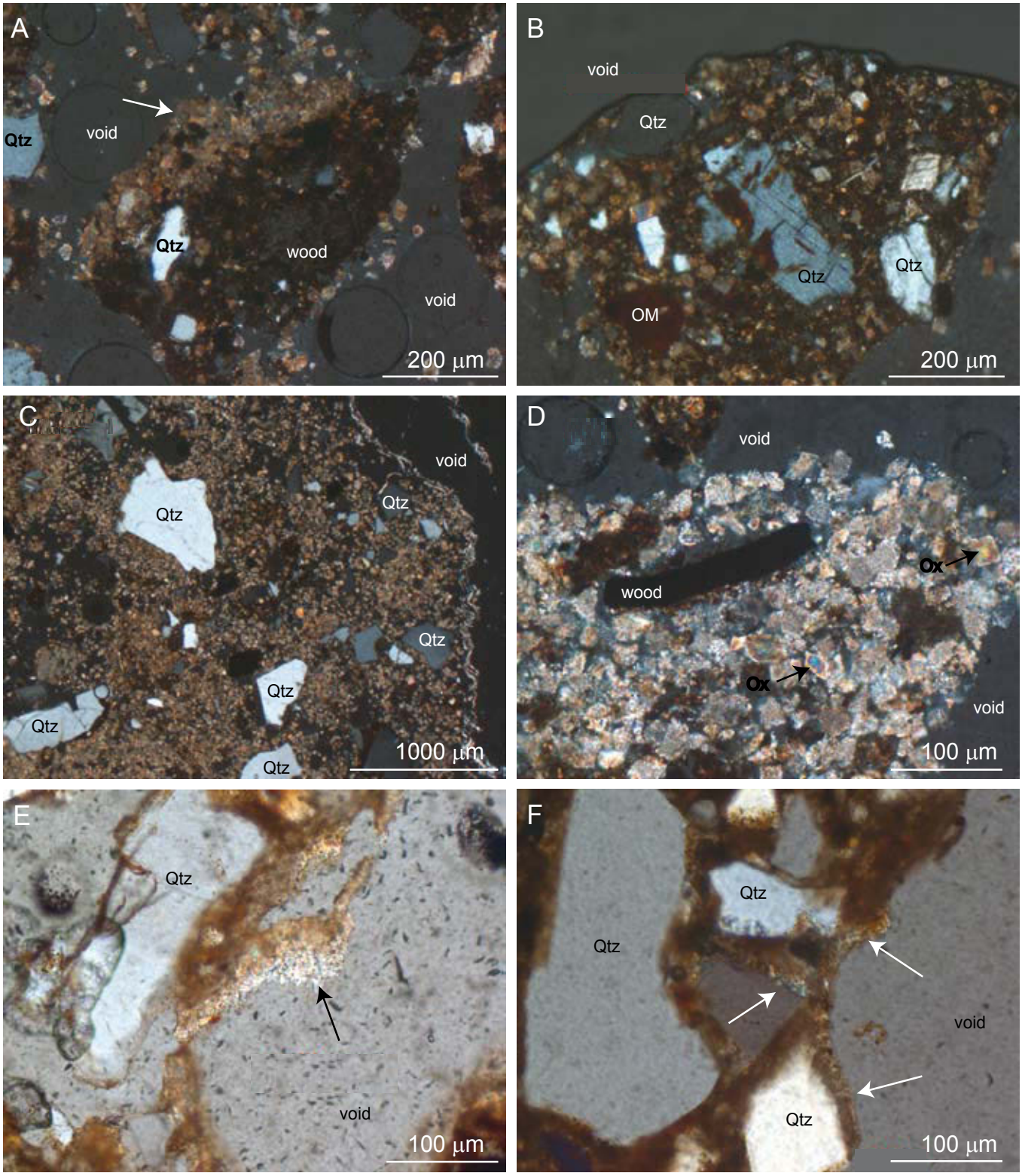


Fig. 6- Carbonate features found in soils surrounding M. excelsa *trees. A) Carbonate and oxalate accumulation around a wood remain found at 5 cm under the living* M. excelsa *tree (PL). B) Ped composed of quartz, carbonate, oxalate, and organic matter present at 5 cm under the living* M. excelsa *tree (LP). C and D) Carbonate and oxalate crystals including silicate and organic matter at 5 cm under the living* M. excelsa *tree (PL). E and F) carbonate coatings (arrows) at 40 cm and 50 cm under the living* M. excelsa *tree (PL).*

leaching of carbonate ions in depth, where local supersaturation conditions can allow re-crystallisation. In the case of a sloping system, carbonate ions can also be leached away, reaching streams, which eventually will bring them to the oceans, where a biologically carbonate precipitation can take place. In addition, in the soil, sawdust is present and likely results from wood cut and action of termites. One consequence is the release of carbonate crystals and oxalate salts from wood tissues, increasing the carbonate content in the soil first centimetres. Moreover, the stump wood

is partially burnt, accelerating the oxalate transformation into carbonate. Micromorphology confirms the presence of highest carbonate concentrations in smithereens of wood tissues. Charcoal is present in soils as well (Fig. 7) evidencing savannah burning, a current practice providing quick and fresh growing for cattle of nomadic people Peul (Lerebours-Pigeonnière and Ménager 2001). The transformation of oxalate crystals into carbonate during combustion is carried out when the temperature exceeds 470°C (Canti 2003). This process affects the soil first centimetres and resulting carbonate crystals retain the calcium oxalate habit and can therefore be considered as a calcium carbonate pseudomorphosis on Ca-oxalate (Cailleau 2005).

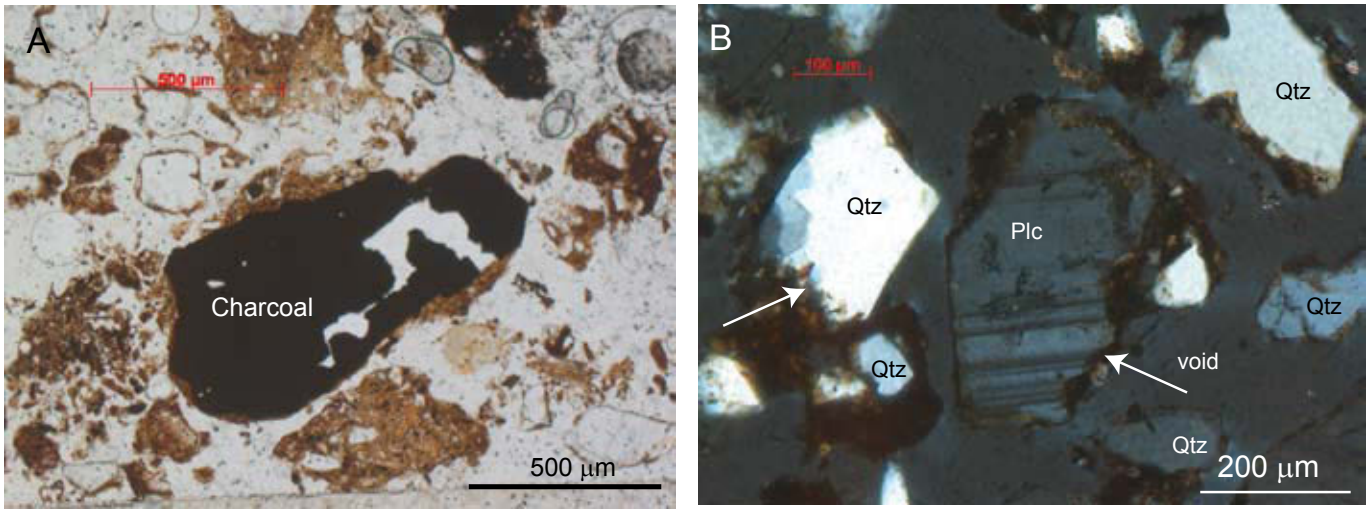


Fig. 7- Thin section details showing in A (natural light) burned wood tissues probably resulting from the bushfi e practice and in B (crossed-polarized light) silicates with corrosion gulfs (arrows). Plagioclases are probably one of the main calcium primary source.

X-ray diffraction analyses on Burkina Faso soil fractions and *M. excelsa* wood show that carbonate is constituted by low magnesian calcite, with various concentrations of Mg, from pure calcite (0% MgCO3) to high magnesian calcite (max 8% MgCO3; Fig. 8). In fact, magnesium is present in bedrock and soils. Detected carbonate has a low magnesium calcite stoichiometry, and is present in wood as well as in the soil. Oxalotrophic bacteria were found on wood surface from

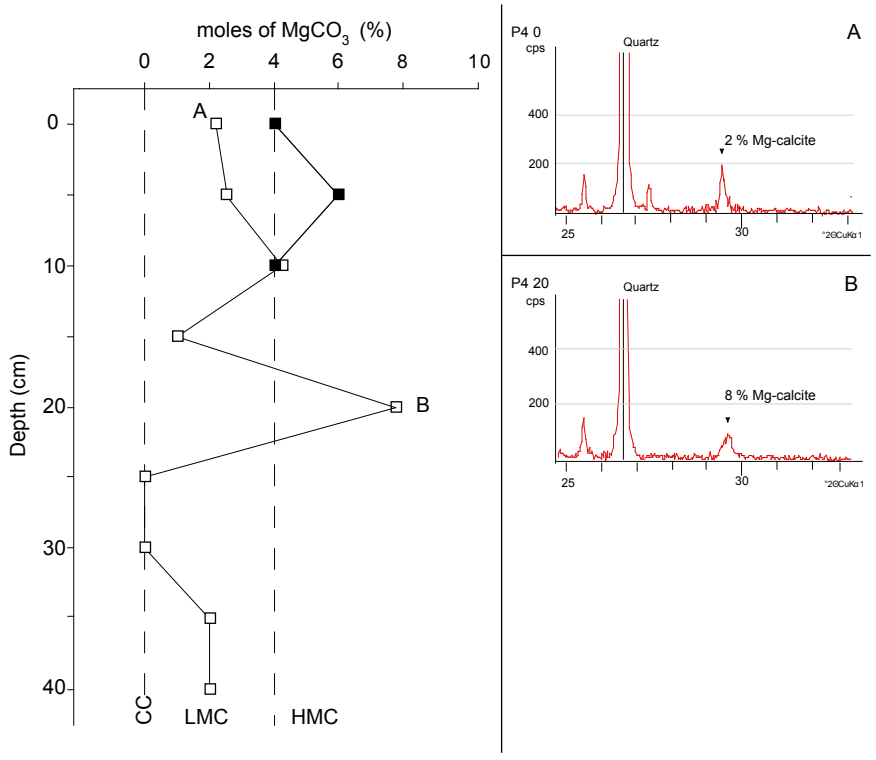


Fig. 8- White squares indicate the magnesium percentage found for the profile under the living M. excelsa *tree (P4) and black square the values calculated for the soil under the* M. excelsa *stump. A and B are XR spectra from P4 profile at 0 cm and 20 cm deep respectively. CC: Calcium carbonate; LMC: Low magnesian calcite; HMC: high magnesium calcite.*

oxalogenic Indian (Pr. Aragno personal communication) and Bolivian trees (M. Mota, pers. com.). Low magnesium-calcite has also been found in Cameroon and Ivory Coast soils surrounding oxalogenic trees (Cailleau 2005). Precipitation of this kind of low magnesium carbonate could be the result of a pure physicochemical process (e.g. supersaturation), or driven by microorganisms (Kübler 1992; Braissant 2005; Dupraz et al. 2009). Because carbonate formation is in this case the consequence of the oxalate-carbonate pathway, it is possible that the oxalate involved is a magnesium oxalate, such as glushinskite [Mg(C2O4) · 2 H2O], which is commonly associated with plants (Cowgill 1989; Garvie 2003; Monje and Baran 2005), fungi (Adamo and Violante 2000; Kolo and Claeys 2005; Gadd 2007), or lichens (Wilson et al. 1980; Adamo and Violante 2000; Burford et al. 2003). Moreover, fungi and bacteria can influence the cationic species of carbonate during biochemical processes (Braissant 2005). Magnesium is preferentially associated with fungal hyphae because fungi are metalophile. The ionic difference in carbonate species can be the result of the oxalate consumption by different oxalotrophic bacteria due to their different affinity for a specific cation (Braissant 2005). This affinity can depend on the available links associated to the cell wall as well as the chemical nature of the link sites (Braissant 2005). Nevertheless, there is no doubt that the oxalate-carbonate pathway allows the accumulation of alkali cations. This accumulation is the end-product of an immobilisation of Ca and Mg related to the carbonate precipitation.

One limiting factor that manages the carbon immobilization is calcium (Ca), and to a lesser extent, magnesium (Mg) availability. Primary Ca and Mg sources are silicates that show, in the analyzed soil profiles, dissolution gulfs (Fig. 7). Silicate weathering provides the necessary Ca and/or Mg to fix the atmospheric CO_2 and form a long-term carbon sink. The weathering rate of a mineral in a given environment can be considered as a function of intensity (temperature, moisture, pH and Eh) and capacity (specific surface area and nature of the mineral) factors (McKeague and Cline 1963). Silicate weathering counterbalances the volcanoes and the metamorphic CO2 emissions and thus regulates the level of atmospheric CO_2 during geological times (Urey 1952), following these equations:

$$CaSiO_3 + CO_2 \rightarrow CaCO_3 + SiO_2$$
$$MgSiO_3 + CO_2 \rightarrow MgCO_3 + SiO_2$$

Physical, chemical, and biochemical processes can modify silicate structure. Fragmentation and fracturing (physical agents) driven by climate (wind and frost) and biology (fungal hyphae, tree roots, burrowing organisms, and biomineralizing organisms) increase the crystal surface exposition facilitating chemical attack. Chemical attack is caused by water through hydration, hydrolysis, and dissolution processes. Silicate hydrolysis, the main dominant process observed in tropical environments, follows the equation below:

$$CaAl_2Si_2O_8 \text{ (anorthite)} + 3\ H_2O + 2\ CO_2 \rightarrow Al_2Si_2O_5(OH)_4 \text{ (kaolinite)} + Ca^{2+} + 2\ HCO_3^-$$

Depending on the CO_2 amount (pCO_2) dissolved in the water, the process that prevails is the acidolysis or the hydrolysis. Subsequently, the formed carbonic acid can: 1) enter in the water-table, 2) follows the $HCO_3^- \leftrightarrow H^+ + CO_3^{2-}$ equilibrium (see above), and/or 3) be transformed by the carbonic anhydrase and follows this reaction:

$$H_2O + CO_2 \leftrightarrow H_2CO_3 \leftrightarrow HCO_3^- + H^+$$

in order to maintain the acid-alkaline balance. In the presence of water, organisms influence silicate weathering by their metabolism, with the production of acids, ligands, CO_2, biofilms, etc., or by active ion uptake, equilibrium displacing, changes in redox conditions, etc. Some of the chemical reactions and processes that control the CO_2 concentration of natural surface waters include weathering of minerals, photosynthesis and respiration, anaerobic bacteria consumption of organic matter (e.g., sulfate reduction, respiration), and carbon dioxide dissolution and ex-solution (Andersen 2002). Alkaline conditions (pH > 9) lead to silicate dissolution enhancement, whereas a very acidic environment (pH < 3) can alter silicate structure (Millot et al. 1977). Alkaline environments are the result of alkaline media induced by bacterial

oxalotrophy (Braissant 2005; Verrecchia et al. 2006), or alkaline water-solution containing dissolved carbonate after they passed through the carbonate phase (Millot et al. 1977).

4. Conclusions

Evidence of the impact of *M. excelsa* tree on oxalate and carbonate contents in soils has been demonstrated. Organic carbon is present mainly as wood remains that contain oxalate and carbonate. Oxalate concentrations in Burkina Faso soils are in the same order of magnitude as those found under *M. excelsa* stumps from Ivory Coast and Cameroon (Cailleau 2005). In these soils, the concentration of oxalate is more important in the first horizon, where the biological activity is more efficient. In the Ak horizon, lower values in oxalate content could indicate a major area of oxalate consumption (oxalotrophy). Carbonate content in ferralsols is unusual but well demonstrated. This carbonate is the result of oxalate oxidation performed by bacteria. Carbonate is expressed as different features and results from various processes. Transformation of oxalate into carbonate influences soil pH, making the latter abnormally alkaline for such tropical conditions. Organic matter, organic acids and carbonates present under the oxalogenic tree, promote an unusual accumulation of Ca and Mg, compared to other tropical soils and can be considered as a carbon trapping system.

References

Adamo P, Violante P (2000). Weathering of rocks and neogenesis of minerals associated with lichen activity. Appl Clay Sci 16:229-256.

Andersen CB (2002). Understanding carbonate equilibria by measuring alkalinity in experimental and natural systems. J. Geosci Education 50:389-403.

Arnott HJ, Pautard FGE (1970). Calcification in plants. In: Biological calcification, pp 375-476. Edited by Schraer H. Amsterdam: North-Holland Publishing Company.

Bosu PP, Cobbinah JR, Nichols JD, Nkrumah EE, Wagner MR (2006). Survival and growth of mixed plantations of *Milicia excelsa* and *Terminalia superba* 9 years after planting in Ghana. Forest Ecol Manag 233 (2-3):352-357.

Braissant O (2005). Carbonatogénèse bactérienne liée au cycle biogéochimique oxalate-carbonate. Université de Neuchâtel. 214 pp.

Braissant O, Cailleau G, Aragno M, Verrecchia EP (2004). Biologically induced mineralization in the tree *Milicia excelsa* (Moraceae): its causes and consequences to the environment. Geobiology 2 (1):59-66.

Braissant O, Cailleau G, Dupraz C, Verrecchia EP (2003). Bacterially induced mineralization of calcium carbonate in terrestrial environments: the role of exopolysaccharides and amino acids. J Sediment Res 73 (3):485-490.

Braissant O, Verrecchia EP, Aragno M (2002). Is the contribution of bacteria to terrestrial carbon budget greatly underestimated? Naturwissenschaften 89 (8):366-370.

Burford EP, Kierans M, Gadd GM (2003). Geomycology: fungi in mineral substrata. Mycologist 17 (3):98-107.

Cailleau G (2005). Cycle du carbone et biominéralisation carbonatée en milieu continentale: la diagenèse des phases oxalate-carbonate. Université de Neuchâtel. 254 pp.

Cailleau G, Braissant O, Dupraz C, Aragno M, Verrecchia EP (2005). Biologically induced accumulations of $CaCO_3$ in orthox soils of Biga, Ivory Coast. Catena 59:1-17.

Cailleau G, Braissant O, Verrecchia EP (2004). Biomineralization in plants as a long-term carbon sink. Naturwissenschaften 91 (4):191-194.

Campbell WG, Fisher RC (1932). The composition and origin of "stone" in Iroko wood (*Chlorophora excelsa*, Benth. and Hook. f.). Emp For J 11:244-245.

Canti MG (2003). Aspect of the chemical and microscopic characteristics of plant ashes found in archaeological soils.

Catena 54:339-361.

Carozzi AV (1967). Recent calcite-cemented sandstone generated by the equatorial tree Iroko (*Chlorophora excelsa*), Daloa, Ivory Coast. J Sediment Petrol 37 (2):597-600.

Carvalho S, de Oliveira F, Vaz H (2004). Situation des ressources génétiques forestières de la République démocratique de Sao Tomé-et-Principe. Service de la mise en valeur des ressources forestières; Document de travail FGR/63F; Division des ressources forestières FAO, Rome, Italie. 42 pp.

Certini G, Corti G, Ugolini FC (2000). Vertical trends of oxalate concentration in two soils under *Abies alba* from Tuscany (Italy). J Plant Nutr Soil Sc 163 (2):173-177.

Cobbinah JR, Wagner MR (1995). Phenotypic variation in *Milicia excelsa* to attack by *Phytolyma lata* (Psyllidae). Forest Ecol Manag 75 (1-3):147-153.

Cowgill UM (1989). A naturally occurring alpha magnesium oxalate dihydrate from the northern Jordan Valley (Israel). Mineral Mag 53 (4):505-507.

Devineau J-L (1976). Données préliminaires sur la litière et la chute des feuilles dans quelques formations forestières semi-décidues de moyenne Côte-d'Ivoire. Oecol Plant 11 (4):375-395.

Dupraz C, Reid RP, Braissant O, Decho AW, Norman RS, Visscher PT (2009). Processes of carbonate precipitation in modern microbial mats. Earth-Science Rev 96:141-162.

Fox TR, Comerford NB (1990). Low-molecular-weight organic acids in selected forest soils of the Southeastern USA. Soil Sci Soc Am J 54 (4):1139-1144.

Franceschi V (2001). Calcium oxalate in plants. Trends Plant Sci 6 (7):331.

Franceschi VR, Horner HT (1980). Calcium oxalate crystals in plants. Bot Rev 46 (4):361-427.

Franceschi VR, Nakata PA (2005). Calcium oxalate in plants: Formation and function. Annu Rev Plant Biol 56:41-71.

Gadd GM (2004). Mycotransformation of organic and inorganic substrates. Mycologist 18 (2):60-70.

Gadd GM (2007). Geomycology: biogeochemical transformations of rocks, minerals, metals and radionuclides by fungi, bioweathering and bioremediation. Mycol Res 111 (1):3-49.

Garvie LAJ (2003). Decay-induced biomineralization of the saguaro cactus (*Carnegiea gigantea*). Am Min 88:1879-1888.

Harris CM (1933). Stone in *Chlorophora excelsa* B. and H., Iroko. Emp For J 12:229-238.

Hodgkinson A (1977). Oxalic acid in biology and medicine. London. Academic Press. 325 pp.

Jansen JWA (1974). Timber trees of Liberia; University of Liberia, Monrovia. UNDP/SF/FAO College of Agriculture and Forestry Project; University of Liberia, Monrovia. 83 pp.

Khammar N, Martin G, Ferro K, Job D, Aragno M, Verrecchia E (2009). Use of the frc gene as a molecular marker to characterize oxalate-oxidizing bacterial abundance and diversity structure in soil. J Microbiol Meth 76 (2):120-127.

Kolo K, Claeys P (2005). In vitro formation of Ca-oxalates and the mineral glushinskite by fungal interaction with carbonate substrates and seawater. Biogeosciences Discuss 2 (2):451-497.

Kübler B (1992). Calcites magnésiennes. Identification et dosage par diffraction X de $MgCO_3$ dans la solution solide. Cahiers de l'Institut de Géologie, Laboratoire de Minéralogie, Pétrographie et Géochimie; Université de Neuchâtel, Institut de Géologie série AX, N.22, 15 pp.

Kuzyakov Y, Shevtzova E, Pustovoytov K (2006). Carbonate re-crystallization in soil revealed by ^{14}C labeling: Experiment, model and significance for paleo-environmental reconstructions. Geoderma 131:45-58

Lerebours-Pigeonnière A, Ménager M-T (2001). Les atlas de l'Afrique: Burkina Faso: Groupe Jeune Afrique: les éditions du Jaguar. 62 pp.

McKeague JA, Cline MG (1963). Silica in soils. Adv Agron:339-396.

Millot G, Nahon D, Paquet H, Ruellan A, Tardy Y (1977). L'épigenie calcaire des roches silicatées dans les encroûtements carbonatés en pays subaride antiatlas. Maroc. Sci Géo Bull 30 (3):129-152.

Monje PV, Baran EJ (2005). Evidence of formation of glushinskite as a biomineral in a Cactaceae species. Phytochemistry 66 (5):611-614.

Nakata PA (2003). Advances in our understanding of calcium oxalate crystal formation and function in plants. Plant Sci 164 (6):901-909.

Nguyen C (2003). Rhizodeposition of organic C by plants: mechanisms and controls. Agronomie 23 (5-6):375-396.

Nichols JD, Wagner MR, Agyeman VK, Paul B, Cobbinah JR (1998). Influence of artificial gaps in tropical forest on survival, growth, and *Phytolyma lata* attack on *Milicia excelsa*. Forest Ecol Manag 110 (1-3):353-362.

Ofori DA, Cobbinah JR (2007). Integrated approach for conservation and management of genetic resources of Milicia species in West Africa. Forest Ecol Manag 238 (1-3):1-6.

Ofori DA, Newton AC, Leakey RRB, Grace J (1996). Vegetative propagation of *Milicia excelsa* by leafy stem cuttings: effects of auxin concentration, leaf area and rooting medium. Forest Ecol Manag 84 (1-3):39-48.

Ouinsavi C, Sokpon N, Bada O (2005). Utilization and traditional strategies of in situ conservation of iroko (*Milicia excelsa* Welw. C.C. Berg) in Benin. Forest Ecol Manag 207 (3):341-350.

Prior J, Cutler D (1992). Trees to fuel Africa's fires: Trees are a vital source of firewood in rural Africa, but the wrong ones turn savannas into desert. New Sci 135:35-39.

Tu S, Guo Z, Sun J (2007). Effect of oxalic acid on potassium release from typical chinese soils and minerals. Pedosphere 17 (4):457-466.

Urey HC (1952). The planets: their origin and development. Yale University Press. S.Miller, Science, 245 pp.

Verrecchia EP, Braissant O, Cailleau G, Aragno M (2006). The oxalate-carbonate pathway in soil carbon storage: the role of fungi and oxalotrophic bacteria. In: Fungi in biogeochemical cycles, Gadd GM (ed). Cambridge University Press. pp 289-310.

Wilson MJ, Jones D, Russell JD (1980). Glushinskite, a naturally occurring magnesium oxalate. Mineral Mag 43:837-840.